Tree-ring Growth Modelling Applied to Bayesian Dendrochronology

Masoud Muhammed Hassan

Thesis submitted to the University of Sheffield for the degree of Doctor of Philosophy in Statistics

School of Mathematics and Statistics

University of Sheffield

December 2016

Acknowledgements

Having expressed my thanks to the Almighty God who enabled me to perform this thesis, I would like to express my gratitude to the following people for their help and support during my PhD study here in Sheffield.

- I am deeply in the debt of my first supervisor **Professor Caitlin Buck** for all her time, effort, advice and helpful criticism. I am grateful for all the things I have learned from her through all the four years we have worked together. It has been my honour to work with such kind and great person, and I cannot only count her as my supervisor, but also as my close friend and role model.

- I am also grateful to my second supervisor **Dr. Timothy Heaton** for his support and constructive suggestions which made this study possible.

- Many thanks go to **Mr. Geoff Boden** for his support with IT and providing another pair of eyes to read through this thesis.

- My thanks go to **Dr. Emma Jones**, for our collaboration and her helpful comments through interesting discussion at the beginning of this project.

- Thanks to my funding body, Ministry of Higher Education and Scientific Research, Kurdistan Regional Government-Iraq, and Financial Support at from the University of Sheffield which all made this study possible.

- Many thanks go to all my colleagues and staff members in School of Mathematics and Statistics, for their friendship and help.

- Thanks to my **mother, sister** and **brothers** for all the valuable things they have taught me and for all the things that they motivate me to do. I am very grateful for their wise words and encouragement during my hard times.

- Finally, a special thank goes to **Mrs. Huda Ferman**, my love and partner for her support, and giving me the incredible joy of taking care of my children (**Maawa** and **Muhammed**) along these years.

Abstract

Classical dendrochronology involves using standard statistical methods, such as correlation coefficients and t-values to crossmatch undated tree-ring width sequences to dated 'master' chronologies. This crossmatching process aims to identify the 'best' offset between the dated and undated sequences with a view to providing a calendar date estimate for the undated trees.

Motivated by the successful and routine use of Bayesian statistical methods to provide a fully probabilistic approach to radiocarbon dating, this thesis investigates the practicality of using a process-based forward model known as 'VSLite' at the core of Bayesian dendrochronology. The mechanistic VSLite model has the potential to capture key characteristics of the complex system that links climate to tree-ring formation. It allows simulated, dated tree-ring chronologies to be generated at any geographical location where historical climate records exist. Embedding VSLite within a Bayesian approach to tree-ring dating allows combination of both ring-width data and any available prior information. Additionally, instead of identifying the 'best' calendar date estimate, the Bayesian approach allows provision of probabilistic statements about a collection of possible dates, each with a specific (posterior) probability.

The impact of uncertainty in the VSLite input parameters on the model output has been systematically investigated in this thesis, and the VSLite-based approach to Bayesian tree-ring dating has been explored using both simulated and real data. Results of implementing the new VSLite-based approach are compared with those using current classical and Bayesian approaches. An option for reducing the need for preprocessing data is also investigated via a data-adaptive rescaling approach. Having established the effectiveness of using the mechanistic forward model as the core for Bayesian dendrochronology, the practicality of adopting it to aid in dating in the absence of suitable local master chronologies is also explored.

Contents

Chapter 1

Introduction and Motivation

1.1 Background

Dendrochronology is a science that studies patterns of tree-ring widths of the same species in order to date processes and events over time and space. Each year a tree grows a new extra ring, and the width of that ring relies largely on the weather conditions prevalent during the growing season, and other factors, including the type of soil, and the tree's strife for light and nutrients. It is assumed that trees within the same geographical region receive the same climatic signal throughout a given year because they are exposed to similar climatic growth conditions, but this signal varies from year to year (Litton and Zainodin, 1991). Consequently, the width of these rings also appears to be variable in sequence, reflecting the effect of climate variation in different seasons. Good growing seasons usually provide wide rings, whereas the poor ones produce narrow rings. This pattern is the key to both dendrochronology (using the pattern of tree-ring growth to date timbers) and dendroclimatology (using the pattern of tree-ring growth as an indicator to monitor ecological processes and reconstruct past climate). For more information about dendrochronology and dendroclimatology, the reader is referred to Cook *et al.* (1990); Fritts (1976); Vaganov *et al.* (2006).

Dendrochronologists use patterns of annual ring-widths to date timbers by matching a group of trees from the same geographical location one with another

to ensure that every single ring is matched to its exact date of formation. This process is called "cross-matching" or "cross-dating" and is now usually based on statistical techniques (detailed in Chapter 2) which are used to measure the similarity between the cross-matched sequences. Before the patterns of tree-ring widths are used to date undated timbers, it is necessary to build a master chronology, an extremely long ring-width sequence that is created by averaging ring-widths from a large number of continuously overlapping older timbers. A cross-dating process is then applied to date undated timbers by cross-matching them with the master chronology.

Over the past decades, many efforts have been made to evolve statistical models of ring-width growth to be used for dendrochronology. The earlier statistical models were typically based on extending linear, empirically-determined relationship between tree-ring "indices" (preprocessed data, described in Section 2.1) and climate. Fritts (1976) suggested that such a model of tree-ring growth (described in Section 3.1) relies on the assumption that a climatic signal is common to all the trees grown in the nearby area plus some noise (error) which accounts for non-climatic factors. This simple statistical model was then investigated by several other researchers including Zainodin (1988) and Litton and Zainodin (1987, 1991) who proposed a fully model-based method for tree-ring dating and cross-matching sequences. A successful use of the model for dating trees, using classical methods such as t-values, was introduced by Litton and Zainodin (1991).

Following the adoption of Markov Chain Monte Carlo (MCMC) methods by the Bayesian research community, the simplicity and linearity of this statistical model made it a promising candidate to be used in a fully Bayesian framework. A Bayesian approach to tree-ring dating, using the statistical model, was first investigated by Buck *et al.* (1996). Tree-ring data and prior knowledge about the unknown dates were combined in a Bayesian framework to match a group of undated trees to a larger and longer group of dated trees (master chronology) from

the same geographical region.

1.2   Motivation for Thesis

The Bayesian approach proposed by Buck *et al.* (1996) has been explored most recently by Jones (2013) with a view to making it a routine practice in dendrochronology. She developed a series of methods for formalising the matching of undated timbers to a dated master chronology, thus allowing the user community to obtain full posterior date densities. The Bayesian approach proposed by Jones (2013) is fully probabilistic and provides a basis for the implementation of a Bayesian approach to tree-ring dating. However, this approach was not well-received by some in the dendrochronology community as it relies on a very simple descriptive statistical model of tree-ring growth (described in Section 3.1) which does not capture the mechanism of the ring-width growth during the growing season and formation of ring-widths. Additionally, it requires the tree-ring data to be fully processed (detailed in Section 2.1) in order to obtain stationary sequences prior to any representation of the data in the model and the matching process.

Recently, a mechanistic process-based model called VSLite (Tolwinski-Ward *et al.*, 2013) (described in Section 3.2.2) has become available which links ring-width growth to climate variables (temperature and precipitation), and provides dated tree-ring sequences. The VSLite model is a simplified version of the Vaganov-Shaskin model (Vaganov *et al.*, 2006) (detailed in Section 3.2.1) which captures the mechanism of key characteristics of the complex system that links tree-ring growth to climate. We are interested in exploring the use of the VSLite forward model to tree-ring dating within the Bayesian framework. The motivation behind this Bayesian investigation is to provide a routine method for dating similar to the one that successfully and routinely used in Bayesian radiocarbon dating, through modern radiocarbon calibration software such as OxCal (Bronk Ramsey, 1995) and BCal (Buck *et al.*, 1999).

The current project aims to use a stochastic version of the VSLite model at the core of Bayesian tree-ring dating by adding the matching process to the model and implementing it in the Bayesian framework. The new VSLite-based matching approach is implemented alongside the statistical-based approach of Jones (2013) as a building block for developing a fully Bayesian framework for tree-ring dating. Initially, we explore the strengths and weaknesses of the two approaches, but our ultimate goal is to develop a single coherent framework that can be recommended to professional dendrochronologists.

1.3   Thesis Objectives

This thesis focusses on the study of Bayesian tree-ring dating using both statistical and mechanistic models. In particular, we aim to investigate the possibility of using a mechanistic forward model (described in Section 3.2.2) at the core of Bayesian dendrochronology. The following are the main objectives of the thesis.

1. Search the literature for classical methodologies used by dendrochronologists for tree-ring dating, and the latest statistical and mechanistic, process-based, models used for describing the relationship between ring-width growth and climate.

2. Evaluate the process-based VSLite model and explore the uncertainty in its output using variance-based sensitivity analysis under Gaussian process emulation.

3. Investigate a Bayesian implementation of the VSLite model to tree-ring dating, which allows the formal use of prior information about the unknown date of timbers, thereby providing posterior date estimates at each possible offset rather than using the traditional t-value approach that is currently being used.

4. Examine several prior distributions for the VSLite model parameters, and adopt the most appropriate one.

5. Evaluate the efficiency and efficacy of the Bayesian approach to dendrochronology using VSLite model by comparing its implementation and results with those proposed by Jones (2013) (using a descriptive statistical model). Hence use the results obtained to recommend adoption of Bayesian models to professional dendrochronologists in their day-to-day work.

6. Investigate the use of less-processed data (detrended but not prewhitened or normalised) for tree-ring dating by considering data-adaptive rescaling for the cross-matched sequences.

7. Investigate a new VSLite-based approach for tree-ring dating in the presence of missing master chronologies by matching undated tree-ring sequences to a pseudo-master chronology generated from the VSLite model.

1.4 Thesis Structure

The remainder of this thesis is outlined as follows. In **Chapter 2**, we review existing classical statistical techniques used by dendrochronologists. The reader is introduced to several filtering methods used to remove the growth trend (detrending) and autocorrelation (prewhitening) from the raw ring-widths to prepare data for cross-matching. We then discuss the advantages and limitations of these filtering methods. The matching process and available dating methods (both classical and Bayesian) are then briefly reviewed before moving to describe the process of constructing tree-ring chronologies.

Chapter 3 describes two different models for ring-width growth, a descriptive statistical model and a mechanistic forward model, both of which are used within this thesis for implementation of Bayesian dendrochronology. Then the descriptive statistical approach for crossmatching trees and its Bayesian implementation are

described before moving on to explain the mechanistic VSLite model and its structure and components.

In **Chapter 4**, we implement the VSLite model at different locations around the world with a view to examining the efficiency of the model. We then investigate the uncertainty in the VSLite model output by exploring different sources of error in the model. Such uncertainties include those relating to: the model parameters, the model inputs climate data and error in the model structure. We then systematically explore the impact of uncertainty in the VSLite parameters on the model redoutput variability by conducting a Bayesian sensitivity analysis using Gaussian process emulation. A variance-based sensitivity analysis is then used to quantify the impact of each parameter on the model output variability.

Chapter 5 provides a Bayesian approach to estimate VSLite growth threshold parameters, considering three different prior distributions. The Bayesian approach and MCMC techniques are then used to estimate the main site-specific growth threshold parameters of the VSLite model for several UK chronologies (both Quercus and Pinus trees). The sensitivity of posterior estimates to the prior choices and to the tree species is also examined before moving on to use the VSLite model for the Bayesian tree-ring dating.

In **Chapter 6**, we extend the Bayesian approach to tree-ring dating by using the VSLite model at the core of the matching process; replacing the descriptive statistical model used by Jones (2013). We implement the new VSLite-based approach within the Bayesian framework, and investigate its efficiency using several simulation experiments. We then make a comparison between the results obtained from the descriptive statistical and VSLite-based models for tree-ring dating.

In **Chapter 7**, we address the issues associated with the need for filtering and normalising tree-ring data when dating timbers. We consider a method to improve cross-matching in dendrochronology by adding a scale parameter to the model

which accounts for the rescaling between the two crossmatched sequences. This allows us to use less-processed data (detrended but not prewhitened or normalised) for tree-ring dating. The method is evaluated using both simulated and real data.

Chapter 8 builds on the work introduced in Chapter 7 by addressing the problem of matching undated timbers when no appropriate master chronology exists. We consider a VSLite-based approach by first replacing a missing master-chronology for a site of interest by a pseudo-master chronology generated from the VSLite model using available climatic records. Hence, we match undated timbers to the pseudo-master chronologies and make inferences about the matching process in the Bayesian framework using a two-stage MCMC method. To test the efficiency of the approach, we match individual (and also groups of) trees to pseudo-local master chronologies.

Chapter 9 summarises the research work and draws conclusions from it. Recommendations are then offered about the routine use and application of Bayesian dendrochronology and plans for future work are outlined.

Chapter 2

Existing Statistical Methodologies in Dendrochronology

Statistical methods and techniques play a significant role and are widely used in tree-ring science, both in dendrochronology and dendroclimatology. Without the use of statistics and statistical methods, this field of science may not work very well. This is because analysing patterns of tree-ring widths relies on a statistical understanding of such data. For example, annual ring-width data is a time-series sequence, and for dendrochronologists to be able to work effectively with these types of data, they usually use time-series techniques which is a significant branch of statistics. Dendrochronological studies and analysis depend on a series of statistical procedures. It starts from preprocessing data to remove any age-trend from data via fitting a curve to the raw tree-ring sequences, then statistical measures such as correlation coefficient and Student's $t-$value are used in crossmatching ring-width sequences and hence providing a calendar date for an undated timber. More recently, Bayesian statistical approaches have also been used in dendrochronology to match undated trees to the dated sequences in the Bayesian framework. Therefore, statistical methods and techniques have been widely used in the core of tree-ring science to analyse patterns of ring-widths for both dendrochronological and palaeoclimatological studies. This chapter reviews existing statistical methods used for analysing patterns of tree-ring width data.

2.1 Preprocessing Tree-ring Data

Tree-ring width sequences store several information including the age of the tree, short-term climatic signal and long-term growth trends (Fritts, 1976). Before using tree-ring data for crossmatching, the data should be preprocessed in order to remove any age growth effect and non-climatic factors from raw data. The following sections describe how the dendrochronologist preprocesses the data to remove the trends, before crossmatching a pair of sequences. The ring-width indices that are preprocessed are used to match two single sequences. Preprocessing tree-ring data includes three main steps: detrending (remove age trend from data), prewhitening (remove autocorrelation), and standardizing (obtain a stationary time-series). These three main steps along with their methods and procedures are detailed below.

2.1.1 Detrending

Detrending is a statistical process of removing trend from tree-ring width sequences. One of the main non-climate factors that exists in ring-width data is age growth trend, such as negative exponential or negative slope. When the tree is younger it usually grows faster, and a wider ring is formed. As the tree ages, the growth of ring-width slows down. Thus, before dating timbers in dendrochronology or reconstructing past climate from tree-ring width, this age-related trend must be identified and removed from raw ring-width measurements for physical and statistical reasons. Physically to remove the geometry impacts of the tree by removing age-growth trend; and statistically to obtain stationary time-series sequences which are comparable. This can be done by one of the detrending methods described below. Therefore, detrending is an important preparation step for any dendrochronology or dendroclimatology study in order to remove tree-specific signal and reveal the stationary part of the climate signal. Detrended ring-width series is a dimensionless sequence with a particular mean and homoscedastic variance (Cook *et al.*, 1990). There are many detrending methods suggested in the literature, and here we summarise the most familiar ones used by the user communities.

2.1.1.1 Differencing Method

This is the simplest way for detrending ring-width data. A tree-ring width sequence that has a trend in mean can be transformed to a stationary sequence by evaluating the first differences (Fritts, 1976),

$$y_t = x_t - x_{t-1}$$

where x_t is a raw ring-width in year t; $t = 1, 2, ..., n$, n is the length of annual ring-width sequence, and y_t is the detrended ring-width index which takes the difference between the raw measurement in year t and $t-1$. The first-differencing method is most usable with a linear trend in mean; however, higher differencing orders, such as $y_t - y_{t-1}$, can also be used if the trend is not only in mean, but also in the rate of change of the mean.

Differencing methods are very simple to use for removing trends from data and decreasing the variance of the sequences. Despite their simplicity they can some times be problematic because they tend to increase the variance of data and produce spurious high-frequency variation if the trend is not in mean (Fritts, 1976). In that case the ring-width sequences are over-detrended.

2.1.1.2 Logarithmic Differencing

If the first and second order differencing methods fail to remove the trend from data, then logarithmic differencing method can be used. It is very similar to the first-differencing method. Given a non-stationary raw ring-width data, x_t, the detrended ring-width index y_t can be obtained by taking the difference between the logarithm of the raw ring-width in year t and $t-1$,

$$y_t = \ln(x_t) - \ln(x_{t-1}).$$

This method of detrending has been investigated and tested by several dendrochronologists including Steward (1983) and Okasha (1987). The main disadvantage of this technique is that it cannot be used if the sequence is already stationary for it may introduce an extra autocorrelation into the ring-width data (Okasha, 1987).

Thus, under this method, the stationarity of raw data must be first inspected to avoid over-detrending.

2.1.1.3 5-Point Moving Average

This method was first developed and used by Baillie and Pilcher (1973) to remove the trend from raw ring-width data, and is also know as "Baillie and Pilcher's Filter". It removes the low frequency influences from data by taking the arithmetic logarithm of a percentage of five-point moving average. Mathematically, the tth ring-width index from this method can be defined as

$$y_t = \ln(\frac{5x_t}{x_{t-2} + x_{t-1} + x_t + x_{t+1} + x_{t+2}}),$$

where x_t is the raw measurement at year t and y_t is its detrended ring-width index.

In order to examine how good this method is, Zainodin (1988) proposed matching a pair of contemporary ring-width sequences, after detrending, to test whether they crossmatch at the true offset or not. With a particular dataset of tree-rings used in his thesis, he found that the method by Baillie and Pilcher (1973) was better than other available methods to remove age trend from raw data. He established that this simple, yet reliable, method provided relatively useful results. Jones (2013) also followed Zainodin (1988) in using this filtering method in her thesis as it is simple and produces good results.

2.1.1.4 Negative Exponential Curves

The raw ring-widths, in most cases, vary from the pith (the innermost layer of stems of trees) to bark (the outermost layer of stems of trees), as shown in Figure 2.1. This was discovered and noted by Matalas (1962). He suggested that the age growth trend in raw ring-width data can be represented by a negative exponential function and fits this to the raw data. This is one of the most common methods used by the dendrochronologists to justify the raw ring-width and removing any age

trend from the data. In this detrending technique, a negative exponential curve, g_t, is fitted to the raw sequences to model the age trend in the data, and then a value of each raw measurement, x_t, is divided by expected value from estimated curve to provide a detrended index, y_t. The negative exponential curve is defined as

$$\hat{g}_t = \hat{a}e^{-\hat{b}t}$$

where $\hat{g}_t$ is the growth curve estimated from data, $t = 1, 2, \ldots, n$ is the length of the sequence, and a and b are constant coefficients (intercept and slope) to be estimated. Fritts (1963) found that the measured ring-widths are a non-stationary time-series sequences, because the absolute variation in measured tree-ring data decreases monotonically from the pith.
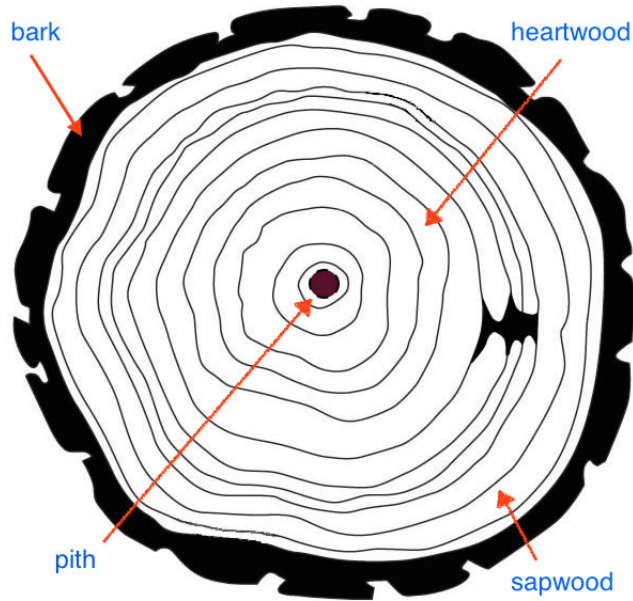
Figure 2.1: A diagram to show a cross section of the trunk of a tree with annual growth rings.

Having estimating an appropriate curve for the growth rates that are associated with the change of tree-geometry over time, a non-stationary sequence can be transformed into a stationary one (Fritts *et al.*, 1969) as follows. The raw measurement (x_t) at year t transforms into its ring-width index (y_t) by dividing the raw

rings by the estimated growth curve ($\hat{g}_t$),

$$y_t = \frac{x_t}{\hat{g}_t}.$$

Any age related growth is removed from the data, and the variance is scaled so that it is almost the same over the whole length of the ring-width sequence.

2.1.1.5   Modified Negative Exponential Curves

This is a new updated version of the previous method suggested by Fritts *et al.* (1969). They realised that the method of fitting negative exponential curve was only working for trees with 100-200 rings, and provided an unreliable curve for older trees. This is because, as the number of rings increases the expected curve tends to zero. Thus, a modified negative exponential curve was suggested by Fritts *et al.* (1969) to estimate the age growth trend and then remove it from the raw ring-width data (Fritts, 1976). The estimated growth curve using this method is:

$$\hat{g}_t = \hat{a}e^{-\hat{b}t} + \hat{c},$$

where $\hat{a}, \hat{b}, \hat{c}$ are constant coefficients to be estimated in such a way that the sum of square of differences of the estimated curve, $\hat{g}$, and the actual ring-width sequence, x, is minimised.

In his investigation to check the adequacy of fitting exponential curves to the growth trend of North American trees, Fritts (1976) argued that the modified method is efficient for most of the data they used as the produced ring-width indices have a lower variance and the mean index value is closer to 1.0. This method was then investigated and recommended by many other dendrochronologists including Cairns (2005); Cook *et al.* (1990); Jones (2013); Warren (1980); Warren and MacWilliam (1981).

Throughout this thesis, experiments using raw data will be detrended to remove the age trend effects using the method of modified negative exponential alongside other methods.

2.1.1.6 Linear Regression Line

Some times raw ring-width sequences gradually change in level over time or have unusual growth pattern that cannot be accommodated by the negative exponential curves. In such cases, a simple linear function can be used for fitting the growth trend in the raw data. The easiest detrending method is to fit the least square regression line to raw ring-width sequences that are relatively short. Under this method of detrending, the growth trend can be represented by a simple linear regression

$$\hat{g}_t = \hat{a} + \hat{b}t,$$

where $\hat{g}_t$ is the estimated growth trend, $\hat{a}$ and $\hat{b}$ are estimated regression coefficients. Then the detrended ring-width index, y_t, is produced by dividing actual raw ring-width, x_t, by the estimated growth trend, $\hat{g}_t$,

$$y_t = \frac{x_t}{\hat{g}_t}.$$

2.1.1.7 Cubic Smoothing Spline

Instead of fitting a curve to the whole ring-width sequences (previous three methods), a smoothing spline can be used to fit a curve made up of cubic polynomial pieces in between data points. A cubic spline to remove age growth from raw ring-width sequences was first suggested by Cook (1981) after looking at the work of Reinsch (1967), who fitted a smoothing spline to data which were subject to unwanted experimental error.

Cook (1981) applied a smoothing spline consisting of different cubic polynomials joined together between the data points, known as knots. The polynomials between these knots join together smoothly as the first and second derivatives are continuous. Because the curve is built of piecewise cubic polynomials, one area of the tree-ring sequence with a particular behaviour can be modelled differently to another area of the sequence that behaves differently. For more details about this method the reader is referred to Reinsch (1967) and Cook (1981). The detrended indices are obtained by dividing raw ring widths by the estimated curve from the

cubic spline.

Cook (1981) thought that his suggested method removes all the trend from data and takes into account the impact of the former year's growth on the present year's (autocorrelation). However Okasha (1987) showed that the ring-width indices obtained from this method are still correlated. Okasha (1987) and Cairns (2005) found that Cook's method does not remove enough growth effect from raw ring-width data, hence causing autocorrelation. Thus, instead of fitting to the raw ring-width, Okasha (1987) fitted a cubic spline to logarithms of the raw ring-width data. He claims that his method of fitting a cubic spline worked better for detrending and removing the age growth trend from data in the datasets he used.

2.1.1.8 Digital Filtering

Another detrending method was suggested by Munro (1984) for removing the age trend effect from the raw ring-width data. This method describes the growth curve as a linearly filtered version of the actual sequence. A smoothed growth estimate of the original sequence can be obtained by weighting the individual observations from the digital filter, and then subtracting the estimated smooth growth curve from the actual ring-width data to obtain the ring-width indices:

$$y_t = \log(x_t) - \sum_{k=-f}^{f} \zeta_k \log(x_{t+k}),$$

where x_t are the actual ring-width data, $\{\zeta_k\}$ is a set of filter weights, f is the length of the filter, y_t are the detrended indices, and $t = f + 1, f + 2, \ldots, t - f$.

Munro (1984) and Wigley *et al.* (1987) suggested this digital filtering for detrending raw ring-width data as it removes the long-term growth trend from data. The authors concluded that the filter should be able to enhance the high frequency variance present but still keep a reasonable amount of autocorrelation.

Several detrending methods have been described in this section. At this point the dendrochronologists can use the ring-width indices of two overlapping sequences for crossmatching with a view to dating them, as detailed in Section 2.2. However, some researchers including Laxton and Litton (1983); Steward (1983); Yamaguchi

(1986); Zainodin (1988), have noted that the ring-width indices are still autocorrelated which is detrimental to crossmatching. Therefore, they suggest further processing of ring-width indices to remove the autocorrelation remaining in the data after detrending. In what follows we describe the method of removing this autocorrelation in a process known as 'prewhitening'.

2.1.2 Prewhitening

Prewhitening is a statistical process of removing autocorrelation from time-series data. Such autocorrelation usually occurs in tree-ring sequences when the growth of a ring in one year is related to the growth of the ring in the next and/or previous years (Laxton and Litton, 1983). Therefore, although the process of detrending successfully removes the growth trend from data, it does not necessarily remove the autocorrelation. Cross-matching autocorrelated ring-width sequences might cause an increase in spurious matches. This was first noted by Yamaguchi (1986) in his investigation where he demonstrated by examples that spurious matches can arise between autocorrelated sequences. Thus, he suggested using a method, known as prewhitening, to remove the autocorrelation in the ring-width sequences before any crossmatching can be done.

Laxton and Litton (1983) suggest that after detrending tree-ring width measurements and producing ring-width indices, it is worth checking if the data is clear of any autocorrelation before using them in the matching process. If the detrended ring-width indices are still autocorrelated, the data should be processed more in order to remove any autocorrelation. In the following sections, we describe the existing methods proposed by dendrochronologists to remove the autocorrelation from ring-width indices.

2.1.2.1 Fitting AR(p) Model

The autoregressive model, AR(p), was first suggested by Laxton and Litton (1983) to prewhiten autocorrelated tree-ring sequences. Following Box et $al.$ (1994), the autoregressive process of order p is defined as,

$$y_t = a_1 y_{t-1} + \cdots + a_p y_{t-p} + \epsilon_t,$$

and $y_1, \ldots, y_t$ are detrended ring-width indices, $a_1, \ldots, a_p$ are autoregressive parameters of order p to be estimated, and ϵ's are the white noise with a normal distribution $N(0, \sigma^2)$.

Laxton and Litton (1983) used this model to remove the autocorrelation from ring-width indices. They first removed the growth effect from the raw tree-ring sequence using the detrending method suggested by Baillie and Pilcher (1973) which is described in Section 2.1.1.3, and then prewhitened the sequence using AR(p) model. Laxton and Litton (1983) concluded that there is an overall improvement in cross-matching when using the prewhitened sequences for matching sequences. They also suggested using their method in all sequences before cross-dating.

Wigley et $al.$ (1987) made a comparison among variety of methods for detrending and prewhitening. They commented that no single method appeared to be better than another as one method might appear preferable on one test, whereas in others it might be reversed and be the least preferable. However for prewhitening their data, Wigley et $al.$ (1987) suggested fitting an autoregressive model AR(p) as it is simple and takes into consideration the growth effects in the previous years.

2.1.2.2 Fitting ARMA(p, k) Model

One of the most familiar methods for removing autocorrelation from time-series data is the autoregressive-moving average model, ARMA, for the autocorrelated data. Box et $al.$ (1994) defined the ARMA(p, k) process with p autoregressive and k moving average orders, as follows

$$Y_t = a_1 Y_{t-1} + \cdots + a_p Y_{t-p} + \epsilon_t + b_1 \epsilon_{t-1} + \cdots + b_k \epsilon_{t-k},$$

where $Y_1, \ldots, Y_t$ are random variables and the tree-ring indices $y_1, \ldots, y_t$ are realisations of their values at time t. $a_1, \ldots, a_p$ and $b_1, \ldots, b_k$ are model parameters for p autoregressive and k moving average orders respectively, and ϵ's are the white noise with a normal distribution $N(0, \sigma^2)$.

Fitting ARMA(p, k) model includes three steps. First, identifying the order of the model; i.e. finding the value of p and k. This is usually obtained from the plot of autocorrelation function, ACF, and partial autocorrelation function, PACF. Second, the model is fitted to estimate unknown parameters, $a_1, \ldots, a_p$ and $b_1, \ldots, b_k$, using methods such as, maximum likelihood and least squares. Finally, checking the efficiency of the fitted model to ensure that it is reliable. The reader is referred to Box *et al.* (1994, p.184) for more details about these three steps (using ACF and PACF plots in model selection, estimating parameters of ARMA(p, k) model, and diagnostic checks for the fitted model).

The model is fitted to the detrended indices, and the residuals from the model are then used as the prewhitened indices required for crossmatching process. This method has been used by several dendrochronologists in the literature, including Monserud (1986); Okasha (1987); Steward (1983); Yamaguchi (1986).

Steward (1983) examined the use of ARMA(p, k) models for the prewhitening of tree-ring sequences in a number of Quercus trees in the UK. In her investigation, she tested fitting several ARMA(p, k) models with different orders, and found that an ARMA$(1, 2)$ was the most appropriate model for the vast majority of her data. Steward (1983) stated that her selected model seems very reasonable as the climate in one year would affect the ring-width growth in the following years due to the fact that tree stores energy and food supplies from the previous year.

Okasha (1987) also investigated the use of ARMA models in his thesis. He stated that the most appropriate filtering method is the one which not only removes the age trends from the data but also removes the autocorrelation. He fitted some ARMA(p, k) models to his data, with different p and k orders, and defined k as the number of previous years that the weather conditions have affected the

18

growth of ring-width index. Okasha (1987) found that fitting an ARMA(p, k) model to ring-width indices and hence crossmatching sequences increased the chances of obtaining correct dates since they decrease the autocorrelation in the sequences.

Independently, Yamaguchi (1986) and Monserud (1986) also advocated the use of ARMA(p, k) models for removing the autocorrelation present in the ring-width indices. They concluded that ARMA$(1, 1)$ was the best model for prewhitening the ring-width sequences.

A comparison also made by Cairns (2005) on some filtering methods to produce ring-width indices. Among ten filters he tested, Cairns (2005) found that the ARMA(p, k) model was the 'best' filter as it removes both low frequency variance (cycles with wavelengths greater than eight years) and high frequency variance (cycles with wavelengths less than eight years) from raw data. Whereas, other filters he examined tend to only remove the low frequency variance. Cairns (2005) justified the use of the ARMA model by the evidence made by Steward (1983) which states that it is sensible to consider that the growth in the current year is affected by weather conditions in previous years.

2.1.2.3   Method of Zainodin (1988)

Zainodin (1988) also examined the use of ARMA model for prewhitening tree-ring data in his investigation. He suggested that fitting these types of models might not be suitable for dendrochronology as it adds more complicated procedures which require some knowledge of time series analysis that should not be assumed for dendrochronologists. He also pointed out that, quite often, dendrochronologists deal with large numbers of samples, and so a non-subjective approach would be more suitable. For this purpose, he suggested using a simpler method which does not require estimating parameters p and k. In order to choose an ARMA model from several competing models, Zainodin (1988) used an Akaike Information Criterion (AIC) which is the most well-known model selection criterion, suggested by Akaike

19

(1973). AIC takes into consideration the number of model parameters $(a_1, \ldots, a_p$ and $b_1, \ldots, b_k)$ and how well it fits the data (errors in the model predictions).

For fitted ARMA sequences of length t, the AIC is defined to be:

$$AIC = -2\ln(\text{maximised likelihood of the fitted ARMA(p, k)}) + 2(p + k + 1).$$

A number of models are fitted to the data and the one with the smallest AIC value is chosen as the 'best' model.

2.1.2.4 Fitting ARMA-GARCH Models

After his investigation on comparing trend removal filters, Cairns (2005) settled on using $\text{ARMA}(p, k)$ models to detrend and prewhiten a logged tree-ring sequence for beech trees. However, he noted that when fitting $\text{ARMA}(p, k)$ models to tree sequences, there were areas of particularly large residuals that were observed from examining index plots of the residuals. He declared that "these patches do not indicate significant positive autocorrelation, but the occurrence of autoregressive conditional heteroscedasticity, ARCH" (Cairns, 2005, p.94). The family of time series models known as ARCH and generalized autoregressive conditional heteroscedastic (GARCH) models attempt to model its occurrence in time-series data.

Under the $\text{ARMA-GARCH}(p, k, r, s)$ model, the conditional mean of the detrended ring-width sequence is modelled by $\text{ARMA}(p, k)$ model of p and k orders, and its error variance, σ_t^2, (which is a non-constant variance in tree-ring sequences) is modelled by a $\text{GARCH}(r, s)$ process with r and s orders. The model is defined as follows,

$$y_t = \sum_{i=1}^{p} a_i y_{t-i} + \epsilon_t + \sum_{i=1}^{k} b_i \epsilon_{t-i}, \quad \epsilon_t \sim N(0, \sigma_t^2),$$

$$\sigma_t^2 = \phi_0 + \sum_{i=1}^{r} \phi_i \epsilon_{t-i}^2 + \sum_{i=1}^{s} \theta_i \sigma_{t-i}^2$$

where $y_1, \ldots, y_t$ are detrended ring-width indices, $a_1, \ldots, a_p$ and $b_1, \ldots, b_k$ are $\text{ARMA}(p, k)$ model parameters, and ϵ's are the white noise with a normal dis-

tribution $N(0, \sigma_t^2)$, ϕs and θs are GARCH(r, s) model parameters.

Cairns (2005) used Markov chain Monte Carlo methods under the Bayesian paradigm to estimate unknown parameters of the model for preprocessing tree-ring data before crossmatching. He then used residual sequences from his model as ring-width indices ready for use in the matching process. Cairns (2005) also showed by examples that the ARMA-GARCH model was able to remove both low and high frequency variance from the data he used. He concluded that the use of the ARMA-GARCH model as a filter provided a robust methodology for cross-matching tree-ring sequences. He also claimed that his new method of preprocessing data appeared to reduce the number of spurious matches when used for crossmatching timbers. Although Cairns (2005) used Bayesian methods to develop a technique for preprocessing and removing age trend from raw data, he did not use such Bayesian methods at the core of dating process. However, in this thesis we aim to use such Bayesian methods at the core of tree-ring dating.

In this section several methods have been described that are used by dendrochronologists to remove autocorrelation from tree-ring sequences and provide normally distributed ring-width indices appropriate for the use in the crossmatching process. The next section describes the normality of the produced ring-width indices.

2.1.3 Standardizing Indices

Dendrochronologists usually seek for fully standardized ring-width sequences to be used in the crossmatching process. The stationarity of these sequences is required so that they should be statistically identical and comparable to each other before crossmatching them. It is often assumed that after detrending (removing age trend) and prewhitening (removing autocorrelation) the produced ring-width indices are stationary and approximately normally distributed. If this is the case then the ring-width indices can be crossmatched to each other; otherwise, the indices must

be standardized.

Many researchers, who have suggested methods for filtering tree-ring data, assumed that their methodologies provide normally distributed indices. However, when investigating the normality of produced indices, Munro (1984) and Zainodin (1988) found that this is not always true. For example, Munro (1984) showed that the ring-width indices obtained from applying the detrending method by Baillie and Pilcher (1973) were not normally distributed but close to a normal distribution. In his assessment for normality of the produced indices, Zainodin (1988) detrended his data using the method by Baillie and Pilcher (1973) (Section 2.1.1.3), and then prewhitened them using the method by Box *et al.* (1994) (Section 2.1.2.2). He then assessed the normality of the indices produced by examining normal probability plots. Despite detrending and prewhitening his tree-ring width data, Zainodin (1988) found that the distribution of the indices was symmetric but probably heavier in tails than a normal distribution.

Thus, it is not guaranteed that the ring-width indices produced from filtering methods are necessarily fully normally distributed. If the normality of the sequences is essential for the analysis, it can be further processed by some transformation methods, such as standard z-scores of indices, which is the most commonly used method. Formally, the standardisation of the ring-width indices $y_1, \ldots, y_t$ of length t is

$$z_t = \frac{y_t - \bar{y}}{\sigma_y},$$

where $\bar{y}$ is the mean of ring-width sequence, and σ_y is its standard deviation. The standardised sequence z has a zero mean and a standard deviation of one.

2.1.4 Limitations of Preprocessing Data

Preprocessing raw ring-width data includes three main steps: detrending, prewhitening and normalising. The detrending process seems reasonable and logical due to the geometry and biological aspects of the trees. It is an important process which

removes the age growth trend from raw ring-width data and reveals the stationary part of the climate signal. However, the prewhitening step is rather more complicated and not a necessary process for filtering tree-ring data. It is a complicated procedure which requires some knowledge of time series analysis that should not be assumed for dendrochronologists. Furthermore, there might be an impact of this additional filtering process. The main structure and characteristics of the ring-width data, and a part of its climatic signal will be lost if the data are over-processed.

Thus, it is essential to double check the behaviour and the structure of the tree-ring width data before using them in the matching process in order to ascertain that the data are not over-processed and there is enough climatic signal information remaining in the data that makes the matching process both doable and useful. The problem of over-processing tree-ring width data is tackled in more detail in Chapter 7. Rather than extra filtering and removing more characteristics from the data, we will consider a very simple statistical model for matching process which will take into account the impact of rescaling between the two crossmatched sequences using less-processed data.

2.2   Tree-ring Dating: Concepts and Methods

2.2.1   Matching Process

Having successfully prepared tree-ring width data by preprocessing them to remove age trend and autocorrelation, the patterns of the obtained ring-width indices from the same geographical location can then be compared with one another in order to date them. This comparison is known as "cross-matching", and it is important in dendrochronology for it allows dendrochronologists to, ultimately, build chronologies for a region of interest as shown in Fig. 2.2.

Crossmatching is considered to be the base principle of dendrochronology. Matching patterns of two ring-widths sequences allows dendrochronologists to identify the
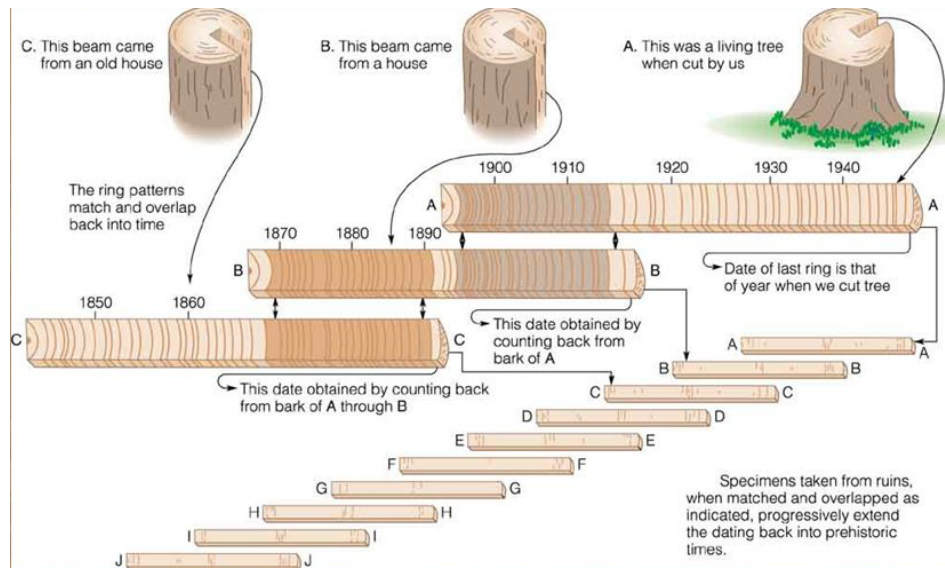
Figure 2.2: A graphical explanation of dendrochronological process from Stokes and Smiley (1968) with permission.

correct date in which each ring-width was composed. This enables estimating the construction date of an ancient building, by matching patterns of timbers taken from the building and crossmatching them with the patterns from nearby living trees. The crossmatching process requires tools and techniques for matching ring-width patterns. There are several methods used by dendrochronologists for dating tree-ring width sequences. Preference for crossmatching techniques varies by countries and institutions. This section reviews existing methods for crossmatching two tree-ring sequences.

2.2.2 Classical Crossmatching

Following are some classical statistical methods used by dendrochronologists to crossmatch patterns of two ring-widths sequences.

2.2.2.1 Time-series Plots

Two ring-width sequences can be matched visually by systematically shifting the two time-series plots against one another in order to locate areas of similarity in the patterns of the ring-widths (Fritts, 1976). If the pattern identified is consistent in both samples, the two sequences can be assumed to be matched at a correct offset. This method tends to be used initially by the dendrochronologists alongside formal statistical methods. Figure 2.3 shows crossmatching of two trees aligned together.
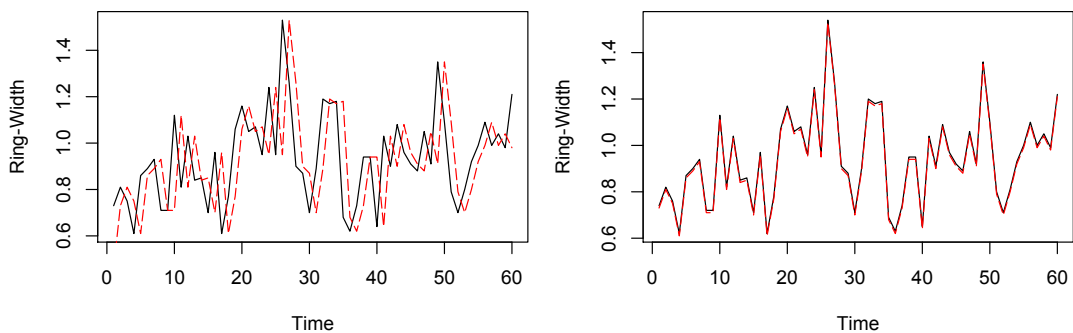
Figure 2.3: Plot of comparing time-series graph of two actual ring-width samples. Sample 1 (*dashed line*) is matched to sample 2 (*solid line*) at wrong offset (*left panel*) and correct offset (*right panel*). The tree-ring widths are measured in millimetres.

The main advantages of this method are: it is very simple to use either by hand or using computers, it can be used without the need for preprocessing data as it uses raw ring-width data, and no expertise is required to understand the results. However, the main disadvantage is that it is an informal way for detecting the similarity between the two sequences, and cannot provide dendrochronologists with quantitative results for dating. Thus, under the use of this method, different researchers might have different decisions for choosing the correct offset. This is because it does not provide a magnitude measure for quantifying the degree of similarity between the two sequences at each possible offset.

2.2.2.2 Skeleton Plots

Skeleton plotting method involves visually inspecting tree-ring width by marking the pattern of narrow and wide ring-widths for each sequence on a graph, and crossmatching each series to one another in order to identify any similar patterns between the two samples (Maxwell *et al.*, 2011), see an example of a skeleton plot for a tree-ring sequence in Figure 2.4.
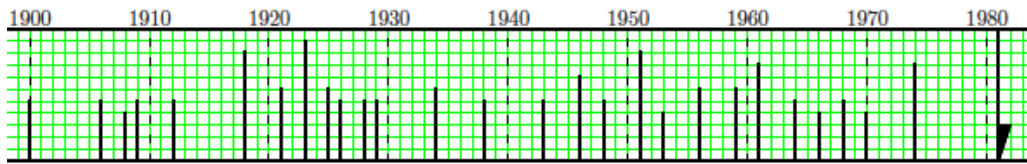
Figure 2.4: An example of a skeleton plot for a tree-ring sequence of 80 years.

The plot has a horizontal scale of years, in which the width of the youngest ring is marked at the left and subsequent rings are recorded to the right of this. Skeleton plots visually show the pattern of wide and narrow rings within a tree-ring sequence. Narrow rings are shown by a vertical line and rings which do not show much variability to adjacent rings in the sequence, known as complacent rings, are omitted. The height of the lines indicates how narrow the ring is. The skeleton plots are systematically shifted against each other in order to locate areas of similar patterns.

The skeleton plot is created for each sample, and these plots are then compared with one another in order to build a master chronology (detailed in Section 2.3) and date individual samples by matching them to a dated chronology. Skeleton plotting is a useful technique but it might be time-consuming, and dendrochronologists might prefer to only use marker rings for each tree sequence to speed the crossmatching process.

2.2.2.3   Trending Method

Trending, or "coefficient of parallel variation" method, is another technique used for crossmatching tree-ring sequences. The raw ring-width is either going up (+) or down (−) from one ring to the next. When two ring-width sequences are aligned, the number of agreement pairs in which the direction of trend is the same for both sequences is counted. The percentage of years with the same trend is computed. For example, a 70% trend indicates that for 70% of the pairs, both sequences went upward in the same years or downward in the same years. When two samples are crossmatched, the percentage score of the trend (tr) with agreeing pairs is defined as:

$$tr = \frac{q_a}{q} \times 100,$$

where q_a is the number of pairs with agreeing trends, and q is the number of overlapped rings between the two samples. The percentage of disagreeing pairs is simply $1 - tr$. The trend score is evaluated at all possible offsets between the two sequences, and the offset with the highest tr value is assumed to be the 'best' offset of the match. Trends greater than 60-70% are assumed to be acceptable for matching.

The benefit of this method is that it does not require any preprocessing of data as it uses raw ring-width data. However, as highlighted by Baillie and Pilcher (1973), this dating method can not take into consideration magnitude of the year-to-year variation, and thus it is a "non-parametric" algorithm. Furthermore, a significant matching is found by this method only when the two sequences have a long overlap with high trend scores. Thus, Baillie and Pilcher (1973) suggested using a parametric method which considers the size of the yearly width variations.

2.2.2.4   Cross-Correlation Coefficient Method

This method was first suggested by Baillie and Pilcher (1973). Let there be two stationary samples of ring-width indices, y_1 and y_2, of length l_1 and l_2 respectively. Let also there be at least q rings in common between the two sequences resulting in

$l_1 + l_2 - 2q + 1$ possible offsets (Δ). Now, let $r(y_1, y_2, \Delta)$ be the Pearson correlation coefficient between the two standardised sequences, y_1 and y_2, at offset Δ. The match with the highest r value is considered as the 'best' match between the two sequences.

The cross-correlation coefficient $r(y_1, y_2, \Delta)$ at offset Δ, with q overlapping rings can be calculated as:

$$r(y_1, y_2, \Delta) = \begin{cases} \frac{\sum_{i=1}^{q}(y_{1i+\Delta}-\bar{y}_1)(y_{2i}-\bar{y}_2)}{\sqrt{\sum_{i=1}^{q}(y_{1i+\Delta}-\bar{y}_1)^2(y_{2i}-\bar{y}_2)^2}}, & \text{if } \Delta \geq 0 \\[3mm] \frac{\sum_{i=1}^{q}(y_{1i}-\bar{y}_1)(y_{2i-\Delta}-\bar{y}_2)}{\sqrt{\sum_{i=1}^{q}(y_{1i}-\bar{y}_1)^2(y_{2i-\Delta}-\bar{y}_2)^2}}, & \text{if } \Delta < 0 \end{cases} \tag{2.1}$$

where y_{1i} and $y_{1i+\Delta}$ are the ith and $(i+\Delta)$th indices from the sequence y_1, and y_{2i} and $y_{2i+\Delta}$ are the ith and $(i+\Delta)$th indices from the sequence y_2, and

$$\bar{y}_1 = \begin{cases} \sum_{i=1}^{q} \frac{y_{1i+\Delta}}{q}; & q = \min(l_{1-\Delta}, l_2), \quad \text{if } \Delta \geq 0 \\[3mm] \sum_{i=1}^{q} \frac{y_{1i-\Delta}}{q}; & q = \min(l_1, l_{2+\Delta}), \quad \text{if } \Delta < 0 \end{cases}$$

$$\bar{y}_2 = \begin{cases} \sum_{i=1}^{q} \frac{y_{2i+\Delta}}{q}; & q = \min(l_{2-\Delta}, l_1), \quad \text{if } \Delta \geq 0 \\[3mm] \sum_{i=1}^{q} \frac{y_{2i-\Delta}}{q}; & q = \min(l_2, l_{1+\Delta}), \quad \text{if } \Delta < 0. \end{cases}$$

This method was investigated by several dendrochronologists including Cook *et al.* (1990); Steward (1983); Wigley *et al.* (1987); Yamaguchi (1986). Unlike the three previous methods of dating tree-rings, this one requires the raw ring-width measurements to be fully preprocessed, since it depends on the fact that the sequences to be matched are stationary (detrended, prewhitened and normalised).

2.2.2.5 t-value Method

As the value of r in the previous method does not take into consideration the length of overlap between the two matched sequences, a Student's t-value is suggested which does take that into account. Baillie and Pilcher (1973) proposed calculating t-values from given r values obtained from cross-correlation coefficients (Section

2.2.2.4). The t-value method is a significant measurement in terms of the overlap length, q. "It provides a measure of the probability of the observed value of r having arisen by chance" (Baillie and Pilcher, 1973, p.11). This method is now routinely used by dendrochronologists to decide how good the match is between the two ring-width sequences when crossmatching.

For the t-value calculation to be a valid measure of significance, it must be assumed that the sequences of tree-ring indices are independent observations that follow a normal distribution with mean zero and constant variance. Baillie and Pilcher (1973) tested this distributional assumption on sample sets of data and found them to follow a normal distribution.

Student's t-value for each possible offset, Δ, between the two sequences, y_1 and y_2, is calculated as follows,

$$t(y_1, y_2, \Delta) = \frac{r\sqrt{q-2}}{\sqrt{(1-r^2)}},$$

where q is the number of overlapping rings between the two sequences, $\Delta = 1, 2, \ldots, l_1 + l_2 - 2q + 1$ is the all possible offsets, r is a correlation coefficient at each possible offset calculated from Equation 2.1. As the value of r increases, the t-value increases, and this indicates that the two samples are matching well at offset Δ.

Baillie and Pilcher (1973) used a threshold t-value of 3.5 to indicate a good acceptable match for tree-ring dating, which gives a 0.1% significance level for overlaps greater than 100 rings. The higher the t-value, the better the match is between the two sequences. Since then this arbitrary threshold value has become a routine practice in dendrochronology. However, it does not suggest that any offset with higher than this threshold t-value is correct, and there might be a cases where the match with a t-value of ≤ 3.5 gives a correct date or a t-values ≥ 3.5 gives an incorrect date (Wigley $et\ al.$, 1987).

When two contemporary ring-width sequences are matched to each other, a t-value is calculated for each offset between the two sequences, and there must be at least one t-value that emerges as higher than the rest. This method of dating tim-

bers has been used by many dendrochronologists, including Baillie (1977, 1995); Bridge (1988); Brown *et al.* (1986); Hillam (1998); Mills (1988); Orton (1983); Pilcher (1990); Pilcher *et al.* (1995); Sander and Levanic (1996); Walker (2005). Throughout this thesis we will use this method as a classical approach to be compared with our developed Bayesian approaches.

Although the t-value measurement is now routinely used by many dendrochronology labs for dating undated trees, it cannot formally include prior information about the unknown date for the undated sequences. Hence we aim, in this thesis, to provide an alternative probabilistic measurement which allows providing a distribution of all possible offsets between crossmatched sequences and also allows formal combination of data and prior information about the unknown date of the undated timbers.

2.2.2.6 Fisher's z-value Method

Having calculated the correlation coefficient $r(y_1, y_2, \Delta)$ for each possible offset between two standardised (stationary) ring-width sequences, dendrochronologists usually transform the obtained r value into either a t-value or z-value, in which the latter is used by Litton and Zainodin (1991); Munro (1984); Okasha (1987) for dating sequences. They used z-value as a similarity measure between the two crossmatched sequences. The higher the z-value, the better the match is between the two sequences. The offset with the highest z-value is considered to be a 'best' match between the two crossmatched sequences. Fisher's z-value is calculated as follows

$$z(y_1, y_2, \Delta) = 0.5 \ \ln\left(\frac{1+r}{1-r}\right),$$

and it is normally distributed with mean $\mu(z_\Delta) = \frac{1}{2}\ln(\frac{1+\rho}{1-\rho})$, and variance $V(z_\Delta) = \frac{1}{q-3}$; where q is the number of overlapping years between the two sequences. It is assumed that the two crossmatched sequences, with q pairs of independent observations from a bivariate normal distribution, has underlying correlation r. If the

two sequences are not contemporary, then $\rho = 0$ and $z \sim N(0, (q-3)^{-1})$ (Buck *et al.*, 1996; Jones, 2013).

Both Okasha (1987) and Steward (1983) recommended the use of Fisher's z-value method as a 'best' measure for crossmatching ring-width indices. However, in his comparison between z-value and t-value statistics, Zainodin (1988) found that the efficiency of both measures are similar and he described them as equally good methods.

Closing remark

Several classical methods have been described in this section which are routinely using by dendrochronologists for crossmatching tree-ring width sequences and dating them. Despite the fact that classical dendrochronology is a successful technique, many tree-ring width sequences remain undated. Jones (2013) highlighted that with the current existing classical methods and approaches, the average success for dating trees in the UK is between 60-70%. This varies from one geographical location to another, for instance the success rate of dating trees in South West England is only approximately 30-40%.

2.2.3 Bayesian Crossmatching

Motivated by the successful use of Bayesian statistical approaches to radiocarbon dating (Buck *et al.*, 1996), the practicality of a similar Bayesian framework to tree-ring dating has been studied by Jones (2013). The data and prior information about the unknown date of the undated trees are combined together to provide a posterior probability of a date match at a particular offset rather than providing classical measures described in Section 2.2.2. Under the Bayesian paradigm, the matching process involves evaluating the likelihood of the model parameters at every possible date offset which allows the posterior distribution of the unknown date to be estimated.

31

In her attempt to develop such a Bayesian approach to crossmatching ring-width sequences, Jones (2013) used a very simple statistical model suggested by Litton and Zainodin (1991), which is described in Section 3.1. This linear model represents the relationship between the tree-ring index and the underlying climate signal which is common to all trees grown within that geographical location.

Jones (2013) highlighted two main advantages of using Bayesian approach to tree-ring dating over the traditional statistical methods. Firstly, instead of identifying the 'best' calendar date estimate for the undated sequences, it allows provision of probabilistic statements about a collection of possible date estimates each with a specific posterior probability. Furthermore, the Bayesian approach allows formal inclusion of prior information, both about the calendar age of undated timbers and about parameters of the underlying statistical model. Thus, the key difference between the Bayesian and classical dating is the use of prior information in cross-matching process. In Bayesian dating, when informative prior knowledge about the undated timbers is available, it should be used in the dating process; otherwise, one can use noninformative priors. The Bayesian approach for tree-ring dating and its implementation by Jones (2013) are detailed in Sections 3.1.3 and 3.1.4 respectively.

2.3 Constructing Chronologies

Having successfully matched single samples with one another (using one of the methods described in Section 2.2), the next step is to build chronologies which is the ultimate target of almost all dendrochronological studies. Once pairwise matching has been successful, groups of samples are said to be matched if and only if, for example, for samples A, B and C, the following three conditions hold:

- A and B match at offset $\Delta(A,B)$,

- B and C match at offset $\Delta(B,C)$,

- thus implies that A and C match at offset $\Delta(A,C)$.

If the dendrochronologist is satisfied (via such pairwise matching) that the groups of samples have a strong enough match to be considered to have ring-widths that have grown in the same year, then a site chronology can be established by averaging the ring-widths that are aligned at the same offset Δ. See Section 2.3.3 for details on how this is done.

A master chronology is an average (arithmetic mean) ring-width sequence for a specific species in a particular region, which is built from matching a group of successively long tree-ring width sequences (Buck and Millard, 2004; Cook *et al.*, 1990). In order to build the master chronology, the absolute date of at least one tree ring should be known. The master chronology forms the reference against which new ring sequences might be matched and dated. It is assumed that the trees of same species at the same geographical locations share the same climatic signal, and one of the main purposes of building master chronologies is to enhance this climatic signal. The master chronology is either "local" or "regional", both are described as follows.

2.3.1 Local Master Chronology

A 'local' or 'site' master chronology is a sequence created from crossmatching a group of trees from a particular location. A site can be defined as a group of timbers from an ancient building, such as a church, or a specific geographical location where several trees have grown, such as a forest. A reliable site chronology can be created from 8–10 trees with the same species (Jones, 2013).

To create a site chronology, tree-ring samples with an overlap of at least 40 rings are crossmatched in pairs (using one of the classical or Bayesian methods given respectively in Sections 2.2.2 and 2.2.3), and the 'best' matches are determined (Laxton and Litton, 1988). Then a site chronology is created by grouping pairwise matching samples and averaging the ring-widths sequences that are aligned at the same offset. A length of the site chronologies varies from 100 to 500 years depending on the length of single trees. For example, a local site chronology of

Sheffield has covered 249 years which is built from 20 individual Quercus trees (using a method described in Section 2.3.3), and it goes back to 1759 AD.

2.3.2 Regional Master Chronology

A "regional" master chronology is a long sequence created from crossmatching a group of site chronologies from a particular region. Regional master chronologies tend to represent a larger geographical area than site chronologies. A region can be defined as a county or country which covers several site chronologies. This regional master chronology serves as a "reference" for crossmatching tree-ring width sequences.

When local chronologies have been established (by the method in Section 2.3.3), the average ring-width produced at an offset Δ represents the climatic signal at that site for that offset. The signal will be enhanced after taking the average ring-width from a group of samples in a site, thus eliminating some of the noise that is present. The local site chronologies can be treated as single ring-width sequences and crossmatched as described in Section 2.2. The local site chronologies may show similarities in ring pattern over wider regional areas, for example single samples from separate woodlands within a close geographical proximity may not crossmatch with confidence, yet the local site chronologies of each woodland may do so.

The regional chronology often covers a larger number of years than a local chronology, and its length varies from 200 years to more than 1000 years. For example, the East Midlands chronology established by Laxton and Litton (1988) covered 1100 years (882–1981 AD) which was built from 59 local master chronologies. In her simulation study to test the Bayesian implementation for tree-ring dating, Jones (2013) generated 50, 100, and 200 year long sequences as local master chronologies, and 200, 500, and 1000 year long sequences as regional master chronologies. Litton and Zainodin (1991) suggest that a regional master chronology should at least include 5 to 10 site chronologies.

Master chronologies can also be created from relatively long lived trees from

the same species, and must be a continuous chronology without any missing ring. Building good and reliable master chronologies is an essential process for successful dating. Without well established master chronologies, many timber samples will remain undated, and the matching process is impossible.

2.3.3 Method of Construction

After successfully obtaining pairwise crossmatching from one of the matching methods described in Section 2.2, and being satisfied that the sequences are cross-matched at the correct offset, master chronologies can be created by combining these pairwise matches. Several methods have been used by dendrochronologists to combine ring-width sequences into a master chronology (Baillie, 1982). The simplest and most widely used way is by averaging a group of standardized ring-widths indices present in a particular year, which requires a large enough number of rings replicated each year (Cook *et al.*, 1990; Fritts, 1976). Let y_{ti} be the ring-width index value for a particular year t from tree i, where $i = 1, \ldots, I$ and I is the number of trees observed in a specific geographical location, then the value of the master chronology at year t is:

$$C_t = \sum_{i=1}^{I} \frac{y_{ti}}{I}$$

where C_t is an estimate of the climatic signal in year t, $t = 1, 2, \ldots, n$, and n is the length of the master chronology C.

Master chronologies can be constructed from either raw ring-widths or preprocessed indices. However, Okasha (1987) recommended that a master chronology is a better estimate of the climatic signal when I trees which are detrended, prewhitened and standardized are used. He stated that when raw ring-widths are used (which are non-stationary and autocorrelated), it can hide changes in the climate between years. Throughout this thesis, this simple averaging (arithmetic mean) method will be used for building chronologies.

2.3.4 Matching Trees to a Dated Master Chronology

When the process of constructing a master chronology is complete, new undated sequences (individual or site chronology) can be matched to the master chronologies in order to date them. This can be done by using the same methods of cross-matching tree-ring patterns of two individual trees (described in Section 2.2). The undated sequence is compared to the dated master chronology at every possible offset Δ, and the match with the highest t-value (classical matching) or the highest posterior probability (Bayesian matching, discussed in Chapter 6) is determined as the 'best' match. The date of the undated sequence can then be obtained for the correct offset from the master chronology.

2.4 Summary of Chapter

This chapter has reviewed the existing statistical methods in both dendrochronology and dendroclimatology. Preprocessing and filtering tree-ring data has been introduced which consists of three main steps: detrending (remove age growth trend), prewhitening (eliminate autocorrelations), and normalising (obtain stationary sequences). This preprocessing usually prepares the tree-ring data prior to dating them. Crossmatching processes, and methods for detecting the similarity between tree-ring width sequences were then reviewed, along with the process of constructing master chronologies and dating undated timbers. The following chapter introduces modelling the relationship between ring-width growth and climate using statistical and mechanistic models.

Chapter 3

Modelling Ring-Width Growth: Statistical & Mechanistic Models

Introduction

One of the most scientific ways to understand the nature of any phenomenon is by creating a model for the process or event. A model is a simplification of reality, and mathematical equations are quantitative models of the corresponding processes. In tree-ring science such models are usually built to understand the nature of the growth of trees and their relationship with the environment in general, and climate in particular. Two types of models, mechanistic (often deterministic) and descriptive (usually statistical), have been developed for such relationships. Existing mechanistic models for tree-ring growth are more complex than the descriptive statistical ones because they encompass many processes and interrelationships, and some of them also have a hierarchical structure. On the other hand, descriptive statistical models are simpler which enables managing and handling uncertainty in the model, but can only evaluate the potential relationship between the data and the corresponding process without studying the mechanism of the phenomenon under study. Thus, both types of models have their own advantages and limitations, and the preference of the model type varies between user communities. The dendrochronology community focuses on using statistical models that

37

are easy to use for cross-matching sequences and dating undated timbers. However, dendroclimatologists have concentrated on using mechanistic forward models for climate-tree-ring relationships in order to invert them and reconstruct climate from trees. Both communities have addressed the behaviour of ring-widths during the growth season.

In this chapter, two well-known statistical and mechanistic models for tree-rings are reviewed in order to be used later in the cross-matching process in the Bayesian framework. A descriptive statistical model by Litton and Zainodin (1991) is given in the next section, and implementing the model for Bayesian dendrochronology by Jones (2013) is also discussed. In the subsequent section, a mechanistic forward model, VS (Vaganov *et al.*, 2006), and its simplified version, VSLite (Tolwinski-Ward *et al.*, 2011), are introduced. Thereafter, statistical methods for evaluating the models and exploring the uncertainty in their outputs are briefly reviewed. These include both standard "sensitivity analysis" (Saltelli *et al.*, 2000) and "Bayesian sensitivity-analysis" (Oakley and O'Hagan, 2004).

3.1   Simple Statistical Model

A simple statistical model for preprocessed tree-ring data was first suggested by Fritts (1976) which represents the relationship between climatic signal and observed ring-width indices. This model assumes that the tree-ring index in year t is equal to the underlying climatic signal which is common to all trees within a particular geographical area plus some noise due to non-climatic effects. The model was then used by Litton and Zainodin (1991) in seeking to find a more formal way of using statistical models for tree-ring dating and cross-matching sequences. The model is defined as follows,

$$y_{ti} = u_t + \epsilon_{ti} \tag{3.1}$$

where y_{ti} is the fully-processed (detrended, prewhitened and normalised) ring-width index at year t for tree i, u_t indicates the underlying climatic signal in year t, and ϵ_{ti} denotes the noise of tree i in year t.

3.1.1 Model Assumptions

Following are the assumptions about the model:

- the width of (raw) tree-rings is influenced by several factors including: the age of the tree (referred to as growth trend), climate variables such as temperature and precipitation (referred to as climatic signal), and other non-climatic factors (referred to as noise).

- the age-related growth trend must be removed from the data by using one of the detrending methods described in Section 2.1.1.

- the climatic signal, u_t, is common to all trees within a particular geographic region which experiences similar climatic conditions, but this signal differs from year-to-year.

- the noise component ϵ_{ti} includes all other non-climatic factors, such as soil condition, site location, presence of pest and disease, and competition among trees for sunlight.

- the signal u_t and the noise ϵ_{ti} are assumed to be independent for mathematical convenience. They both follow independent and identically normally distributed each with mean 0 and variance σ_u^2 and σ_e^2 respectively; $u_t \sim N(0, \sigma_u^2)$ and $\epsilon_{ti} \sim N(0, \sigma_e^2)$.

- the ring-width index y_{ti} follows independent and identically normally distributed with mean 0 and variance $\sigma_u^2 + \sigma_e^2$.

- the signal-to-noise ratio (S), which identifies the strength of similarities among groups of tree-ring samples, is defined as

$$S = \frac{\sigma_u^2}{\sigma_e^2}; \quad \sigma_u^2, \ \sigma_e^2 > 0 \quad \implies \quad S > 0, \tag{3.2}$$

where σ_u^2 and σ_e^2 are respectively the variance of the climatic signal u_t and the variance of the noise ϵ_{ti}. The value of S indicates the nature of the area where the trees come from. The larger the value of S, the more similar the trees are.

3.1.2 Using the Statistical Model for Dating

The model described in Equation (3.1) has successfully been used by Litton and Zainodin (1991) for dating ring-width sequences using classical methods. The following are the three possible ways for matching tree-ring sequences using the descriptive statistical model.

Crossmatching Two Samples

Let two trees i and i' ($i \neq i'$) from the same geographical region be compared for the purpose of dating. The correlation coefficient r between the two matched samples for the same year t can be calculated as follows:

$$r(y_{ti}, y_{ti'}) = \frac{\sigma_u^2}{\sigma_u^2 + \sigma_e^2} = \frac{S}{S+1},$$

and the correlation between these two indices from different years is equal to zero (Litton and Zainodin, 1991). Therefore, the similarity between the two samples can be evaluated via the signal-to-noise ratio, S. As the value of S increases, the correlation r between the two crossmatched ring-width sequences increases and the similarity between them increases too.

The correlation coefficient between any pair of contemporary tree-ring sequences from the same geographic location can be calculated, hence the matrix of pairwise correlations takes the form:

$$
\begin{bmatrix}
1 & r & r & \dots & r \\
r & 1 & r & \dots & r \\
r & r & 1 & \dots & r \\
\vdots & \vdots & \vdots & \ddots & \vdots \\
r & r & r & \dots & 1
\end{bmatrix}
$$

To investigate the model, Litton and Zainodin (1991) used two different datasets from locations that are 55km apart. They found that the correlation coefficients between trees in the same geographical region are greater than the correlation coefficients between trees in different regions.

Crossmatching a Sample to a Chronology

Under the same assumptions of the model in equation 3.1, a single tree-ring sample y_{ti} can be matched to a well replicated average sequence $\bar{y}_{t.}$ at the same year t, and the correlation between the two sequences would be:

$$r(y_{ti}, \bar{y}_{t.}) = \frac{\sigma_u^2}{\sqrt{(\sigma_u^2 + \frac{\sigma_e^2}{I})(\sigma_u^2 + \sigma_e^2)}} = \frac{S}{\sqrt{(S + I^{-1})(S + 1)}},$$

where $\bar{y}_{t.}$ is the average sequence created from I samples of ring-width indices from the same region, with $E(\bar{y}_{t.}) = 0$ and $Var(\bar{y}_{t.}) = (\sigma_u^2 + \frac{\sigma_e^2}{I})$.

Zainodin (1988) concluded that the correlation between a sample and an average sequence at the same geographical region is always greater than that between the two individual sequences; $r(y_{ti}, \bar{y}_{t.}) > r(y_{ti}, y_{ti'})$.

Crossmatching Two Chronologies

Similarly, the statistical model can also be used for crossmatching two averaged sequences. Let $\bar{y}_{t.}$ and $\bar{y}_{t.'}$ be two chronologies created from I_1 and I_2 trees respectively, with zero means and variances, $Var(\bar{y}_{t.}) = \sigma_u^2 + \frac{\sigma_e^2}{I_1}$ and $Var(\bar{y}_{t.'}) = \sigma_u^2 + \frac{\sigma_e^2}{I_2}$, respectively. The correlation coefficient between the two crossmatched chronologies is:

$$r(\bar{y}_{t.}, \bar{y}_{t.'}) = \frac{\sigma_u^2}{\sqrt{(\sigma_u^2 + \frac{\sigma_e^2}{I_1})(\sigma_u^2 + \frac{\sigma_e^2}{I_2})}} = \frac{S}{\sqrt{(S + \frac{1}{I_1})(S + \frac{1}{I_2})}}.$$

Zainodin (1988) also noted that a higher correlation coefficient is obtained between the two averaged chronologies than between an average and a sample or two individual samples; i.e.

$$r(\bar{y}_{t.}, \bar{y}_{t.'}) > r(y_{ti}, \bar{y}_{t.}) > r(y_{ti}, y_{ti'}),$$

thus, grouping trees from the same climatic region is preferable for tree-ring dating when using the statistical model.

3.1.3 A Bayesian Approach to the Statistical Model

A Bayesian approach to statistical tree-ring dating was first investigated by Buck *et al.* (1996). Ring-width data and prior information about the unknown dates were combined in the Bayesian framework when matching a group of undated trees (site chronology) to a larger and longer group of dated trees (master chronology) from the same region. The Bayesian approach to tree-ring dating can be summarised as follows.

Let the dated master chronology be of length l, and let the undated site sequence be of length l^* and consist of I trees. Then the sample correlation coefficient r_Δ is calculated at each possible offset Δ when the site chronology is crossmatched to the master chronology:

$$r_\Delta = \sqrt{\frac{S}{S + S' + I^{-1}}},$$

where $\Delta = 1, 2, \ldots, (l - l^* + 1)$ is the number of all possible date offsets between the two sequences, S is a regional and S' is a subregional signal-to-noise ratio, in which the latter indicates that trees from different sides of a region respond slightly differently to the climate. These correlation coefficients r_Δ are then transformed into Fisher's z_Δ-values (as described in Section 2.2.2.6) with mean $\mu(z_\Delta) = \frac{1}{2} \ln(\frac{1+r}{1-r})$, and variance $V(z_\Delta) = \frac{1}{l^* - 3}$.

Now let Δ^* be the true unknown date of the first ring-width index for the undated sequence, and let $\mathbf{y}$ represent both the data of the master chronology and the averaged site chronology, the likelihood is then defined as

$$p(\Delta^* = \Delta, \mathbf{y}) = \exp\left\{\frac{-1}{2V(z_\Delta)}(z_\Delta - \mu(z_\Delta))^2\right\}.$$

Assuming no informative prior knowledge about the true date, the prior probability that Δ^* takes the true offset position Δ is defined as:

$$p(\Delta^* = \Delta) = \frac{1}{l - l^* + 1},$$

so that each date within the interval of all possible dates $(l - l^* + 1)$ between the two sequences is equally likely.

Therefore, using Bayes' theorem we usually combine the likelihood, $p(\mathbf{y}|\Delta^* = \Delta)$, and the prior, $p(\Delta^* = \Delta)$, to obtain the posterior distribution as follows

$$p(\Delta^* = \Delta|\mathbf{y}) = p(\mathbf{y}|\Delta^* = \Delta) \, p(\Delta^* = \Delta).$$

Since the prior distribution is noninformative (and in this case is constant), the posterior distribution for the unknown start date stays normal as follows

$$p(\Delta^* = \Delta|\mathbf{y}) = \exp\left\{\frac{-1}{2V(z_\Delta)}(z_\Delta - \mu(z_\Delta))^2\right\}.$$

As the posterior distribution is continuous and the estimated dates should be discrete, the posterior estimates are discretized to years in the possible interval. For further information about this Bayesian approach, the reader is referred to Buck *et al.* (1996, p. 342–348).

Most recently, this approach has been implemented by Jones (2013) with a view to making it routine practice in dendrochronology. She used simulated data and trees of known age to evaluate the efficiency of the Bayesian implementation of the model using both informative and non-informative priors for the unknown dates.

3.1.4 Bayesian Implementation by Jones (2013)

Jones (2013) added a new parameter β to the statistical model in Equation 3.1 and then implemented it in the Bayesian framework to match the undated site chronologies to the dated master chronologies. The β parameter represents the population mean of the standardised ring-width indices which is assumed to have zero mean to ensure the stationarity of the model. The new model becomes

$$y_{ti} = \beta + u_t + \epsilon_{ti}, \tag{3.3}$$

where β is the mean of the ring-width indices and it is expected to be close to zero, and all other components are the same as those for the original model in Equation 3.1.

The Bayesian implementation involves simultaneously fitting the model and sequentially matching the undated site chronology to the dated master chronology

with a view to identifying the offset with the highest probability of a match and thus the most likely date for the undated chronology. Following is a brief summary of Jones' Bayesian implementation of tree-ring dating.

3.1.4.1   Model Notation

Jones (2013) defined the notation of her model implementation as follows. Let the dated master chronology be of length l years, and comprise I trees. Let the start and end dates of the dated master chronology be Δ_s and Δ_e, respectively, so that $l = \Delta_e - \Delta_s + 1$. For tree i, $i = 1, 2, \ldots, I$, let δ_i be the start date of the tree i, l_i be its age (length of the sequence) in years, and $\delta_i + l_i - 1$ be its felling date. Similarly, let the undated site chronology be of length l^* years, and have I^* trees. Let Δ^* be the unknown start date of the undated site chronology. For tree i, $i = n+1, \ldots, I + I^*$, let $\delta_i = \Delta^* + h_i$ be its unknown start date (where $h_i \geq 0$, is the offset of tree i relative to Δ^*), l_i^* be the length of the tree, and $\delta_i + l_i^* - 1$ be the end date of the tree.

Now, the dating process starts by consecutively matching the undated site chronology to the dated master chronology at all possible offsets from $t = \Delta_s - l^* + q$ to $t = \Delta_e + l^* - q$, where q is the minimum overlap of rings between the dated and undated sequences. Therefore, the total number of all possible offsets between the two sequences is equal to $l + l^* - 2q + 1$.

3.1.4.2   The Likelihood

The tree-ring width indices follow a normal distribution with mean $\beta + u_t$ and variance σ_e^2. Let $\mathbf{y}^D = (y_1, \ldots, y_I)$ and $\mathbf{y}^{UD} = (y_{I+1}, \ldots, y_{I+I^*})$ represent the indices for all dated and undated trees, respectively, so that the indices for all trees together are $\mathbf{y} = (\mathbf{y}^D, \mathbf{y}^{UD}) = (y_1, \ldots, y_n, y_{I+1}, \ldots, y_{I+I^*})$. The likelihood of the dated and undated master chronologies can be given respectively as,

$$p(\mathbf{y}^D | \beta, \mathbf{u}, \sigma_u^2, \sigma_e^2) \propto \prod_{i=1}^{n} \left[\prod_{t=\delta_i}^{\delta_i + l_i - 1} (\frac{1}{\sigma_e^2})^{\frac{1}{2}} \exp(-\frac{1}{2\sigma_e^2}(y_{ti} - \beta - u_t)^2) \right]$$

$$p(\mathbf{y}^{UD}|\beta, \mathbf{u}, \sigma_u^2, \sigma_e^2, \Delta^*) \propto \prod_{i=n+1}^{n+n^*} \left[\prod_{t=\Delta^*+r_i}^{\Delta^*+r_i+l_i-1} (\frac{1}{\sigma_e^2})^{\frac{1}{2}} \exp(-\frac{1}{2\sigma_e^2}(y_{ti} - \beta - u_t)^2) \right],$$

and the likelihood of all data can be obtained by combining both the likelihood of the undated site and dated master chronologies as follows

$$p(\mathbf{y}|\beta, \mathbf{u}, \sigma_u^2, \sigma_e^2, \Delta^*) \propto p(\mathbf{y}^D|\beta, \mathbf{u}, \sigma_u^2, \sigma_e^2) \; p(\mathbf{y}^{UD}|\beta, \mathbf{u}, \sigma_u^2, \sigma_e^2, \Delta^*).$$

3.1.4.3   The Priors

In order to make inference about the unknown parameters $(\beta, \sigma_u^2, \sigma_e^2, \Delta^*)$, Jones (2013) defined prior distributions for each parameters; $p(\beta)$, $p(\sigma_u^2)$, $p(\sigma_e^2)$, and $p(\Delta^*)$. The choice of a suitable prior distribution for each of these parameters is discussed in Chapters 5 and 6.

3.1.4.4   The Posterior

Using Bayes' theorem, which allows us to combine the likelihood of data and the prior information about the unknown parameters, the joint posterior distribution of the model parameters is given by

$$p(\beta, \mathbf{u}, \sigma_u^2, \sigma_e^2, \Delta^*|\mathbf{y}) \propto p(\mathbf{y}|\beta, \mathbf{u}, \sigma_u^2, \sigma_e^2, \Delta^*) \; p(\beta) \; p(\sigma_u^2) \; p(\sigma_e^2) \; p(\Delta^*).$$

Jones (2013) applied Markov chain Monte Carlo methods under the Bayesian paradigm to estimate the unknown model parameters. Throughout this thesis we will be using the term "Jones' approach" to indicate to this Bayesian implementation of the statistical model for tree-ring dating.

3.1.5   Pros and Cons of the Statistical Model

The descriptive statistical model by Litton and Zainodin (1991) assumes that tree-ring width is a combination of a climatic signal which is common to all trees grown in a specific area plus some noise which accounts for the non-climatic factors. This simple model is easy to use since it assumes a linear relationship between ring-width indices and climatic signal. However, this model has the following limitations:

- it does not capture the mechanism of the growth process during the growing season and formation of tree-ring widths.

- it is not able to simulate dated ring-width indices (trees with known age) for a specific geographical location.

- it requires the ring-width data to be fully processed (detrended, prewhitened and normalised) in order to obtain stationary sequences prior to any representation of the data in the model.

- as with all other classical methods of dating, the Bayesian approach by Jones (2013), which uses this descriptive model, still requires the data to be fully preprocessed prior to the matching process.

These four limitations will be addressed in the remainder of this thesis by investigating the use of mechanistic forward models (described below) which provide an alternative and more realistic way to model the growth process and tree-ring formation. Such forward models aim to capture the mechanisms of main characteristics of the complex system of growth which directly relates climate to the tree-ring width. Under the mechanistic models, the environmental variables, such as temperature, rainfall and sunlight link to the biological processes occurring within raw ring-widths during the growing season. By directly modelling the way in which raw ring-widths arise, the need for fully preprocessing data will be removed.

An extension to the Jones' approach to Bayesian tree-ring dating is investigated in Chapter 6. The extension includes replacing the descriptive statistical model by a more realistic, mechanistic forward model (known as VSLite and described in Section 3.2.2) to be used at the core of the dating process. The use of both statistical and mechanistic models in the Bayesian tree-ring dating are studied, and the comparisons between them are also described in that chapter. In Chapter 7 a new Bayesian approach is investigated which allows less preprocessing of data prior to the matching process. This will be implemented via adding an extra parameter to the model to account for a rescaling between the two sequences before dating.

3.2 Mechanistic Forward Models

Most of the previous approaches to dendrochronology depend on extending simple linear statistical models which relate tree-ring width indices to a univariate climatic signal. These models require the raw ring-width data to be preprocessed (detrending: removing the trend of age-related growth, and prewhitening: removing the autocorrelation from tree-ring width indices) (Fritts, 1976; Jones, 2013; Litton and Zainodin, 1991). Such models provide crucial understanding of the climate-tree-ring relationship, yet are restricted by several methodological presumptions, such as linearity and stationarity (Tolwinski-Ward *et al.*, 2011). To investigate the possibility of using non-stationary and non-linear models for ring-width growth, members of the dendroclimatology research community, including Evans *et al.* (2006); Guiot *et al.* (2014); Tolwinski-Ward *et al.* (2011); Vaganov *et al.* (2006); Zhang *et al.* (2011), have recently examined the use of mechanistic models which study the physical and biological processes by which the tree-ring widths are formed. Such mechanistic models usually link climate variables to the growth of the ring-widths through a physical process, and remove the need for the data to be fully processed, hence providing potential for dendrochronologists to deal directly with less processed data. This section describes a mechanistic process-based model, called "VS" and its simplified version "VSLite".

3.2.1 VS Model

The Vaganov-Shaskin model, known as "VS", is a simple mechanistic model introduced by Vaganov *et al.* (2006) which aims to capture the main response of tree-ring growth to the climate. The VS is one of the most recent, popular and widespread process-based models which enables simulating seasonal growth and tree-ring formation, by modelling the effects of daily meteorological data (temperature, soil moisture and sunlight) on ring-width growth. The VS model depends on the following assumptions (Vaganov *et al.*, 2006).

1. It is a deterministic model which studies the complex system of the biological

structure of ring-width growth.

2. Ring-width growth is mainly determined by external climate variables such as temperature, soil moisture and sunlight.

3. The principle of limiting factors, growth is limited by the most critical factor in demand (Fritts, 1976), is used for restricting the main factors of growth rate.

4. The VS model runs on daily time-step which requires as inputs daily meteorological data (temperature and precipitation) which enables simulating tree-ring sequences at any geographical area around the world where such data exist.

Despite some limitations (described in Section 3.3.1.3), the VS model remains one of the most accepted physiological models which used for modelling coniferous trees in a variety of regions and under different climatic conditions.

3.2.1.1   Model Description

Under the VS model, the daily growth response of tree-ring width, $G(t)$, is determined by three partial growth functions as follows:

$$G(t) = G_E(t) \times min\{G_T(t), G_M(t)\} \tag{3.4}$$

where $t = 1, 2, \ldots, 365$ days in a calendar year, $G_E(t), G_T(t)$, and $G_M(t)$ are respectively the partial growth response to daily solar radiation, daily temperature and daily soil moisture. These three partial functions are independent, and the calculation of each of them is briefly described below.

Partial Growth Response to Sunlight $G_E(t)$

The growth of a tree is affected by the supply of sunlight (solar irradiation) during the vegetation period. If a tree receives poor light, the photosynthesis will be

decreased and thereby cambial activity, so that narrow ring-widths will be formed (Schweingruber, 1988). Consequently, solar radiation indirectly affects the growth rate and tree-ring formation through the photosynthetic tissues. The partial growth response to sunlight $G_E(t)$ is a function of site latitude, solar angle, and hour angles (day-length) (Touchan *et al.*, 2012), and it can be calculated as follows:

$$G_E(t) = E/E_0 \tag{3.5}$$

and

$$E = \left\{ \cos(h_s)\sin\phi\sin(d) + \cos\phi\cos(d)\sin(h_s) \right\}$$

where:

- E is incoming irradiation.
- E_0 is direct solar irradiation for the earth, which is constant and approximately equal to 1360 $W\,m^{-2}$ (Touchan *et al.*, 2012).
- ϕ is geographic latitude (in radians).
- d is declination angle for the geographic latitude, and h_s is hour angle for the geographic latitude. For more information about the importance of these two parameters in the model, the reader is referred to Vaganov *et al.* (2006).

Partial Growth Response to Temperature $G_T(t)$

Tree-ring width is directly influenced by temperature during the growing season. Fritts (1976) showed that high temperature usually leads to reduced net photosynthesis which thereby leads to less production of food and therefore narrow rings are formed. By the same token, cool temperature during the growing season leads to decreased physiological activities of the tree and shortening the growing season, therefore it results in reduced rates of cell division, thereby fewer xylem cells are produced and narrow rings are formed. The partial growth rate to temperature is represented by a piece-wise linear function (see Figure 3.1).
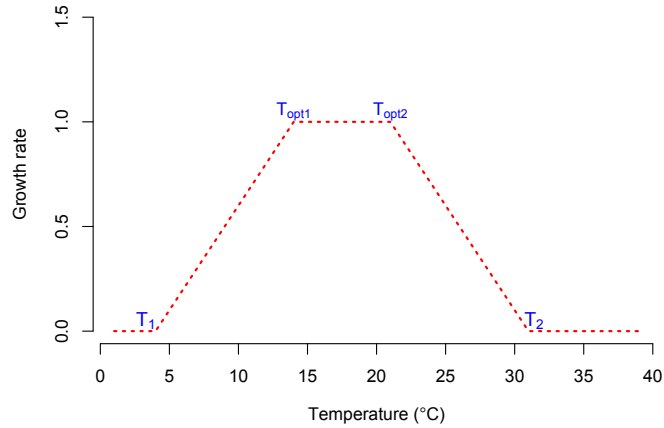
Figure 3.1: An illustrative graph of piece-wise ramp function of partial growth response to temperature G_T.

Seasonal tree growth begins at the minimum temperature for growth T_1 and it increases linearly from T_1 to the first optimum growth (T_{opt1}) then the growth curve remains steady and optimal growth rate is maintained from T_{opt1} to T_{opt2}, before the growth starts to decline linearly between T_{opt2} and T_2. It is assumed in the model that there is no growth when the temperature is less than T_1 or greater than T_2 (i.e. growth does not occur outside the range $T_1 \leq T \leq T_2$).

Partial Growth Response to Soil-Moisture $G_M(t)$

The availability of water in the soil is the most influential factor affecting the growth rate of ring-width and formation of wood. Without sufficient water, most trees do not grow well. Similar to the $G_T(t)$, growth response to soil moisture $G_M(t)$ is defined as a piece-wise linear function, see Fig. 3.2. G_M is the most complex component of the overall growth response function $G(t)$ in the VS model (Equation 3.4).

The daily soil moisture contents M_t are not available, but can be calculated given daily climate variables using a 'Leaky Bucket' water balance model (Haung *et al.*, 1996; Vaganov *et al.*, 2006), as follows.
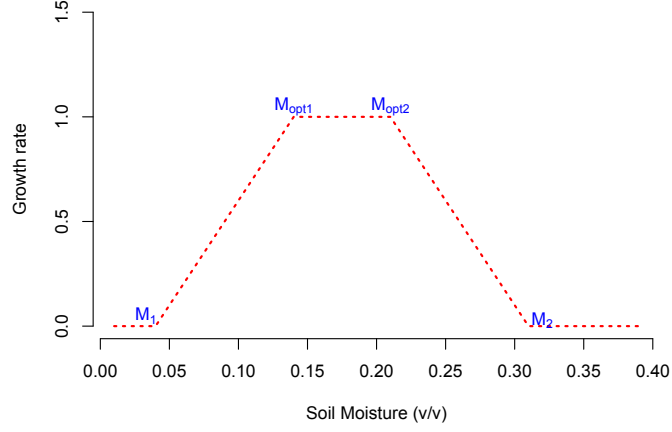
$$\frac{dM_t}{dt} = P_t - E_t - R_t - Q_t \tag{3.6}$$

Figure 3.2: An illustrative graph of piece-wise ramp function of partial growth curve to soil-moisture G_M.

where P_t is a mean precipitation, E_t is a mean evapotranspiration, R_t is a net streamflow divergence, and Q_t is a net groundwater loss at time t. These four components are defined as follows.

- The streamflow divergence (R_t) is a sum of a surface runoff (F_t) and a sub-surface base flow runoff (O_t),

$$
\begin{aligned}
R_t &= F_t + O_t \\
&= P_t \Big[\frac{M_{t-1}}{M_x}\Big]^{\alpha_c} + \frac{\alpha_a}{1+\alpha_b} M_{t-1},
\end{aligned}
$$

  where M_x is a maximum capacity of soils to hold water, M_{t-1} is the previous day's soil moisture content, α_a, α_b and α_c are the model parameters to be estimated, and their estimated values by Haung *et al.* (1996) are given in Table 3.1.

- The net ground water loss, Q_t, is calculated as

$$
Q_t = \frac{\alpha_a \alpha_b}{1+\alpha_b} M_{t-1}.
$$

- The evapotranspiration, E_t, is calculated as

$$
E_t = \frac{M_{t-1}}{M_{max}} E_p,
$$

51

where E_p is the evapotranspiration rate per month and calculated given mean monthly temperature, sunlight, and number of days in the month. The reader is referred to Haung *et al.* (1996, p. 1352) for more details about the calculation of E_p.

- The daily precipitation function P_t is defined as:

$$P_t = \min(a_1 P, P_x) = \begin{cases} a_1 P & \text{if } a_1 P < P_x \\ P_x & \text{if } a_1 P \geq P_x \end{cases}$$

where $(a_1 P)$ is a total daily precipitation, P_x is the maximum daily precipitation for saturated soil, and a_1 is the part of precipitation which captured by the crown of trees, which depends on the geographical area, slope, climate and soil type (Vaganov *et al.*, 2006).

3.2.1.2 VS Model Parameterisation

VS model is multi-parametric, and the main parameters used in the VS model can be seen in (Vaganov *et al.*, 2006, Chapter 7). Most of the parameters in the model have a biological meaning; however, the large number of the parameters (40) is a challenging issue, since it affects the simplicity and efficiency of its implementation. Additionally, making inferences about these parameters requires a considerable effort. Thus, Vaganov *et al.* (2006) used two methods for evaluating the model parameters. The first one assumes that if there is enough experimental information about tree species, growth threshold parameters, climate conditions and region, then the VS model parameters can be defined prior to making any calculation. If no information is available, then the second approach is to approximate starting values for the model parameters, as a first-step calculation, and then slightly change one parameter at time and observe the agreement between generated and observed ring-width chronologies. If the correlation between the two chronologies shows sufficient agreement, then the model with those particular parameters will be considered a good fit.

3.2.1.3   Advantages and Limitation of the VS model

The main strength point of VS model is the potential of applying it to different tree species, such as Quercus and Pinus, although it was first designed and applied particularly for conifer trees. Moreover, the investigation of this model by several researchers including Anchukaitis *et al.* (2006); Evans *et al.* (2006); Shi *et al.* (2008); Touchan *et al.* (2012); Vaganov *et al.* (2006) show the efficiency of the model. They implemented the model for different species in various regimes, and showed that the model works well under a range of environmental conditions, such as dry, wet, arid, semi-arid and monsoon climates.

Vaganov *et al.* (2006) suggested that their simulation model can be used as a complement to the empirical-statistical models of dendrochronology and dendroclimatology in order to assess more accurately the climate-tree growth relationship. This is because the growth rate of trees to climate is usually non-linear (Fritts, 1976), and it might differ in different climate regimes, leading to insufficiency of using classical statistical methods that only assume linear growth response to climate. Therefore, evaluation of such models is necessary to evaluate the statistical modelling of past climate, and make them reliable and more adequate. Furthermore, linear empirical-statistical analyses alone cannot reveal a biological mechanism for variability of tree-ring width growth (Shi *et al.*, 2008; Touchan *et al.*, 2012). Hence, underlying physiological processes which relate tree-rings growth to climate are essential, particularly for palaeoclimatological investigations, both in order to reconstruct accurately the past climate and also to help better interpret the process of growth. The VS model can also be used for dendrochronological studies (Vaganov *et al.*, 2006) by considerably reducing the number of model parameters to become simpler and hence to be used in the matching process for dating sequences. This will give a new opportunity for dendrochronologists to reveal the influence of climate variables to dendrochronological data via studying the mechanism of ring-width growth and also to reveal the effect of non-climatic factors which they usually represent only as noise.

However, there are some limitations of the VS model. Firstly, implementation

relies on access to daily meteorological data of temperature, precipitation, soil moisture and sunlight from local weather stations. These types of data are not available for places where the meteorological stations are absent, and even where they are found, they are limited to a short period of time, typically not more than 200 years. Thus, applications of this model to archaeological dating and chronological studies are rather limited. Secondly, all the processes and parameters are usually fixed. Thus, uncertainty of the parameters and of the model itself are ignored. However, when modelling any physical or biological process it is important to evaluate the models and study their uncertainties before using them. It is desirable, for example, to make a statistical inference about the unknown parameters, which will be helpful to understand the accuracy of the model itself. Under the current version of the VS, this would not be easy to achieve or maybe impossible due to the large numbers of the model parameters.

3.2.1.4 VS Model Applications

In order to investigate whether tree-ring width sequences can be modelled as a function of climatic variables, Anchukaitis *et al.* (2006) utilised the deterministic VS to model the seasonal growth and tree-ring formation of Pinus trees in the USA. Ring-width chronologies were simulated in their investigation using daily climate records from south-east USA for the period (AD 1920-2000). Then a comparison was made between modelled and observed sequences to explore the efficacy of the model. They implied that the model is reliable for simulating tree-ring chronologies, which also used to assess and explicate the climate-tree-ring growth relationships.

Evans *et al.* (2006) also used the VS model to investigate and interpret tree-ring data in different climates. Daily station records data were used to generate tree-ring chronologies in two large areas of north USA and Russia. Then, simple statistical measurements, such as mean and correlations were applied to make a comparison between modelled and observed sequences. The study concluded that

the model was relatively insensitive to the model parameters, and the VS model was able to simulate accurately intra-seasonal to inter-decadal climate variability for relatively large regional areas.

In order to investigate the growth response of trees in (semi-arid north central China) to climate variations, Shi *et al.* (2008) applied the VS model and successfully simulated local tree-ring width chronologies from daily meteorological records. They concluded that the VS model was able to simulate ring-width sequences, evaluate the climate-tree growth relationship, and produce physically interpretable results. Their results emphasized that moisture availability directly affects the tree-ring formation only during May to August. Their study also suggested that ring-width is sensitive to the end of the growth season, and not very sensitive to beginning (Shi *et al.*, 2008). Hence, late end of the growth season results in forming wide rings, whereas narrow rings are produced in years with an earlier end of growth season.

3.2.2   VSLite Model

VSLite, developed by Tolwinski-Ward *et al.* (2011), is a significantly simpler version of the VS model of tree-ring growth, which requires site latitude, monthly temperature and precipitation data as inputs (see Figure 3.3). The motivation behind providing VSLite was to develop the efficiency and simplicity of the full VS simulation model, in order (eventually) to be able to estimate the model parameters, with a view to providing information about the uncertainty in parameters and hence in the model itself.

The VSLite model differs from the full VS in the following aspects:

- VSLite uses monthly, rather than daily, average climate data as inputs, since the monthly meteorological records are more widely available than daily data.

- VSLite has fewer (11) parameters than the VS (40). This is not just because
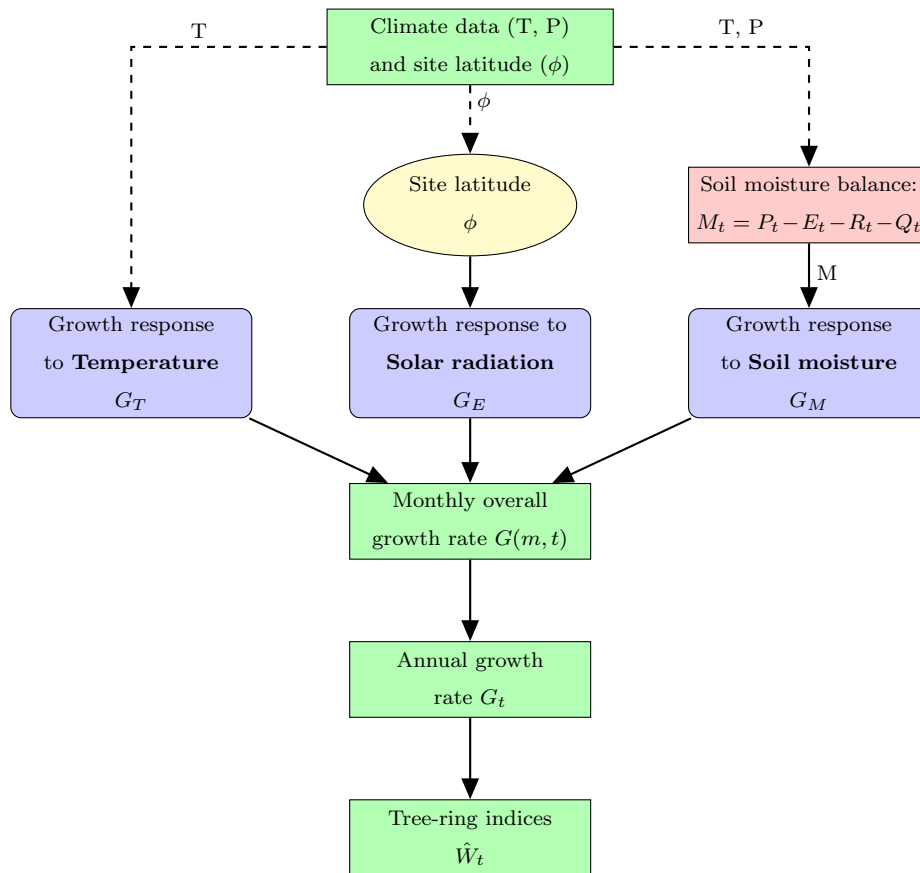
Figure 3.3: Schematic representation of the VSLite model which shows the relationship between climate variables and simulated ring-width indices.

only key parameters of the growth rate process are present, but also because modelling of cell growth in the cambial zone (a cell generator that is between the wood and inner bark), which is significant component of the full VS model, is entirely absent in VSLite.

- This reduction in input data and decrease in the number of model parameters results in an enhancement of computer run-time. VSLite is approximately 30 times faster than the full VS model (Tolwinski-Ward *et al.*, 2011).

- VSLite model links the climate variables directly to tree-ring width growth.

3.2.2.1 VSLite Model Components

For each modelled month (m) in each modelled year (t) in the VSLite model, a monthly growth response to temperature $G_T(m, t)$ is evaluated by:

$$G_T(m,t) = \begin{cases} 0 & \text{if } T(m,t) \leq T_1; \\ \frac{T(m,t)-T_1}{(T_2-T_1)} & \text{if } T_1 \leq T(m,t) \leq T_2; \\ 1 & \text{if } T_2 \leq T(m,t) \end{cases} \tag{3.7}$$

where $T(m, t)$ is the monthly average temperature for month m and year t, T_1 is a temperature threshold parameter below which the growth of ring-width cannot occur, and T_2 is a threshold above which the growth process is insensitive to the climate variability.

The monthly soil moisture contents $M(m, t)$ can be calculated given monthly temperature and precipitation, using the "Leaky Bucket" water balance model, detailed in Section 3.2.1.1. Then, similar to the calculation of $G_T(m, t)$, a monthly growth response to soil moisture $G_M(m, t)$ is calculated as:

$$G_M(m,t) = \begin{cases} 0 & \text{if } M(m,t) \leq M_1; \\ \frac{M(m,t)-M_1}{(M_2-M_1)} & \text{if } M_1 \leq M(m,t) \leq M_2; \\ 1 & \text{if } M_2 \leq M(m,t) \end{cases} \tag{3.8}$$

where $M(m, t)$ is the monthly average soil moisture for month m and year t, M_1 is a soil moisture threshold parameter below which growth process is not occurring, and M_2 is a threshold parameter which the growth is insensitive to soil moisture variability.

Therefore, the overall monthly growth response of tree-ring widths to climate is:

$$G_{(m,t)} = G_E(m,t) \times \min\left\{G_T(m,t), G_M(m,t)\right\} \tag{3.9}$$

where $G_E(m, t)$ is a monthly growth response to solar irradiation derived from trigonometric functions of a geographic latitude ϕ as detailed in Section 3.2.1.1.

3.2.2.2 Tree-ring Formation

A time-series of annual tree-ring width growth is produced by summing the overall monthly growth responses $G(m, t)$ over the 12 months,

$$G_t = \sum_{m=1}^{12} G_{(m,t)}, \tag{3.10}$$

and the simulated ring-width index $\hat{W}_t$ at year t is obtained by standardising the annual growth response, and is given by:

$$\hat{W}_t = \frac{G_t - \bar{G}}{\sqrt{\sigma_G^2}}, \tag{3.11}$$

where $\bar{G}$ and σ_G^2 are the mean and standard deviation of the annual growth sequence respectively. Thus, $\hat{W} \sim N(0, 1)$ is the sequence of annual ring-width indices simulated from the VSLite model.

3.2.2.3 VSLite Model Parameterisation

The VSLite model has 11 parameters, listed in Table 3.1. The first four parameters T_1, T_2, M_1, and M_2, are the growth threshold parameters which control the simulated non-linear temperature $G_T(m, t)$ and soil moisture $G_M(m, t)$ growth curves. Tolwinski-Ward *et al.* (2011) assumed that the value of T_1 should be larger than zero (freezing) and less than or equal to 9^oC, whereas the value of T_2 should be greater than T_1 and less than or equal to 24^oC. Similarly, wide reasonable intervals have been given to the two soil moisture growth threshold parameters (M_1 and M_2) (Tolwinski-Ward *et al.*, 2011), and their optimal intervals are given in Table 3.1.

The last seven parameters in the Table are related to the calculation of the soil-moisture contents using Leaky Bucket water balance model (Haung *et al.*, 1996). Given temperature and precipitation data, and globally fixed water balance parameters, the monthly soil moisture contents can be obtained via the Leaky Bucket hydrology model. These seven parameters are assumed to be constant in space and time, because they are indirectly affecting the growth of ring-width. These parameters were estimated by Haung *et al.* (1996), and their values are given in Table

Parameter	Description	Value
T_1	Threshold temperature for $g_T > 0$	[0°C, 9°C]
T_2	Threshold temperature for $g_T = 1$	[10°C, 24°C]
M_1	Threshold soil moisture for $g_M > 0$	[0, 0.1] v/v
M_2	Threshold soil moisture for $g_M = 1$	[0.1, 0.5] v/v
M_x	Maximum moisture held by soil	0.76 v/v
M_m	Minimum moisture held by soil	0.01 v/v
α_a	Runoff parameter 1	0.093 month^{-1}
α_b	Runoff parameter 2	5.8
α_c	Runoff parameter 3	4.886
d_r	Depth of root system	1000 mm
M_0	Initial value for previous month's moisture	0.20 v/v

Table 3.1: VSLite model parameters as defined by Tolwinski-Ward *et al.* (2011).

3.1. These parameters were measured in millimetres, but Tolwinski-Ward *et al.* (2011) transformed them to volumetric measures via dividing them by a rooting depth (d_r) parameter. The value of d_r is taken from the full VS model. M_0 which is the initial value for the previous month's soil moisture content indicates that the model has lags, and therefore it cannot be simulated for a single month, but rather for a whole sequence.

3.2.2.4 VSLite Model Applications

The VSLite model was applied by Tolwinski-Ward *et al.* (2011) to simulate 277 local Pinus chronologies in North America, and by Breitenmoser *et al.* (2014) to simulate 2271 different tree-species sequences in around the world. To examine the efficiency and efficacy of the VSLite to simulate tree-ring width series, a comparison was made between simulations derived from the model and the real observed ring-width chronologies. Tolwinski-Ward *et al.* (2011) used simple statistical methods such as correlation coefficients and graphical comparisons to assess the adequacy of

their model. They showed that simulations by the VSLite has skilfully represented climate-driven variability of real ring-width sequences. Thus, they conclude that VSLite is able to produce more realistic and physically interpretable results than the statistical models.

In addition to using simple statistical methods utilised by the model developers, we will use more formal techniques and a more systematic analytical method for checking the model adequacy and exploring the uncertainty in model outputs. This method is detailed in the next Chapter.

Closing Remark

In this section two well-known mechanistic models for simulating tree-ring width growth, VS and VSLite, have been reviewed. Since the main target of this thesis is to investigate the potential of using the VSLite model for Bayesian dendrochronology, we will evaluate the model and investigate the uncertainty of its outputs before progressing to implementation of the model for dating purposes. This is in order to evaluate the model and ensure that its uncertainty is controllable. In the next sections, we review two statistical approaches which have been developed for exploring and managing uncertainty in computer models.

3.3 Sensitivity Analysis

Before applying a computer model, such as the VSLite model, to practical problem solving, the adequacy of the model should be evaluated in order to investigate its capability to reproduce the mechanism of the process under study. Different statistical methods and approaches are developed to examine the efficiency of such models. Sensitivity Analysis (SA) is one of these methods used to determine the most influential parameters of the model by examining the impact of changing input parameters, and observing their effect on the model output. SA offers a systematic investigation of a model's response to perturbations of input parameters. It is a very

useful way to understand the model's response behaviour, examine the accuracy of the model, identify the most influential input parameters and rank them in terms of their impact on the output. In addition to this, SA helps model developers to identify which input parameters are not influential and can be ignored in order to simplify the model, and to make decisions about where the model needs to be improved in order to reduce its variability.

Probabilistic sensitivity analysis approaches are categorized as either local or global (Saltelli *et al.*, 2000). A Local Sensitivity Analysis (LSA) is performed when input parameters are varied one-at-a-time around some fixed point with a view to observing their impacts on the model output. However, a Global Sensitivity Analysis (GSA), also called "variance-based sensitivity analysis", is performed when all input parameters are varied simultaneously over their entire uncertainty space, typically using probability distributions for each parameter, and the impact on the variability of the model output is observed. For more information about LSA and GSA and their application, the reader is referred to Saltelli *et al.* (2000, 2008, 2004).

The sensitivity analysis can be conducted for any computer model, such as the VSLite, by obtaining multiple runs of that model using random input configurations based on Monte Carlo sampling, which is computationally expensive. However, an alternative approach called Bayesian Sensitivity Analysis (BSA), is now more commonly used, which builds an emulator (approximation of the model) for the model under investigation, and then the sensitivity analysis is performed on the emulator.

3.4 Bayesian Sensitivity Analysis

Bayesian Sensitivity Analysis (BSA) aims to understand the sensitivity of the model output variations to change in the input parameters using a Gaussian process (GP) model. Widely used methods to conduct SA, developed by Saltelli *et al.* (2000, 2008), depend on Monte Carlo sampling techniques (Bowman, 1990) to estimate sensitivity measures (described in Section 3.4.2 below). Unfortunately, the

classical approaches of SA by Saltelli *et al.* (2000) are computationally expensive and require a large number of model runs. OHagan (2004, p. 1291) states that "Even for a model that takes just one second to run, a comprehensive variance-based sensitivity analysis may require millions of model runs". To overcome this difficulty, Gaussian Process regression models, known as GP emulators, have been proposed to implement SA. Thus, if the model to be evaluated is computationally expensive, the Bayesian SA can be used instead to explore the uncertainty of the model output without having to run the model many times. In the BSA approach, we learn about model uncertainty from only one run of the computer model by creating an emulator for the model.

The statistical theory and mathematical principles of using BSA to perform global sensitivity analysis (GSA) were first suggested by Oakley and O'Hagan (2004). Under BSA, each model parameter is defined by a probability distribution, and hence the Gaussian emulator can be built (as described in Section 3.5.1 below) using training data which are obtained from running the model at carefully chosen design points. McKay *et al.* (1979) suggested Latin hypercube sampling for choosing such design points which guarantees that each input parameter is well represented in the design. The BSA approach consists of two main stages. First, building a statistical emulator for the computer model from a set of training points. Second, using the created emulator to calculate sensitivity measures of interest.

The main advantage of using the Bayesian sensitivity approach and Gaussian process emulators to conduct SA is that no additional runs of the original model are needed to compute sensitivity measures. This is a good improvement, especially for complex computer models.

3.4.1   Building a Gaussian Processes Emulator

A Gaussian processes emulator is an approximation of the model (simulator), and it was first suggested by Sacks *et al.* (1989) as a method for emulating computer models. The GP emulator usually considers the simulator as an unknown func-

tion $f(\mathbf{x})$, which is used to estimate model output, and hence quantify the model uncertainty.

The reason for considering the computer model $f(\mathbf{x})$ as an unknown function is because model output is unknown till we run the model. Therefore, our prior information about $f(\mathbf{x})$ can be modelled by a GP with a particular mean and covariance function (Haylock and OHagan, 1996). Then the prior knowledge will be updated as new data are received. Building an emulator for complex and computationally expensive models is a very useful technique for performing sensitivity analysis of the model under study.

In short, building a Gaussian process emulator for any computer model (such as the VSLite) requires the following main four procedures respectively.

1. Formulating the prior mean and covariance function for the emulator.

2. Defining prior distributions for hyper-parameters of the emulator.

3. Generating design points for the model parameters using a sampling technique, for example, a Latin Hyper-cubic method (McKay *et al.*, 1979).

4. Running the model at the input parameter configurations specified in the design.

Oakley and O'Hagan (2004) describe the process of building GP emulators as follows. Given input parameters, $\{\mathbf{x_1}, \ldots, \mathbf{x_n}\}$, the prior uncertainties about the corresponding outputs $\{f(\mathbf{x_1}), \ldots, f(\mathbf{x_n})\}$ are considered via a multivariate normal distribution with mean function defined by

$$E\{f(\mathbf{x})|\ \beta^*\} = \mathbf{h}(\mathbf{x})^T\ \beta^*,$$

and covariance function between output points defined as

$$\mathrm{cov}\{f(\mathbf{x}), f(\mathbf{x}')|\sigma^2\} = \sigma^2 c(\mathbf{x}, \mathbf{x}'),$$

where $\mathbf{h}(\mathbf{x})$ indicates a vector of regression, β^* is the corresponding regression coefficients, σ^2 is the variance of the GP emulator which determines the overall

scale of the model, and $c(\mathbf{x}, \mathbf{x}')$ denotes the correlation matrix whose elements are defined as

$$c(x, x') = \exp\{-(x - x')^T \omega \, (x - x')\},$$

and $\omega = \mathrm{diag}(\omega_1, \ldots, \omega_n)$ is the diagonal matrix of roughness parameters, which indicate how strongly the emulator responds to each particular parameter.

The design points are then used for estimating unknown hyper-parameters (σ^2, β^*) of the GP emulator. Conjugate priors, the normal inverse gamma distribution, are chosen for σ^2 and β^* so that

$$p(\beta^*, \sigma^2) \propto \sigma^{-\frac{1}{2}(d+p+2)} \exp\left(-[(\beta^* - z)^T V^{-1}(\beta^* - z) + a]/(2\sigma^2)\right).$$

The choice of the prior specification for these two hyper-parameters is problem-specific, but Oakley and O'Hagan (2002, 2004) used a weak (conjugate) form for the prior:

$$p(\beta^*, \sigma^2) \propto \sigma^{-2}.$$

Latin hypercube sampling is then utilised to generate n design points for each input parameter, and the model is run at such design points to obtain a set of training data ($\mathbf{y}$). Then, the posterior distribution of the GP emulator is obtained by conditioning on the prior distributions of hyper-parameters and the obtained data $\mathbf{y}$. Conditional on roughness parameters ω and the data, the corresponding outputs have a multivariate t-distribution,

$$[f(\mathbf{x})|\omega, \mathbf{y}] \sim t_{n+p}\{m^*(x), \hat{\sigma}^2 c^*(\mathbf{x}, \mathbf{x}')\}, \qquad (3.12)$$

where $m^*(\mathbf{x})$ and $c^*(\mathbf{x}, \mathbf{x}')$ are respectively a posterior mean and covariance functions, and p indicates the number of coefficients (number of input parameters plus one) in the mean function.

The quality of the obtained GP emulator importantly relies on the number of design points, distribution of design points in the input sample space, and their hyper-parameter values. For more information about the Gaussian process emulations and building emulators, the reader is referred to (Kennedy and O'Hagan,

2001; Oakley and O'Hagan, 2002, 2004; OHagan, 2004).

3.4.2   Estimating the Sensitivity Measures

Once the emulator is built, its posterior distribution, Equation 3.12, can be used to infer several measures relevant to the sensitivity analysis, which are described in the following subsections.

3.4.2.1   Main Effects and Interactions

The main effects of any input parameter is the impact of changing the value of that input over its random space, and the interactions are the impact of changing two or more inputs together. The Sobol sensitivity decomposition, defined by Saltelli *et al.* (2000), states that any $f(\mathbf{x})$ is decomposed as follows,

$$y = f(\mathbf{x}) = E(Y) + \sum_{i=1}^{d} z_i(\mathbf{x}_i) + \sum_{i<j} z_{ij}(\mathbf{x}_{ij}) + \sum_{i<j<k} z_{ijk}(\mathbf{x}_{ijk}) + \cdots + z_{1,2,\ldots,d}(\mathbf{x}),$$

where

$$z_i(\mathbf{x}_i) = E(Y|\mathbf{x}_i) - E(Y),$$

is the main effect of $\mathbf{x}_i$, and

$$z_{i,j}(\mathbf{x}_{i,j}) = E(Y|\mathbf{x}_{i,j}) - z_i(\mathbf{x}_i) - z_j(\mathbf{x}_j) - E(Y),$$

is the first-order interaction between inputs i and j which gives information about the combined influence of the two inputs. Further terms indicate higher order interactions, and their impacts are typically small and are eliminated.

The main effects and interactions measures are evaluated from the posterior of the GP emulator.

3.4.2.2   Variance-based Sensitivity Factors

Variance-based sensitivity factors are the most popular measures to quantify the proportion of the output variance attributable to each individual input parameter.

The full variance decompositions are only meaningful when the input parameters are independent from one another (Saltelli *et al.*, 2000), and this has been assumed by the model developers (Tolwinski-Ward *et al.*, 2011). Assuming the independence of input parameters, the variance decomposition, defined by Saltelli *et al.* (2000), is

$$Var(Y) = \sum_{i}^{d} V_i + \sum_{i<j} V_{ij} + \sum_{i<j<k} V_{ijk} + \cdots + V_{1,2,\ldots,d},$$

where $Var(Y)$ indicates total variance of the output, d denotes number of input parameters to the model, V_i is the partial variance or "main effect variance" of input $\mathbf{x_i}$ on Y, and is given by

$$V_i = Var\{E(Y|\mathbf{x_i})\},$$

and V_{ij} is the joint effect (interaction) of the two input parameters $\mathbf{x_i}$ and $\mathbf{x_j}$ on Y, and is given by

$$V_{ij} = Var\{z_{i,j}(\mathbf{x}_i, \mathbf{x}_j)\}.$$

Another useful sensitivity measure is a "total effects variance" V_{Ti} which quantifies the amount of variation caused by the input $\mathbf{x_i}$ and any interaction involving $\mathbf{x_i}$ (i.e. for each input $\mathbf{x_i}$, the total effect is equal to the main effect for $\mathbf{x_i}$ plus all interactions including $\mathbf{x_i}$)

$$V_{Ti} = Var(Y) - Var\{E(Y|\mathbf{x}_{-i})\},$$

where $\mathbf{x}_{-i}$ indicates all input parameters except $\mathbf{x_i}$. All measures are usually converted to proportions via dividing by the total variance, as follows

$$S_i = \frac{V_i}{Var(Y)},$$

$$S_{Ti} = \frac{V_{Ti}}{Var(Y)},$$

where S_i is called the **main effects factor**, and S_{Ti} is called the **total effects factor** of the individual parameter $\mathbf{x}_i$. A high value of the main effect factors for a particular parameter indicates that the uncertainty of the model output can be decreased frequently by learning a true values of that parameter. For each given

66

input parameter of the model $\mathbf{x}_i$, the difference between the total effects factor (S_i) and main effects factor (S_{Ti}) is a measure of the amount of interaction effect derived from $\mathbf{x}_i$.

Variance-based sensitivity approach is a simple and useful method which can be used to identify significant and insignificant parameters of the VSLite model, and quantifies the effect of each parameter on the model outputs. The Bayesian sensitivity analysis and all the sensitivity measures can be computed using a freely available software package (GEM-SA; Gaussian Emulation Machine for Sensitivity Analysis, http://www.tonyohagan.co.uk/academic/GEM/index.html). The package was first developed by Kennedy and O'Hagan (2001) for the Centre for Terrestrial Carbon Dynamics (CTCD).

3.5   Summary of Chapter

In this chapter two different types of model, statistical and mechanistic, were described for simulating tree-ring width growth. A well-known descriptive statistical model by Litton and Zainodin (1991) was reviewed first, and its implementation for the Bayesian dendrochronology by Jones (2013) was then described. This was followed by consideration of the advantages and limitations of the statistical model in the tree-ring dating. Next, two mechanistic models, VS and VSLite, were reviewed; of which the latter model will be the main focus of the remainder of this thesis. Sensitivity analysis for computer models was then reviewed followed by Bayesian Sensitivity Analysis which uses Gaussian process to build an emulator for the model under investigation. Thereafter, the variance-based sensitivity measures were also reviewed which can be estimated from posterior of the emulator. In the next chapter, VSLite model will be implemented to simulate tree-ring width sequences at different geographical locations around the world, and the model's efficiency will be checked. Bayesian Sensitivity Analysis will be used systematically to investigate uncertainty in the VSLite model output. This will include examining the impact of each model parameter on the model output variablity.

Chapter 4

Exploring Uncertainty in the VSLite Model

The mechanistic VSLite model was described in the previous chapter, and a stochastic version of the model will be used at the core of Bayesian tree-ring dating in the next chapters. Before accomplishing that, it is essential to evaluate the model and to check its adequacy to ensure that the model is reliable. Furthermore, it is useful to identify which of model parameters are more influential on the model's output variability. This is typically done in order to pay more attention to the significant parameters and to make inferences about them when fitting the model for cross-matching tree-ring width sequences. In this chapter, we implement and evaluate the VSLite model by exploring the uncertainty in the model output. We apply the Bayesian Sensitivity Analysis for the model in order to quantify the contribution of each model parameter to the model output variation.

4.1   VSLite Model Implementation

In order to investigate the uncertainty in the VSLite model, we have implemented the model at different geographical areas around the globe. For this purpose, the VSLite model has been implemented in R programming environment (R Core Team, 2015). Although the VSLite code was originally written by Tolwinski-Ward

et al. (2011) in MATLAB, we have written new code for two reasons. First, the code will be changed, eventually, to include the tree-ring matching process in the Bayesian framework and to make inference about the model parameters. We prefer not to do this in MATLAB, as it is proprietary (rather than free open source software) and this has costs implications for the users. Second, R was built and designed for substantial statistical modelling and inference. Before using the new code for the model implementation, the accuracy of the R-code was tested to ensure that exactly the same results as the original Matlab code are obtained. For this purpose, the model has been ran using the two codes, and the results were compared which were similar to four decimal places; therefore, the new R-code written was as accurate as the original code.

In this model evaluation, the new R implementation of the model (henceforward known simply as VSLite) was run at many different places in the USA, the UK and Europe, to simulate tree-ring width sequences. The VSLite model outputs (simulated) were compared to actual (observed) ring-width indices at the same location to check the model adequacy. Four geographical locations (sites) each with different climate conditions are presented here as examples of this model evaluation. Information of the data for these four sites are given in Table 4.1.

Site	Taxon	ITRDB code	Latitude	Longitude	Time span
Site 1	Pinus	ca530	36.45	-118.22	1901-1984
Site 2	Pinus	ca544	34.17	-117.12	1901-1984
Site 3	Pinus	ca615	39.02	-122.82	1901-1984
Site 4	Pinus	co523	39.32	-106.08	1901-1984

Table 4.1: Information of tree-ring data for four sites in the USA.

The following sections describe observed and simulated ring-width sequences for the four sites, along with exploration of the model efficiency via investigation of the uncertainty in the model outputs.

4.1.1 Observed Tree–Ring Data

Tree-ring data were chosen to overlap with the meteorological data, for the period 1901 to 1984 AD. The reason for this choice of period (84 years) is the availability of climate data and tree-ring observations. All the observed tree-ring data were taken from the International Tree-Ring Data Bank (`http://www.ncdc.noaa.gov/paleo/treering.html`). For each tree, the data include raw ring widths, the calendar date of the first ring, longitude and latitude at which the tree grew, and tree species. To remove any growth trends, the observed raw ring-widths data (x_{ti}) are detrended (using the method described in Section 2.1.1.5) to give tree-ring indices (y_{ti}). A local site chronology C_t, for each of the four locations, is also constructed by grouping and averaging the obtained ring-width indices (using the method detailed in Section 2.3). Then, the site chronologies are standardised to give

$$W_t = \frac{C_t - \bar{C}}{\sigma_C},\tag{4.1}$$

where C_t indicates site chronology's ring-width index at year t, $\bar{C}$ and σ_C are mean and standard deviation of the observed site chronology respectively. Thus, $W_t \sim N(0,1)$ is the annual observed site chronology.

4.1.2 Simulating Ring-Width Sequences from VSLite

The VSLite model allows simulation of tree-ring width sequences at any geographical location around the world where climate data records exist, requiring, in particular, input of the form monthly temperature and precipitation averages along with site latitude.

Climate Data Records

The monthly meteorological data, used in this investigation, are not observational data but gridded model outputs. Time-series of monthly temperature and precipitation were estimated by Harris *et al.* (2014), and can be freely obtained from the Climate Research Unit, CRU-3.21 dataset (`http://badc.nerc.ac.uk/data/cru/`).

The CRU time-series data cover the global surface at 0.5^o latitude $\times 0.5^o$ longitude spatial resolution from 1901 to 2013, and are based on the climate records from meteorological stations. Therefore, these monthly temperature and precipitation estimates are available as gridded output in an appropriate format for use as input to VSLite. The uncertainty in CRU data varies from one area to another depending on the number of meteorological stations used in the interpolation of model output. For example, the uncertainty in such data estimates for African regions is higher than that for Europe and North America, due to the number of meteorological stations recording real observational data. Nevertheless, these historical CRU time-series are currently the most accurate and reliable climate data outputs available in monthly time-steps (Harris *et al.*, 2014).

Partial Growth Functions

Selecting the CRU time series from the grid-point with the nearest half-degree latitude distance for the four sites of interest, VSLite was used to simulate ring-width sequences for each site (as detailed in Section 3.2.2). Partial growth responses to temperature $G_T(m,t)$ and soil moisture $G_M(m,t)$ were calculated by applying the Equations 3.7 and 3.8 respectively. The results for the four chosen sites are given in Figure 4.1.

Figure 4.1 shows the partial growth responses to temperature $G_T(m,t)$ and soil moisture $G_M(m,t)$ calculated from the VSLite model. It is clear that the growth at sites 1 and 4 are temperature-limited as the overall monthly growth response is determined by the lower value of these two partial growth functions (G_T and G_M). At these two sites the mean partial growth response to temperature is almost 0 in the coldest months, and peaks only in the summer time. The mean growth curve response to soil moisture is constant over the whole growing season reflecting adequate access to water throughout the year. On the other hand, the mean modelled partial growth responses for sites 2 and 3 show clearly how the overall monthly growth response is affected by an interaction between soil moisture and tempera-
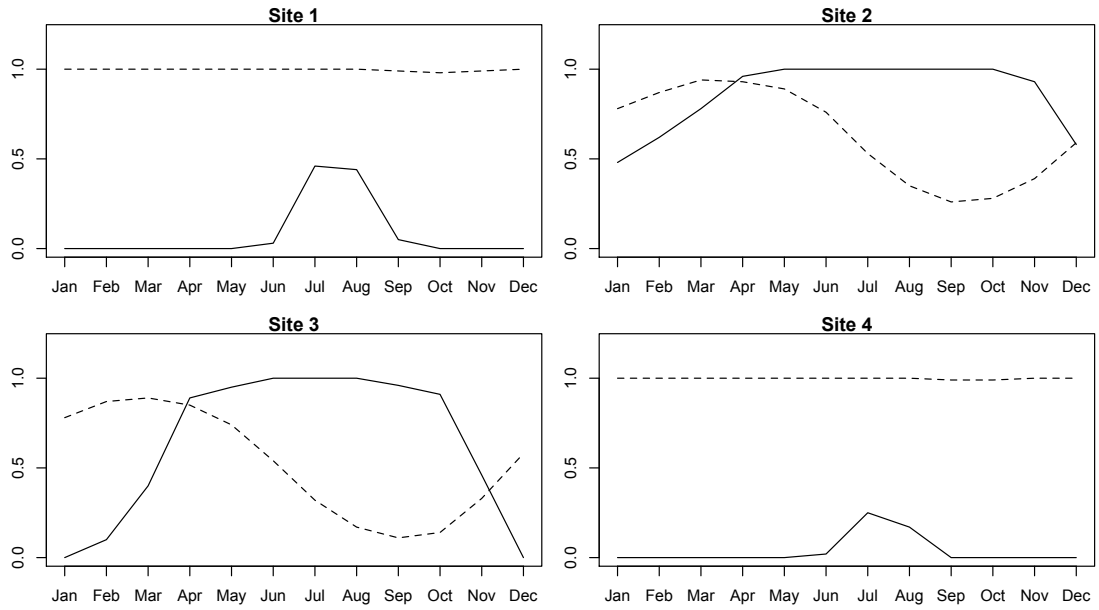
Figure 4.1: Monthly partial growth response to temperature, G_T (*solid line*) and soil moisture, G_M (*dashed line*) at four different sites in the USA, modelled from the VSLite model.

ture. Growth is moisture-limited during spring, summer and autumn as the G_M curves fall below the G_T curves, and it is temperature-limited only in the winter months. Thus, the VSLite model has captured the climate driven variable(s) at each site, and it is easy to interpret the model outputs in terms of the climate controls on simulated partial growth functions. This suggests that, at least at these four sites, the VSLite model can determine whether growth is dominated by temperature or soil moisture, or a combination of the two.

Tree-ring Formation

The partial growth response functions were then used to obtain monthly overall growth responses, $G(m,t)$, using Equation 3.9. The VSLite-based simulated annual ring-width sequence $\hat{W}_t$, for each site, was then obtained by summing the overall growth response function over the 12 months, as detailed in Equation 3.10. These simulated ring-width sequences are given in Figure 4.2.
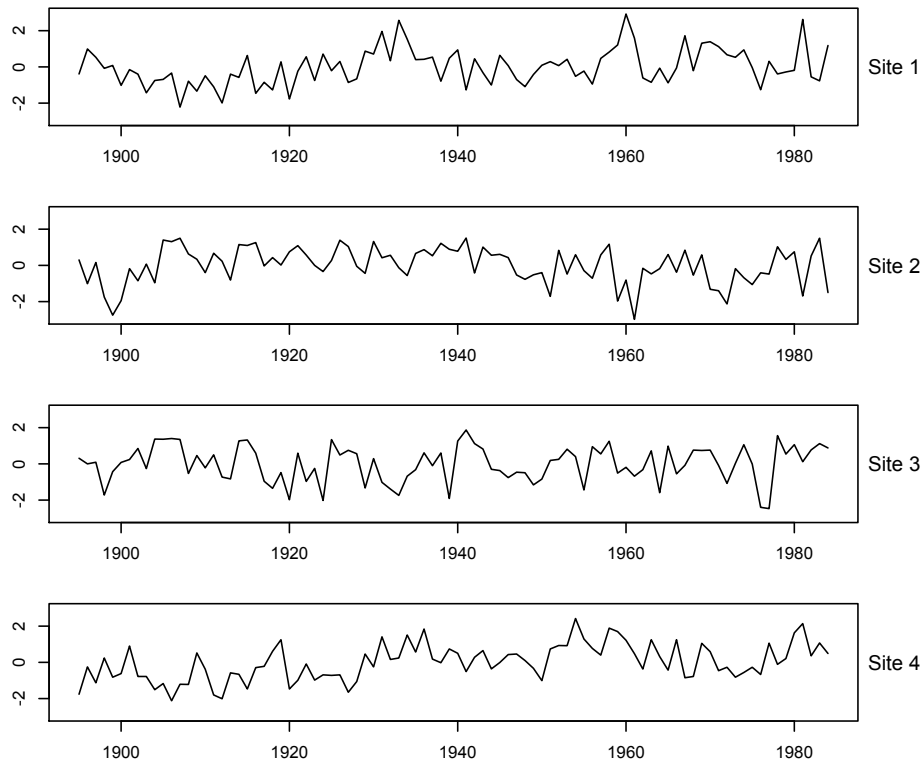
Figure 4.2: Plot of simulated ring-width indices from the VSLite model at four different sites in the USA. The x-axes are calendar dates and y-axes are ring-width indices.

Figure 4.2 shows time-series of simulated ring-width sequences from the VSLite model at the four chosen sites in the USA. Each ring-width sequence is generated from the model as a function of site-specific partial growth response to temperature G_T, soil moisture G_M and solar irradiation G_E.

4.1.3   Model Evaluation

For each site in this model evaluation, an actual ring-width chronology was obtained. A simulated site chronology was also generated from the VSLite model. These two sets of data enable us to make an initial valuation of the capability and behaviour of VSLite model to simulating ring-width sequences.

Graphical Comparison

Both the observed and simulated time-series were plotted together to check the similarity between the pattern of the two sequences (Figure 4.3). This quick visual comparison was made for the four sites to identify any relationships between the two data sets. The similarity in patterns between the two chronologies indicates the capability of VSLite model to capture the climatic variability within tree-ring sequences at each site. The more similar the two chronologies, the better the VS-Lite model output.
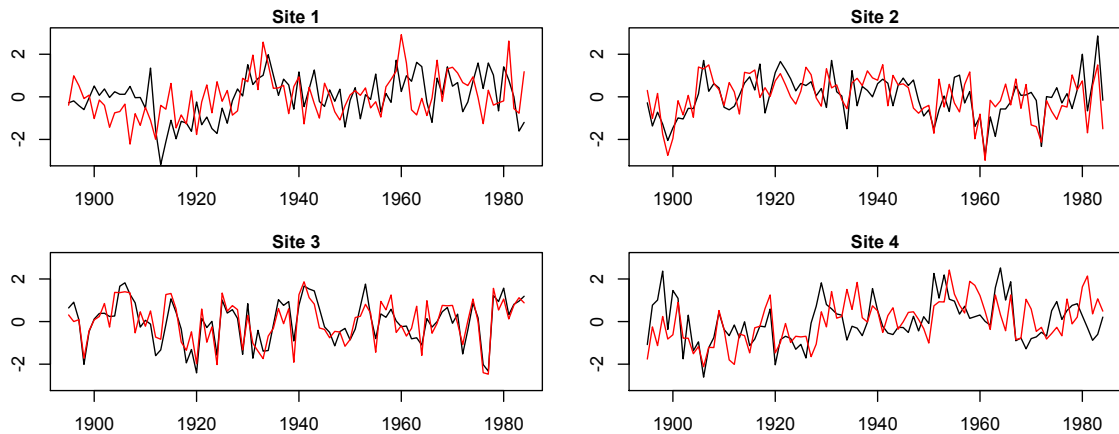
Figure 4.3: Plot comparing observed (*black*) and simulated (*red*) ring-width sequences generated from the VSLite model at four different sites in the USA. The x-axes are calendar dates and y-axes are ring-width indices.

Figure 4.3 shows the results of comparing observed and simulated chronologies. It shows that the VSLite model has performed better in sites 2 and 3 than in sites 1 and 4. This is because there are better agreement and similarities in the patterns between simulated and observed chronologies in sites 2 and 3. This indicates that the uncertainty in the model outputs for sites 1 and 4 is higher, and the performance of the VSLite model is not very good compared to the other two sites. This visual comparison, as means by which to explore the uncertainty in the model outputs, but not sufficient to quantify or describe the differences. More formal statistical methods are needed to quantify the model uncertainty.

Although the VSLite model was generally able to simulate ring-width sequences under different environmental conditions at various locations, the efficiency of the model varies from one site to another. This uncertainty in model output occurs because of either uncertain site-specific climate data (temperature and precipitation), uncertain model parameters, or error in model structure. Thus, before moving on to examine the use of the VSLite model to the Bayesian dendrochronology, which is the main aim of this thesis, it is worth studying the sources of any uncertainty within the model with a view to controlling them, and hence decreasing the model output variability.

4.2 Sources of Uncertainty in the VSLite Model

There are multiple sources of error in any process-based model. Here we adopt the classification offered by Kennedy and O'Hagan (2001) who identify three main sources as described below.

- **Uncertainty in model input parameters**: the uncertainty in the VSLite model input parameters emerges because they relate to either observed or estimated physical phenomena most (or all) of which are uncertain. Such uncertain input parameters can be represented as a probability distribution and then controlled by making statistical inferences and learning about the true values of the model parameters from data.

- **Uncertainty in data inputs**: this type of uncertainty in the VSLite model arises when climate model gridded outputs (instead of observational records) are used as input into VSLite model to simulate tree-ring-width sequences. Observational historical monthly climate data do not exist for all geographical locations around the globe, and these data records are therefore modelled from nearby meteorological stations. Even if such data exist, we might imprecisely record them. The uncertainty in the input data for climate models

is usually assumed small enough to be ignored (Harris *et al.*, 2014) and we follow this convention here for mathematical convenience.

- **Uncertainty in model structure**: this refers to the case where we are not certain about the true structural relationships within a model. As the models are approximations of the real process, we are not certain about the most appropriate way to represent them in our model. This type of uncertainty in the tree-ring width models can be controlled by the model developers (biologists and botanists) by further studying the mechanism and the nature of ring-width growth and improving their knowledge about the climate-tree-ring relationships.

  Exploring in detail this source of VSLite model uncertainty is beyond the scope of this research project, because that is largely done better by those with knowledge of the biology, and indeed some of those with that knowledge have already began to do that work, including Evans *et al.* (2014); Tolwinski-Ward (2015). This type of model uncertainty has also been explored by performing external discrepancy analysis (Bayarri *et al.*, 2007; Strong and Oakley, 2014).

Three different possible sources causing uncertainties in the VSLite model output have been defined. The first of these uncertainty sources is statistically controllable, and can be explored by performing the Bayesian sensitivity analysis described in Section 3.4. Therefore, in this thesis, we concentrate on exploring uncertainties in the model output due to the uncertain input parameters.

In what follows in this chapter we investigate the uncertainty in VSLite model parameters via applying the Bayesian sensitivity analysis (BSA). The contribution of each parameter to the model's output variability is quantified using variance-based sensitivity measures (detailed in Section 3.4.2), and the parameters are therefore ranked in terms of their influences on the model output variation.

4.3 Bayesian Sensitivity Analysis of VSLite Model

Bayesian sensitivity analysis (BSA), discussed in Section 3.4, is conducted for the VSLite model in order to quantify and assess how change in the model outputs can be attributed by changing each input parameter $\mathbf{x}_i$; where $i = 1, \ldots, p$, and p is the number of the VSLite model parameters of interest. Model input parameters that have a significant impact on the output were identified by evaluating variance-based sensitivity measurements, main effects and total effects described in Section 3.4.2. These measures are then used to rank model parameters in terms of their contribution to the model output variability.

The following steps are used to carry out the BSA for the VSLite model:

- **Identification of the input parameter uncertainty**

  We first represent the uncertainty space and configuration of a probability density for each of the input parameters. The information on the uncertainty of the parameter ranges is commonly estimated either based on physical reasoning or only from experts, whilst the mathematical representation of the probability distributions might be either theoretically known or to be considered.

  All the eleven VSLite model parameters (given in Table 4.2) were allowed to vary in the Bayesian Sensitivity Analysis. The first four parameters are the main growth threshold parameters which control the simulated non-linear growth response to temperature and soil moisture. The minimum and maximum values for these four parameters were taken from experts' opinion in the literature (Haung *et al.*, 1996; Tolwinski-Ward *et al.*, 2013, 2011; Vaganov *et al.*, 2006). The next seven parameters are related to the monthly soil moisture computation $M(m, t)$, which are estimated from monthly temperature $T(m, t)$ and precipitation $P(m, t)$ data, via a "Leaky Bucket" sub-model, introduced in Section 3.2.1. The "optimal" values of these seven parameters

were estimated by Haung *et al.* (1996), and then were widely used as globally optimal values in the literature. To perform the BSA, we varied these 7 parameters by $\pm 25\%$ around their original (optimal) values, and this variation allowed remaining parameters in their well-defined sample spaces.

A summary of the resulting ranges (lower and upper values) for all VSLite parameters are presented in Table 4.2. As no information is available on the prior probability densities for each model input parameter, uniform distributions were assigned for the input parameters. We defined the uniform prior for each model parameter through the lower and upper values given in Table 4.2.

Parameter	Description	Min	Max
T_1	threshold temperature for $g_{\mathbf{T}} > 0$	1	9
T_2	threshold temperature for $g_{\mathbf{T}} = 1$	10	24
M_1	threshold soil moisture for $g_{\mathbf{M}} > 0$,	0	0.1
M_2	threshold soil moisture for $g_{\mathbf{M}} = 1$,	0.10	0.5
M_x	maximum soil moisture held by soil	0.67	0.96
M_m	minimum soil moisture held by soil	0.008	0.013
α_a	runoff parameter 1	0.07	0.116
α_b	runoff parameter 2	4.35	7.25
α_c	runoff parameter 3	3.666	6.106
d_r	root (bucket) depth	750	1250
M_0	initial value for previous month's soil	0.15	0.25

Table 4.2: Summary of the VSLite model parameters to be used for the implementation of the Bayesian Sensitivity Analysis of the model.

- **Selecting design points**

  To fill the design space for the sensitivity analyses, a Latin Hypercube Design (LHD) was used. LHD is a popular approach for space-filling designs for computer experiments proposed by McKay *et al.* (1979). It assures that all

parts of the range of each parameter are well covered in the sample space. This space-filling approach divides the input space into regions of equal probability and randomly assigns points that are distributed evenly across the probability-space.

We used the GEM-SA (`http://www.tonyohagan.co.uk/academic/GEM/index.html`) software to create the Latin Hypercube design points for the VSLite model parameters. The software only requires the number of input parameters (p), the number of design points (d), and each parameter space range (upper and lower values). The VSLite model has 11 parameters ($p = 11$). The size of the finite set of design points required for building emulators is supposed to be equal to number of parameters d times ten ($d = p \times 10$) (Oakley and O'Hagan, 2004; OHagan, 2004), ensuring full coverage of the parameter space. In the VSLite model case, $d = 11 \times 10 = 110$ design points.

- **Constructing the GP emulator**

  Having successfully selected the design points for the input parameter space, the simulator (VSLite model) was evaluated at d selected design points to produce the "training set" $\mathbf{y}_i$, $i = 1, \ldots, d$. Then, the Gaussian process regression, detailed in Section 3.4, was fitted to the training data $\mathbf{y}$ to build an emulator for the VSLite model. The created emulator was then used as a surrogate for VSLite to conduct the sensitivity analysis.

- **Estimating the sensitivity measures**

  Finally, all the sensitivity measures, the main and total effects factors (described in Section 3.4.2), for all model parameters were computed using the posterior distribution of the constructed GP emulator. Consequently, the impact of each of the VSLite model parameter was quantified, and the most influential parameters of the model were determined.

4.4 Results

This section contains plots of results for the experiments suggested in the previous section. The Bayesian sensitivity analysis was performed for the VSLite model at 26 different geographical locations around the world for which climate data records (temperature and precipitation) and real tree-ring width data (Quercus or Pinus) are available. These site were chosen randomly, and the reason for choosing these two species is that they are the two most reliable tree-species for dendrochronological and palaeoclimatological studies. The locations were also selected to cover a wide range of climates. Figure 4.4 shows the distribution of these locations on the map. The geographical information and tree species of each of the selected sites are given in Table 4.3.
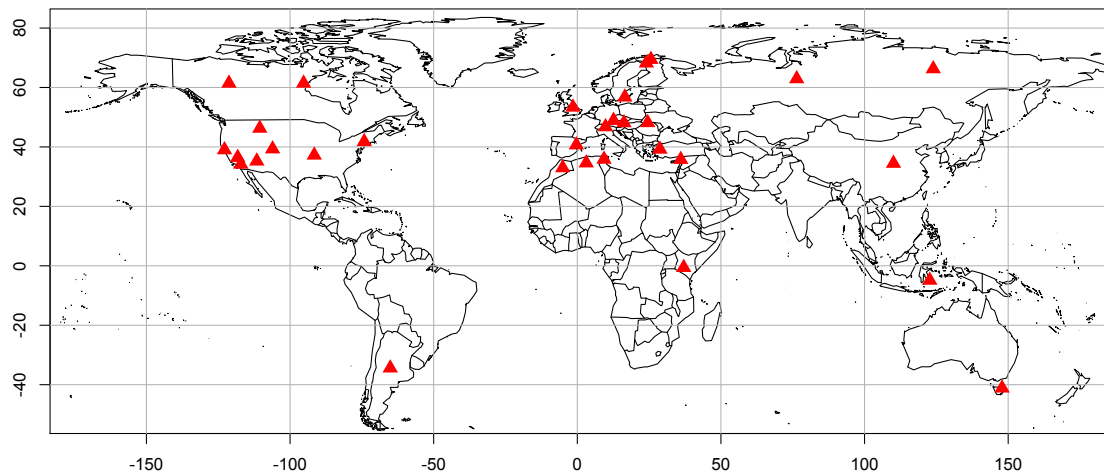
Figure 4.4: Locations of the 26 sites chosen to perform the Bayesian sensitivity analysis for the VSLite model. Horizontal lines represent latitudes and vertical lines are longitudes.

To perform Bayesian sensitivity analysis for the VSLite model parameters at each of the 26 geographical sites shown in Figure 4.4, monthly climate records (temperature and precipitation) were used to run the model at each site. These climate records were obtained from the Climate Research Unit CRU (CRU-TS3.21 dataset), described in Section 4.1.2. A simple function was written in R to se-

Site	Site code in ITRDB	Taxon	Country	Latitude	Longitude	Chronology length
1	morc018	Quercus	Morocco	32.97	-5.07	1450-1980
2	ca544	Pinus	USA /CA	34.17	-117.12	1707-1988
3	chin056	Pinus	China	34.47	110.08	1458-2005
4	alge003	Pinus	Algeria	34.6	3.12	1854-2006
5	az564	Pinus	USA/AZ	35.23	-111.57	1931-2003
6	syri003	Pinus	Syria	35.78	36.02	1882-2001
7	tuni003	Pinus	Tunisia	35.85	9.3	1874-2003
8	ca530	Pinus	USA/CA	36.45	-118.22	917-1987
9	ca615	Quercus	USA/CA	39.02	-122.82	1642-1996
10	turk039	Pinus	Turkey	39.23	28.78	1792-2004
11	co523	Pinus	USA/CO	39.32	-106.08	1050-1985
12	spai020	Quercus	Spain	40.67	-0.33	1763-1991
13	mt125	Quercus	USA/MT	46.27	-110.53	1602-2009
14	swit179	Quercus	Switzerland	46.77	9.82	1733-2005
15	aust111	Pinus	Austria	48.12	16.25	1766-1995
16	ukr001	Quercus	Ukraine	48.15	24.52	1676-2003
17	germ059	Quercus	Germany	48.92	12.62	1917-2001
18	brit064	Quercus	UK	51.07	-1.38	1629-2009
19	brit012	Quercus	UK	51.8	-1.12	1781-1978
20	brit053	Quercus	UK	53.37	-1.5	1759-2003
21	swed313	Pinus	Sweden	56.77	16.55	1858-2006
22	cana301	Quercus	Canada	61.43	-121.27	1689-1998
23	russ155	Pinus	Russia	62.93	76.38	1726-1994
24	russ205	Quercus	Russia	66.28	123.92	1551-2007
25	finl072	Pinus	Finland	68.22	24.05	1724-2006
26	norw007	Pinus	Norway	69.42	25.63	1698-2001

Table 4.3: Summary of geographical information for 26 sites chosen to perform the Bayesian sensitivity analysis for the VSLite model. They are sorted by site latitudes.

lect the nearest half-degree of gridded climate output for each site. These time series of monthly climate can be obtained from the Climate Research Unit website (http://badc.nerc.ac.uk/data/cru/).

The Bayesian sensitivity analysis was performed at each of these 26 sites separately, and then the results of the analysis were compared to understand the behaviour of the model at different locations with various climate conditions. By way of illustration, the following section shows the results of performing the BSA for the VSLite model parameters at a single site (Sheffield, UK).

4.4.1 Applying BSA for the VSLite Parameters at Sheffield

Using several steps for the Bayesian sensitivity analysis (discussed in detail in Section 4.3), we performed a sensitivity study for the VSLite model at our illustration site (Sheffield). The target was to examine how sensitive the simulated ring-width indices from the model to each individual VSLite parameter, so that one can learn about the true values of the most influential parameters with a view to reducing the uncertainty in the model output. To evaluate variance-based sensitivity factors, the following steps were undertaken.

First, we specified a minimum and maximum value for each of the eleven input parameters of the model, and then a probability distribution (uniform), based on the available information about the parameter, was defined for each model parameter. Second, a combination of 110 design points of the input parameters were generated using a Latin-Hypercube design method (described and discussed in Section 4.3), to obtain a good representation of the sample space of each parameter. We then ran the VSLite model at those generated design points to provide the training data, $\mathbf{y}$, of the model output. The Gaussian process regression (described in Section 3.4) was then fitted to the training data and an emulator for the VSLite model was built. Finally, we calculated the sensitivity analysis measures from the posterior distribution of the VSLite emulator. The following are the results of conducting the BSA for the VSLite model at our illustration site (Sheffield).

4.4.1.1 Emulator Performance

The accuracy of the constructed emulator should be checked before using it to perform the sensitivity analysis for model parameters. The performance of the GP emulator can be examined by the quantitative values of both the variance of the emulator (σ^2) and the value of the "roughness parameter" ($\boldsymbol{\omega}$) for the model parameters. The values of these hyperparameters show the quality of the emulator. σ^2 determines the overall performance of the model and it is scaled from zero to

one, which measures the quality of the fit of the emulator to the original model code. The lower the value of σ^2, the better the created emulator is; where zero indicates perfect emulator. Roughness hyperparameters $\boldsymbol{\omega}$ provide estimates of the smoothness for each parameter, which determine how strongly the created emulator responded to each particular parameter. At our chosen site, Sheffield, the variance of the constructed emulator was ($\sigma^2 = 0.4861$) which indicates that the model parameters show only moderate divergence from linearity, hence suggesting that our constructed emulator is good and well approximated the original VSLite model. Furthermore, the values of the roughness parameters are as follows,

$$\begin{aligned}
\boldsymbol{\omega} &= \big[\omega_1, \omega_2, \ldots, \omega_{11}\big] \\
&= \big[0.55,\ 1.32,\ 0.23,\ 0.63,\ 0.28,\ 0.11,\ 0.10,\ 0.29,\ 0.14,\ 0.23,\ 0.80\big].
\end{aligned}$$

These values are relatively low (less than one) for most of the VSLite model parameters which implying that the emulator responds smoothly to most of the input parameter variations, and hence the created emulator is a useful representation of the VSLite model.

Having constructed a good emulator for the VSLite model, the sensitivity analysis measures can be inferred from the resulting emulator. The following subsections show the SA results for the VSLite model in Sheffield.

4.4.1.2   Main Effects and Total Effects

The main and total effects factors (detailed in Section 3.4.2) for each of the model parameters were calculated in order to examine the impact of each of them, and identify the most influential parameter(s) affecting the variability in the simulated tree-ring width indices by the VSLite model. The main effect of any input parameter measures (in percentage) the impact of changing the value of that parameter over its input space; while the total effects of any parameter measures the main effects of that parameter plus all the pair-wise interactions with all other parameters simultaneously.

Table 4.4 shows results of performing SA of the VSLite model at our illustration site, Sheffield. The parameters, with considerable main effects on the model output variability, are highlighted in grey. The total effects factors were also calculated, which indicates how each VSLite parameter contributed to the model output variation when all its interaction with the other model parameters are considered.

Input parameters	Main effects (%)	Total effects (%)
T_1	18.07	21.85
T_2	**68.67**	74.53
M_1	0.39	1.29
M_2	0.83	3.12
M_x	0.06	1.77
M_m	0.05	1.02
α_a	0.14	1.14
α_b	0.10	1.75
α_c	0.09	1.14
d_r	0.07	1.65
M_0	0.18	2.27
Total	88.65	

Table 4.4: Main effects and total effects factors for VSLite model parameters at Sheffield site. Highlighted is the most influential parameters.

As shown in Table 4.4, the percentage variance contribution of input parameters varies from 0.05% to 68.67%. The main effects sum to 88.65% of the total variation in model output, indicating that the impact of all possible interactions between model parameters sum to 11.35%. It is clear that the most influential input parameters, with the largest contribution on the model output uncertainty, are T_2 with 68.67% and T_1 with 18.07%. Under the climatic conditions at this geographical location, these two parameters together are responsible for almost 86.74% of the variation in tree-ring width indices simulated from the model. This indicates that any changes in these two parameters will affect the model outputs significantly. Thus, the uncertainty in the model output, at this location, would be decreased noticeably by learning true values of these two parameters.

The results in Table 4.4 also demonstrate that some interactions between the VSLite parameters exist. These can be seen by observing the total effects (column 3) of each parameter, which assess the magnitude of pair-wise interactions of

each individual parameter with all other model parameters. For instance, the total effect of the M_2 shows that although the main effect of this parameter was very low (0.83%), the total effects of this parameter with the others is (3.12%) which suggest that the interaction of parameter with others is relatively influential. In other words, due to its interaction with T_1 and T_2, M_2 is also an important parameter in the model, but its influence is not substantial compared to effects of T_1 and T_2.

Figure 4.5 shows the main effects and the total effects plots for the VSLite model parameters at our illustration site, Sheffield. It provides a visual representation of the sensitivity analysis results represented in Table 4.4.
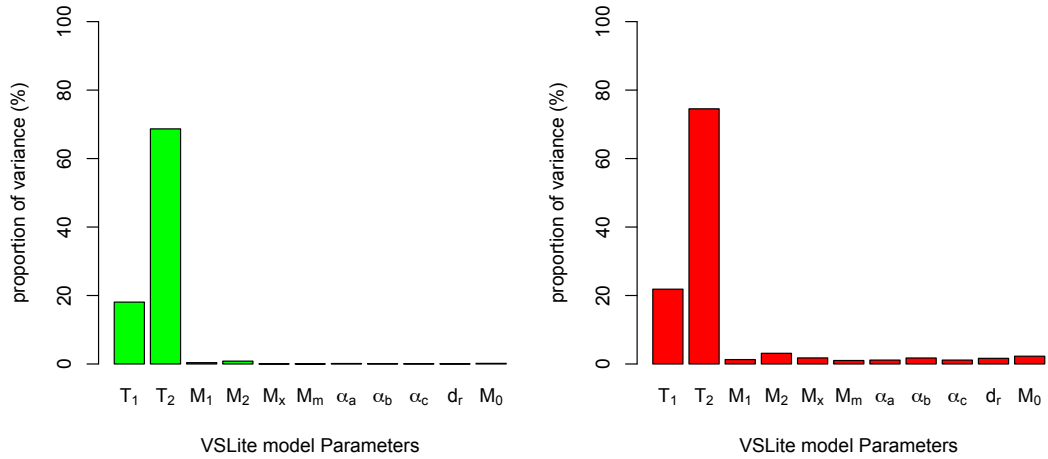
Figure 4.5: Sensitivity of each parameter on variability of the simulated ring-width indices from the VSLite model at Sheffield. Main effects (*left panel*) and total effects (*right panel*) show the contribution of each parameter to the variability of the model output.

This section demonstrates the results of performing the Bayesian sensitivity analysis for the VSLite model at a single geographical location in the UK. As the simulated ring-width indices from the VSLite is a function of monthly climate variables and a combination of model parameters, the model's behaviour might vary from one location to another. Consequently, the sensitivity analysis might also vary for different areas. Therefore, the BSA of the model parameters should be assessed in a variety of locations with different climate conditions. This will help us to understand the contribution of each parameter to the uncertainty in the

model output under different climate conditions.

4.4.2 BSA of VSLite Model at Different Climatic Regions

Bayesian sensitivity analysis of the VSLite model was performed at 26 different locations around the world to study the behaviour of this model globally. Table 4.5 shows a summary of the results obtained.

Site	Site code	Taxon	T_1	T_2	M_1	M_2	M_x	M_m	α_a	α_b	α_c	d_r	M_0	Var (%)
5	morc018	Quercus	18.86	48.41	0.33	9.86	0.12	0.99	0.09	0.09	0.2	0.65	0.31	**79.91**
6	ca544	Pinus	16.40	34.90	0.85	31.14	0.54	0.09	0.35	0.22	0.16	0.33	0.20	**85.18**
7	chin056	Pinus	12.62	36.33	0.22	34.03	0.27	0.41	1.23	0.08	0.06	0.44	0.54	**86.23**
8	alge003	Pinus	19.94	13.69	0.24	36.01	0.11	0.29	0.74	0.08	0.43	0.17	0.33	**72.03**
9	az564	Pinus	13.8	53.35	0.1	6.17	0.19	0.37	0.41	0.24	0.29	0.32	0.31	**75.55**
10	syri003	Pinus	19.09	39.16	0.07	7.38	0.23	0.8	0.36	0.25	0.3	1.07	0.7	**69.41**
11	tuni003	Pinus	19.57	30.23	0.28	14	0.48	0.22	0.16	0.5	0.45	1.46	0.33	**67.68**
12	ca530	Pinus	21.02	61.12	0.49	5.13	0.51	0.24	0.38	0.18	0.11	0.24	0.28	**89.07**
13	ca615	Quercus	10.70	30.50	0.64	36.20	0.77	0.15	0.43	0.57	0.49	0.97	0.31	**81.73**
14	turk039	Pinus	16.91	55.5	0.11	5.89	0.24	0.12	0.19	0.28	0.06	0.19	0.1	**79.59**
15	co523	Pinus	17.30	37.70	0.37	28.40	0.43	0.37	0.25	0.61	0.19	0.81	0.42	**86.85**
16	spai020	Quercus	23.67	38.87	0.19	9.78	0.28	0.58	0.12	0.56	1.06	0.17	0.25	**75.53**
17	mt125	Quercus	12.64	51.66	0.37	11.13	0.66	0.07	0.95	0.09	0.09	0.18	0.43	**78.27**
18	swit179	Quercus	41.55	25.43	0.11	1.29	0.08	0.07	0.23	0.16	0.31	1.42	0.57	**71.22**
19	aust111	Pinus	14.62	52.88	0.32	7.58	0.23	0.36	0.33	0.26	0.14	0.09	0.5	**77.31**
20	ukr001	Quercus	16.97	68.12	0.33	0.15	0.19	0.05	0.31	0.51	0.36	0.33	0.27	**87.59**
21	germ059	Quercus	10.57	67.24	0.32	1.36	0.2	0.08	0.09	0.07	0.08	0.18	0.37	**80.56**
22	brit064	Quercus	14.07	41.12	1.23	21.72	0.84	0.13	0.17	0.38	0.29	0.51	0.64	**84.10**
23	brit012	Quercus	15.03	48.71	0.75	13.35	0.28	0.34	0.22	0.19	0.27	0.43	0.79	**80.36**
24	brit053	Quercus	18.07	68.67	0.06	0.83	0.39	0.05	0.14	0.1	0.09	0.07	0.18	**88.65**
25	swed313	Pinus	16.89	50.81	0.52	10.55	0.27	0.1	0.31	0.31	0.13	0.07	0.12	**80.08**
26	cana301	Quercus	15.25	35.11	0.81	21.95	0.14	0.16	0.84	0.07	0.88	1.06	0.11	**76.38**
27	russ155	Pinus	8.6	49.87	0.13	5.32	0.32	0.57	0.18	0.52	0.66	0.89	0.33	**67.39**
28	russ205	Quercus	8.01	29.83	0.12	31.69	0.1	0.13	0.16	0.3	0.1	0.32	0.59	**71.34**
29	finl027	Pinus	21.2	49.39	0.95	2.07	0.81	0.28	0.42	0.35	0.94	0.11	0.16	**76.68**
30	norw007	Pinus	23.43	44.4	1.44	0.71	0.97	0.15	0.29	0.67	0.92	0.18	0.2	**73.36**

Table 4.5: Summarised results from the Bayesian sensitivity analysis of the VSLite model at 26 chosen sites. The percentage variance attributed to the variation in each individual input parameter in the model (columns 3-13), and the total output variance of the model explained by the main effects at each site (column 14). Highlighted in grey is the input parameter at each site which contributes most to the model output variability.

It is worth noticing from the results in Table 4.5 that three parameters (T_1, T_2 and M_2) contribute most to the model output variability at all locations. The whole uncertainty of the model output (tree-ring width indices) is almost totally controlled by these three parameters, which reveals that the simulation of ring-width indices from the VSLite model are strongly sensitive to these parameters. However, the degree of effect among these three parameters varies from one site to another. For example, the parameters T_1 and T_2 are influential at almost all of the 26 geographic sites with different degree of influence. The only exception are sites "indo005" and "keny002" where M_2 is dominant. M_2 also is very influential at some other sites, such as "arg113", "russ205", and "ca615", and is not at all influential in some others, such as sites "norw007" and "uk001". This suggests that any changes in these three influential input parameters will affect the variability of the model output substantially. Hence, if we want to reduce the model output uncertainty in any particular location we should learn about the true value of the most influential parameters at that location.

To conclude, the VSLite model parameters which have the greatest impact on the simulation of tree-ring width indices at these 26 sites are T_1, T_2 and M_2. However, the growth threshold parameter M_1 appears to have little effect on the model output variability which suggests that the tree-ring growth is insensitive to the lower soil moisture threshold. Similarly, the contribution for each of the other seven VSLite parameters is less than 1%, which indicates that they are not influential on the variability of the model output. This is because the threshold parameters (T_1, T_2, and M_2) directly affect the growth of ring-widths. However, the other 7 model parameters relate to the sub-model used to generate monthly soil moisture content, and so only indirectly affect the formation of tree-rings. Therefore, the most reasonable way is not to investigate the sensitivity of these seven parameters on the tree-ring width simulation, but instead to investigate their impact on the soil moisture simulation (Leaky Bucket model), because they are directly related to this latter model. In other words, if the interest were on understanding the

impact of each of these seven parameters on the soil moisture contents, one can easily perform the BSA for the Leaky Bucket model parameters to investigate that.

Our results are in agreement with those reported by the model developers (Tolwinski-Ward *et al.*, 2011), who suggested that only the four threshold parameters directly control the tree-ring formation through the partial growth response functions to temperature and soil moisture. Thus, it is logical that these parameters have a direct impact on the simulation of tree-rings from the model. Furthermore, they suggested that the impact of these four parameters is likely equal on the formation of tree-rings. However, we show that they are not equally likely effectual, and their contribution to the model output variability varies from one site to another. It is true that these four parameters are driving the uncertainty in the model output, but their ranking in terms of their influences is also site-specific, and varies from one site to another depending on the climatic conditions.

4.4.3   Sensitivity of VSLite Parameters to Climate Data

In the previous section we estimated the main effect factors for each of the VSLite model parameters at 26 different geographical locations. In this section we will summarise the effect of each individual parameter on the model output variability at different climate regions (with different climatic conditions: temperature and precipitation). In order to achieve that, we used an R package called "akima" which implements bivariate interpolation onto a grid for irregularly spaced input data. We utilized "akima" package to draw 3D figures for exploring the effect of the VSLite parameter on the model output variability to understand the influence of each individual parameter under different climates. This would help us to understand under every climatic scenario which model parameter is the most influential.

Figure 4.6 demonstrates the main effects of each of the key VSLite model parameters separately under different climate conditions. The plots in Figure 4.6 confirm
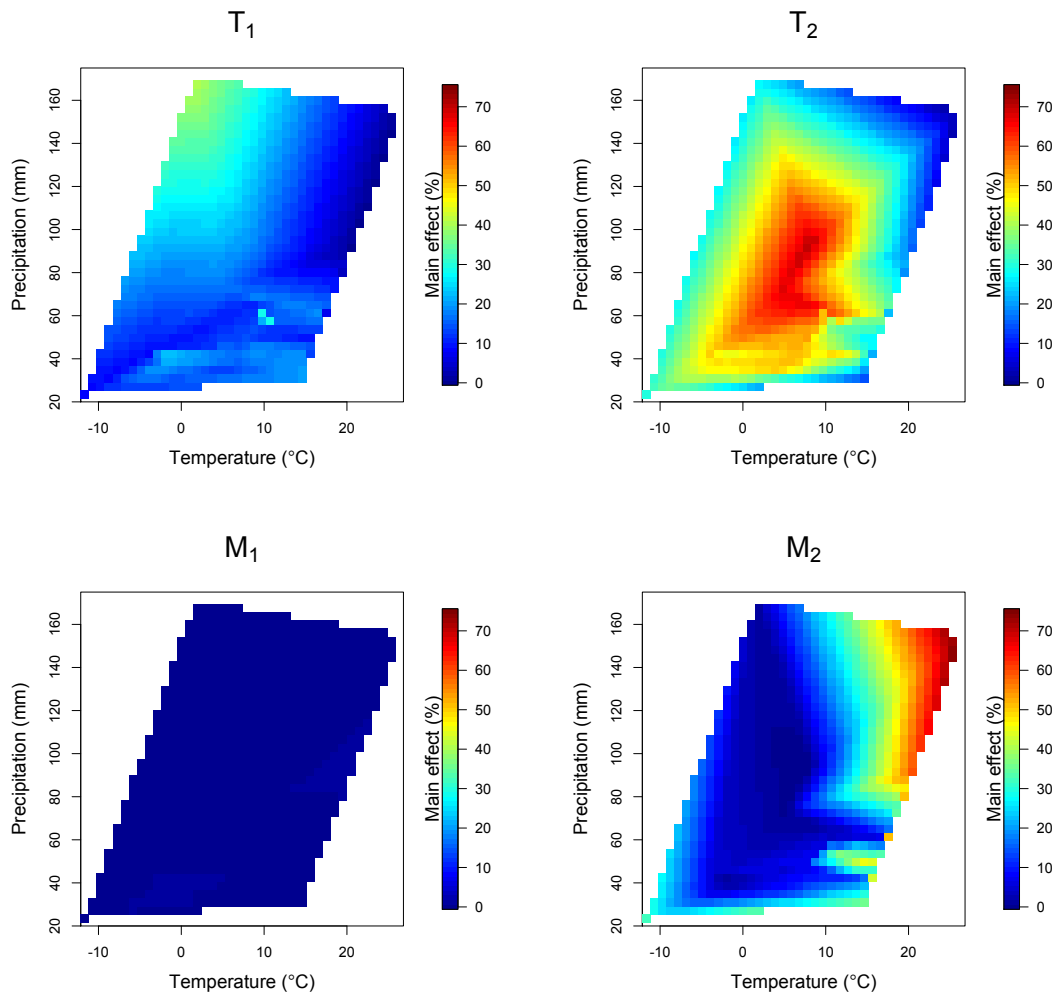
Figure 4.6: The sensitivity of VSLite parameters to the model input variation under different climate variables (mean monthly temperature and precipitation). Various colours represent the percentage of contribution (main effect) of each parameter to the model output variability, where blue is low and red is high.

that three parameters of the VSLite model (T_1, T_2 and M_2) contribute most to the variability of tree-ring widths simulated by the VSLite model. However, the impact of each is clearly not uniform across the climate range. For example, the parameter T_1 (Figure 4.6; top left panel) is influential to the model output variation in regions where temperature is relatively low and precipitation is high, while the parameter T_2 (Figure 4.6; top right panel) plays a significant contribution to the model output variation across a much wider range, but particularly in regions where the temper-

ature is between about $0\,°C$ to $10\,°C$ and the precipitation is between about 50 to 120 mm. The parameter M_1 (Figure 4.6; bottom left panel) has little contribution to the variation in model output in almost all different regions, and the tree-ring simulation from the VSLite model is insensitive to this parameter no matter what the climatic condition is in that region. However, the parameter M_2 (Figure 4.6; bottom right panel) is very influential on the model output variation in regions where the temperature is extremely high and the precipitation is very high too.

Similar to the parameter M_1, the percentage contribution of each of the last seven model parameters to the variability in tree-ring simulation was very small (less than 1%). Since their plots were very similar to that of the parameter M_1, we do not report them here, and the reader is referred to the BSA results for these parameters in Table 4.5.

Figure 4.6 helps us to understand under each climatic condition which input parameter is most important to the variation of the tree-ring width simulation from the VSLite model. The result can be classified and interpreted as follows:

- Cold and wet regions: in the regions when temperature is low and precipitation is high, T_1 and T_2 are influential, M_1 and M_2 are not influential.

- Cold and dry regions: in the regions when temperature is low and precipitation is low, parameters T_2 and M_2 are influential to the model output with T_2 dominant.

- Hot and wet regions: in the regions when temperature is high and precipitation is high, only T_2 and M_2 are influential to the model output with M_2 dominant.

- Hot and dry regions: in the regions when temperature is low and precipitation is high, parameters T_2 and M_2 are influential to the model output.

- Moderate climate: in the regions with moderate temperature and precipitation, parameters T_2 and M_2 are influential to the model output with T_2 dominant.

Therefore, the results of performing the Bayesian sensitivity analysis for the VSLite model enables identifying the most influential input parameters at each climate region, and also ranking/ordering the model parameters in terms of their importance. This is an essential step, especially when we want to make inference about the model parameters and learn about their true values.

The results of performing the BSA for varying all the VSLite model parameters together show that the main growth threshold $(T_1, \ T_2, \ M_1, \ M_2)$ contribute most to the variance in the tree-ring width simulation, with lesser contribution of the parameter M_1. The next step is to investigate the sensitivity of varying just these four parameters with their interactions to the model output variation. In the next section we will ignore the impact of the last 7 parameters, and just explore the sensitivity of the main four growth threshold parameters to the model output variability.

4.4.4 SA of Main Growth-threshold Parameters with their Interactions

The results of performing probabilistic sensitivity analysis, varying all 11 VSLite model parameters together, showed that the contribution of the last 7 parameters to the total variance of tree-ring simulation were very small, and the main growth threshold parameters (T_1, T_2, M_1, M_2) contributed the most to the variance in the tree-ring widths simulation. Consequently, in this section we investigate the sensitivity of these four parameters with their pair-wise interactions to the model output variability, and ignore the effect of the last 7 parameters. This is to examine whether there is any significant effects of any pair-wise interactions between the most influential parameters. We followed the same methodology performed in the previous sections to carry out the BSA; however, instead of varying all the 11 VSLite parameters, we varied just growth response parameters with a view to understanding how changes in these four parameters and their interactions will affect the model output variability. The last 7 parameters of the model were fixed to

their optimal values (given in Table 3.1) which we found in the literature and were used by the model developers (Haung *et al.*, 1996; Tolwinski-Ward *et al.*, 2011; Vaganov *et al.*, 2006). Table 4.6 illustrates the results of performing BSA for the VSLite model at Sheffield site when varying only the main four growth response parameters.

Parameters	Main effects (%)	Total effect (%)
T_1	31.02	34.69
T_2	59.36	64.01
M_1	0.78	4.11
M_2	1.05	4.40
$T_1 T_2$	1.75	
$T_1 M_1$	1.15	
$T_1 M_2$	0.77	
$T_2 M_1$	1.25	
$T_2 M_2$	1.65	
$M_1 M_2$	0.93	
Total	99.71	

Table 4.6: Main effect and pair-wise interactions, and total effects of the main four VSLite model parameters at Sheffield site.

Results in Table 4.6 shows that T_1 and T_2 are the most influential parameters for the variance of the simulated tree-ring widths, with T_2 dominant. The main effects of these two parameters alone sum to 90.38% of the total variance, while that of all four parameters and their interactions sums to 99.71% of the total variance; note that the main effects sum to approximately 100% due to including all the possible interactions. Table 4.6 also provides the effect of pair-wise interactions between model parameters which measure the amount of impact that these pair-wise interactions have on the model output variability. It is worth noticing that although the main effects of the parameter M_1 alone is very low (less than 1%), the interaction of this parameter with the others is rather larger. The main effect of pair-wise interactions $T_1 T_2$, $T_1 M_1$, $T_2 M_1$, and $T_2 M_2$ are relatively high (bigger than 1%), and therefore if taken together they might be influential to the model output variation, a feature of VSLite not explicitly noted by previous authors.

Results in this section show that the variability in the tree-ring widths simulated from the VSLite model, at Sheffield site, are almost totally controlled by the main four growth threshold parameters, which in total with their pair-wise interactions sum to 99.71% of the whole output variance. Similar results were also obtained, but not reported here, for the remaining 29 sites used in our investigations. This means that special attention should be paid to these four input parameters when using the VSLite model for any dendrochronological and palaeoclimatological studies.

4.5   Summary and Conclusions

In this chapter we implemented the VSLite model at different geographical locations around the world. We also applied a Bayesian sensitivity analysis (BSA) for the model which uses a Gaussian process emulator to explore the uncertainty in the model output. An emulator was successfully built for the model and then used to compute a range of variance-based sensitivity measures. To our knowledge, this is a first attempt made to apply this method to the VSLite. It is useful because it enables us to systematically identify the most influential input parameters in the model, and rank them in terms of their influence on the model output (tree-ring widths) variability.

Our results showed that, in general, parameters T_1, T_2 and M_2 appeared to have the biggest contribution to the model output variation. This suggests that the simulation of ring-widths from the VSLite model is strongly sensitive to at least one of these three parameters. The degree of impact among these three parameters however varies from one site to another. For example, T_2 had greatest impact on the model output variation in almost all of the 26 studied sites, whilst the parameter M_2 was very influential at some sites, but less influential in others depending on the climate data used to run the model.

In the next chapter we will utilize the results obtained in this chapter to fit

the VSLite forward model to tree-ring width data of known ages. We will use a Bayesian approach for estimating the most influential parameters in the model with a view to reducing the variability in the simulated ring-width indices before using the model for the dating purposes in the following chapter. The Bayesian approach enables us to combine the tree-ring data and our prior knowledge about the unknown parameters in each site of interest to make inference and learn about the true values of uncertain parameters.

Chapter 5

Bayesian Estimation for VSLite Model Parameters

5.1   Overview

The VSLite model has 11 uncertain parameters which drive the uncertainty in the model output. In the previous chapter we implemented the deterministic version of the model at different geographical locations around the world, and also used sensitivity analysis to explore model output uncertainty then quantitatively identified the most influential parameters in the model. This investigation allowed us to identify the most influential input parameters in the model, and rank them in terms of their influence on the model output variability. We concluded that three of the 11 VSLite parameters were most influential to the model output variability.

In this chapter, we use a hierarchical Bayesian modelling approach (offered in Section 5.3) to fit the VSLite forward model to tree-ring chronologies. This will help us to make inferences about the model error and the most influential uncertain parameters in the model with a view to learning about their true site-specific values. Taking only the most influential parameters into consideration helps to speed up the parametrization process and make inference about the model uncertainty. The main difference between Bayesian and classical inference is that the former allows us to quantify our beliefs about the unknown parameters via prior

distributions. However, the estimation of the VSLite model parameters at any particular region requires the availability of an annual ring-width chronology as well as monthly climate data (temperature and precipitation) for the site of interest. For this purpose, we investigated the Bayesian implementation of the VSLite model at a range of geographic locations in the UK, which has many ring-width chronologies and also has the longest climate data in the world. The available tree-ring chronologies in the UK are described in Section 5.2, and the Bayesian approach is outlined in Section 5.3. Results of applying the Bayesian approach to estimate VSLite growth threshold parameters for Quercus and Pinus trees in the UK are presented in Section 5.4.

5.2 Tree-ring Chronologies in the UK

Tree-ring data of two tree-species, Quercus and Pinus (the two most popular species used by dendrochronologists and dendroclimatologists) were chosen to fit the VSLite model and make Bayesian inferences about model parameters. The tree-ring data of known age for a range of geographical locations in the UK were obtained from the International Tree-ring Data Bank (ITRDB). The locations vary in the number of trees and the time period they cover. Figure 5.1 illustrates the geographic distribution of the selected locations that are chosen due to the availability of tree-ring width data of known age and their overlapped climatic records. The locations are well spread around the UK.

To avoid double use of the same dataset in the inference problem, the individual tree-ring data, at each site, were split into two equal groups, training (50%) and testing (50%) data. The training data were used in this chapter for estimating the VSLite growth threshold parameters. The testing data will be used in the following chapters for Bayesian implementation of the VSLite model and matching process (cross-matching undated sequences to a dated master chronology).

For each of the UK locations, a time-series of monthly temperature, $\mathbf{T}$, and precipitation, $\mathbf{P}$, data were also obtained from the Climate Research Unit (CRU-
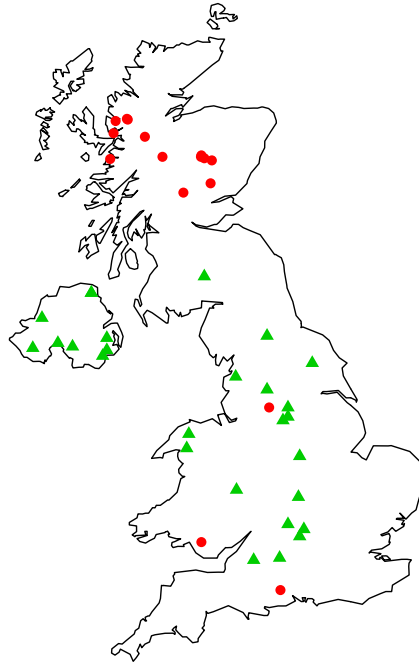
Figure 5.1: Distribution of the UK tree-ring chronologies of known age. *Circles* indicate Pinus and *triangles* indicate Quercus trees.

TS3.21), described in Section 4.1.2. These are not observational data but gridded model outputs estimated by Harris *et al.* (2014) using climate observations from meteorological stations. For each site, the nearest half-degree of these data were chosen and used as inputs to the VSLite model to generate ring-width sequences.

5.3 Bayesian Approach to Estimating VSLite Parameters

The VSLite model (introduced in Section 3.2.2) provides a useful tool for representing the relation between climate and ring-width growth. In the previous chapter, we showed that a simulated chronology's response to local climate variables was driven mostly by three growth threshold parameters (T_1, T_2, and M_2) which link the climate to the modelled ring-width indices. Therefore, if we need to control the uncertainty in the VSLite model output, and then eventually use the model

for cross-matching sequences, it is likely to be important to learn about the true values of these key parameters for any specific site under study.

With this motivation in mind, we used a Bayesian parameter estimation approach (Tolwinski-Ward *et al.*, 2013) to estimate the growth threshold parameters of the VSLite forward model. Tolwinski-Ward *et al.* (2013) originally applied their approach to Pinus trees in the USA alone. Additionally, they used noninformative, flat priors for the unknown parameters. In this chapter, we develop the Bayesian approach to use more realistic and informative priors and to estimate the growth threshold parameters, not only for Pinus but for Quercus trees as well, in the UK. The reason for choosing the UK for this investigation is the availability of relatively long observational climate records, which allows us, eventually, to investigate the use of the VSLite model for cross-matching ring-width sequences for dendrochronology (not just dendroclimatology as the original authors did). The four site-specific growth threshold parameters T_1, T_2, M_1 and M_2 can be estimated given actual ring-width chronologies under the Bayesian framework as follows. Although M_1 is not an influential parameter (as investigated in the previous chapter), we include it here in our Bayesian inference in order to compare our results with those obtained by model developers.

5.3.1 The Model

The ring-width indices y_t in year t (at the site of interest) is modelled as a VSLite model output $\hat{W}_t$ plus stochastic noise ϵ_t,

$$y_t = (\sqrt{1 - \sigma_\epsilon^2})\hat{W}_t + \epsilon_t, \tag{5.1}$$

where ;

- $y_t = (y_1, y_2, \ldots, y_n)$ is the observed site chronology of ring-width indices of length n years, obtained from using the method described in Section 2.3.

- $\hat{W}_t = (W_1, W_2, \ldots, W_n)$ is the deterministic VSLite estimate (as detailed in Equations 3.7 to 3.11) of a tree-ring width sequence of length n years

given monthly temperature $\mathbf{T}$ and precipitation $\mathbf{P}$ inputs, the model growth response parameters $\theta = (T_1,\ T_2,\ M_1,\ M_2)$, and site latitude ϕ,

$$\hat{W}_t = f(\mathbf{T}, \mathbf{P}, \phi, T_1, T_2, M_1, M_2).$$

For more information about calculating $\hat{W}_t$, the reader is referred to the description of the VSLite model in Section 3.2.2.

- $\epsilon_t = (\epsilon_1, \epsilon_2, \ldots, \epsilon_n)$ is the stochastic noise (error) vector accounting for both non-climatic factors (soil conditions, competition for light and nutrients, the presence of pests and diseases, and attack by humans or animals) and for influences of time series of processes that VSLite was not able to capture. ϵ_t follows an independent and identically distributed (i.i.d.) normal distribution with mean 0 and variance σ_ϵ^2, i.e. $\epsilon_t \sim N(0, \sigma_\epsilon^2)$.

- $\sigma_\epsilon^2 = \mathrm{Var}(\epsilon_t)$, is the variance of the model errors, and $\sigma_\epsilon^2 \leq 1$.

- Since both the time series of data and of VSLite output are standardized to have zero mean and unit variance, the sum of the climatic signal variance and the model noise variance is 1. "The coefficient $\sqrt{1 - \sigma_\epsilon^2}$ on the estimate from VSLite gives the proportion of the observed data's standard deviation that can be explained by VSLite as signal" (Tolwinski-Ward *et al.*, 2013, p.1483), and therefore the signal-to-noise ratio is $R = \frac{1 - \sigma_W^2}{\sigma_W^2}$.

5.3.2 The Likelihood

Given the data vector $y_t = (y_1, y_2, \ldots, y_n)$ of observed ring-width indices, the time-series of monthly climatic variables, and the VSLite growth threshold parameters, the likelihood for the model is defined as

$$p(\mathbf{y}|\mathbf{T}, \mathbf{P}, \boldsymbol{\theta}, \sigma_\epsilon^2) \propto \exp\left\{ -\frac{1}{2\sigma_\epsilon^2}(y_t - \sqrt{1 - \sigma_\epsilon^2}\hat{W}_t)^2 \right\}. \tag{5.2}$$

Note that the dependence on the VSLite growth threshold parameters $\theta = (T_1, T_2, M_1, \text{ and } M_2)$ is implicit in the deterministic estimate of the VSLite model out-

put $\hat{W}_t$, and σ_ϵ^2 indicates the error variance associated with the model uncertainty.

5.3.3 Specifying Priors

Under the Bayesian paradigm prior distributions are needed in order to make inference about the unknown parameters T_1, T_2, M_1, M_2, and σ_ϵ^2. For the mathematical convenience, all model parameters are assumed to be mutually independent (Tolwinski-Ward *et al.*, 2013), and this allows definition of the joint prior distribution as the product of individual prior models for each,

$$p(T_1, T_2, M_1, M_2, \sigma_\epsilon^2) = p(T_1) \ p(T_2) \ p(M_1) \ p(M_2) \ p(\sigma_\epsilon^2).$$

5.3.3.1 Prior for growth threshold parameters

Site-specific growth threshold parameters (T_1, T_2, M_1, and M_2) are necessary due to different climatic conditions and tree species. The selection of the prior distributions for these four parameters are based on a survey of current literature pertaining to biological growth thresholds in trees. Unlike the VSLite model developers (Tolwinski-Ward *et al.*, 2013) who used broad uniform and beta priors, we suggest using gamma distributions to represent our beliefs about the four VSLite growth threshold parameters.

We used gamma distribution priors for these parameters for two reasons. First, the gamma distribution has a non-negative range and a density function with slowly decaying tails, which makes it widely used for describing skewed data; and this is a feature of the VSLite partial growth response curves to temperature and soil moisture, which are functions of the growth threshold parameters. Second, the gamma distribution allows us to explore values for the VSLite growth threshold parameters outside the "optimal" ranges given in Table 3.1, which were defined by Tolwinski-Ward *et al.* (2011) for Pinus trees. This flexibility would allow us to apply the model not just to Pinus trees, but also to other species, such as Quercus trees.

We chose the mean of our gamma prior for each of the four growth response parameters to be equal to those used by the model developers (Vaganov *et al.*, 2006). In addition, we modelled our gamma priors with shape (α) and scale (β) parameters consistent with general scientific interpretation (determined by experts and given in Table 3.1) about the tree growth responses to both temperature and soil moisture variables. The Gamma distribution is defined by

$$
f(x) = \begin{cases} \frac{1}{\Gamma(\alpha)\ \beta^{\alpha}}\ x^{\alpha-1}e^{-x/\beta}, & \text{for } x \geq 0 \\ 0 & \text{otherwise} \end{cases}
$$

with $\alpha, \beta \geq 0$ and

$$
\Gamma(\alpha) = \int_0^{\infty} x^{\alpha-1}\exp(-x)\ dx.
$$

The expected value and variance of the Gamma distribution are $E(x) = \alpha\beta$ and $V(x) = \alpha\beta^2$, respectively. Figure 5.2 shows probability density functions for the Gamma with a selection of shape and scale parameters.

We use gamma distributions to represent our prior beliefs about the unknown growth parameters of the VSLite model as follows. For the parameter T_1, the minimum threshold temperature for ring-width growth to occur, we defined a gamma prior distribution $T_1 \sim \Gamma(\alpha_{T_1}, \beta_{T_1})$ with shape $\alpha_{T_1} = 10$ and scale $\beta_{T_1} = 0.5$ supported on the range $[0, \infty]$ which covers the optimal range of the T_1 parameter. This prior gives a mean of $5\,°C$ which is consistent with the widely accepted values suggested by Korner (2012).

There is little information available about T_2, the maximum threshold parameter which ring-width growth is no longer sensitive to temperature variabilities, in the literature. Vaganov *et al.* (2006) used a default value of $17\,°C$ in their case studies to simulate tree-ring sequences at different geographical locations. We define a
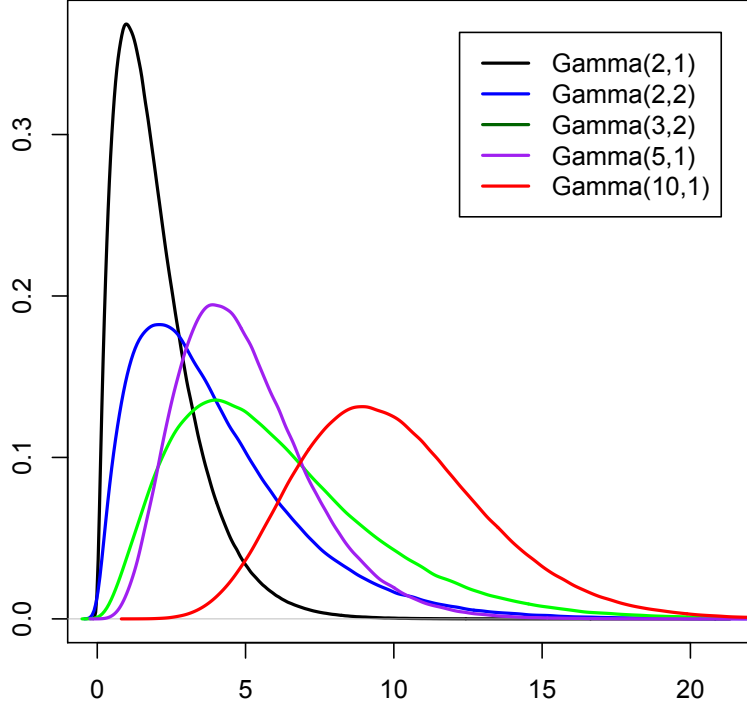
Figure 5.2: Probability density function of Gamma with different shape and scale parameters.

gamma prior distribution for this parameter as,

$$T_2 \sim \Gamma(\alpha_{T_2} = 34, \beta_{T_2} = 0.5).$$

The above prior gives a mean of $17\,^{\circ}\mathrm{C}$ which is very close to that used by Evans *et al.* (2006); Shi *et al.* (2008); Tolwinski-Ward *et al.* (2013); Touchan *et al.* (2012).

Similarly, we chose Gamma prior distributions for the two soil moisture growth threshold parameters M_1 and M_2 as follows,

$$M_1 \sim \Gamma(\alpha_{M_1} = 3.5, \ \beta_{M_1} = 0.01),$$

$$M_2 \sim \Gamma(\alpha_{M_2} = 2.5, \beta_{M_2} = 0.1),$$

where these two priors gives a mean of 0.035 and 0.25 for M_1 and M_2 respectively.

These two means are very close to those used by Tolwinski-Ward *et al.* (2013) as default values.

Prior for σ_ϵ^2

The prior for the model error variance σ_ϵ^2 was chosen to be conjugate. In the Bayesian hierarchical model, the inverse-gamma distribution is often used for the model variance parameter due to the conjugacy properties between the normal and inverse-gamma distributions which simplifies the sampling procedure (Gelman, 2006; Gilks *et al.*, 1996). Accordingly, the prior distribution for σ_ϵ^2 was chosen to be inverse-gamma with parameters $\alpha_\epsilon = 0.01$ and $\beta_\epsilon = 0.01$,

$$\sigma_\epsilon^2 \sim \text{Inv-Gamma}(\alpha_\epsilon = 0.01, \beta_\epsilon = 0.01).$$

Due to the use of a conjugate prior for this parameter the resulting posterior distribution is also inverse-gamma.

In summary we have the prior distributions for the VSLite model parameters listed in Table 5.1.

Parameters	Prior
T_1	Gamma($\alpha_{T_1} = 10, \beta_{T_1} = 0.5$)
T_2	Gamma($\alpha_{T_2} = 34, \beta_{T_2} = 0.5$)
M_1	Gamma($\alpha_{M_1} = 3.5, \beta_{M_1} = 0.01$)
M_2	Gamma($\alpha_{M_2} = 2.5, \beta_{M_2} = 0.1$)
ϵ	Normal($0, \sigma_\epsilon^2$)
σ_ϵ^2	Inv-Gamma($\alpha_\epsilon = 0.01, \beta_\epsilon = 0.01$)

Table 5.1: Table of prior distributions for VSLite parameters.

5.3.4 Obtaining Posterior Distributions

Given prior distributions for the unknown parameters, listed in Table 5.1, and an expression for the ring-width data, through the likelihood, given in Equation 5.2, we can obtain the joint posterior distribution of the VSLite parameters using Bayes' theorem,

$$
\begin{aligned}
p(\boldsymbol{\theta}, \sigma_\epsilon^2 | \mathbf{y}, \mathbf{T}, \mathbf{P}) \propto & \, p(\mathbf{y}|\mathbf{T}, \mathbf{P}, \boldsymbol{\theta}, \sigma_\epsilon^2) \, p(\boldsymbol{\theta}, \sigma_\epsilon^2) \\
\propto & \, p(\mathbf{y}|\mathbf{T}, \mathbf{P}, T_1, T_2, M_1, M_2, \sigma_\epsilon^2) \, p(T_1) \, p(T_2) \, p(M_1) \, p(M_2) \, p(\sigma_\epsilon^2) \\
\propto & \prod_{t=1}^{n} (\frac{1}{\sigma_\epsilon^2})^{\frac{1}{2}} \exp \left\{ -\frac{1}{2\sigma_\epsilon^2}(y_t - \sqrt{1 - \sigma_\epsilon^2}\hat{W}_t)^2 \right\} \times T_1^{(\alpha_{T_1} - 1)} \, e^{-T_1/\beta_{T_1}} \times \\
& T_2^{(\alpha_{T_2} - 1)} \, e^{-T_2/\beta_{T_2}} \times M_1^{(\alpha_{M_1} - 1)} \, e^{-M_1/\beta_{M_1}} \times M_2^{(\alpha_{M_2} - 1)} \, e^{-M_2/\beta_{M_2}} \times \\
& \left(\sigma_\epsilon^2\right)^{-(\alpha_\epsilon + 1)} \exp \left(-\frac{\beta_\epsilon}{\sigma_\epsilon^2} \right).
\end{aligned}
$$

Unfortunately, we are unable to analytically evaluate the posterior distribution above. However, we can use a Markov Chain Monte Carlo (MCMC) method which allows sampling from the full conditional distribution for each model parameter. In what follows we briefly describe the MCMC sampling procedures for the VSLite model parameters. For more information about general MCMC sampling algorithms, the reader is referred to Gilks *et al.* (1996).

5.3.5 Sampling Procedure

A Metropolis-Hastings algorithm within a Gibbs sampler, which is a standard MCMC sampling approach, is utilised in order to draw samples from the posterior distributions of the model parameters. These procedures can be outlined as follows.

1. Choose starting values $T_1^{(0)}, T_2^{(0)}, M_1^{(0)}, M_2^{(0)}$, and $\sigma_\epsilon^{2(0)}$

2. for $j = 1$ to N_{mcmc} (MCMC sample size)

   a) Draw a proposed value T_1' from the prior distribution of T_1.

   b) Calculate the likelihood of the proposed value,
      $p(\mathbf{y}|\mathbf{T}, \mathbf{P}, T_1', T_2^{(j-1)}, M_1^{(j-1)}, M_2^{(j-1)}, \sigma_\epsilon^{2(j-1)})$.

c) Calculate the likelihood of the current value,

$p(\mathbf{y}|\mathbf{T}, \mathbf{P}, T_1^{(j-1)}, T_2^{(j-1)}, M_1^{(j-1)}, M_2^{(j-1)}, \sigma_\epsilon^{2(j-1)})$.

d) With probability $\min\left\{1, \frac{p(\mathbf{y}|\mathbf{T},\mathbf{P},T_1',T_2^{(j-1)},M_1^{(j-1)},M_2^{(j-1)},\sigma_\epsilon^{2(j-1)})}{p(\mathbf{y}|\mathbf{T},\mathbf{P},T_1^{(j-1)},T_2^{(j-1)},M_1^{(j-1)},M_2^{(j-1)},\sigma_\epsilon^{2(j-1)})}\right\}$ set $T_1^{(j)} = T_1'$; otherwise, set $T_1^{(j)} = T_1^{j-1}$.

e) Repeat steps (a to d) to update T_2, using parameters $(T_1^{(j)}, M_1^{(j-1)}, M_2^{(j-1)}, \sigma_\epsilon^{2(j-1)})$.

f) Repeat steps (a to d) to update M_1, using parameters $(T_1^{(j)}, T_2^{(j)}, M_2^{(j-1)}, \sigma_\epsilon^{2(j-1)})$.

g) Repeat steps (a to d) to update M_2, using parameters $(T_1^{(j)}, T_2^{(j)}, M_1^{(j)}, \sigma_\epsilon^{2(j-1)})$.

h) Sample a value for $\sigma_\epsilon^{2(j)}$ from its full conditional distribution,

$p(\sigma_\epsilon^2|\mathbf{y}, \mathbf{T}, \mathbf{M}, T_1^{(j)}, T_2^{(j)}, M_1^{(j)}, M_2^{(j)})$.

3. Repeat step (2) until the Markov Chain reaches equilibrium.

4. After the burn-in period and thinning the subsequent iterations of step (2) using a suitable thin interval (discussed in Section 5.3.8), the resulted iterations are used as samples from the posterior.

5.3.6   Full Conditional Distributions

The full conditional distribution for each model parameter can be obtained from the joint posterior distribution above given all other parameters. Occasionally the conditional posterior distribution obtained has a standard distribution form, and hence a Gibbs update, which is a standard MCMC sampling method (Geman and Geman, 1984), can be used to sample draws from the obtained distribution. Alternatively, if the derived conditional distribution is not a standard distribution, then a Metropolis-Hastings update (Hastings, 1970), which is a more general MCMC sampling method can be performed. The full conditional posterior distributions for each VSLite parameters are defined below.

Conditional Posterior Distribution for Growth threshold Parameters

The calculation of the full conditional posterior distribution is similar for each of the four VSLite growth threshold parameters $\boldsymbol{\theta} = (T_1, T_2, M_1, M_2) = (\theta_1, \theta_2, \theta_3, \theta_4)$. With prior $\theta_i \sim \Gamma(\alpha_i, \beta_i)$, and the likelihood $p(\mathbf{y}|\mathbf{T}, \mathbf{P}, \boldsymbol{\theta}, \sigma_\epsilon^2)$, the full conditional distribution for each of the four VSLite parameter θ_i is

$$p(\theta_i|\mathbf{y}, \mathbf{T}, \mathbf{P}, \boldsymbol{\theta}_{-i}, \sigma_\epsilon^2) \propto p(\theta_i) \, p(\mathbf{y}|\mathbf{T}, \mathbf{P}, \boldsymbol{\theta}, \sigma_\epsilon^2)$$

$$\propto \theta_i^{(\alpha_i-1)} \exp\left(\frac{-\theta_i}{\beta_i}\right) \exp\left\{-\frac{1}{2\sigma_\epsilon^2}(y_t - \sqrt{1 - \sigma_\epsilon^2}\hat{W}_t)^2\right\}$$

$$\propto \theta_i^{(\alpha_i-1)} \exp\left\{-\left(\frac{\theta_i}{\beta_i} + \frac{1}{2\sigma_\epsilon^2}(y_t - \sqrt{1 - \sigma_\epsilon^2}\hat{W}_t)^2\right)\right\}.$$

where $i = 1, 2, 3, 4$, and $\boldsymbol{\theta}_{-i}$ denotes the vector of the four growth threshold parameters except θ_i. The conditional distributions for the parameters $\boldsymbol{\theta}$ are not standard distributions, thus we use the Metropolis-Hastings instead of a Gibbs update.

The Conditional Posterior Distribution of σ_ϵ^2

With prior $p(\sigma_\epsilon^2) \sim \Gamma^{-1}(\alpha_\epsilon, \beta_\epsilon)$, and likelihood $p(\mathbf{y}|\mathbf{T}, \mathbf{P}, \boldsymbol{\theta}, \sigma_\epsilon^2)$, the full conditional distribution of σ_ϵ^2 is

$$p\left(\sigma_\epsilon^2|\mathbf{y}, \mathbf{T}, \mathbf{P}, \boldsymbol{\theta}\right) \propto p(\sigma_\epsilon^2) \, p(\mathbf{y}|\mathbf{T}, \mathbf{P}, \boldsymbol{\theta}, \sigma_\epsilon^2)$$

$$\propto \left(\sigma_\epsilon^2\right)^{-(\alpha_\epsilon+1)} \exp\left(\frac{-\beta_\epsilon}{\sigma_\epsilon^2}\right) \times \exp\left\{-\frac{1}{2\sigma_\epsilon^2}(y_t - \sqrt{1 - \sigma_\epsilon^2}\hat{W}_t)^2\right\}$$

$$\propto \left(\sigma_\epsilon^2\right)^{-(\frac{n}{2}+\alpha_\epsilon+1)} \exp\left\{-\frac{1}{2\sigma_\epsilon^2}\left(\sum_{t=1}^{n}(y_t - \sqrt{1 - \sigma_\epsilon^2}\hat{W}_t)^2 + \beta_\epsilon\right)\right\}.$$

This has the form of inverse-gamma density. Thus the posterior distribution of $\sigma_\epsilon^2 \sim \Gamma^{-1}(a_\epsilon, b_\epsilon)$ where $a_\epsilon = (\frac{n}{2} + \alpha_\epsilon)$, and $b_\epsilon = \frac{1}{2}\sum_{t=1}^{n}(y_t - \sqrt{1 - \sigma_\epsilon^2}\hat{W}_t)^2 + \beta_\epsilon$.

5.3.7 Further Exploring Hierarchy in Model Parameters

Given the hierarchical nature of the Bayesian modelling structure discussed in this thesis, we could further extend the inference problem for the model parameters

by adding another hierarchy layer to the priors of the VSLite growth threshold parameters, and hence allow for the unknown hyperparameters to be updated from data. This is statistically defined as follows.

$$\mathbf{y}|\mathbf{T}, \mathbf{P}, T_1, T_2, M_1, M_2, \sigma_\epsilon^2 \sim N(\sqrt{1 - \sigma_\epsilon^2} \; \hat{W}_t, \sigma_\epsilon^2)$$

$$\sigma_\epsilon^2 \sim \text{Inv-Gamma}(\alpha_\epsilon, \beta_\epsilon)$$

$$T_1|\alpha_{T_1}, \beta_{T_1} \sim \text{Gamma}(\alpha_{T_1}, \beta_{T_1})$$

$$\alpha_{T_1} \sim U(a_1, b_1)$$

$$\beta_{T_1} \sim U(a_2, b_2)$$

$$T_2|\alpha_{T_2}, \beta_{T_2} \sim \text{Gamma}(\alpha_{T_2}, \beta_{T_2})$$

$$\alpha_{T_2} \sim U(a_3, b_3)$$

$$\beta_{T_2} \sim U(a_4, b_4)$$

$$M_1|\alpha_{M_1}, \beta_{M_1} \sim \text{Gamma}(\alpha_{M_1}, \beta_{M_1})$$

$$\alpha_{M_1} \sim U(a_5, b_5)$$

$$\beta_{M_1} \sim U(a_6, b_6)$$

$$M_2|\alpha_{M_2}, \beta_{M_2} \sim \text{Gamma}(\alpha_{M_2}, \beta_{M_2})$$

$$\alpha_{M_2} \sim U(a_7, b_7)$$

$$\beta_{M_2} \sim U(a_8, b_8),$$

although other options for modelling the hyper-priors would clearly be available.

The values of the all 18 hyperparameters $(\alpha_\epsilon, \beta_\epsilon, a_1, \ldots, a_8, b_1, \ldots, b_8)$ would be determined in a way that makes the prior broad and vague to allow for the hyperparameters to be updated from data; hence the suggestion of uniform flat priors. However, we do not implement this model in this thesis for two reasons. First, it would add considerably to the computational time as we would need to update nine parameters $(\alpha_{T_1}, \alpha_{T_2}, \alpha_{M_1}, \alpha_{M_2}, \beta_{T_1}, \beta_{T_2}, \beta_{M_1}, \beta_{M_2}, \sigma_\epsilon^2)$, instead of five. We prefer to avoid this extension, because eventually (in the following chapters) we need to use the model for a matching process as part of the dendrochronological dating which adds its computational expensive. Second, there is substantial information available about the optimal values of growth threshold parameters provided in the

literature, which we use to help define priors for the model parameters without necessarily needing to add another hierarchy layer.

5.3.8 MCMC Convergence

When performing an analysis using MCMC method, it is essential to check the convergence (i.e. stationarity) of the chain for each parameter to ensure that it has converged to the target distribution so that we can make inferences. Reaching convergence is thus a key implementation issue associated with any MCMC-based method. There are several types of convergence diagnostics that can be used to achieve this goal. In Bayesian statistics, we do not only depend on one diagnostic method, but rather more than one, to check the convergence of parameters. Consequently, we used several diagnostics listed below for assessing the stationarity of MCMC chains, in this and following chapters.

- **Visual inspection**

  Visually inspecting a time series (trace plot) of the chain for each parameter to see whether the sequences are moving around the parameter space or get "stuck" in certain areas. If the MCMC iterations are mixing well (moving around the parameter space), and the chain does not take a long time to move around the parameter space, then it is assumed that the chain has converged to its stationary distribution.

- **Different starting values**

  Different starting values were used to generate several different MCMC chains for each parameter. When the trace plots of such chains overlap one another after a suitable burn-in and all lead to the same estimates for the true posterior distributions, then we assume the chain has converged.

- **Raftery and Lewis diagnostic**

  The Raftery and Lewis diagnostic technique (Raftery and Lewis, 1992) was also utilized for each parameter in order to estimate the total run length of

MCMC needed, to be discarded as a burn-in period (number of iterations throwing away at the beginning of Markov chain), and the appropriate thinning interval (discard all but every nth observation) required to produce an independence between the stored output values. In almost all cases in our experiments, the MCMC reached its stationary distribution after a short period of burn-in. Thus, a period of 1000 iterations were chosen to be used as burn-in.

- **Gelman and Rubin**

  A more formal and reliable diagnostic technique by Gelman and Rubin (1992) was also applied for checking the MCMC stationarity. The idea behind this diagnostic technique is to run two or more MCMC chains from very different starting values to see if they converge to an identical distribution.

  This technique can be summarised as follows. Suppose we generate k MCMC chains each of length $2k$, and we discard the first k iterations as burn-in. Then, we calculate the within chain (V) and between-chain (V') variances,

  $$V = \frac{1}{k} \sum_{j=1}^{k} \frac{1}{n-1} \sum_{i=1}^{n} (Y_{ij} - \bar{Y}_j)^2,$$

  $$V' = \frac{n}{k-1} \sum_{j=1}^{k} (\bar{Y}_j - \bar{\bar{Y}})^2$$

  where n is the number of iterations (sample size) in each chain, Y_{ij} is the i-th generated value of chain j, $\bar{Y}_j = \frac{1}{n} \sum_{i=1}^{n} Y_{ij}$, and $\bar{\bar{Y}} = \frac{1}{k} \sum_{j=1}^{k} \bar{Y}_j$.

  The variance of the stationary distribution can then be estimated as a weighted average of within-chain and between-chain variances.

  $$\hat{\text{Var}}(Y) = \frac{n-1}{n} V + \frac{1}{n} V'.$$

  Now the Gelman and Rubin $\hat{R}$ factor can be calculated as $\hat{Q} = \sqrt{\frac{\hat{\text{Var}}(Y)}{V}}$.

Gelman and Rubbin (1992) suggest that a value of $\hat{Q}$ below 1.1 should be acceptable indication of a converged MCMC. If $\hat{Q}$ is greater than 1.1, then the chain is not converged yet and the sampler should rerun for a larger number of iterations until it has converged and stationarity has been achieved.

This diagnostic test is used for all experiments in the next sections to check the MCMC convergence for all parameters. We ran three MCMC chains with 10000 iterations each after a burn-in period of 1000 iterations. Whenever it suggests that the sampler has not converged, then the MCMC was run for a greater number of samples until it had converged.

Since it is common practice in Bayesian statistics to use more than one diagnostic method to check the convergence of MCMC chains, we did not depend on only one method, but different diagnostics (listed above) were implemented, in this and following chapters, for checking the convergence of MCMC chains. The posterior estimate plots and diagnostic checking, in this thesis, were calculated using two R packages, "*boa*" (Smith, 2007) and "*coda*" (Plummer *et al.*, 2006).

A Bayesian approach has been defined for estimating the uncertain VSLite model parameters with all necessary notation and prior distributions required. The full conditional distribution for all parameters have been detailed leading to the Metropolis-Hastings within Gibbs sampling procedure required for the Bayesian MCMC implementation. Experiments are now needed to investigate the Bayesian implementation before moving on to use the model for the matching process and tree-ring dating.

5.4 Estimating VSLite Model Parameters for the UK Chronologies

This section contains results of the experiments to estimate the VSLite model parameters at a range of UK locations discussed in Section 5.2. We applied the Bayesian approach, described in Section 5.3, to estimate the VSLite growth response parameters independently at each of the 40 sites in the UK. The parameter estimation at each site was conditioned on the associated actual ring-width index chronology, $\mathbf{y}$, and observed monthly climate data series, $\mathbf{T}$ and $\mathbf{P}$.

The results presented in this section are the Bayesian approach estimates of the four VSLite growth threshold parameters (T_1, T_2, M_1, and M_2) and the model error parameter, σ_ϵ^2. The posterior estimates of the model parameters vary from one site to another, and for the two tree types, Quercus and Pinus. The full posterior distributions of the model parameters, at each site, provided information about the relationship between climate and ring-width and the uncertainty in the model parameters that links them. Two examples of experiments, one of Quercus and one of Pinus, are presented here. Collective results from the other 38 sites are summarised and plotted in Section 5.4.3.

At each site, we implemented the Bayesian approach and provide a table and histogram plot for the posterior estimates of the main VSLite parameters. Each table contains summary statistics including mean, 1st quartile, 2nd-quartile (median), 3rd-quartile, and 95% highest probability density (HPD) interval of the posterior distribution for each parameter. Tables also contain the number of iterations that the MCMC chains were thinned by and how many iterations were required to ensure that the chains had converged and thus the results were reproducible. All posterior estimates of the model parameters are reproducible to two decimal places. Posterior histogram and MCMC convergence checking for each experiment are not reported but have been undertaken, using the diagnostic methods described in Section 5.3.8. The following are results of the Bayesian parameter estimation for two representative sites in the UK, one with Quercus trees (Sheffield, $53.37^o N$

and $-1.50^o E$) and one with Pinus trees (Porter Brook, $53.50^o N$ and $-1.95^o E$).

5.4.1 Results for "Sheffield" Site with Quercus Trees

This section provides detailed results from implementing the Bayesian methodology and the MCMC algorithm for one representative Quercus tree site. The tree-ring data and monthly climate records for this geographical location were both obtained from the ITRDB and the CRU, respectively.

With extreme starting values set for the model parameters $(T_1, T_2, M_1, M_2, \sigma_\epsilon^2)$, we have a MCMC chain of length 10,000, after 1000 iterations burn-in (on the advice of the convergence diagnostic methods described in Section 5.3.8) and after the MCMC chain had been thinned every 10 iterations. After being satisfied that the MCMC chain for each parameter had converged, the associated summary statistics in Table 5.2 and marginal posterior distributions shown in Figure 5.3 were obtained.

Parameter	Mean	1st Qu	2nd Qu	3rd Qu	95% HPD	
					Lower	Upper
T_1	6.08	6.09	4.89	7.17	2.81	8.97
T_2	15.48	15.04	13.73	16.87	11.63	20.08
M_1	0.036	0.034	0.028	0.047	0.032	0.073
M_2	0.537	0.531	0.437	0.639	0.09	0.85
σ_ϵ^2	0.69	0.68	0.63	0.74	0.55	0.82

Table 5.2: Posterior estimates for VSLite parameters at Sheffield, from the converged MCMC chains of length 10,000 iterations.

The mean, first, second and third quartiles reported in Table 5.2 denote the central location tendency estimates of the VSLite growth threshold parameters $(\hat{T}_1, \hat{T}_2, \hat{M}_1,$ and $\hat{M}_2)$ at this particular location. These point estimates allow us to interpret the behaviour of the climate response to tree-ring growth at this geographical location. We can see for instance that the mean posterior estimate of T_1, which is the minimum threshold temperature for ring-width growth to occur, is
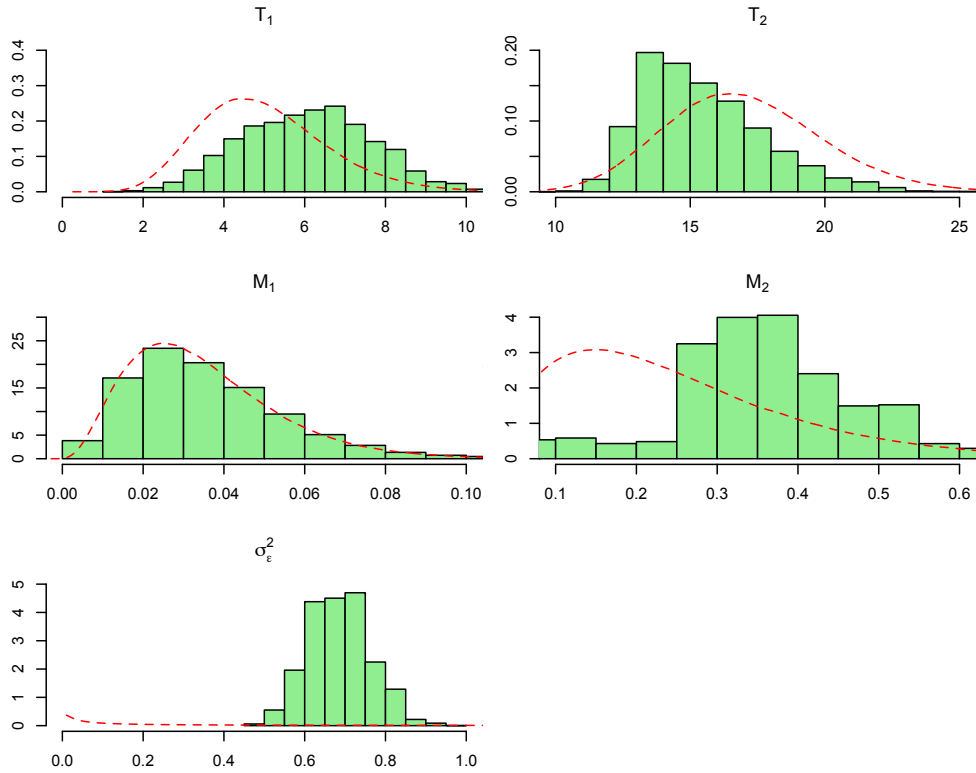
Figure 5.3: Prior density (*dashed line*) and histogram plots of the marginal posterior distributions estimated by applying the MCMC sampling approach to estimating the VSLite model parameters at Sheffield site.

equal to 6.08 at this geographical location. Similarly, the mean posterior estimate of T_2, which is the temperature above which tree-ring growth is no longer sensitive to temperature, is equal to 15.48. Our estimates of the model parameters are in agreement with the currently debated temperature and soil moisture thresholds (discussed in Section 5.3.3). The HPD indicates the highest probability density interval for each parameter which covers a region of $(1 - \alpha) \times 100\%$ of the posterior density including the mode assuming uni-modal marginal distribution. We can use HPD intervals to check where the most of the posterior probability lies. For instance, a 95% HPD of the lower temperature threshold parameter, T_1, indicates that we are 95% sure that the value of T_1 lies in the interval [2.81, 8.97]. It is worth noticing that the HPD of the upper temperature threshold parameter, T_2

has exceeded its optimal range, which suggests that different prior distributions might give different optimal range for each parameters. The spread of the posterior estimates for the model parameters in Figure 5.3 reveals the variability in their estimated values and the degree to which both the tree-ring and climate data informed the estimated parameter values. In other words, the sensitivity of the posterior estimates to the choice of prior distributions demonstrate the extent to which whether the data or the prior informed the estimated posteriors most. Accordingly, the degree of Bayesian learning, at this particular site, varies between parameters as we can see that there is enough information in the data to learn about model parameters except for the parameter M_1 which tends to be entirely dominated by the prior distribution used.

5.4.2 Results for "Porter Brook" Site with Pinus Trees

Similarly, we show results of implementing the Bayesian approach for a representative Pinus tree site in the UK, called "Porter Brook".

Table 5.3 and Figure 5.4 show respectively summary statistics and histogram plots of the estimated posterior distributions for VSLite model parameters (T_1, T_2, M_1, M_2, and σ_ϵ^2) at the Porter Brook site.

					95% HPD	
Parameter	Mean	1st Qu	2nd Qu	3rd Qu	Lower	Upper
T_1	3.56	3.55	2.86	4.23	3.55	5.62
T_2	12.19	11.65	10.85	14.88	11.65	20.28
M_1	0.041	0.038	0.025	0.053	0.038	0.094
M_2	0.56	0.45	0.44	0.72	0.45	0.93
σ_ϵ^2	0.64	0.63	0.58	0.69	0.63	0.79

Table 5.3: Posterior estimates for VSLite parameters at Porter Brook, from the converged MCMC chains of length 10,000 iterations.

It is clear from the results of these two representative sites that despite using the same prior for the unknown growth threshold parameters, some evidence for
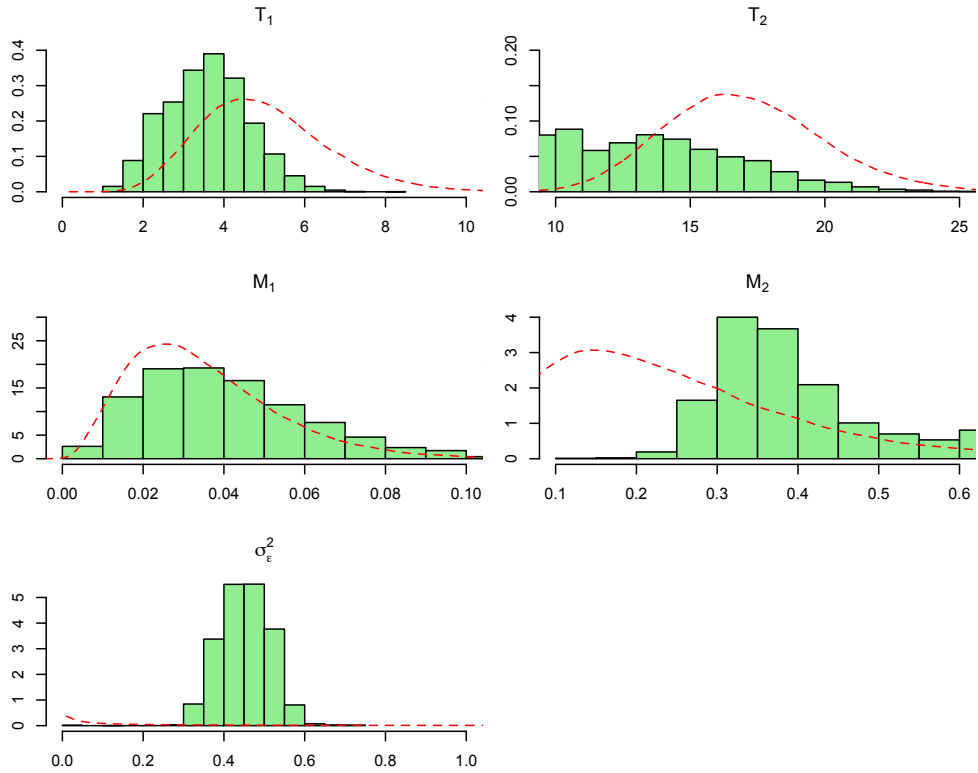
Figure 5.4: Histogram plots of the marginal posterior distributions estimated by applying the MCMC sampling approach to estimating the VSLite model parameters at Porter Brook site.

species-dependent distributions exists. For Pinus trees, our estimates of temperature threshold parameters, T_1 and T_2, are lower than for Quercus trees, while M_2 is higher for Pinus trees. These indicates that the Pinus trees are more sensitive to lower temperature and higher soil moisture conditions. However, there is no such evidence for species-dependence for parameter M_1 at these two representative sites since the results showed that the VSLite does not model this parameter very well and thus we learn little about M_1 from the data.

Although these two geographical locations, Sheffield and Porter Brook, are very close and thus exposed to similar climates, the VSLite model behaves slightly differently to different tree-species. Figure 5.5 shows the distribution of differences between posterior estimates for the VSLite parameters from two different tree-

115

species (Quercus and Pinus).
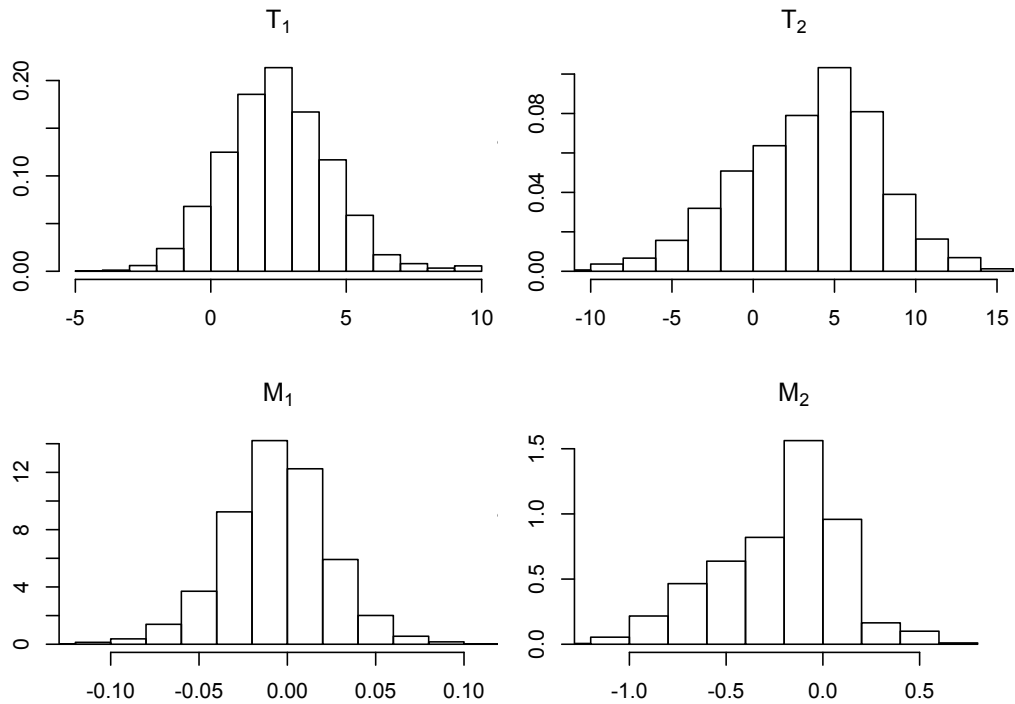
Figure 5.5: Histogram plots of the pairwise differences between our posterior estimates for the VSLite growth threshold parameters from two different tree-species (Quercus and Pinus) at two geographically close sites (Sheffield and Porter Brook).

As we can see that the distribution of differences are skewed to the right for parameter T_2, while it is skewed to left for the parameter M_2, which indicates that there is some differences between tree-species. Furthermore, the scale of differences for these two parameters (T_2 and M_2) seems very large compared with their optimal ranges. These variations in the estimates of the growth threshold parameters between Quercus and Pinus trees are noticeable, which might reflect the adaptation of Pinus trees to lower temperature and higher soil moisture growth threshold values.

5.4.3 Sensitivity of Posterior Estimates to Prior Choices

In this section we used three different prior distributions to implement the Bayesian approach and make inference about the VSLite model parameters at 40 sites in the UK. The posterior estimates resulted from using our proposed gamma priors, detailed in Section 5.2, compared to the uniform and beta priors suggested by the model developers (Tolwinski-Ward *et al.*, 2013). This enables us to check the sensitivity of the posterior estimates to the prior used. We examined the performance of each of the three proposed prior distributions for the VSLite model parameters by comparing the posterior density estimates (Figure 5.6) and summary statistics (Table 5.4) from the resulting posterior distributions using each of the three proposed priors. Based on the experiments for all the UK chronologies, the posterior estimates for the unknown model parameters at each site were obtained from the MCMC and the performance of the prior distributions were evaluated.

Figure 5.6 and Table 5.4 show respectively the marginal posterior density estimates and summary statistics (posterior median) for the VSLite parameters obtained from the MCMC chains using the three prior distributions under consideration (Uniform, Beta and Gamma). We are interested in calculating and reporting a summary statistic and choose the posterior median, because it is probably the best compromise in being robust for heavy tailed densities.

The results of our experiments show that there is some difference between the estimated posteriors using different prior distributions except for the M_1 parameter, about which we appear to learn little from the data. The degree of Bayesian learning for the other three parameters varies from one site to another. Specifically, posterior densities of the upper growth thresholds, T_2 and M_2, show that there is reliably enough information in the data to make inference about these two parameters. By contrast, the posterior density estimates for the parameter T_1 at most sites, especially for Quercus trees, are close to the prior distribution used.

117
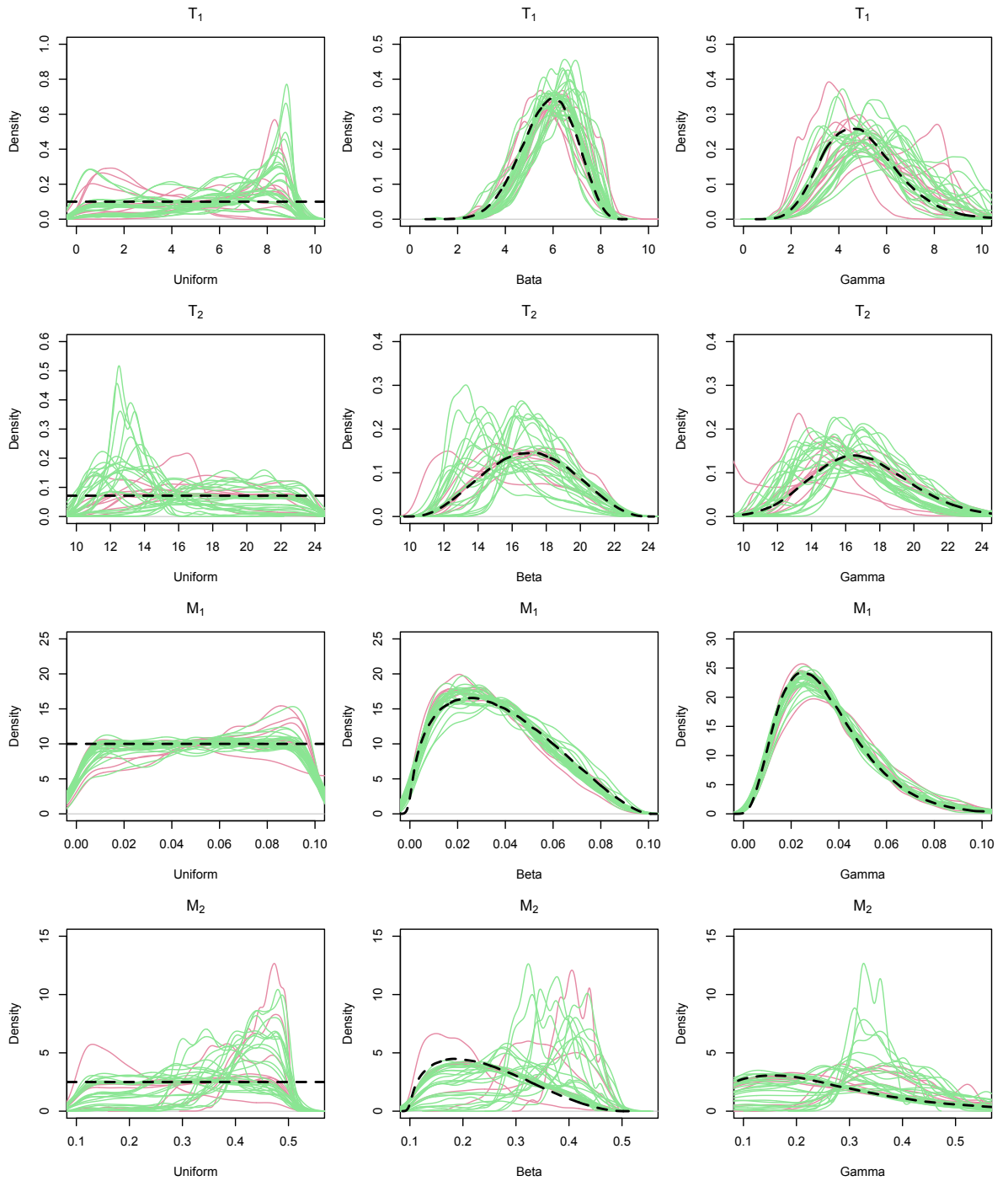
Figure 5.6: Prior (*dashed line*) and estimated posterior (*solid line*) densities for the four VSLite growth threshold parameters $\hat{T}_1$, $\hat{T}_2$, $\hat{M}_1$, and $\hat{M}_2$ at 40 different sites in the UK for two tree types, Quercus (*green*) and Pinus (*red*).

Site	Code	Lat.	Long.	Taxon	Uniform				Beta				Gamma			
					T_1	T_2	M_1	M_2	T_1	T_2	M_1	M_2	T_1	T_2	M_1	M_2
1	brit64	51.07	-1.38	Quercus	5.68	13.07	0.051	0.43	5.94	14.07	0.034	0.4	5.23	15.4	0.032	0.49
2	brit002	51.37	-2.32	Quercus	6.35	15.71	0.050	0.38	6.13	15.12	0.033	0.34	5.48	15.8	0.032	0.39
3	brit063	51.4	-1.7	Quercus	5.19	18.58	0.047	0.32	5.88	16.64	0.031	0.28	4.87	16.57	0.031	0.25
4	brit061	51.7	-1.22	Quercus	5.91	16.73	0.050	0.35	6	16.55	0.032	0.29	5.35	16.55	0.031	0.3
5	brit4	51.8	-1.12	Quercus	4.49	18.47	0.064	0.42	5.83	16.86	0.041	0.37	4.9	17.26	0.036	0.4
6	brit059	51.87	-1.5	Quercus	6.14	13.41	0.052	0.43	5.97	14.45	0.034	0.39	5.31	15.46	0.032	0.48
7	brit031	52.25	-1.25	Quercus	5.55	19.6	0.049	0.32	5.94	17.85	0.032	0.27	5.2	17.84	0.031	0.25
8	brit010	52.35	-2.73	Quercus	6.6	13.76	0.052	0.44	5.99	14.82	0.034	0.38	5.39	15.52	0.032	0.48
9	brit011	52.82	-1.22	Quercus	6.26	13.85	0.052	0.37	6.06	15.25	0.033	0.3	5.51	15.27	0.032	0.34
10	brit2	52.93	-3.92	Quercus	6.35	15.16	0.043	0.34	6.05	15.69	0.033	0.32	5.53	15.74	0.032	0.36
11	brit040	53.13	-3.87	Quercus	2.83	12.87	0.066	0.48	5.64	13.96	0.044	0.48	4.26	15.4	0.036	0.57
12	brit12	53.32	-1.62	Quercus	6.96	16.51	0.041	0.27	6.24	16.98	0.033	0.25	5.9	16.53	0.031	0.22
13	brit053	53.37	-1.5	Quercus	7.51	12.84	0.053	0.45	6.38	13.61	0.033	0.4	6.09	15.04	0.032	0.53
14	rit033	53.5	-1.5	Quercus	6.11	16.56	0.033	0.25	6.11	16.56	0.033	0.25	5.68	15.97	0.031	0.24
15	brit035	53.75	-2	Quercus	4.28	19.76	0.057	0.36	5.5	17.56	0.037	0.33	4.47	18.03	0.034	0.34
16	brit013	53.93	-2.75	Quercus	7.92	13.44	0.052	0.43	6.46	14.57	0.033	0.33	6.65	15.31	0.032	0.45
17	brit6	54.4	-7	Quercus	4.92	19.68	0.053	0.34	5.72	17.71	0.034	0.3	4.83	17.93	0.032	0.3
18	brit11	54.12	-0.92	Quercus	4.66	15.74	0.051	0.37	4.98	16.23	0.033	0.25	5.78	16.29	0.032	0.29
19	brit057	54.22	-5.93	Quercus	8.33	14.04	0.050	0.41	6.54	15.53	0.032	0.26	7.21	15.59	0.032	0.36
20	brit044	54.33	-7.6	Quercus	4.98	16.41	0.054	0.39	5.72	15.81	0.036	0.37	4.85	16.72	0.033	0.41
21	brit058	54.35	-6.65	Quercus	6.29	15.59	0.049	0.26	6.03	16.03	0.032	0.24	5.56	16.05	0.032	0.21
22	brit028	54.47	-5.83	Quercus	6.27	14.72	0.050	0.32	6.04	15.64	0.033	0.27	5.54	15.66	0.031	0.28
23	brit001	54.75	-7.38	Quercus	7.32	17.05	0.049	0.3	6.35	17.14	0.033	0.24	6.03	16.93	0.031	0.22
24	brit	55.1	-6.2	Quercus	6.8	16.32	0.049	0.28	6.19	16.59	0.032	0.24	5.79	16.49	0.031	0.21
25	brit7	55.33	-3.5	Quercus	6.5	17.52	0.048	0.3	6.13	17.02	0.032	0.26	5.49	16.83	0.032	0.23
26	brit021	56.63	-3.35	Quercus	7.82	16.46	0.049	0.28	6.38	17.4	0.032	0.24	6.12	17.08	0.032	0.21
27	brit017	56.95	-3.32	Pinus	2.64	13.72	0.058	0.34	4.75	14.6	0.036	0.32	4.39	13.69	0.034	0.28
28	brit049	56.97	-5.75	Pinus	4.33	15.72	0.049	0.31	5.04	15.63	0.032	0.24	5.2	15.5	0.031	0.23
29	brit022	56.98	-3.5	Pinus	5.25	16.38	0.052	0.33	5.92	13.96	0.025	0.31	4.97	15.46	0.032	0.26
30	brit015	57	-3.58	Pinus	6.88	17.59	0.040	0.29	5.38	15.92	0.029	0.19	5.92	15.57	0.030	0.14
31	brit020	57.02	-3.57	Pinus	4.72	13.04	0.049	0.31	5.06	15.82	0.032	0.24	5.26	15.66	0.031	0.23
32	brit024	57.28	-4.92	Pinus	2.09	16.43	0.051	0.32	4.42	14.92	0.033	0.25	4.36	14.99	0.031	0.22
33	brit048	57.33	-5.67	Pinus	2.56	16.1	0.050	0.28	4.75	13.92	0.033	0.24	4.91	15.87	0.031	0.22
34	brit016	57.5	-5.62	Pinus	4.29	15.05	0.050	0.32	5.48	14.29	0.028	0.27	5.09	14.48	0.031	0.25
35	brit018	57.52	-5.33	Pinus	6.11	16.36	0.049	0.3	5.08	16.01	0.032	0.24	5.31	14.82	0.031	0.22
36	brit026	57.53	-5.35	Pinus	4.51	16.48	0.051	0.32	5.53	14.5	0.028	0.28	5.12	15.68	0.031	0.24
37	brit019	50.95	-1.68	Pinus	4.77	16.58	0.051	0.3	5.14	15.05	0.031	0.24	5.26	14.89	0.032	0.22
38	brit10	51.62	-3.57	Pinus	3.2	14.65	0.053	0.34	4.95	15.33	0.034	0.31	4.83	15.29	0.033	0.32
39	brit032	53.5	-1.95	Pinus	5.14	14.76	0.050	0.3	5.08	15.91	0.032	0.24	5.47	15.76	0.032	0.22
40	brit038	54.22	-2.3	Pinus	3.39	14.24	0.053	0.32	4.91	15.26	0.034	0.3	4.93	14.23	0.032	0.31

Table 5.4: Medians of the posterior distribution for the VSLite parameters at 40 sites in the UK (given in Figure 5.1), using three different priors. Calculated from the converged MCMC chains of length 10,000. Lat indicates latitude and Long indicates longitude.

In regards the effect of the prior choices on the Bayesian estimates, the beta and gamma priors tend to produce posterior estimates with smaller variances than

using the uniform priors. As expected, when using uniform priors for the unknown parameters, the posterior probability estimates tend to be widely spread over the "optimal" range of the growth threshold parameters (as shown in Figure 5.6, first column), hence the posterior distributions have larger variances. On the other hand, using beta and gamma priors tend to provide posterior estimates that are more concentrated, hence the posterior variances are smaller. This suggests that uniform priors should only be used for representing beliefs about the VSLite growth threshold parameters when there is insufficient knowledge available in the literature about the "optimal" values for these uncertain parameters. Hence, this flat priors can be useful when using the VSLite model for other tree-species which we have no (or limited) information about their growth threshold parameters. However, for our chosen tree-species (Quercus and Pinus) in this thesis, there is a substantial amount of information provided by biologists and botanists in the literature about the optimal values of the growth threshold parameters for Quercus and Pinus trees. Thus, it is logical and statistically reasonable (from a Bayesian perspective) to use this information in the statistical inference via considering appropriate priors for these unknown parameters. Consequently, we will be using gamma priors for the VSLite growth threshold parameters in our investigation of the model for Bayesian tree-ring dating in the next chapters.

Results in Table 5.4 show the posterior medians of VSLite parameters at each of the 40 sites in the UK. The posterior medians of the lower threshold temperature, T_1, for all the UK sites fall within 2–9 °C (using uniform prior), 4–7 °C (using beta prior) and 4–7.5 °C (using gamma prior); whereas the posterior medians of the upper threshold temperature T_2 fall within 12–20 °C (using uniform prior) and 14–18 °C (using beta or gamma priors). Similarly, the posterior medians of the lower threshold soil moisture M_1 fall within 0.03–0.07 (using uniform prior), 0.03–0.045 (using beta prior) and 0.03–0.037 (using gamma prior); while the posterior medians of the upper threshold soil moisture M_2 fall within 0.25–0.50 (using uniform prior), 0.15–0.50 (using beta prior) and fall within 0.1–0.6 (using gamma prior).

5.5   Summary of Chapter

The number of different potential prior distributions for the unknown parameters in the Bayesian inference can cause difficulties in choosing the best one, especially when these priors do not produce similar results. Thus, in this chapter, we investigated a Bayesian analysis using various prior distributions for estimating VSLite parameters at a range of the locations across the UK. Alongside the two priors used by Tolwinski-Ward *et al.* (2013), we also investigated using a gamma prior for the unknown growth threshold parameters with the target means similar to those of the beta priors. We found that the gamma distribution was more appropriate for representing our beliefs about the VSLite parameters.

The sensitivity of the posterior estimates to different priors used was also examined. From this analysis we found that it is essential to select priors for the VSLite parameters carefully, especially when there is not enough biological information available about the growth threshold parameters for the tree-species under study. In such cases, the posterior estimates become more sensitive to the prior used, and hence the choice of the appropriate priors become more relevant. Thus, in remainder of this thesis we will be using gamma priors, which are more suitable for the VSLite growth threshold parameters.

In the next chapter the Bayesian approach for the VSLite model implemented in this chapter will be extended to include a matching step to be used for Bayesian tree-ring dating. The inference problem will remain similar, but an extra parameter will be added to the model to account for cross-matching ring-width sequences and hence providing a posterior probability of a match at each possible offset.

Chapter 6

Bayesian Dendrochronology Using VSLite Model

Cross-matching (or cross-dating) is a process of matching a group of trees from the same (or neighbouring) geographical location one with another and thus, if one or more is of known age, dating each ring in all trees to their exact year of formation. Traditionally, statistical methods (detailed in Chapter 2) such as cross-correlation coefficients and t-values are used to match undated ring-width sequences to a dated master chronology (a group of dated trees). However, in this chapter a Bayesian approach for tree-ring dating using the VSLite model is introduced. This new, probabilistic approach involves simultaneously fitting the VSLite model and matching the undated trees to a dated site chronology, and hence identifying the posterior probability of a match at all possible offsets between the two sequences. The Bayesian approach enables us to combine the tree-ring data and the prior information about the unknown date of the sequences, and hence make Bayesian inferences about the matching process and the true values of the uncertain model parameters. Before implementing the VSLite model for cross-matching ring-width sequences, it is worth briefly summarising the matching process.

6.1 Matching Process

Suppose we wish to match an undated Quercus ring-width sequence to a dated master chronology (an average of a group of Quercus tree-ring sequences for a particular region). Both the undated sequence and the master chronology must be from the same tree species, grown in the same geographic area, and have received the same climatic conditions. In classical dendrochronology, the two sequences are compared both visually and statistically in order to detect any similarity between them. The comparison is made year-by-year at all possible offsets, and typically the one with the highest t-value or z-score is considered to provide a calendar date for the undated sample. However, in Bayesian dendrochronology, the aim is to provide a posterior probability of the match at all possible offsets between the two sequences; and hence provide the calendar date for the undated sequence which has the highest probability.

6.1.1 Matching Notation

Following the methodology of Jones (2013), we define the notation of the matching process as follows. Let the dated master chronology be of length l years, and comprise I trees. Let the start and end dates of the master chronology be Δ_s and Δ_e, respectively, so that $l = \Delta_e - \Delta_s + 1$. For tree i, $i = 1, 2, \ldots, I$, let δ_i be its start date of the tree i, l_i be its age (or length of growth) in years, and $\delta_i + l_i - 1$ be its felling date. Similarly, let the undated site chronology be of length l^* years, and have I^* trees. Let Δ^* be the unknown start date of the undated site chronology. For tree i, $i = I + 1, \ldots, I + I^*$, let $\delta_i = \Delta^* + r_i$ be its unknown start date (where $r_i \geq 0$, is the offset of tree i relative to Δ^*), l_i^* be the length of the tree, and $\delta_i + l_i^* - 1$ be the end date of the tree.

Now, the dating process starts by consecutively matching the undated site chronology to the dated master chronology at all possible offsets from $t = \Delta_s - l^* + q$ to $t = \Delta_e + l^* - q$, where q is the minimum overlap of rings between the dated and undated sequences (discussed in Chapter 3). Therefore, the total number of

all possible offsets between the sequences is equal to $l + l^* - 2q + 1$.

q is crucial when matching ring-width sequences, because considering a small number of overlapping rings between the two sequences will increase the chances of matching the undated sequence at the wrong offset. Dendrochronologists tend to use 40-50 rings of overlap between dated and undated sequences, and Laxton and Litton (1988) suggest that q of less than 40 rings are assumed to be unreliable for matching process.

6.2 Bayesian Approach to Tree-ring Dating

Here we extend the VSLite model to include the cross-matching process of tree-ring width sequences, and implement it via a Bayesian paradigm which combines both the likelihood of data and the prior information about the unknown age of the undated tree. We add an extra parameter Δ^* (the unknown date of the undated sequence) to the Bayesian approach of the VSLite model (outlined in Section 5.3), and then implement it for dating purposes (making inferences about the matching process). The following sections describe the Bayesian implementation of the VS-Lite model for matching process.

6.2.1 Model Implementation

6.2.1.1 The Likelihood

The VSLite forward model, given in Equation 5.1, provides tree-ring width indices which follow a normal distribution with mean $(1 - \sigma_\epsilon^2)^{\frac{1}{2}} \hat{W}_t$ and variance σ_ϵ^2.

Now, let $\mathbf{W} = (W_1, W_2, \ldots, W_t)$ be the vector of climatic signals (tree-ring width growth) for years $1, 2, \ldots, t$, and let $\mathbf{y}_i = (y_{\delta_i}, \ldots, y_{\delta_i + l_i - 1})$ be the vector of ring-width indices for tree i. Let $\mathbf{y}^D = (y_1, \ldots, y_I)$ and $\mathbf{y}^{UD} = (y_{I+1}, \ldots, y_{I+I^*})$ represent the indices for all dated and undated trees, respectively. Then the indices for all trees (dated and undated) are $\mathbf{y} = (\mathbf{y}^D, \mathbf{y}^{UD}) = (y_1, \ldots, y_I, y_{I+1}, \ldots, y_{I+I^*})$.

- Likelihood of the dated chronology

Under the VSLite forward model, the likelihood of the dated site master chronology for $i = 1, 2, \ldots, I$ trees with each tree i being dated is:

$$p(\mathbf{y}^D|\mathbf{T}, \mathbf{P}, \boldsymbol{\theta}, \sigma_\epsilon^2) \propto \prod_{i=1}^{I} \left[\prod_{t=\delta_i}^{\delta_i + l_i - 1} (\frac{1}{\sigma_\epsilon^2})^{\frac{1}{2}} \exp(-\frac{1}{2\sigma_\epsilon^2}(y_{ti} - \sqrt{1 - \sigma_\epsilon^2}\hat{W}_t)^2) \right].$$

Note that the dependence on the four VSLite growth threshold parameters $\boldsymbol{\theta} = (T_1, T_2, M_1, M_2)$ is implicit in the deterministic estimate of the growth signal $\hat{W}_t$.

- Likelihood of the undated chronology

Now, let the likelihood of the undated site master chronology for $i = (I + 1), (I + 2), \ldots, (I + I^*)$ trees be:

$$p(\mathbf{y}^{UD}|\mathbf{T}, \mathbf{P}, \boldsymbol{\theta}, \sigma_\epsilon^2, \Delta^*) \propto \prod_{i=I+1}^{I+I^*} \left[\prod_{t=\Delta^*+r_i}^{\Delta^* + r_i + l_i - 1} \left(\frac{1}{\sigma_\epsilon^2}\right)^{\frac{1}{2}} \exp(-\frac{1}{2\sigma_\epsilon^2}(y_{ti} - \sqrt{1 - \sigma_\epsilon^2}\hat{W}_t)^2) \right].$$

Where;

- Δ^*: is the unknown start date of the undated site chronology.

- $l^* + l - 2q + 1$: is the number of all possible offsets between the dated and undated sequences.

- $\Delta = (\Delta_s - l^* + q, \ \Delta_s - l^* + q - 1, \ldots, \ \Delta_s - 1, \Delta_s, \ \Delta_s + 1, \ldots, \ \Delta_e - q + 1)$ are all possible start dates for the undated site chronology.

- The likelihood of all data

The likelihood of all data can be obtained by combining both the likelihood of the dated and undated site master chronologies as follows,

$$p(\mathbf{y}|\mathbf{T}, \mathbf{P}, T_1, T_2, M_1, M_2, \sigma_\epsilon^2, \Delta^*) \propto p(\mathbf{y}^D|\mathbf{T}, \mathbf{P}, T_1, T_2, M_1, M_2, \sigma_\epsilon^2) \times$$
$$p(\mathbf{y}^{UD}|\mathbf{T}, \mathbf{P}, T_1, T_2, M_1, M_2, \sigma_\epsilon^2, \Delta^*).$$

6.2.1.2 The Priors

In order to implement the matching process and make inferences about the unknown parameters (T_1, T_2, M_1, M_2, σ_ϵ^2, Δ^*), prior distributions are needed for all six uncertain parameters. We use gamma priors for the four growth threshold parameters and inverse-gamma for the model error parameter, σ_ϵ^2. These priors have been described in detail in the previous chapter. The reader is referred to Section 5.3.3 for more details about the prior distributions for these five parameters. The prior for the sixth parameter Δ^* is defined as follows.

Prior for Δ^*

As no information is available about the unknown date of the undated ring-width sequences, we assume that each date within the interval of all possible dates is equally likely. Therefore, we simply assume that Δ^* lies somewhere within the range of the dated chronology to which we are matching and thus used a noninformative uniform prior distribution for the unknown date as follows,

$$p(\Delta^*) \sim U\{a_\Delta, \ldots, b_\Delta\},$$

where, $a_\Delta = \Delta_s - l^* + q$, and $b_\Delta = \Delta_e + l^* - q$ are the minimum and maximum possible offsets for the unknown date, respectively.

6.2.1.3 The Posterior

By combining the prior distributions for all unknown parameters and expression for the ring-width data through the likelihood, the joint posterior distribution of the VSLite parameters and matching process is given by

$$p(\boldsymbol{\theta}, \sigma_\epsilon^2, \Delta^* | \mathbf{y}, \mathbf{T}, \mathbf{P}) \propto p(\mathbf{y} | \mathbf{T}, \mathbf{P}, \boldsymbol{\theta}, \sigma_\epsilon^2, \Delta^*) \; p(\boldsymbol{\theta}, \sigma_\epsilon^2, \Delta^*)$$

$$\propto p(\mathbf{y}^D | \mathbf{T}, \mathbf{P}, \boldsymbol{\theta}, \sigma_\epsilon^2) \; p(\mathbf{y}^{UD} | \mathbf{T}, \mathbf{P}, \boldsymbol{\theta}, \sigma_\epsilon^2, \Delta^*) \; p(\boldsymbol{\theta}) \; p(\sigma_\epsilon^2) \; p(\Delta^*)$$

$$\propto p(\mathbf{y}^D | \mathbf{T}, \mathbf{P}, T_1, T_2, M_1, M_2, \sigma_\epsilon^2) \; p(\mathbf{y}^{UD} | \mathbf{T}, \mathbf{P}, T_1, T_2, M_1, M_2, \sigma_\epsilon^2, \Delta^*) \times$$

$$p(T_1) \; p(T_2) \; \pi(M_1) \; p(M_2) \; p(\sigma_\epsilon^2) \; p(\Delta^*)$$

$$\propto \prod_{i=1}^{I} \left[\prod_{t=\delta_i}^{\delta_i + l_i - 1} \left(\frac{1}{\sigma_\epsilon^2} \right)^{\frac{1}{2}} \exp\left(-\frac{1}{2\sigma_\epsilon^2} (y_{ti} - \sqrt{1 - \sigma_\epsilon^2} \hat{W}_t)^2 \right) \right] \times$$

$$\prod_{i=I+1}^{I+I^*} \left[\prod_{t=\Delta^*+r_i}^{\Delta^*+r_i+l_i-1} \left(\frac{1}{\sigma_\epsilon^2} \right)^{\frac{1}{2}} \exp\left(-\frac{1}{2\sigma_\epsilon^2} (y_{ti} - \sqrt{1 - \sigma_\epsilon^2} \hat{W}_t)^2 \right) \right] \times$$

$$\left[T_1^{(\alpha_{T_1} - 1)} \; e^{-T_1/\beta_{T_1}} \right] \left[T_2^{(\alpha_{T_2} - 1)} \; e^{-T_2/\beta_{T_2}} \right] \left[M_1^{(\alpha_{M_1} - 1)} \; e^{-M_1/\beta_{M_1}} \right] \times$$

$$\left[M_2^{(\alpha_{M_2} - 1)} \; e^{-M_2/\beta_{M_2}} \right] \left[(\sigma_\epsilon^2)^{-(\alpha_\epsilon + 1)} \; e^{-\left(\frac{\beta_\epsilon}{\sigma_\epsilon^2} \right)} \right] \left[\frac{1}{l + l^* - 2q + 1} \right].$$

Again, the joint posterior distribution above cannot be evaluated analytically, thus we use MCMC sampling method to update model parameters. The full conditional distributions for all parameters are obtained and can be found in Appendix I.

6.2.2 Sampling Algorithm: Metropolis-Hastings

A Metropolis-Hastings algorithm within a Gibbs sampler was used to estimate the posterior distributions of the unknown parameters. The procedure used for this MCMC sampling can be outlined as follows.

1. Choose starting values $T_1^{(0)}, T_2^{(0)}, M_1^{(0)}, M_2^{(0)}, \sigma_\epsilon^{2(0)}$, and $\Delta^{*(0)}$.

2. for $j = 1$ to N_{mcmc} (MCMC sample size)

   a) Draw a proposed value T_1' from the prior distribution of T_1.

   b) Calculate the likelihood of the proposal,
   $$p(\mathbf{y} | \mathbf{T}, \mathbf{P}, T_1', T_2^{(j-1)}, M_1^{(j-1)}, M_2^{(j-1)}, \sigma_\epsilon^{2(j-1)}, \Delta^{*(j-1)})$$

   c) Calculate the likelihood of the current value,
   $$p(\mathbf{y} | \mathbf{T}, \mathbf{P}, T_1^{(j-1)}, T_2^{(j-1)}, M_1^{(j-1)}, M_2^{(j-1)}, \sigma_\epsilon^{2(j-1)}, \Delta^{*(j-1)})$$

d) With probability $\min\left\{1, \dfrac{p\left(\mathbf{y}|\mathbf{T},\mathbf{P},\, T_1',\, T_2^{(j-1)},\, M_1^{(j-1)},\, M_2^{(j-1)},\, \sigma_\epsilon^{2\,(j-1)},\, \Delta^{*(j-1)}\right)}{p\left(\mathbf{y}|\mathbf{T},\mathbf{P},\, T_1^{(j-1)},\, T_2^{(j-1)},\, M_1^{(j-1)},\, M_2^{(j-1)},\, \sigma_\epsilon^{2\,(j-1)},\, \Delta^{*(j-1)}\right)}\right\}$ set $T_1^{(j)} = T_1'$; otherwise, set $T_1^{(j)} = T_1^{j-1}$.

e) Repeat steps (a to d) to update T_2, using parameters $(T_1^{(j)}, M_1^{(j-1)}, M_2^{(j-1)}, \sigma_\epsilon^{2\,(j-1)})$.

f) Repeat steps (a to d) to update M_1, using parameters $(T_1^{(j)}, T_2^{(j)}, M_2^{(j-1)}, \sigma_\epsilon^{2\,(j-1)})$.

g) Repeat steps (a to d) to update M_2, using parameters $(T_1^{(j)}, T_2^{(j)}, M_1^{(j)}, \sigma_\epsilon^{2\,(j-1)})$.

h) Sample a value for $\sigma_\epsilon^{2\,(j)}$ from its full conditional distribution,
$p(\sigma_\epsilon^2|\mathbf{y}, \mathbf{T}, \mathbf{P}, T_1^{(j)}, T_2^{(j)}, M_1^{(j)}, M_2^{(j)}, \Delta^{*(j-1)})$

i) Sample a value for $\Delta^{*(j)}$ from its full conditional distribution,
$p(\Delta^*|\mathbf{y}, \mathbf{T}, \mathbf{P}, T_1^{(j)}, T_2^{(j)}, M_1^{(j)}, M_2^{(j)}, \sigma_\epsilon^{2\,(j)})$

3. Repeat step (2) until the Markov Chain reaches equilibrium.

4. After the burn-in period and thinning the subsequent iterations of step (2), the resulted iterations are used as samples from the posterior.

5. End.

The MCMC convergence for the model parameters $(T_1, T_2, M_1, M_2, \sigma_\epsilon^2)$ were checked, using the diagnostic methods summarised in Section 5.3.8, to make sure that the MCMC chains had reached their stationarity. However, since the parameter Δ^* is a discrete variable, it was difficult to ascertain a diagnostic test to ensure that the chain had converged. Instead, a check on the reproducibility of the results was conducted via running each test using three different random seeds. The posterior probabilities for Δ^* for each seed after a specified number of iterations were compared. This determined how many iterations are needed to produce reproducible results for Δ^*.

6.3 Simulating Data for Model Implementation

In order to examine the MCMC implementation and the behaviour of the VSLite-based matching process, we simulated ring-width indices using the VSLite forward

model (given in Equation 5.1). The following parameters, based closely on those of (Jones, 2013), need to be considered for the data simulation.

(1) **Signal-to-noise ratio**

The signal-to-noise ratio (SNR) is a measurement that describes how similar a group of tree-ring width samples are within a chronology. As the variance of the model noise σ_ϵ^2 decreases, the signal-to-noise ratio increases and the similarity among the trees increases, and vice-versa. For simulating data to test the Bayesian implementation of the VSLite model, we used a range of SNR values (given in Table 6.1) to mimic different types of data. Since the tree-ring data are normally distributed with mean 0 and variance 1, the sum of the climatic signal variance and the model noise variance is 1. Thus, different SNR can be obtained by adopting different values for the model noise variance σ_ϵ^2.

SNR	σ_ϵ^2	SNR	σ_ϵ^2
0.1	0.8999	1.1	0.4762
0.2	0.8333	1.2	0.4545
0.3	0.7692	1.3	0.4348
0.4	0.7143	1.4	0.4167
0.5	0.6667	1.5	0.4000
0.6	0.6250	1.6	0.3846
0.7	0.5882	1.7	0.3704
0.8	0.5556	1.8	0.3571
0.9	0.5263	1.9	0.3448
1.0	0.5000	2.0	0.3226

Table 6.1: Different signal-to-noise ratios (SNR) with corresponding model noise variance σ_ϵ^2, used for simulating data for exploring the Bayesian implementation of the VSLite model.

(2) **Deterministic growth signal $\hat{W}_t$**

The deterministic estimate of the climatic signal $\hat{W}_t$, detailed in Section 3.2.2,

is the main component of VSLite via which W_t is modelled as a function of monthly climatic data, site latitude, and growth threshold parameters.

(3) **The dated master chronology**

Dated master chronologies are required for the cross-matching process. Dated samples were simulated by adding normally-distributed noise, $N(0, \sigma_\epsilon^2)$, to the simulated climatic signals $\hat{W}_t$. A dated master chronology was then obtained by grouping of simulated trees, with the following parameters.

- The length of the dated master chronology (l)

  The length of dated site master chronologies in the UK varies from one site to another. For simulating data for our model implementation and matching process, we mimicked reality by simulating local site master chronologies of length $150, 200$, and 250 years.

- Number of samples (I) in the dated master chronology.

  The number of trees in the dated master chronologies also varies from one site to another in the UK. For the experiments that follow, we simulated chronologies with 10 samples.

- The length of individual trees (l_i) in the dated master chronology.

  We randomly simulated trees of length ($75 \leq l_i \leq 150$) to mimic real trees in the UK database of the dated site chronologies.

(4) **Minimum overlap between dated and undated site chronologies**.

For simulating data for the Bayesian model implementation and matching process, we followed Jones (2013) to use $q = 50$ as a minimum overlap between dated and undated site master chronologies.

(5) **The undated site chronology**.

An undated site chronology was obtained by grouping simulated trees, with the following parameters:

- The length of the undated site chronology (l^*).

  The length of the undated site chronology should be shorter than the length of the dated master chronology, $l^* \leq l$, to ensure the matching process. Thus, we considered undated site chronologies of length 100 and 50 years.

- Number of samples (I^*) in the undated site chronology.

  The number of individual trees in the undated site chronologies should also be less than or equal to the number of individual trees in the dated site chronologies, $I^* \leq I$. Therefore, chronologies with $10, 5, 2$, and 1 samples were simulated.

- The length of the individual trees (l_i^*) in the undated site chronology.

  Randomly selected simulation trees of length ($50 \leq l_i \leq 100$) were considered to mimic real undated trees in the UK database.

(6) **The true offset of the undated site master chronology**.

We followed Jones (2013) to fix the true offset of the undated site chronology to the dated master chronology at $t = 100$. This helped us to compare the results for different experiments, as well as comparing results of the Bayesian approach to the classical ones.

6.3.1 Pseudo-code for Data Simulation

In order to simulate tree-ring width indices for use in testing our approach for matching an undated site chronology to a dated master chronology, the following algorithm was used,

1. Specify l, I, Δ_s and Δ_e for the dated site master chronology.

2. Identify l^* and I^* for the undated site master chronology.

3. Determine a SNR and hence σ_ϵ^2 for data.

4. Identify q, the minimum overlap between the two sequences.

5. Calculate $l + l^* - 2q$, the length of the climatic signal vector required.

6. Generate a deterministic $\hat{W}_t$ from climatic data:

   - Specify the site of interest, and find its latitude ϕ.

   - Obtain monthly climatic data $\mathbf{T}$ and $\mathbf{P}$.

   - Calculate the monthly soil moisture content $\mathbf{M}$.

   - Calculate G_T, G_M, G_E, and overall growth G_t.

   - Obtain $\hat{W}_t$.

7. Simulate a dated master chronology:

   - Create an $(l \times I)$ matrix, by taking a subset of length (l) from the climatic signal $\hat{W}_t$ and replicate it (I) times.

   - Simulate an $(l \times I)$ noise matrix from $N(0, \sigma_\epsilon^2)$

   - Sum the two matrices to give a matrix of ring-width indices $\mathbf{y^D}$.

8. Simulate an undated site chronology:

   - Calculate all possible offsets, $l + l^* - 2q + 1$.

   - Choose an offset Δ^* from $t = \Delta_s - l^* + q$ to $\Delta_e - l^* - q$.

   - Create an $(l^* \times I^*)$ matrix, by taking a subset of length (l^*) from $t = \Delta^*, \ldots, \Delta^* + l^* - 1$, and replicate it (I^*) times.

   - Simulate an $(l^* \times I^*)$ noise matrix from $N(0, \sigma_\epsilon^2)$.

   - Sum the two matrices to give a matrix of undated ring-width indices $\mathbf{y^{UD}}$.

9. Use dated and undated data for the model implementation in matching process.

The algorithm above was used to simulate data for each experiment in the next section.

6.4 VSLite-based Crossmatching Experiments

This section outlines experiments of matching undated ring-width sequences to a dated master chronology using the VSLite model and the data simulation algorithm outlined in Section 6.3.1. A selection of experiments are reported in this section, and several complementary ones are given in Appendix II.

For each experiment in this section, a Bayesian implementation of the VSLite model and the matching process was applied, along with the traditional method (t-value) to make a comparison between our approach and the classical one.

For each experiment, the model parameters ($T_1, T_2, M_1, M_2, \sigma_e^2$, and Δ^*) were estimated and the posterior plots and their MCMC convergence were checked. A range of diagnostic checks, detailed in Section 5.3.8, were used for checking the MCMC convergence. As the interest here was in estimating the posterior probability of the date match at each possible offset, in this section we only report results related to this parameter. Results for other parameters were close to those reported in the previous chapter. Each table contains the model noise (σ_ϵ^2) and signal-to-noise ratio (SNR) used to simulate the tree-ring data used in the Bayesian parameter estimation and matching process along with the posterior probability of the date match at each possible offset, the posterior mean for $\hat{\sigma}_\epsilon^2$ and results of matching the same sequences using the classical tree-ring dating approach (t-value).

6.4.1 Matching short (50-year) undated site chronology

This section illustrates results from the experiment to match an undated site chronology with **1** sample covering **50** years, to a dated master chronology with **10** samples covering **200** years (at Sheffield site, $\phi = 53.37$). The true offset is **100**, and the minimum overlap between the dated and undated chronologies is **50**. We ran a MCMC sample of length 100,000 iterations and discarded the first 10000 iterations as burn-in period. The MCMC were then thinned every 10 iterations and the results were reproducible after 9000 iterations.

Table 6.2 shows results of the experiment of matching the dated and undated chronologies summarised above, from a subregion with a signal-to-noise ratios vary from 0.9 to 0.1.

SNR	σ_ϵ^2	Posterior Probability		$\hat{\sigma}_\epsilon^2$	t-value
		Offset	Probability		
0.9	0.5263	100	1.00	0.538	5.703
		98	0.00		2.823
0.8	0.5556	100	1.00	0.5692	4.261
		98	0.00		2.827
0.7	0.5882	100	1.00	0.6039	3.912
		98	0.00		2.826
0.6	0.625	100	0.97	0.6334	3.542
		98	0.01		2.693
		14	0.00		2.431
0.5	0.6667	100	0.86	0.6802	3.123
		98	0.07		2.743
		14	0.04		2.414
		109	0.01		2.121
0.4	0.7143	100	0.63	0.742	2.793
		98	0.24		2.654
		14	0.06		2.374
		75	0.02		2.013
0.3	0.7692	100	0.34	0.7844	2.891
		98	0.28		2.744
		14	0.19		2.190
		109	0.11		2.064
0.2	0.8333	98	0.41	0.8517	2.61
		100	0.32		2.601
		14	0.12		2.366
		109	0.08		2.237
0.1	0.8999	98	0.13	0.9228	2.423
		149	0.06		2.296
		104	0.05		1.968
		100	0.03		1.862

Table 6.2: Results of matching undated trees to a dated master chronology using our extension of the VSLite model. A Bayesian probabilistic estimate of a match at the true offset is compared with the classical results (t-value). The signal-to-noise ratio (SNR) for the simulate ring-widths used in the experiments varies from 0.9 to 0.1.

We can see from the table that when the signal-to-noise ratio (SNR) is grater than or equal to 0.7, the posterior probability of a match at the correct offset is 1. When SNR is 0.6, the posterior probability estimate of the match at the true offset is 0.97, and the classical t-value is 3.542. The posterior probability estimates at other offsets were almost zero, and their t-values were less than 3.5. This is the minimum threshold value used by dendrochronologists when using the classical method for matching ring-width sequences (Baillie and Pilcher, 1973; Cook *et al.*, 1990). However as the SNR decreased to 0.5, the posterior probability estimate of the match at the true offset decreased to 0.86, and so on.

Therefore, we can see that the posterior estimate of the match depends on the signal-to-noise ratio; as SNR decreases, the climatic signal variance decreases, the similarity among individual trees within the chronology decreases and hence the posterior probability estimate of a match at the true offset also decreases, and vice versa.

Figure 6.1 shows, the histograms of the posterior distributions for the model parameters for the experiment outlined above, when the signal-to-noise ratio is $SNR = 0.5$. The first four histograms illustrate the estimated temperature and soil moisture growth threshold parameters ($\hat{T}_1$, $\hat{T}_2$, $\hat{M}_1$, $\hat{M}_2$) which were discussed in detail in the previous chapter. The last two histogram plots in Figure 6.1 illustrate respectively the posterior estimate of the model noise parameter $\hat{\sigma}_e^2$ and the posterior probability of the match at all possible offsets. The highest posterior probability of a match was equal to 0.86 at the true offset.

Our approach has successfully provided posterior probabilities of a match at all possible offsets, and has provided a date with the highest posterior probability.
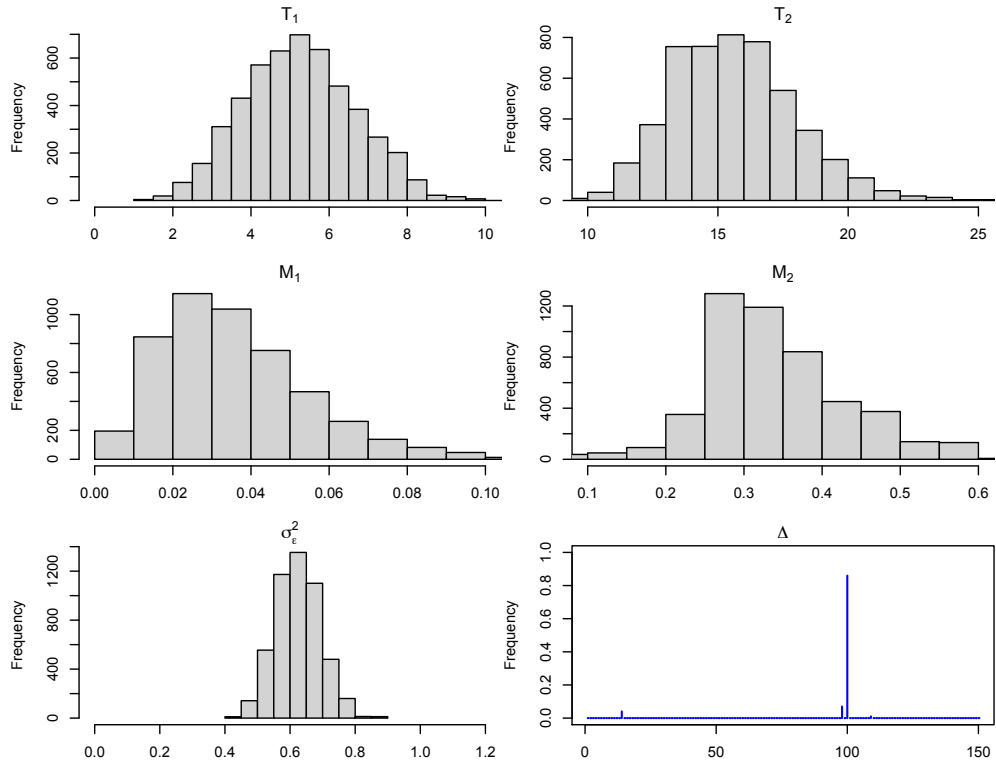
Figure 6.1: Plot of the posterior distribution of the VSLite model parameters $\hat{T}_1$, $\hat{T}_2$, $\hat{M}_1$, $\hat{M}_2$, $\hat{\sigma}_\epsilon^2$ and $\hat{\Delta}^*$ for the experiment of matching an undated tree-ring width sequence covering 50 years to a dated site master chronology containing 10 samples, covering 200 years, when the signal-to-noise ratio of the simulated tree-ring data was 0.5.

6.4.2 Matching long (100-year) undated site chronology

This section includes results of the experiment of matching an undated site chronology covering **100** years, to a dated master chronology with **10** samples covering **200** years (at Sheffield site, $\phi = 53.37$). The true offset is **100**, and the minimum overlap between dated and undated sequences is **50**. The MCMC of length 200,000 iterations were sampled after discarding the first 20000 iterations as burn-in period. The MCMC were then thinned every 10 iterations and the results were reproducible after 10000 iterations.

Table 6.2 illustrates results of the experiment of matching an undated site chronology of length 100 years to a dated master chronology of length 200 years.

SNR	σ_ϵ^2	Posterior Probability		$\hat{\sigma}_\epsilon^2$	t-value
		Offset	Probability		
0.6	0.625	100	1.00	0.6207	8.211
		48	0.00		2.629
0.5	0.6667	100	1.00	0.6623	7.859
		48	0.00		2.713
0.4	0.7143	100	1.00	0.7098	6.289
		48	0.00		2.803
0.3	0.7692	100	1.00	0.7648	5.679
		48	0.00		2.891
0.2	0.8333	100	0.99	0.830	5.362
		48	0.00		2.95
0.1	0.8999	100	0.82	0.9018	3.997
		48	0.06		2.882
		95	0.03		2.671
		135	0.02		2.487

Table 6.3: Results of matching undated site chronologies of length 100 years to a dated master chronology of length 200 years using our extension of the VSLite model. A Bayesian probabilistic estimate of a match at the true offset is compared with the classical results (t-value). The signal-to-noise ratio (SNR) used to generate the simulated tree-ring data for these experiments vary from 0.6 to 0.1.

Table 6.2 shows the Bayesian matching results compared with the classical one. Results of both methods were consistent, as the highest t-value and the posterior probability of 1 were provided for the match at the true offset for SNR greater than or equal to 0.3. When the SNR is 0.1, the results of both methods were still consistent, but with the lower posterior probability (0.82), and lower t-value (3.997) at the true offset. Again, the posterior probability estimate of the match at the true offset depends on the signal-to-noise ratio. As the SNR decreases, the posterior probability estimate decreases, and vice-versa.

Results obtained from these two experiments, along with those reported in Ap-

pendix II, show how the Bayesian implementation of the VSLite model and the matching process can provide the dendrochronologist with probabilistic evidence of a match at a date (in terms of a posterior probability). The Bayesian matching results were consistent with the classical ones (t-value) in all the experiments undertaken here. Furthermore, even when the classical method fails to match the undated sequences to its true offset with an acceptable t-value (greater than or equal to 3.5), the Bayesian matching process provides evidence for dating by offering posterior probabilities for all possible offsets of the match.

6.5   Comparison between Results from VSLite and Jones' Models for Dating

In order to assess the ability of our extension to the VSLite model in the matching process, a comparison was made between the results obtained from the Bayesian implementation of this model and those obtained from the Bayesian implementation of Jones (described in Section 3.1.4). For the two models to be comparable, we considered experiments with the same signal-to-noise ratio, and with the same random seeds used to simulate ring-width indices from the two models. Then posterior probability of a match at the true offset were compared.

We undertook several such experiments but only one of these is reported here. All the remaining results can be found in Appendix III.

Table 6.4 shows results of using three different approaches (VSLite-based approach, Jones' approach and t-value based approach) to match an undated sample covering **50** years to a dated site master chronology with **10** samples covering **200** years. For the high signal-to-noise ratios, both VSLite approach and Jones' approach successfully provide a posterior probability of 1.00 for the match at the true offset. In other words, when considering high SNR for data, the performance of the two models was indistinguishable. However, as the signal-to-noise ratio decreased

SNR	σ_ϵ^2	VSLite Model			Jones' Model			t-value
		Offset	Prob.	$\hat{\sigma}_\epsilon^2$	Offset	Prob.	$\hat{\sigma}_\epsilon^2$	
0.9	0.526	100	1.00	0.54	100	1.00	0.55	5.70
		98	0.00		5	0.00		2.82
0.8	0.556	100	1.00	0.57	100	1.00	0.57	4.26
		98	0.00		5	0.00		2.57
0.7	0.588	100	1.00	0.604	100	0.98	0.60	3.91
		98	0.00		5	0.2		2.63
0.6	0.625	100	0.97	0.633	100	0.87	0.64	3.54
		98	0.01		5	0.10		2.69
		14	0.00		7	0.02		2.43
0.5	0.667	100	0.86	0.680	100	0.55	0.68	3.12
		98	0.07		5	0.33		2.74
		14	0.04		7	0.05		2.41
0.4	0.714	100	0.63	0.74	5	0.51	0.73	2.79
		98	0.24		100	0.21		2.65
		14	0.05		7	0.07		2.37
0.3	0.769	100	0.34	0.784	5	0.44	0.79	2.89
		98	0.29		7	0.14		2.74
		14	0.21		45	0.08		2.19
		109	0.13		84	0.07		2.06
0.2	0.833	98	0.41	0.851	84	0.31	0.86	2.61
		100	0.32		5	0.20		2.60
		14	0.12		7	0.08		2.37
		109	0.08		45	0.07		2.24

Table 6.4: Results of matching 1 undated tree of length 50 years to a dated master chronology, with 10 samples, covering 200 years, when using three methods (based on the VSLite model, Jones' model and traditional t-value approach). The signal-to-noise ratio (SNR) for the simulated tree-ring width data used in these experiments varies from 0.9 to 0.2. The posterior estimate of the match at the true offset depends on the signal-to-noise ratio. As the SNR decreases, the posterior probability decreases, and vice-versa.

the performance of the two models changed, and the VSLite approach tends to provide higher posterior probabilities of a match at the true offset. For example, when $SNR = 0.5$ the VSLite model provided a posterior probability for the match at the true offset of 0.86 while Jones' model provided a posterior probability of just 0.55.

Furthermore, results in Table 6.4 also illustrate that when the Jones' approach failed in matching an undated sample to a dated master chronology, the VSLite model successfully matched the sample at the true offset. For example, when the signal-to-noise ratio is $SNR = 0.4$, the VSLite model has successfully matched the undated sample to the dated master chronology at the true offset with a posterior probability equal to 0.63. However, Jones' model led to the highest posterior probability (0.51) being associated with an incorrect offset, and it provided a lower posterior probability (0.21) of a match at the true offset. Table 6.4 also shows that the mean posterior estimate of the model noise parameter $\hat{\sigma}_e^2$ were very similar from both approaches and were close to the true values used to generate the tree-ring width data.

6.6   Summary and Conclusion

In this chapter, a new Bayesian approach was introduced for matching undated trees to dated master chronologies. The approach uses the VSLite model at the core of the dating process and is otherwise based closely on the approach of Jones' (described in Section 3.1.4). Results from the VSLite-based matching approach were compared to those using the approach of Jones for several simulated data experiments. Experiments in this chapter showed that:

- there is a strong relationship between the signal-to-noise ratio used to simulate data and the posterior probability of a match at the true offset. As signal-to-noise ratio increases, the model noise variance decreases and the similarity among individual samples within the chronology increases; thus the posterior probability of a match at the true offset increases.

- as the number of samples (I^*) in the undated site chronology increases, the posterior probability of a match at the true offset also increases.

- when considering low signal-to-noise ratio for data, the approach based on the VSLite model outperforms that using Jones' model by providing larger

posterior probabilities of a match at the true offset. However, when considering high signal-to-noise ratio for data, both models perform similarly.

The aim here was not primarily to compare a probabilistic Bayesian approach with the traditional method when cross-dating trees, but rather to investigate the relative behaviour of the Bayesian method using different models (one purely statistical and the other process-based). Results provided in this chapter suggest that the process-based modelling approach using the VSLite model performed better, especially when the signal-to-noise ratio is low, and this might be for the following reasons.

(1) In the simple statistical model, Jones' approach (described in Section 3.1), tree-ring width simulations are simply generated by summing a simulated climatic signal ($W_t \sim N(0, \sigma_w^2)$) and model noise ($\epsilon_{ti} \sim N(0, \sigma_\epsilon^2)$) for a specified σ_w^2 and σ_ϵ^2. However, tree-ring width simulations from the VSLite forward model are generated in a more realistic way by capturing the mechanisms of key features of the biological processes within trees during the growing season, which links climate variables to ring-width growth and tree-ring formation.

(2) The statistical model can only capture the variation of ring-width indices annually (year-to-year). However, the VSLite model captures the variation of ring-width growth in a monthly time-step (month-to-month).

(3) Unlike the statistical model, VSLite is able to simulate dated ring-width indices (trees with known age) at any specific geographical location. This is due to the use of dated climate variables (temperature and precipitation) as inputs to the model.

(4) The statistical model requires the ring-width data to be fully processed (detrended, prewhitened and normalised) in order to obtain stationary sequences prior to any representation of the data in the model. However, the VSLite does not require the data to be fully processed, and it has the potential of

using less-processed data. This will be addressed in the next chapter.

In this chapter we have demonstrated that the VSLite model can successfully be used in the matching process when using simulated data. The next chapter will investigate the Bayesian implementation of the model and matching process for less-processed data. This will be more interesting statistically, as it will remove the preprocessing step from data and allow the dendrochronology community to work directly with the real tree-ring width data instead of ring-width indices.

Chapter 7

Bayesian Tree-ring Dating Using Data-adaptive Rescaling

A Bayesian framework for tree-ring dating was introduced in the previous chapter using either our extension to the VSLite (mechanistic forward model), or using the simple statistical model by Jones (2013). The two models were implemented along with the traditional dendrochronology methods. All the current approaches, classical and Bayesian, in dendrochronology usually use fully preprocessed data, which is intended to remove tree-specific signal and reveal the stationary part of the climate signal. Preprocessing raw ring-width data includes three main steps: detrending, prewhitening and normalising (all detailed in Section 2.1). However, the disadvantage of fully preprocessing data is that some of the essential structure and characteristics of raw ring-width data are lost, and more climate signal is removed than is necessary. Additionally, current available methods apply the preprocessing procedures on the dated and undated sequences separately, and do not take into account any effect of the rescaling between the two sequences before matching (this is explained by an illustrative example in the next section). To our knowledge this problem has not been addressed before by dendrochronologists.

In order to tackle this issue in this chapter, we introduce a new simple and more general Bayesian approach for tree-ring dating, which aims to use less-processed data (only detrended, not prewhitened or normalised) for matching undated ring-

width sequences directly to the dated master chronology. The model also involves two new scaling and translating parameters (α and β) which both ensure that the two sequences are on the same scale before matching them. Thus, our approach keeps the first preprocessing step (detrending) which is inevitable, because trees grow faster when they are younger, and removing this age-related growth trend seems sensible and essential. Furthermore, the new approach also allows for single trees to be matched to the dated master chronologies, as well as matching pairs of individual trees which is used for constructing chronologies.

This chapter is structured as follows. Section 7.1 gives the motivation behind introducing this new model by an illustrative example. Section 7.2 outlines the new model with the rescaling parameter and its Bayesian implementation for the matching process. Section 7.3 includes results of implementing the model for Bayesian matching using both real and simulated data. The main conclusions and a summary of the chapter are exist in Section 7.4.

7.1 Motivation

The motivation behind introducing a new model (detailed in Section 7.2) was to use less-processed data in the matching process and allow for the rescaling between dated and undated sequences, which are not considered in the current dendrochronology methods. When crossmatching an undated tree (short) to a master chronology (long), the undated sequence might match to any short interval in the long master chronology which has different climate fluctuations as shown in Figure 7.1, top panel. These intervals could have quite different climate variation, therefore it is not appropriate to put the undated sequence on the same scale as the master chronology, without taking into consideration the effect of rescaling between the two sequences. Furthermore, different trees might respond in different ways to climate; some of them might have bigger fluctuations than the others. Thus, of course, we need to rescale the dated and undated sequences when crossmatching, but without fixing the scale (as currently used by dendrochronologists).

This is because the scale factor used for rescaling one of them is based on the whole long period (master chronology) while the one used for the another sequence is based on a short period (undated tree). Instead, we need a method to allow the data to tell us what kind of scale the dated and undated sequences should have, which therefore allows rescaling them together inside the model likelihood when matching them. The limitation with the current dating methods, and hence the need for a new suggested approach, is illustrated by the following example.
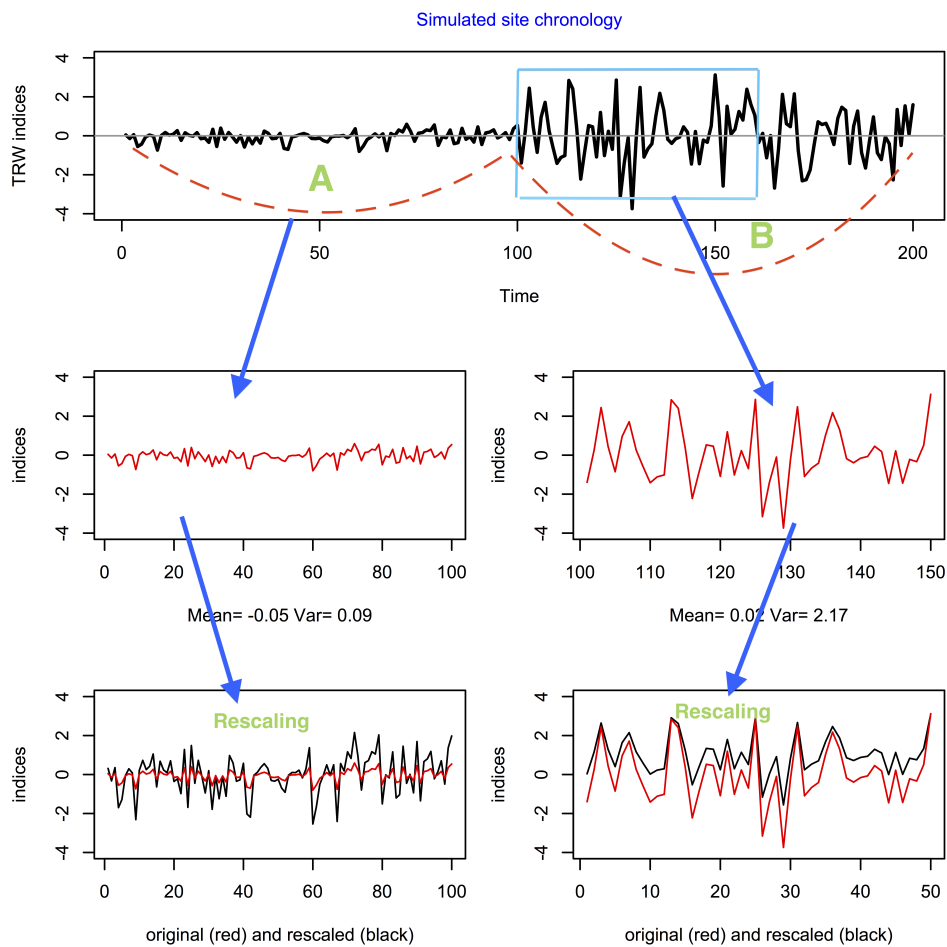
Figure 7.1: A plot to show the effect of separately rescaled two subsections of undated ring-width sequences taken out from a dated master chronology. Simulated site chronology (*top panel*), two different undated sequences (*middle panel*), the two undated sequences and their rescaled version (*bottom panel*).

7.1.1 Illustrative Example

Suppose there is a fully-processed tree-ring site master chronology (y^D) of length $l = 200$ years, with zero mean and variance one, which has some flat and some wiggly sections, as shown in Figure 7.1. Let A and B be two subsections of the dated master chronology of length l_A and l_B respectively. With the current dating methods, if we take out a subsection (either flat or wiggly) of this chronology to be considered as undated sequence and try to re-date it, then there are two potential ways that the matching process might go wrong, due to the following issues:

- Scaling: the dated and undated sequences are not on the same scale.

- Translating: the dated and undated sequences are shifted from one another.

These two issues are illustrated clearly in Figure 7.1. If we take out, for example, a subsection A (Figure 7.1, middle panel) from the master chronology and assume it to be undated and hence match it again to the master chronology, then we will obtain a perfect match (i.e. the undated sequence will be matched to its correct offset). However, in the traditional dating approach we do not do this, but instead we rescale (reprocessing) the undated sequence again to have zero mean and variance one (Figure 7.1, bottom panel) in order to put it on the same scale with the master chronology. Despite the fact that the rescaled sequences still have the same shape/pattern, the scale changes significantly, and the sum of squared differences between the rescaled and the original sequences (as mentioned in Equation 7.2) is quite large. Hence, it will not match to its correct offset because the two sequences are no longer on the same scale.

This indicates that the undated tree has grown less/more fast by the factor α, because some trees might have more extreme responses to climate conditions than others. The effect of this rescaling factor is totally ignored in the current dating methodologies. Therefore, we should allow for this rescaling factor to be considered in the model itself (inside the matching process) by adding an extra parameter (α) to account for the rescaling between dated and undated sequences rather than reprocessing the undated sample to be put on the same scale as the dated master.

Another example where the matching process might not work is when there is a translation (shift) in the mean of the undated sequence; when dating a small time-period which is unrepresentative of longer master chronology. If we take, for example, a short subsection from a wiggly part of the master chronology (Figure 7.1, middle right panel) and assume it to be undated and match it to the master chronology, we will have a perfect match to its correct offset. However, if we rescale it to have a zero mean and match it again to the master chronology (with the current dendrochronology methods), we do not obtain a good match because it might match to any short interval in the long master chronology which has different climate fluctuations of such short-periods.

Again, the effect of this shifting factor is entirely ignored in the current dating methodologies. Therefore, we should also allow for this translation effect to be considered in the model used for the matching process.

Thus, within our new approach (described in the next section) we consider the impact of the two issues mentioned above by adding two extra parameters (α and β) to the model to allow for the rescaling and translation effects between the cross-matched sequences prior to matching them.

7.2   A Modified Model with Rescaling Factor

The relationship between the undated tree-ring width sequences (y^U) and the dated master chronology (y^D) is described as,

$$\alpha \, y_i^U = \beta \; + \; y_{i+\Delta}^D + \; \epsilon_i, \tag{7.1}$$

where

y_i^U: is the detrended undated ring-width sequence of length l^*.

y_i^D: is the detrended dated master chronology of length l.

α: is the rescaling parameter between the dated and undated sequences.

β: is the population mean of the undated ring-width indices.

Δ: is the possible offset (unknown start date) of the undated sequence.

ϵ_i: is the model noise (error), which follows an independent and identically distributed (i.i.d.) normal distribution with mean 0 and variance σ_e^2.

7.2.1   Bayesian Implementation of the Modified Model

The model described above was used for the matching process (detailed in Section 6.1) in a Bayesian framework to match undated trees to dated master chronologies with a view to providing posterior probability of a match at all possible offsets. The Bayesian paradigm allows combining both the likelihood of data and prior information about the unknown date of the undated tree, as follows.

7.2.1.1   The Likelihood

Let the likelihood of the undated sequence y^U given the dated master chronology y^D and the unknown parameters α, β, σ_e^2, Δ be:

$$p(\mathbf{y}^U|\alpha,\beta,\sigma_e^2,\Delta,\mathbf{y}^D) \propto \prod_{i=1}^{l^*} \left(\frac{1}{\sigma_e^2}\right)^{\frac{1}{2}} \exp\left\{ -\frac{1}{2\sigma_e^2}(\alpha\ y_i^U - \beta - y_{i+\Delta}^D)^2\right\}, \qquad (7.2)$$

where;

- $l + l^* - 2q + 1$: is the total number of all possible offsets between the dated and undated sequences; and q is the minimum overlap of rings between them.

- $\Delta = (\Delta_s - l^* + q, \Delta_s - l^* + q - 1, \ldots, \Delta_s - 1, \Delta_s, \Delta_s + 1, \ldots, \Delta_e - q + 1)$ are all possible offset (start date) for the undated tree-ring sample; where Δ_s and Δ_e are the start and end dates of the dated master chronology.

7.2.1.2   The Priors

To make inferences about the model parameters in the matching process under the Bayesian paradigm, prior distributions are needed for the unknown parameters α, β, σ_e^2, and Δ.

Prior for α

The parameter α, is the rescaling parameter between the dated and undated trees. To choose a suitable prior for this parameter, it should satisfy these two conditions.

(i) It should be positive ($\alpha > 0$) as it is a scaling factor which indicates that one of the two sequences might grown faster than the other.

(ii) It should be symmetric so that for any numbers a and b with $1 < a < b$; $P(a < \alpha < b) = P(1/b < \alpha < 1/a)$. This will allow us to consider a rescaling on either tree (i.e. dated or undated) in a symmetric fashion. However, the prior on β parameter (described below) might not allow for this, but as close as possible.

Therefore, we chose our prior distribution for α to be log-normal, with parameters $(\mu_\alpha, \sigma_\alpha^2)$, which satisfies the two conditions above. We chose μ_α to be equal to zero in order to satisfy the symmetry property. For the experiments in this chapter we used a log-normal prior distribution for α, with $\mu_\alpha = 0$, and $\sigma_\alpha = 0.25$, which gives a density mode of 1 (see Figure 7.2).

The log-normal density as a prior for α can be parametrised with μ_α and σ_α as follows,

$$f(\alpha) = \frac{1}{\alpha \sqrt{2\pi}\sigma_\alpha} \exp\left\{\frac{-1}{2\sigma_\alpha^2}(\log \ \alpha - \mu_\alpha)^2\right\}.$$

The expected value and the variance of α are:

$$E(\alpha) = e^{(\mu_\alpha + 1/2\sigma_\alpha^2)}$$

$$\mathrm{Var}(\alpha) = e^{2\mu_\alpha + \sigma_\alpha^2}(e^{\sigma_\alpha^2} - 1).$$

Figure 7.2 shows log-normal distribution priors with different values for hyper-parameters μ_α and σ_α.
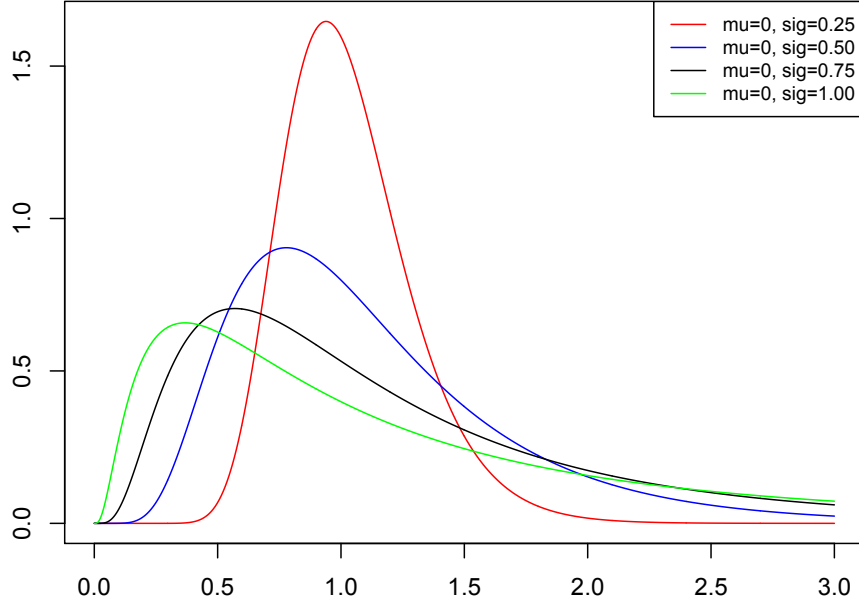
Figure 7.2: Probability density function of log-normal with different parameters.

Prior for β

The parameter β is the population mean of the undated ring-width sequence. Again, for the similar reason to (α) mentioned above, this parameter should have a symmetric distribution with a mean close to zero, because we have no prior information that one tree is having an offset from the other one. Accordingly, an appropriate prior distribution for this parameter would be normally distributed with zero mean and variance k, where k is a constant to be determined. For the experiments in this chapter we used a noninformative prior for β, with a large value of k of 100.

Prior for σ_e^2 and Δ

The prior distribution for the model noise (σ_e^2) and the unknown date of the undated sequence (Δ) will be the same as those used in the previous chapters. The reader is referred to Section 5.3.3 and 6.2.1 for more details about the prior distributions for these two parameters.

7.2.2 The Posterior

Using Bayes' theorem, by combining the prior for all unknown parameters and the likelihood, the joint posterior distribution of the unknown parameters is given by

$$p(\alpha, \beta, \sigma_e^2, \Delta | \mathbf{y}^D, \mathbf{y}^U) \propto p(\mathbf{y}^U | \alpha, \beta, \sigma_e^2, \Delta, \mathbf{y}^D) \; p(\alpha) \; p(\beta) \; p(\sigma_e^2) \; p(\Delta)$$

$$\propto \prod_{i=1}^{l^*} \Big(\frac{1}{\sigma_e^2}\Big)^{\frac{1}{2}} \exp\Big\{ -\frac{1}{2\sigma_e^2}(\alpha \; y_i^U - \beta - y_{i+\Delta}^D)^2 \Big\} \times$$

$$\frac{1}{\alpha \; \sigma_\alpha \sqrt{2\pi}} \exp\Big\{ -\frac{1}{2}\Big(\frac{\ln \alpha - \mu_\alpha}{\sigma_\alpha}\Big)^2 \Big\} \times \Big(\frac{1}{k}\Big)^{\frac{1}{2}} \exp\Big(\frac{-\beta}{2k}\Big) \times$$

$$\big(\sigma_e^2\big)^{-(a_e+1)} \exp\Big(\frac{-b_e}{\sigma_e^2}\Big) \times \Big(\frac{1}{l + l^* - 2q + 1}\Big).$$

7.2.3 Full Conditional Distributions for Parameters

To apply the MCMC we should find the conditional distribution for each model parameter given all the other parameters. The full conditional distribution for each parameter were obtained from the joint posterior distribution above, as follows.

The Conditional Distribution of $(\alpha | \beta, \sigma_e^2, \Delta, \mathbf{y}^D, \mathbf{y}^U)$

With the prior distribution of $\alpha \sim$ log-normal$(\mu_\alpha, \sigma_\alpha)$, and the likelihood of data $p(\mathbf{y}^U | \alpha, \; \beta, \; \sigma_e^2, \; \Delta, \; \mathbf{y}^D)$, the full conditional posterior distribution of α is:

$$p(\alpha | \beta, \sigma_e^2, \Delta, \mathbf{y}^D, \mathbf{y}^U) \propto p(\mathbf{y}^U | \alpha, \beta, \sigma_e^2, \Delta, \mathbf{y}^D) \; p(\alpha)$$

$$\propto \prod_{i=1}^{l^*} \Big(\frac{1}{\sigma_e^2}\Big)^{\frac{1}{2}} \exp\Big\{ -\frac{1}{2\sigma_e^2}(\alpha \; y_i^U - \beta - y_{i+\Delta}^D)^2 \Big\} \times$$

$$\frac{1}{\alpha \; \sigma_\alpha \sqrt{2\pi}} \exp\Big\{ -\frac{1}{2}\Big(\frac{\ln \alpha - \mu_\alpha}{\sigma_\alpha}\Big)^2 \Big\}.$$

The full conditional distribution for the α is not a standard distribution, thus we will use the Metropolis-Hastings update instead of the Gibbs sampler for this parameter.

The Conditional Distribution of $(\beta | \alpha, \sigma_e^2, \Delta, \mathbf{y}^D, \mathbf{y}^U)$

A normal distribution is a conjugate prior for the parameter (β) since it results in a posterior distribution that is also normal, and thus it makes the sampling procedures simpler. With the prior distribution of $\beta \sim N(0, k)$, and the likelihood of data $p(\mathbf{y}^U | \alpha, \beta, \sigma_e^2, \Delta, \mathbf{y}^D)$, and with N^* indicating the total number of observations, the full conditional posterior distribution of β is:

$$p(\beta | \alpha, \sigma_e^2, \Delta, \mathbf{y}^D, \mathbf{y}^U) \propto p(\mathbf{y}^U | \alpha, \beta, \sigma_e^2, \Delta, \mathbf{y}^D)\, p(\beta)$$

$$\propto \prod_{i=1}^{l^*} \left(\frac{1}{\sigma_e^2}\right)^{\frac{1}{2}} \exp\left\{ -\frac{1}{2\sigma_e^2}(\alpha\, y_i^U - \beta - y_{i+\Delta}^D)^2 \right\} \times \left(\frac{1}{k}\right)^{\frac{1}{2}}$$

$$\exp\left\{ -\frac{\beta^2}{2k} \right\}.$$

$$\propto \exp\left\{ -\frac{1}{2}\left(\frac{N^*}{\sigma_e^2} + \frac{1}{k}\right)\beta^2 + \left[\frac{1}{\sigma_e^2}\sum_{i=1}^{l^*}\left(\alpha\, y_i^U - y_{i+\Delta}^D\right)\right]\beta \right\}.$$

The full conditional distribution for the parameter β is a standard normal distribution. Thus,

$$p\left(\beta | \alpha, \sigma_e^2, \Delta, \mathbf{y}^D, \mathbf{y}^U\right) \propto N\left(\hat{\mu}_\beta, \hat{V}_\beta\right),$$

where
$$\hat{V}_\beta = \left(\frac{N^*}{\sigma_e^2} + \frac{1}{k}\right)^{-1} \text{ and } \hat{\mu}_\beta = \hat{V}_\beta\left\{ \frac{1}{\sigma_e^2}\sum_{i=1+\Delta}^{l^*}\left(\alpha\, y_i^U - y_{i+\Delta}^D\right) \right\}.$$

The Conditional Distribution of $(\sigma_e^2 | \alpha, \sigma_e^2, \Delta, \mathbf{y}^D, \mathbf{y}^U)$

The calculation of the full conditional distribution of $(\sigma_e^2 | \alpha, \beta, \Delta, \mathbf{y}^D, \mathbf{y}^U)$ is similar to that seen in chapter 5. Therefore, the distribution of the model noise parameter is inverse-gamma

$$p\left(\sigma_e^2 | \alpha, \beta, \Delta, \mathbf{y}^D, \mathbf{y}^U\right) \sim \Gamma^{-1}\left(\frac{N^*}{2} + a_e, \ \sum_{i=1}^{l^*}(\alpha\, y_i^U - \beta - y_{i+\Delta}^D)^2 + b_e \right).$$

The Conditional Distribution of Δ

The calculation of the full conditional distribution of $(\Delta|\alpha, \beta, \sigma_e^2, \mathbf{y}^D, \mathbf{y}^U)$ is very similar to that seen in chapter 6. Therefore, the posterior distribution of Δ is

$$\log\left[p(\Delta|\alpha, \beta, \sigma_e^2, \mathbf{y}^D, \mathbf{y}^U)\right] = -\frac{1}{2\sigma_e^2}\sum_{i=1}^{l^*}(\alpha\ y_i^U - \beta - y_{i+\Delta}^D)^2.$$

The Bayesian implementation of the new model and the matching process have been described in this section with the essential notation. The new approach aims to work with less-processed data, detrended ring-widths, when matching undated sample to a dated master chronology. Experiments are now required to examine the ability of the model in the matching process.

7.2.4 MCMC Sampling Algorithm

A Metropolis-Hastings algorithm within a Gibbs sampler were implemented to draw samples from the posterior distributions of the model parameters. The sampling procedures are outlined as follows.

i) Choose starting values $\alpha^{(0)}, \beta^{(0)}, \sigma_e^{2(0)}$, and $\Delta^{(0)}$.

ii) for $j = 1$ to N_{mcmc}

  1. Update the parameter α by:

   a) Draw a proposed value α' from a suitable proposal distribution $\Psi(\alpha'|\alpha^{(j-1)})$.

   b) Calculate the likelihood of the proposal,
   $p(\mathbf{y}^U|\mathbf{y}^D, \alpha', \beta^{(j-1)}, \sigma_e^{2(j-1)}, \Delta^{(j-1)})$

   c) Calculate the likelihood of the current value,
   $p(\mathbf{y}^U|\mathbf{y}^D, \alpha^{(j-1)}, \beta^{(j-1)}, \sigma_e^{2(j-1)}, \Delta^{(j-1)})$.

   d) With probability $\min\left(1, \frac{p(\mathbf{y}^U|\mathbf{y}^D,\ \alpha',\ \beta^{(j-1)},\ \sigma_e^{2(j-1)},\ \Delta^{(j-1)})}{p(\mathbf{y}^U|\mathbf{y}^D,\ \alpha^{(j-1)},\ \beta^{(j-1)},\ \sigma_e^{2(j-1)},\ \Delta^{(j-1)})} \frac{\Psi(\alpha^{(j-1)}|\alpha')}{\Psi(\alpha'|\alpha^{(j-1)})}\right)$
   set $\alpha^{(j)} = \alpha'$; otherwise, set $\alpha^{(j)} = \alpha^{(j-1)}$.

2. Update β by sampling a value for $\beta^{(j)}$ from its full conditional distribution, $p(\beta|\mathbf{y}^U, \mathbf{y}^D, \alpha^{(j)},\ \sigma_e^{2(j-1)}, \Delta^{(j-1)})$.

3. Update σ_e^2 by sampling a value for $\sigma_e^{2(j)}$ from its full conditional distribution, $p(\sigma_e^2|\mathbf{y}^U, \mathbf{y}^D, \alpha^{(j)},\ \beta^{(j)},\ \Delta^{(j-1)})$.

4. Update Δ by sampling a value for $\Delta^{(j)}$ from its full conditional distribution, $p(\Delta|\mathbf{y}^U, \mathbf{y}^D, \alpha^{(j)},\ \beta^{(j)},\ \sigma_e^{2(j)})$.

iii) Repeat step (ii) until the Markov Chain reaches equilibrium.

iv) All subsequent converged iterations of step (ii) are used as samples from the posterior.

We typically choose a symmetric proposal (i.e. $\Psi(\alpha'|\alpha) = \Psi(\alpha|\alpha'))$ in our Metropolis-Hastings update, hence the acceptance probability simplifies.

7.3 Bayesian Matching Process Experiments

This section outlines experiments of matching undated ring-width sequences to a dated site master chronology using the approach outlined in Section 7.2.1.

For each experiment in this Section, a Bayesian implementation of the model and the matching process is applied, along with the traditional method (t-value) to make a comparison between our approach (using less-processed data with rescaling parameter) and the classical methodology (using fully-processed data without rescaling). The approach has successfully provided posterior probabilities of a match at all possible offsets, and has provided a highest posterior probability for a match at the true offset.

For each experiment, the model parameters (α, β, σ_e^2, and Δ) were estimated in the Bayesian framework via the MCMC sampling. The posterior plots and their MCMC convergence were checked but not reported. Different diagnostic techniques, detailed in Section 5.3.8, were used for checking the MCMC convergence. Following are results of three experiments conducted for matching undated sequences to a dated site master chronology, using both simulated and real data.

7.3.1 Experiment 1: Simulated Data

In order to examine the adequacy of the new modified approach for matching process which takes into account a scaling parameter between the dated and undated sequences, an experiment with simulated data is implemented here. To create an example where the climate variation might alter over different periods of time, we generated a site master chronology of length 300 years as follows (see Figure 7.3). We generated the first and last 100 years of that chronology from $N(0, 2)$ and the second 100 years from $N(0, 0.5)$, and then we combined the three sequences together and normalised to have zero mean and variance one to mimic a fully-processed data-set. As you can see in the Figure 7.3, a subsection of length 100 years was then taken out from a flat part (ring-widths 101 to 200) of the master chronology and assumed to be undated. This undated sequence was then rescaled (so that it has a variance of 1) and matched to the dated master chronology using the new Bayesian approach, Jones' approach and a classical (t-value). The results from the three approaches were then compared and are summarised in Table 7.1.
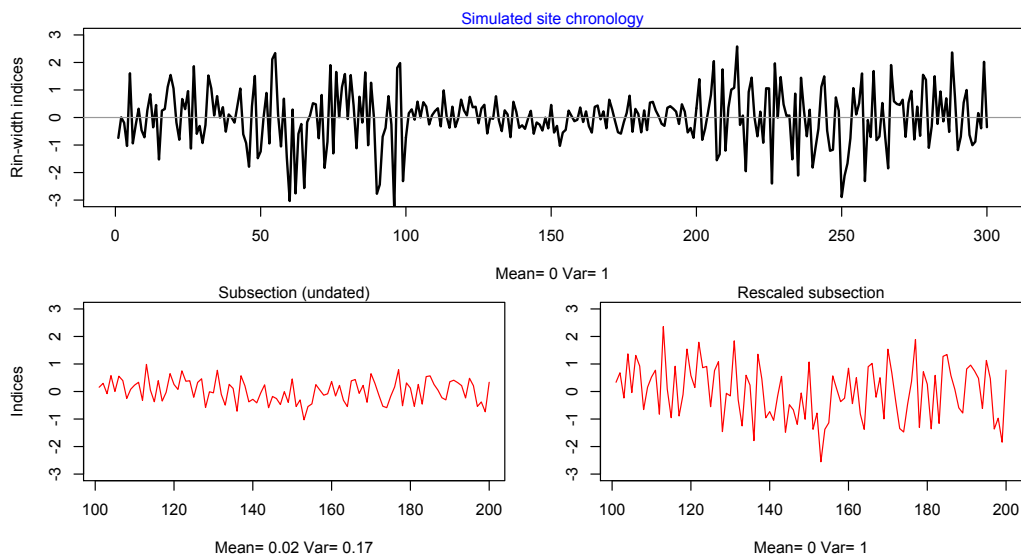
Figure 7.3: Simulated site chronology (*top*) from a normal distribution with zero mean and variance one to mimic the fully-processed data. A subsection of length 100 years (*bottom left*) is taken out and assumed to be undated. The undated sequence is rescaled (*bottom right*) to put on the same scale as the dated chronology.

It is worth noticing that when matching the undated subsection without rescaling (Figure 7.3, bottom left panel) to the master chronology, we will obtain a perfect match (i.e. it will be matched to its correct offset with a scaling of 1 and a shift of 0). However, in the traditional dendrochronology they do not do this, but instead they rescale the undated sequence again so that it has zero mean and variance one (Figure 7.3, bottom right panel) in order to put it on the same scale as the master chronology, but without taking into account the effect of that rescaling.

Results in Table 7.1 show that the new Bayesian approach with the rescaling parameters has provided a high posterior probability estimate of 0.91 for a match at the true offset. In this simulation experiment, the new approach tends to perform better than the current available methods. This is clear in the table, as the classical method and Jones' approach both failed to provide high t-value and high posterior probability of the match at the true offset. Specifically, the classical method has provided a t-value of 3.18 which is under the acceptable threshold value used by dendrochronologists. Similarly, a relatively low posterior probability of only 0.57 was provided by Jones' approach. Unlike the results of our modified approach, the results of the two current methods tend to be unacceptable by the dendrochronologists who are looking for a relatively high posterior probability (≥ 0.70) and high t-value (≥ 3.5) of the match.

New approach		Jones' approach		t-value	
Offset	Posterior Prob.	Offset	Posterior Prob.	Offset	Posterior Prob.
100	0.914	100	0.574	100	3.18
140	0.063	175	0.251	175	2.47
153	0.021	140	0.073	112	2.04
87	0.005	124	0.026	103	1.96

Table 7.1: Results of matching an undated sequences covering 100 years to a dated site master chronology covering 300 years, using our new Bayesian approach, Jones' approach, and the traditional method (t-value). The true offset is 100.

Figure 7.4 shows the histograms of the posterior distributions for the model parameters $\hat{\alpha}$, $\hat{\beta}$, $\hat{\sigma}_e^2$ and $\hat{\Delta}$ when using our new approach which takes into account the impact of data-adaptive rescaling.
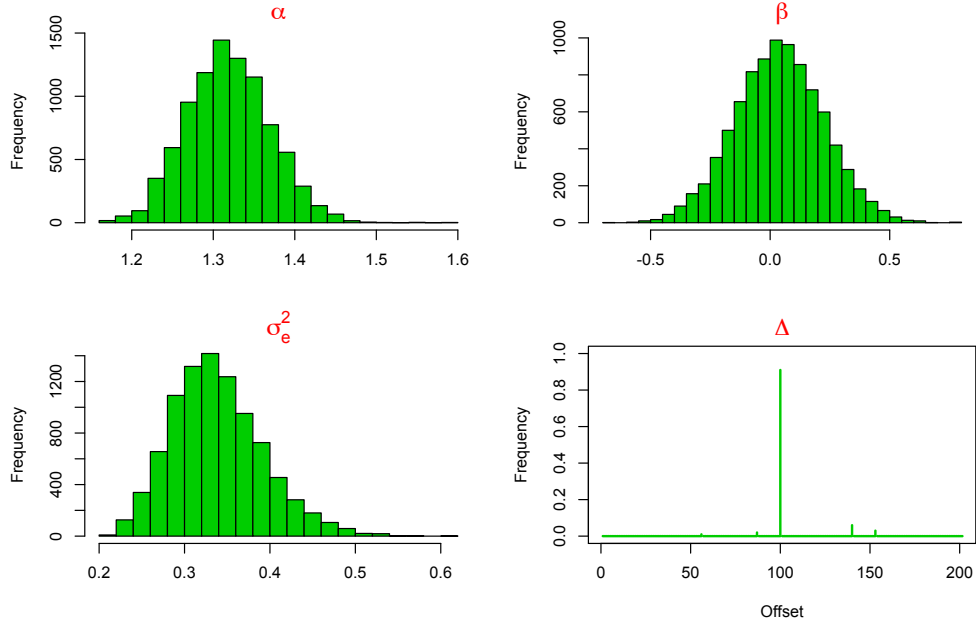
Figure 7.4: Posterior histograms of the model parameters for the experiment of matching undated sequence covering 100 years to a dated site chronology covering 300 years, using our modified approach with simulated data.

This simulation experiment shows the impact of the data-adaptive rescaling between dated and undated sequences prior to matching process. It showed that better dating results with higher posterior probability of a match can be obtained when taking into account a rescaling effect in the model, which ensures that the two sequences are on the same scale before matching them. The effect of the scaling might be influential as results in this experiment showed that a low t-value and a low posterior probability are provided when such data-adaptive rescaling effects are ignored (i.e. the two sequences, one is short and another one is long, are rescaled independently). Therefore, our new method has successfully evaluated the impact of the rescaling via the posterior estimates of the model parameters $\hat{\alpha}$ and $\hat{\beta}$ which both measure the scale and the shift between the dated and undated data.

157

7.3.2 Experiment 2: Real Data (Less-Processed)

The Bayesian approach introduced in Section 7.2.1 allows us to work with less-processed (detrended) data in the matching process. This is due to the rescaling parameter (α) which enables putting the crossmatched sequences on the same scale prior to dating them. Within our new approach, the need for the fully-processed data (which is not desirable) might be removed when matching undated ring-width sequences to a dated master chronology. By using less-processed (only detrended, not prewhitened or normalised) data in the matching process we retain more structures and characteristics of the underlying climatic signal in the data. Furthermore, it would allow the dendrochronology and dendroclimatology communities to work directly with the raw ring-width data when dating timbers and reconstructing past climate.

In order to explore the behaviour of the matching process with less-processed data, we conducted an experiment with real data here. Raw tree-ring width data of 20 Quercus tree samples were obtained from ITRDB for a site in the UK called "Sheffield", `http://www.ncdc.noaa.gov/data-access/paleoclimatology-data/` `datasets/tree-ring`. The length of tree-ring samples at this site varies from 84 years to 245 year as shown in Table 7.2 and Figure 7.5.

Table 7.2 shows descriptive statistics for measured Quercus ring-width data at Sheffield site, and Figure 7.5 shows the time-series plot of both raw ring-width data and detrended sequences for each individual trees at Sheffield site. All the tree-ring series were aligned together with a view to building a site master chronology.

All the tree-ring samples were detrended, using methods detailed in Section 2.1.1, to remove any growth related effect (age-trend) from measured ring-widths. Figure 7.5 (bottom panel) shows the detrended ring-width sequences. One of the detrended samples was then randomly selected (sample EPW19) to be assumed as undated sequence of length 135 years, and the remaining 19 samples were then used to build a dated site master chronology, using methods detailed in Section

Seq	Series	Time Span	No. Years	Corr with Master	Mean	Std dev
1	BPW01	1784 - 2003	220	0.645	1.34	0.651
2	BPW02	1780 - 2003	224	0.480	0.95	0.717
3	BPW03	1812 - 2003	192	0.634	1.67	0.598
4	BPW04	1821 - 2003	183	0.540	1.38	0.786
5	BPW05	1799 - 2003	205	0.583	0.86	0.532
6	BPW06	1777 - 2003	227	0.555	1.50	0.584
7	BPW07	1841 - 2003	163	0.614	0.84	0.417
8	BPW08	1833 - 2003	171	0.596	1.73	0.832
9	BPW09	1808 - 2003	196	0.705	1.72	0.914
10	BPW10	1804 - 2003	200	0.592	0.94	0.917
11	EPW11	1759 - 2003	245	0.601	1.09	0.475
12	EPW12	1864 - 2003	140	0.540	1.51	0.701
13	EPW13	1836 - 2003	168	0.689	1.63	1.016
14	EPW14	1824 - 2003	180	0.554	1.39	1.059
15	EPW15	1831 - 2003	173	0.528	1.37	0.675
16	EPW16	1843 - 2003	161	0.409	1.46	0.795
17	EPW17	1866 - 2003	138	0.617	1.77	0.596
18	EPW18	1917 - 2003	87	0.469	2.68	0.727
19	EPW19	1869 - 2003	135	0.450	1.50	0.622
20	EPW20	1920 - 2003	84	0.349	2.37	0.697

Table 7.2: Summary statistics for raw ring-width data of 20 samples from "Sheffield, Bingham Park Wood and Endcliffe Wood". Columns 3 to 6 show respectively the time span for each sequence, number of years covered by the samples, the correlation between the sequence and the site master chronology, mean and standard deviation of each ring-width sequences.

2.3.3. A site master chronology of length 245 years for this geographical location was successfully built.
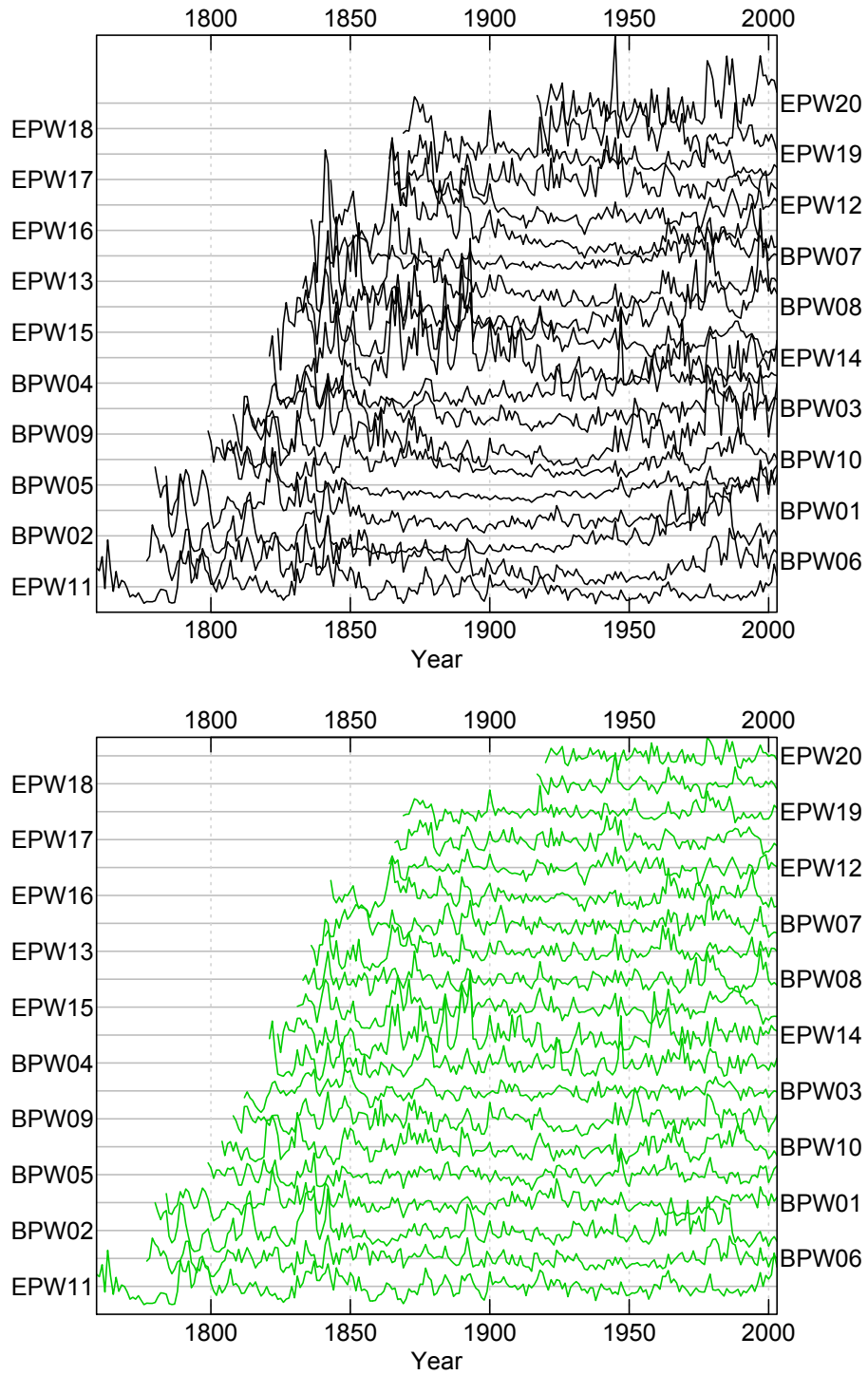
Figure 7.5: A plot of raw ring-width data (*top*) and detrended ring-width indices (*bottom*) at "Sheffield, Bingham Park Wood and Endcliffe Wood".

Figure 7.6 shows the time-series plots of the dated site master chronology built from 19 detrended individual trees, and the undated sample.
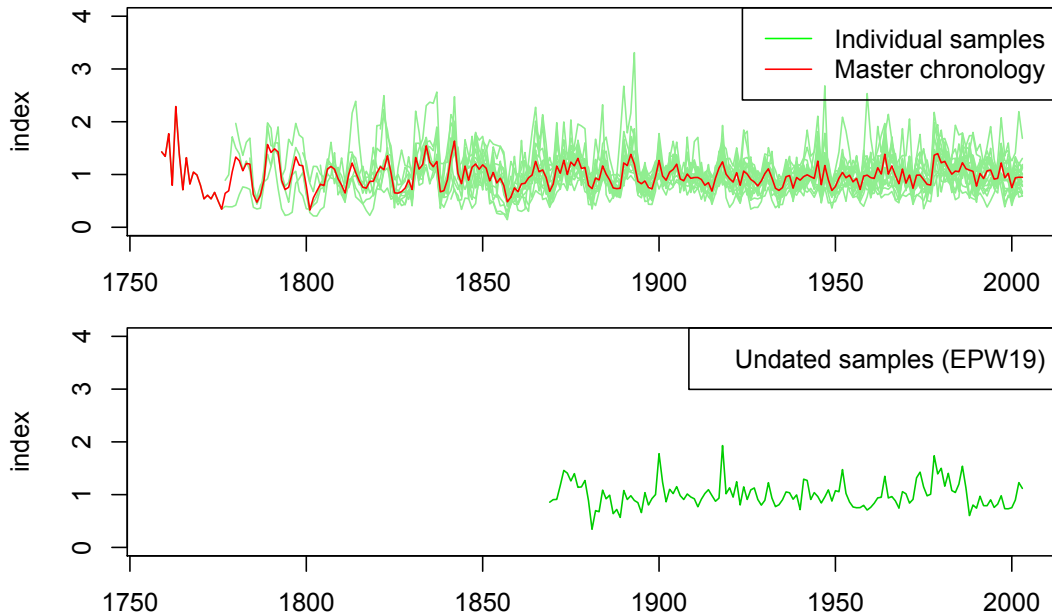
Figure 7.6: Time-series plots of ring-width indices at "Sheffield, Bingham Park Wood and Endcliffe Wood"; *top panel* shows a dated master chronology (*red*) created from 19 individual trees (*green*), and *bottom panel* shows an undated ring-width sequence. All the sequences are only detrended, not prewhitened or normalised.

The undated sample is then matched to the dated site master chronology using our new model which takes into consideration the rescaling between the two sequences. Table 7.3 shows the posterior probability of the match at the main four highest probability offsets, and the mean posterior estimates of the model parameters ($\hat{\alpha}$, $\hat{\beta}$, and $\hat{\sigma}_e^2$). The true date of the undated sequence is AD 1869. The Bayesian implementation of the model has successfully located the undated sample at the correct date offset with a high posterior probability of 0.89. However, the classical method which does not take into account the effect of rescaling between the two sequences, has failed to provide a high t-value for the match at the correct offset. It has provided a t-value of just (3.29) which is under the acceptable threshold value (3.5). This emphasizes the importance of the new approach which

provides more reliable and dependable results for matching ring-width sequences.

Posterior Probability		$\hat{\alpha}$	$\hat{\beta}$	$\hat{\sigma}_e^2$	t-value
Offset	Probability				
1869	0.89	0.248	0.074	0.481	3.29
1863	0.05				3.41
1797	0.02				3.13
1856	0.01				2.61

Table 7.3: Results of the experiment of matching a detrended undated sequence covering 135 years to a dated site master chronology covering 245 years, using our new Bayesian approach and the traditional dendrochronology method (t-value). The true offset of the undated sequence is 1869 AD. The MCMC ran for 10000 iterations with 1000 iterations as burn-in period, and the parameter results have been thinned to every 10 iterations.

This experiment shows the potential of using less-processed data for dating purposes under our new Bayesian approach. In this experiment, although the data were only detrended, the model has successfully matched the undated sample at the true offset with the highest posterior probability. Due to the use of the rescaling parameters (α and β) in the model, the new approach removes the need of the fully processed data in the matching process. In other words, the model only keeps the detrending procedure which is inevitable to remove the age-trends from raw data. This is beneficial for the dendrochronologists which will allow them to keep more structures of climatic signals in their data, and will also allow removing the need for prewhitening and normalising data which are undesirable.

7.3.3 Experiment 3: Matching Individual Trees

The classical tree-ring dating process relies on finding two samples which match properly together. A master chronology is then constructed by matching these two sequences together and then finding more samples which match the first two, and so on. However, sometimes trees may have come from different places and

fail to match with each other, thus building a site chronology will become more difficult, and the timbers therefore remain undated. This is because under classical methodologies, a match with a t-value of less than 3.5 cannot be accepted and the timber remains undated in this case.

In order to examine the ability of our new Bayesian approach for matching individual trees in terms of their posterior probabilities, we used our data in the previous experiment (Section 7.3.2) for this purpose, as follows. Sample 11, which is the longest tree-ring sequence in this geographical location is assumed to be a dated sequence known as "reference". Ten individual samples were also selected randomly and assumed to be undated sequences. Hence the 10 samples were cross-matched against the dated reference to obtain an absolute calendar date for each undated sample.

Table 7.4 shows the results of crossmatching pairs of ten single trees. Every single tree is crossmatched with the "reference" sequence (sample 11) using our new Bayesian approach and the classical method (t-values). Results in Table 7.4 illustrate that the new Bayesian approach has successfully matched each individual tree with the highest posterior probability at its true offset, and there is no match with high posterior probability at the wrong offsets. Specifically, it provided a very high posterior probability (≥ 0.90) for samples (1, 2, 4, 5, and 9), a moderate posterior probability (≥ 0.70) for samples (3, 6 and 8), and a low, but the highest posterior probability for samples 7 and 10.

More interestingly, while the classical method (t-value) failed to match some of the undated sequences at their true offsets, the new Bayesian approach was able to match them with relatively high posterior probabilities. This can be noticed, for example, in samples 3 and 6 when the classical method provided t-values of less than the acceptable threshold value 3.5, but the posterior probabilities were relatively high. This is because the dated and undated samples were not on the same scales before matching, and the classical method does not account for the effect of rescaling them.

This experiment demonstrated that the new Bayesian approach can also be

163

Sample	Offset	Posterior Probability	t-value
Sample 1	**1784**	0.93	5.01
	1759	0.06	3.15
	1802	0.01	2.61
Sample 2	**1780**	0.90	4.45
	1779	0.08	2.15
	1753	0.01	1.76
Sample 3	**1812**	0.70	3.28
	1810	0.16	2.73
	1794	0.09	2.13
Sample 4	**1821**	0.99	5.48
	1782	0.00	3.32
	1819	0.00	1.97
Sample 5	**1799**	1.00	5.62
	1760	0.00	2.89
	1805	0.00	1.81
Sample 6	**1777**	0.79	3.24
	1800	0.11	2.94
	1793	0.06	2.65
Sample 7	**1841**	0.54	2.85
	1784	0.22	2.98
	1782	0.19	1.45
Sample 8	**1833**	0.78	3.71
	1855	0.15	2.92
	1792	0.02	1.75
Sample 9	**1808**	0.92	3.62
	1866	0.06	3.04
	1807	0.01	1.26
Sample 10	**1804**	0.47	2.97
	1818	0.35	2.71
	1817	0.11	2.62

Table 7.4: Results of crossmatching ten undated individual trees to a single dated sequence using our new Bayesian approach and the classical method (t-values). The first (highlighted) offset for each sample is the true offset.

used to match individual trees one with another. The new approach was able to always provide a highest posterior probability at the true offset. Therefore, if (for example) a threshold posterior probability of 0.70 is to be considered for making a decision about good or bad matches, then the majority of the individuals trees in this experiment have been successfully matched at their true offsets, and there is no matches with a highest posterior probability on the wrong offsets.

7.4   Summary of Chapter

In this chapter a Bayesian approach for tree-ring dating has been introduced and examined by different experiments on simulated and real data. The approach takes account of scaling and translating between the dated and undated sequences to ensure that they are on the same scale before cross-matching them. It has taken into consideration the data-adaptive rescaling between the undated tree (which is relatively short and might come from a place with a short period of climate variation) and the dated master chronology (which is relatively long and might come from a place with a long period of climate variation). The new approach involves simultaneously fitting a simple linear model, matching undated trees to a dated master chronology, and hence identifying a posterior probability of a match at each possible offset between the two sequences. The Bayesian matching process includes evaluating the likelihood of the model parameters at every possible date offset which allows the posterior distribution of the unknown date to be estimated.

Bayesian implementation experiments in this chapter show the potential of matching less-processed data with data-adaptive rescaling. The new approach has successfully matched the undated sequence with the highest posterior probability of a match at the true offset. Within this approach, the matching process were applied for less-processed data. This has enabled us of rescaling sequences of different lengths using data-adaptive rescaling, and therefore matching trees that kept more structure of climatic signals in their data. In addition, the new approach has successfully used for matching individual trees with each other, and this is beneficial for building master chronologies.

In the next chapter, the new model introduced here with the rescaling parameter will be linked with the VSLite model to tackle the problem of matching undated trees in the presence of missing master chronologies. The VSLite model will be used to estimate a pseudo-master chronology from dated climate variables, and the missing master will be replaced by the pseudo-chronology generated from VSLite. This will be implemented in a Bayesian framework using a two-stage MCMC method.

Chapter 8

Tree-Ring Dating in the Absence of Master Chronologies

8.1 Introduction and Motivation

In the previous chapter we introduced a linear model for matching undated trees to a dated site master chronology. The model was successfully used to match undated sequences to dated master chronologies under the Bayesian framework. Within that approach, as in all current dendrochronology methods, in order to date any undated ring-width sequences, there must be an existing relatively long dated site or master chronology. This dated sequence is the key to the matching process, without it undated sequences cannot be dated. However, master chronologies are not available for most locations around the world, and are at best only available for limited areas, thus many tree timbers remain undated. For instance, Jones (2013) states that "although dendrochronology is a successful and well practised technique, many timbers sampled do remain undated. The overall success rate for dating timbers in the UK is approximately 60-70%, and this rate varies within sites and within wider geographical locations, for example the success rate of dating timbers in South West England is approximately 30-40%". One of the main reasons for this failure is the lack of master chronology. Therefore, without having such dated chronologies, many actual undated timbers remain undated.

In this chapter we consider the problem of matching undated tree-ring width sequences when the master chronology is missing. We aim to tackle this problem by first replacing a missing master chronology for a site of interest by a pseudo-master generated from the VSLite model using available climatic records. The reason for not directly matching undated sequence to the climate information is because the two types of data (climate and tree-ring) are not comparable, and we aim to transform the climate information into a pseudo chronology to make them comparable. Hence, we match undated timbers to the generated (pseudo) master chronology and make inference about the matching process in a Bayesian framework. Our focus is therefore on areas like South West England where historical climate records exist, but no master chronologies have been established. Although, this method would only work when we have climate data, it would be of great interest to know whether a mechanistic forward model as simple as VSLite has the potential to create tree-ring width chronologies from climate data in areas where we have undated tree-ring data but do not have master chronologies.

This chapter is structured as follows. Modelling the matching undated trees in the presence of missing master chronologies is introduced in Section 8.2. A Bayesian implementation of the model, using a two-stage MCMC method, is detailed in Section 8.3. Methods for measuring uncertainty in the estimated dates for the undated sequences are introduced in Section 8.4. The model implementation algorithm is summarised in Section 8.5. Results from implementing the model for three case studies are reported in Section 8.6, and this is followed by the conclusions and summary in Section 8.7.

8.2 Matching under Missing Chronologies

To model the process of matching undated timbers when master chronologies are missing, we replace the real dated chronology ($\mathbf{y^D}$) given in the model in chapter 7, with a pseudo-master chronology ($\hat{W}$) generated from the VSLite model using

historical climatic records. The model becomes,

$$\alpha \, y_i^U = \beta \; + \; \hat{W}_i + \; \epsilon_i$$

$$= \beta \; + \; f(\mathbf{T}, \mathbf{P}, T_1, T_2, M_1, M_2, \phi) + \; \epsilon_i$$

where;

y_i^U: is the undated ring-width sequences of length l^*.

$\hat{W}_i$: is the dated pseudo-chronology of length l, generated from the VSLite model given monthly temperature ($\mathbf{T}$) and Precipitation ($\mathbf{P}$), VSLite growth response threshold parameters (T_1, T_2, M_1, M_2), and site latitude (ϕ).

α: is the rescaling parameter between the dated and undated sequences.

β: is the population mean of the undated sequences.

ϵ_i: is the error term or noise, which also includes the uncertainty associated with the estimated VSLite output $\hat{W}$. ϵ_i follows a normal distribution with mean 0 and variance σ_e^2.

A Bayesian implementation of this model is offered in the next section. The modified approach involves simultaneously generating a dated pseudo-master chronology from VSLite, fitting the model and match the undated trees to the pseudo-master chronology, and identifying the posterior probability of a match at all possible offsets between the two sequences.

8.3   Bayesian Model Implementation

In the Bayesian framework, we study the posterior probability of the match Δ at all possible offsets, and also seek the posterior estimates for all other parameters in the model $\pi(T_1, T_2, M_1, M_2, \hat{\mathbf{W}}, \alpha, \beta, \sigma_e^2, \Delta | \mathbf{y}, \mathbf{T}, \mathbf{P})$, which we refer to as $\pi(\Theta | \text{data})$. We thus wish to study

$$\pi(\Theta | \text{data}) = \int_{\Theta} \pi(\Theta | \text{data}) \, \pi(\Theta) \, \mathrm{d}\Theta, \tag{8.1}$$

where $\pi(\Theta)$ is the prior distribution of the unknown parameters. The joint posterior distribution $\pi(\Theta | \text{data})$ is integrated using MCMC techniques.

However, implementing this model and estimating the posterior distribution as mentioned above is potentially a challenging problem because of a large number of model parameters. Having explored the convergence properties of Markov chains used to implement the model in the previous chapter, we established that fitting the model itself is not challenging, but the matching process and convergence checking for the model parameters is time consuming. In some circumstances when the highest posterior probability of the match is low, it requires running the MCMC chains for more than $100,000$ iterations to obtain the converged and reproducible results. When implemented in R (R Core Team, 2015), the implementations take more than 3 hours on the currently available MacBook computer with a processing speed of 2.7 GHz and 8 GB RAM.

Adding parameters of the VSLite model to the process and updating these within the MCMC will make the problem even more computationally expensive. Therefore, a more efficient method needs to be added to the existing code. Following the example of others with similar problems (Bhattacharya and Haslett, 2007; Christen and Fox, 2005; Ginting *et al.*, 2011; Haslett *et al.*, 2006) we use a two-stage MCMC sampling which allows us to split our inference problem into two separate tasks, as shown in Figure 8.1.

8.3.1 Two-stage MCMC method

In the two-stage MCMC algorithm, estimation of our posterior distribution $\pi(\Theta|\text{data})$, given in Equation 8.1, can be decomposed into two components representing two discrete tasks:

$$\pi(\Theta|\mathbf{data}) = \underbrace{\pi(\hat{\mathbf{W}}|\mathbf{T},\mathbf{P},T_1,T_2,M_1,M_2)}_{\text{stage 1}}\underbrace{\pi(\alpha,\beta,\sigma_e^2,\Delta|\mathbf{y},\hat{\mathbf{W}})}_{\text{stage 2}}. \qquad (8.2)$$

In the first stage, dated pseudo-chronologies are generated from the VSLite model with given climate data for the site (or region) of interest and estimated growth threshold parameters. The output from this stage is the posterior distri-

169
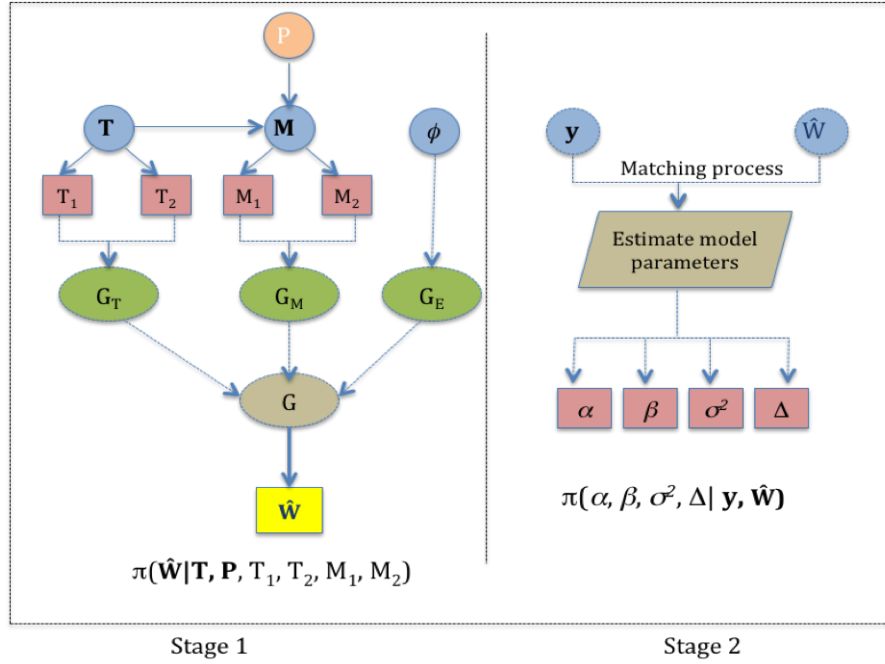
Figure 8.1: Schematic representation of the model for matching undated sequences when no master chronology is available. Stage 1: (*left*) estimating VSLite parameters and generating the dated pseudo-master chronology $\hat{\mathbf{W}}$. Stage 2: (*right*) matching undated sequence to the pseudo-master chronology and estimating the parameters of the dendrochronology model.

bution of dated chronologies $\pi(\hat{\mathbf{W}}|\mathbf{T},\mathbf{P}, T_1, T_2, M_1, M_2)$, and this is referred to as "stage 1" in Figure 8.1 and Equation 8.2. This posterior output is then stored in a large file to be used in the next stage when we match sequences and make inferences about the unknown date for the undated sequences. In the second stage, inferences are made about the model parameters and the matching process $\pi(\alpha, \beta, \sigma_e^2, \Delta|\mathbf{y}, \hat{\mathbf{W}})$. In this stage, the model is fitted using a large number of MCMC iterations, each conditioned on the converged pseudo dated chronology $\hat{\mathbf{W}}$, which is obtained from averaging the posterior samples generated in stage-1.

By separating these two processes, we are making the assumption that the matching process (stage 2) is conditionally independent of the climate data given the generated dated pseudo-master chronologies (stage 1). This is crucial, because

we might need to run the second stage for a very large number of iterations due to the convergence demands, but we do not need such large number of iterations to reach convergence in the first stage. Thus, the two-stage MCMC method contributes to speed up the mixing and convergence overall. As we focus on the posterior probability estimate of the match at all possible offsets (stage 2), the two-stage MCMC method allows us to dedicate most of our computing resources and convergence checking to the second stage, and therefore does not substantially add to the three hour run-time outlined above.

8.3.2 Two-stage MCMC Sampling Procedures

A Metropolis-Hastings algorithm within a Gibbs sampler is used to estimate the posterior distributions of the model parameters $\pi(\Theta|\text{data})$, as follows.

First-stage:

1. Choose starting values for $T_1^{(0)}, T_2^{(0)}, M_1^{(0)}$, and $M_2^{(0)}$.

2. for $j = 1$ to N (MCMC sample size)

   a) Draw a proposed value T_1' from the prior distribution of T_1.

   b) Calculate the likelihood of the proposed value,
   $p(\mathbf{y}^D|\mathbf{T},\mathbf{M},T_1',T_2^{(j-1)},M_1^{(j-1)},M_2^{(j-1)})$

   c) Calculate the likelihood of the current value,
   $p(\mathbf{y}^D|\mathbf{T},\mathbf{M},T_1^{(j-1)},T_2^{(j-1)},M_1^{(j-1)},M_2^{(j-1)})$

   d) With probability $\min\left\{1,\frac{p\left(\mathbf{y}^D|\mathbf{T},\mathbf{M},T_1',T_2^{(j-1)},M_1^{(j-1)},M_2^{(j-1)}\right)}{p\left(\mathbf{y}^D|\mathbf{T},\mathbf{M},T_1^{(j-1)},T_2^{(j-1)},M_1^{(j-1)},M_2^{(j-1)}\right)}\right\}$ set $T_1^{(j)} = T_1'$; otherwise, set $T_1^{(j)} = T_1^{(j-1)}$.

   e) Repeat steps (a to d) to update T_2, using parameters $(T_1^{(j)}, M_1^{(j-1)}, M_2^{(j-1)}, \sigma_\epsilon^{2(j-1)})$.

   f) Repeat steps (a to d) to update M_1, using parameters $(T_1^{(j)}, T_2^{(j)}, M_2^{(j-1)}, \sigma_\epsilon^{2(j-1)})$.

   g) Repeat steps (a to d) to update M_2, using parameters $(T_1^{(j)}, T_2^{(j)}, M_1^{(j)}, \sigma_\epsilon^{2(j-1)})$.

   h) Generate a pseudo-site-chronology vector $\hat{\mathbf{W}}^{(j)}$, based on $T_1^{(j)}, T_2^{(j)}, M_1^{(j)}, M_2^{(j)}$.

3. Repeat step (2) until the Markov Chain reaches equilibrium.

4. Save $\hat{\mathbf{W}}^{(j)}$ to a text file with one chronology per row.

5. Obtain a converged pseudo-chronology, $\hat{\mathbf{W}}$, by averaging (taking a simple arithmetic mean) from all pseudo chronologies $\hat{\mathbf{W}}^{(j)}$ generated in step 4.

6. End of stage 1.

Second-stage:

7. Choose starting values for $\alpha^{(0)}, \beta^{(0)}, \sigma_e^{2(0)}$, and $\Delta^{(0)}$.

8. for $j = 1$ to N (MCMC sample size)

   a) Update α by:

       i. Drawing a proposed value α' from the prior distribution of α.

       ii. Calculate the likelihood of the proposal, $p(\mathbf{y}^U | \hat{\mathbf{W}}, \alpha', \beta^{(j-1)}, \sigma_e^{2(j-1)}, \Delta^{(j-1)})$

       iii. Calculate the likelihood of current value, $p(\mathbf{y}^U | \hat{\mathbf{W}}, \alpha^{(j-1)}, \beta^{(j-1)}, \sigma_e^{2(j-1)}, \Delta^{(j-1)})$.

       iv. With probability $\min \left(1, \frac{p(\mathbf{y}^U | \hat{\mathbf{W}}, \alpha', \beta^{(j-1)}, \sigma_e^{2(j-1)}, \Delta^{(j-1)})}{p(\mathbf{y}^U | \hat{\mathbf{W}}, \alpha^{(j-1)}, \beta^{(j-1)}, \sigma_e^{2(j-1)}, \Delta^{(j-1)})} \right)$ set $\alpha^{(j)} = \alpha'$; otherwise, set $\alpha^{(j)} = \alpha^{(j-1)}$.

   b) Update β by sampling a new value of $\beta^{(j)}$ from its full conditional distribution, $p(\beta | \mathbf{y}^U, \hat{\mathbf{W}}^{(j-1)}, \alpha^{(j)}, \sigma_e^{2(j-1)}, \Delta^{(j-1)})$.

   c) Update σ_e^2 by sampling a new value of $\sigma_e^{2(j)}$ from its full conditional distribution, $p(\sigma_e^2 | \mathbf{y}^U, \hat{\mathbf{W}}^{(j-1)}, \alpha^{(j)}, \beta^{(j)}, \Delta^{(j-1)})$.

   d) Update Δ by sampling a new value of $\Delta^{(j)}$ from its full conditional distribution, $p(\Delta | \mathbf{y}^U, \hat{\mathbf{W}}^{(j-1)}, \alpha^{(j)}, \beta^{(j)}, \sigma_e^{2(j)})$.

9. Repeat step (7) until the Markov Chain reaches equilibrium.

10. After the burn-in period and thinning the subsequent iterations of step (7), the resulting iterations are used as samples from the posterior.

11. End.

8.4 Measuring Uncertainty in Estimated Dates

In order to check the efficiency of the approach suggested in this chapter, we will conduct some experiments at locations where both dated tree-ring data and historical climatic records are available. We will thus compare matching undated trees to both real and pseudo master chronologies, and hence make inferences about the distribution of the unknown dates for the undated timbers. Unlike Jones (2013) who assumed that the match with the highest posterior probability is the only single "best match" for the undated sequence, we will be interested in the whole distribution of all possible offsets with their posterior probabilities. This is because under some circumstances we might have the highest posterior probability at a poor or wrong offset, and for that reason we will study the whole posterior distribution rather than a single match with the highest posterior probability estimate. Therefore, to measure the uncertainty in the estimated dates, we evaluate the following measures which are simple to compute and easy to interpret, especially by non-statisticians.

8.4.1 Loss Function for Matching

The quality of the estimate given the known true date can be described by a loss function and its associated risk. In the current context, a loss (or cost) function is a method of calculating how bad a decision would be if a wrong offset were chosen.

A matching process requires that we specify our matching target, i.e., what we want to achieve. A loss function L for each possible offset from a matching process can be defined as a cost of the difference between possible offset $\hat{\Delta}_i$ and the true offset Δ^*. In this chapter, we use $L(\Delta_i)$ as the cost, or loss, of choosing the offset $\hat{\Delta}_i$ as the possible match for the undated tree. The smaller the value of L, the better the offset is for the undated sequences. There are two commonly used versions of loss functions, the squared loss and the absolute loss. We tend to use the absolute loss function for matching, because it measures the distance between each possible offset and the true offset of the match, and it is easier to understand,

especially for non-statisticians. The loss absolute function for each possible offset can be mathematically defined as

$$L(\Delta_i) = |\hat{\Delta}_i - \Delta^*|$$

where Δ^* is the true offset for the undated sequences, and $\hat{\Delta}_i$ is the possible offset from the matching process. Successful dating occurs when both the number of possible offsets and the cost of each offset are small. To obtain a probability distribution for the loss we simply compute the loss function for each possible offset.

8.4.2 Risk Function

Having evaluated the loss function for each possible offset of the undated sequence, the risk function (or expected loss function) can be defined by taking the expected value of each possible offset with respect to the posterior probability of that offset. The expected loss function for a range of possible offsets to obtain a particular posterior probability (P) can be defined as

$$\begin{aligned} E(L_i \geq P) &= L_1 p_1 + L_2 p_2 + \cdots + L_k p_k \\ &= \sum_{i=1}^{k} L_i p_i \end{aligned}$$

where L_i and p_i are respectively the loss function and the posterior probability of the match for offset i, and k is the number of possible offsets to obtain a posterior probability, P. The expected loss function for the true offset is always equal to zero as the loss of the true offset is zero. We aim to minimise the expected value for the posterior density estimates for all possible offsets between the dated and undated sequences.

8.4.3 Cumulative Posterior Probability

Instead of only providing a single offset with the highest posterior probability of a match, we also estimate the cumulative frequency distribution for posterior

174

probabilities of all possible offsets. This will allow us to evaluate the quality of the matching process in the number of calendar years covered to obtain any particular posterior probability of a match. In other words, the posterior probability of the undated sequences being matched within n calendar years can be evaluated.

Successful dating occurs when the cumulative posterior probability is high, the value of expected losses is low, and the number of possible calendar date offsets included in the matching process is small.

8.4.4 Threshold Probability Value for Bayesian Matching

Classical dendrochronologists usually use a threshold t-value of 3.5 to indicate a good match for tree-ring dating. Baillie and Pilcher (1973) suggested using this value as an arbitrary threshold for the match to be acceptable. Since then, it has become a routinely adopted practice. That said, of course, the higher the t-value, the better the match.

In Bayesian dendrochronology, when matching the dated and undated sequences, the sum of the posterior probabilities of all possible offsets is 1. When there is only one offset with a very high posterior probability between the two sequences, it is easy to indicate it as a best match. However, unfortunately, this is not always the case, and there might be a number of possible offsets each with a rather lower posterior probability. In such cases, to mirror current practice, it seems desirable to have both, the distribution of all possible offsets and a probabilistic threshold value above which a match might reasonably be used in inference.

As mentioned in Chapter 6 several experiments were conducted to match undated sequences to the dated master chronologies using Jones' approach (Jones, 2013). For each experiment, a t-value and a posterior probability of the match were evaluated and compared. Empirical exploration of the results in Chapter 6 suggest that the classical t-value of 3.5 is approximately equivalent to a posterior probability of 0.75, as shown in Figure 8.2. However, we prefer not to use an ar-

bitrary probabilistic threshold value, because we will be providing full probability densities of the match. Nevertheless, if a probabilistic threshold value is demanded by practitioners in the user community, then we (depending on the results of our empirical experiments) suggest a posterior probability of 0.75 as a probabilistic threshold value to be used for the Bayesian dendrochronology. The reason for doing this empirical experiment is to show how the t-values linked to the posterior probabilities might be chosen, by the user community, as an arbitrary probabilistic threshold value for Bayesian dendrochronology. Successful dating occurs when the posterior probability of a match is high; the larger the posterior probability, the better the match is between dated and undated sequences.
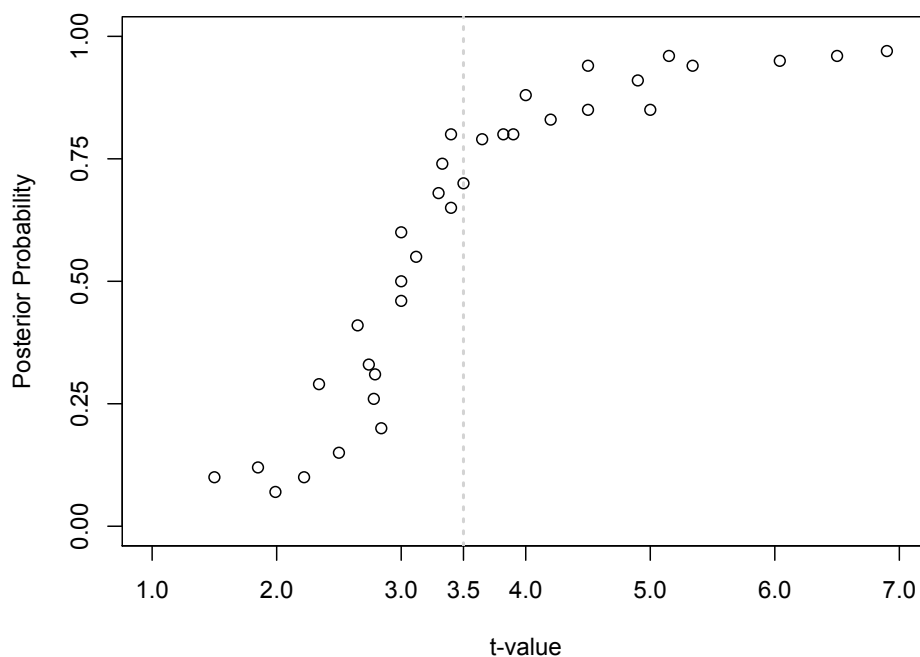
Figure 8.2: Posterior probabilities versus classical t-values obtained from several experiments (conducted in Chapter 6) of matching undated tree-ring sequences to dated master chronologies using Jones' model. Vertical line is 3.5 t-value threshold used by classical dendrochronology.

8.5   Model Implementation Algorithm

To explore the efficiency of the suggested method for dating undated data when site and master chronologies are missing, several experiments were carried out as mentioned in the next section. For each experiment, the following steps were used.

1. Select a geographical site where there exist (I) tree-ring width sequences ($\mathbf{x}$) with known age, then:

   - Divide $\mathbf{x}$ trees into training ($\mathbf{x^t}$) and testing ($\mathbf{x^s}$) data.
   - Detrend $\mathbf{x^t}$ and $\mathbf{x^s}$ data to remove age-trend.
   - Assume $\mathbf{x^s}$ data as undated sequences $\mathbf{y^U}$.
   - Build a site chronology $\mathbf{y^D}$ from training data $\mathbf{x^t}$.

2. Generate a pseudo site chronology $\hat{\mathbf{W}}$ from VSLite model:

   - Specify the site of interest, and find its latitude ϕ.
   - Obtain historical monthly climatic data $\mathbf{T}$ and $\mathbf{P}$.
   - Calculate the monthly soil moisture content $\mathbf{M}$.
   - Make inference about growth response parameters T_1, T_2, M_1, M_2.
   - Calculate partial growths G_T, G_M, G_E, and hence overall growth G_t.
   - Simulate $\hat{\mathbf{W}}$.

3. Match the undated sequences y_i^U to the pseudo site chronology ($\hat{\mathbf{W}}$).

4. Match the undated sequences y_i^U to the real site chronology ($\mathbf{y^D}$).

5. Compare the results obtained from 3 and 4 by evaluating:

   - inferences made about model parameters (α, β, σ_e^2, Δ).
   - the posterior probability of a match at all possible offsets.
   - the loss function and cumulative posterior probability of each offset.

For each experiment in the next section, the algorithm above was used to explore the efficiency of the suggested method when master chronologies are missing.

8.6 Case Study Experiments: Dating under Missing Chronologies

This section provides results of several experiments that examine the accuracy of the new method for matching undated ring-width sequences when master chronologies are missing. As the new method is entirely dependent on the climate data records for generating a pseudo-master chronology, we conduct the methodology at several UK sites where long climate data and many tree-ring width sequences are available. In order to check the efficacy of the new approach, results from matching sequences of known ages are compared, when both real-master and pseudo-master chronologies are used.

8.6.1 Study Specification

Three geographical locations, in the UK, were chosen for the model implementation. The chosen sites are Oxford, Sheffield and Southampton, and following is a summary of the climate and tree-ring data for these sites.

Climate Data

Monthly temperature $\mathbf{T}$ and precipitation $\mathbf{P}$ data for central England and the three selected sites (Oxford, Sheffield and Southampton) were obtained from the Meteorological Office (the United Kingdom's national weather service; `http://www.metoffice.gov.uk`). For central England, the mean monthly data series for temperature began in AD 1659, while precipitation records began in AD 1766 (Manley, 1974; Parker and Horton, 2005; Parker *et al.*, 1992). These are the longest available instrumental records of monthly climate data in the world. Table 8.1 shows the key information for the climate data for the three geographical locations.

Figures 8.3 shows the time-series of mean annual temperature and precipitation for central England and the three chosen sites (Oxford, Sheffield and Southampton).

Site	Name	Latitude	Longitude	Time Span	
				Temperature	Precipitation
Site 1	Oxford	51.76	-1.26	1853-2014	1853-2014
Site 2	Sheffield	53.38	-1.49	1883-2014	1883-2014
Site 3	Southampton	50.91	-1.41	1855-1014	1855-2014
	Central England			1659-2014	1766-2014

Table 8.1: Climate data information for three geographical locations in the UK (Oxford, Sheffield and Southampton), as well as the regional climate data of central England, all obtained from `http://www.metoffice.gov.uk/public/weather/climate-historic`.
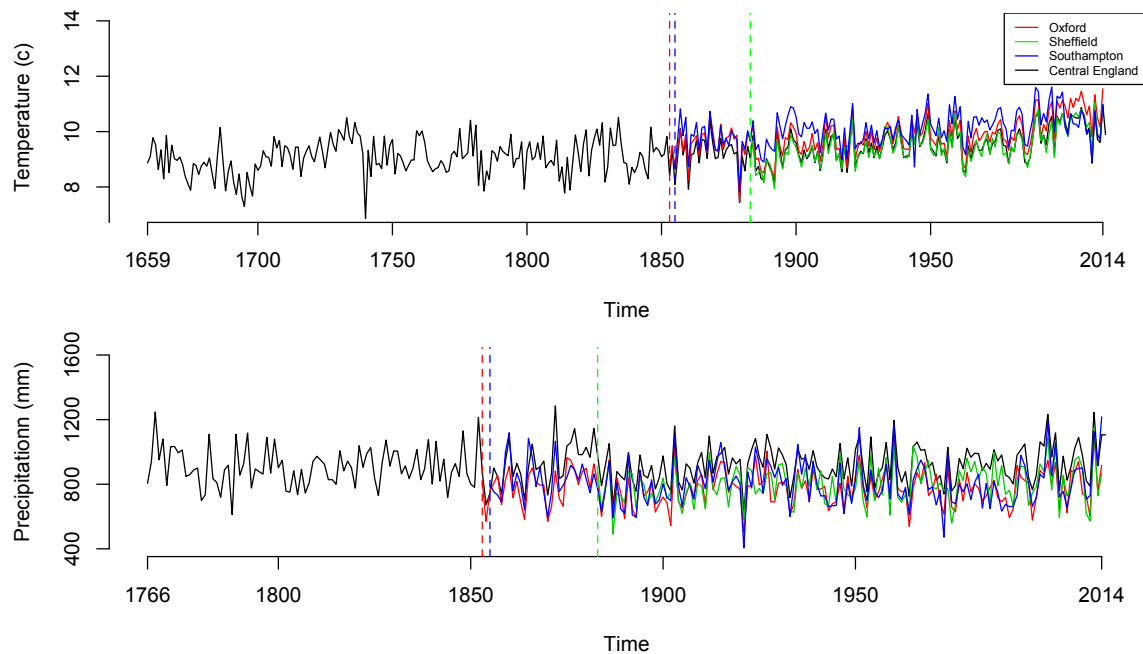
Figure 8.3: Time-series of mean annual temperature (*top*) and precipitation (*bottom*) for central England (*black*) and three geographical locations in the UK, Oxford (*red*), Sheffield (*green*), Southampton (*blue*). Vertical lines indicate starting date in each observation-based time-series.

Tree-ring Data

Tree-ring data were chosen to overlap with the available meteorological data. All the observed tree-ring data were obtained from the International Tree-Ring Data Bank (`http://www.ncdc.noaa.gov/paleo/treering.html`), which is the world's

largest archive of tree ring data. Table 8.2 shows the key information of tree-ring data in our three chosen sites in the UK.

Site	Name	Latitude	Longitude	No. Trees	Time Span	Taxon
Site 1	Oxford	51.8	-1.12	16	1781-1978	Quercus
Site 2	Sheffield	53.37	-1.50	20	1759-2003	Quercus
Site 3	Southampton	51.07	-1.38	26	1800-2009	Quercus

Table 8.2: Tree-ring data information in three geographical locations in the UK (Oxford, Sheffield and Southampton).

It is worth noticing that the difference of distances between the source of climate information (Table 8.1) and tree-ring data (Table 8.2) are not substantial. They are all in the same half-degree of latitude and longitude.

For each site, we divided the individual tree-ring data into two groups of training and testing data. The former was used to build a local site chronology to be utilised in the first MCMC stage when estimating the VSLite growth response parameters, and hence generate a pseudo site chronology derived from the climate data. The testing data were used in the second MCMC stage when matching undated sequences to both real and pseudo site master chronologies.

In what follows, the undated tree-ring width sequences from Sheffield are matched to both real-master and pseudo-master chronologies and the results compared. Results for the other two sites (Oxford and Southampton) can be seen in Appendix IV.

8.6.2   Generating Pseudo Local Site Chronology

Half of the tree-ring width sequences at Sheffield were used to estimate growth response parameters for the VSLite model, and hence a pseudo site chronology was generated from the VSLite model conditioned on monthly climate data, the estimated growth response parameters, and the site latitude. Figure 8.4 shows the simulated pseudo site chronology from the VSLite model at Sheffield.
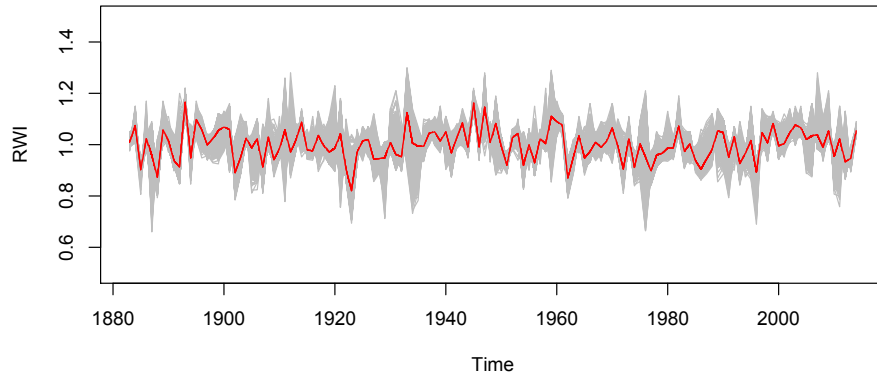
Figure 8.4: Pseudo-site chronologies, $\hat{\mathbf{W}}$, simulated from the VSLite model at "Sheffield" site, given dated climate data records. Grey lines represent n pseudo-chronologies generated, and the red line represents the mean of those n series.

8.6.3   Building Real Site Chronology

Given individual tree-ring width sequences (training data) at Sheffield, a local site chronology which spans the period AD 1759-2003 has been created for this geographical location, using methods detailed in Chapter 2.

8.6.4   Matching Trees to Real and Pseudo Site Chronologies

Table 8.3 shows results of the experiment of matching eight undated sequences from Sheffield to a dated pseudo site chronology of length 132 years generated from the VSLite model, using the Bayesian approach suggested in Section 8.3. Each sequence covered 100 years (from 1904 to 2003 AD) which is the overlapping period with the climate data. Inferences were made about the model parameters and the matching process, and all results reported here are after convergence of the MCMC simulation for the model parameters.

181

Undated Tree	Date	Posterior Probability	Cumulative Posterior Probability	Loss L (Years)	Expected Loss $E(L)$ (Years)
	1904	0.41	0.41	0	0
	1910	0.27	0.68	6	1.62
Sample 1	1894	0.10	0.79	10	2.62
	1887	0.09	0.88	17	4.15
	1905	0.04	0.91	1	**4.19**
	1904	0.33	0.33	0	0
	1898	0.29	0.62	6	1.74
Sample 2	1903	0.20	0.82	1	1.94
	1889	0.07	0.89	15	2.99
	1906	0.03	0.92	2	**3.05**
	1896	0.51	0.51	8	4.08
	1904	0.30	0.81	0	4.08
Sample 3	1893	0.12	0.93	11	**5.40**
	1895	0.05	0.98	9	5.85
	1910	0.01	0.99	6	5.91
	1904	0.34	0.34	0	0
	1887	0.22	0.56	17	3.74
Sample 4	1888	0.19	0.75	16	6.78
	1905	0.11	0.86	1	6.89
	1906	0.04	0.90	2	**6.97**
	1904	0.28	0.28	0	0
	1903	0.27	0.55	1	0.27
Sample 5	1906	0.27	0.82	2	0.81
	1890	0.11	0.93	14	**2.35**
	1895	0.02	0.95	9	2.53
	1904	0.31	0.31	0	0
	1889	0.30	0.61	15	4.50
Sample 6	1912	0.21	0.82	8	6.18
	1887	0.10	0.92	17	**7.88**
	1906	0.04	0.96	2	7.96
	1906	0.30	0.3	2	0.60
	1895	0.23	0.53	9	2.67
Sample 7	1904	0.16	0.69	0	2.67
	1896	0.15	0.84	8	3.87
	1903	0.07	0.91	1	**3.94**
	1904	0.79	0.79	0	0
	1905	0.12	0.91	1	**0.12**
Sample 8	1889	0.05	0.96	15	0.87
	1912	0.01	0.97	8	0.95
	1914	0.01	0.98	10	1.05

Table 8.3: Results of matching eight individual trees of length 100 years from "Sheffield" site. Each tree was matched to the pseudo site chronology of length 132 years, using the Bayesian approach suggested. The true date is 1904, and only 5 possible offsets with the highest posterior probabilities are reported.

Results in Table 8.3 show that the suggested approach has successfully matched the eight undated sequences to the dated pseudo-site chronology. The true date offset always appears among the highest five possible offsets of the match. The cumulative posterior probability and the loss of each possible offset vary among the 8 undated sequences. The expected loss, $E(L)$, of obtaining a cumulative posterior probability ≥ 0.90 is 4.19 years for sample 1, 3.05 years for sample 2, and 5.4 years for sample 3, and so on. Heuristically, the smaller the value of $E(L)$, the better the matching process. Accordingly, sample 8 has the best match among all the undated samples in this geographical location, with a very low expected loss value of 0.12 years.

It is also worth noticing from results in Table 8.3 that although sample 6 has provided the highest posterior probability of the match at the true offset, the matching process for this sample is not as successful as others since the expected loss value is relatively high with 7.88 years. This confirms the importance of investigating the distribution of all possible offsets rather than concentrating on the single offset with the highest posterior probability. Results from two other sites (Oxford and Southampton) are provided in the Appendix IV and are very similar to those reported here.

In order to investigate the adequacy of the suggested approach (when no master chronologies exist), the undated tree-ring width sequences from Sheffield were also matched to real site chronology $\mathbf{y^D}$, and the results were compared to those matched to the pseudo site chronology $\mathbf{\hat{W}}$, generated from the VSLite model. Table 8.4 shows the results of this comparison.

Results in Table 8.4 show that both approaches provide the highest posterior probability of the match at the true offset. However, the probability at that offset is 0.93 when matching to the real site chronology, and 0.41 when matching to the simulated (pseudo) site chronology. Unsurprisingly, the results using the real-site chronology are more satisfactory. However, when such a real site chronology is not

Real Site Chronology					Pseudo Site Chronology				
Offset	PP	CPP	L	$E(L)$	Offset	PP	CPP	L	$E(L)$
1904	0.93	0.93	0	0	1904	0.41	0.41	0	0
1895	0.02	0.95	9	0.18	1910	0.27	0.68	6	1.62
1902	0.01	0.96	2	0.20	1894	0.10	0.78	10	2.62
1922	0.01	0.97	18	0.38	1887	0.09	0.87	17	4.15
1910	0.01	0.98	6	0.44	1905	0.04	0.91	1	4.19
1933	0.00	0.98	29	0.44	1892	0.03	0.94	12	4.55
1927	0.00	0.98	23	0.44	1931	0.02	0.96	27	5.09
1889	0.00	0.98	15	0.44	1933	0.01	0.97	29	5.38
1917	0.00	0.99	13	0.44	1907	0.01	0.98	3	5.42
1935	0.00	0.99	31	0.44	1921	0.00	0.98	17	5.42

Table 8.4: Results of matching an undated sequence (Sample 1) covering 100 years to a real-site chronology and to a pseudo-site-chronology (generated from the VSLite model). The ten highest possible offsets are reported with their posterior probabilities (PP), cumulative posterior probabilities (CPP), loss of offset (L), and the expected loss $E(L)$. The true date of the undated sequences is 1904.

available, the results obtained using the pseudo-chronology are promising. We can demonstrate just how promising they are by considering the loss, L, of each possible offset and their expected loss, $E(L)$, to obtain a cumulative posterior probability of ≥ 0.90.

Table 8.4 shows that when matching to the pseudo site chronology only 5 possible dates with considerable posterior probabilities occur in this experiment, which in order from most to least likely are 1904, 1910, 1894, 1887, 1905. Considering the situation when the real site chronology is missing, the cumulative posterior probability of these five possible offsets taken together accounts for 0.91 posterior probability of the match. We can see that the probability of the undated sequence being dated in the set {1904} is 0.41 with zero expected loss, the probability of it being dated in the set {1904, 1910} is 0.68 with only 1.62 expected loss, and the probability of it being dated in the set {1904, 1910, 1894} is 0.78 with 2.62 expected loss, and so on. Therefore, assuming no real site chronology exist for this site, the undated sequences have been matched to the pseudo site chronology

generated from the VSLite model. This is a useful result for the dendrochronology community as it allows them to date undated timbers even when the site and master chronologies are missing.

8.6.5   Matching Real Site Chronology to Pseudo-Local and Pseudo-Regional Master Chronologies

In the previous experiments we investigated matching individual trees to local pseudo-master chronologies generated from the VSLite model. As it is common practice in dendrochronology to match a group of undated trees to a dated master chronology, here we mimic the same practice by matching an undated site chronology created from a group of individual trees to both pseudo-local and pseudo-regional master chronologies both generated from the VSLite model. The motivation behind this experiment was to examine further the capability of the suggested method to date undated site chronologies, as well as to check whether matching to a local or regional pseudo-master gave better results.

We assume that a group of undated tree-ring data are collected from Sheffield, but that no master chronology exists in this geographical location. Therefore, we use our VSLite-based approach to generate a local pseudo-master chronology from the model given local climate records at Sheffield. Similarly, we generate a regional pseudo-master chronology from the VSLite model given the regional climate records at central England, as detailed in Section 8.6.1. Both simulated pseudo master chronologies (local and regional) are then used in the matching process to provide a calendar date for the undated site chronology, and results from matching to the two master chronologies are compared.

A subset of 100 years from an undated site chronology, which covered the period of 1904-2003 AD, is matched to the simulated local and regional pseudo-master chronologies. The Bayesian model and matching process are implemented, and the results of this experiment are summarised in Table 8.5. All results are after MCMC

185

convergence.

Pseudo Local Chronology					Pseudo Regional Chronology				
Offset	PP	CPP	L	$E(L)$	Offset	PP	CPP	L	$E(L)$
1904	0.44	0.44	0	0	1917	0.24	0.24	13	3.12
1906	0.32	0.76	2	0.64	1898	0.21	0.45	6	4.38
1898	0.09	0.85	6	1.18	1911	0.19	0.64	7	5.71
1905	0.07	0.92	1	1.25	1904	0.18	0.82	0	5.71
1887	0.03	0.95	17	1.76	1885	0.06	0.88	19	6.85
1910	0.02	0.97	6	1.88	1922	0.03	0.91	18	7.39
1889	0.01	0.98	15	2.03	1931	0.01	0.92	27	7.66
1895	0.01	0.99	9	2.12	1903	0.01	0.93	1	7.67
1890	0.00	0.99	14	2.12	1889	0.01	0.94	15	7.82
1896	0.00	0.99	10	2.12	1920	0.00	0.94	16	7.82

Table 8.5: Results of matching an undated site chronology covering 100 years to both local and regional pseudo-master chronologies generated from the VSLite model. The ten highest possible offsets are reported with their posterior probabilities (PP), cumulative posterior probabilities (CPP), loss (L) and expected loss $E(L)$ of each offset. The true offset of the undated sequences is 1904.

Results in Table 8.5 show that the undated site chronology has matched to its true offset with a posterior probability of 0.44 when matching to the local master chronology, and with a posterior probability of 0.18 when matching to the regional master chronology. The expected cost (loss) of obtaining a cumulative posterior probability ≥ 0.90 is only 1.25 years when matching to the local master chronology, whereas it is 7.39 years when matching to the regional master chronology. This indicates that when matching to the local pseudo chronology, the possible offsets of the match are very focused around the true offset with a low expected loss, and the highest posterior probability was provided with the true offset. On the other hand, when matching to the regional pseudo chronology, the possible offsets of the match are very dispersed from the true offset with a high expected loss, and the highest posterior probability was not always provided with the true offset.
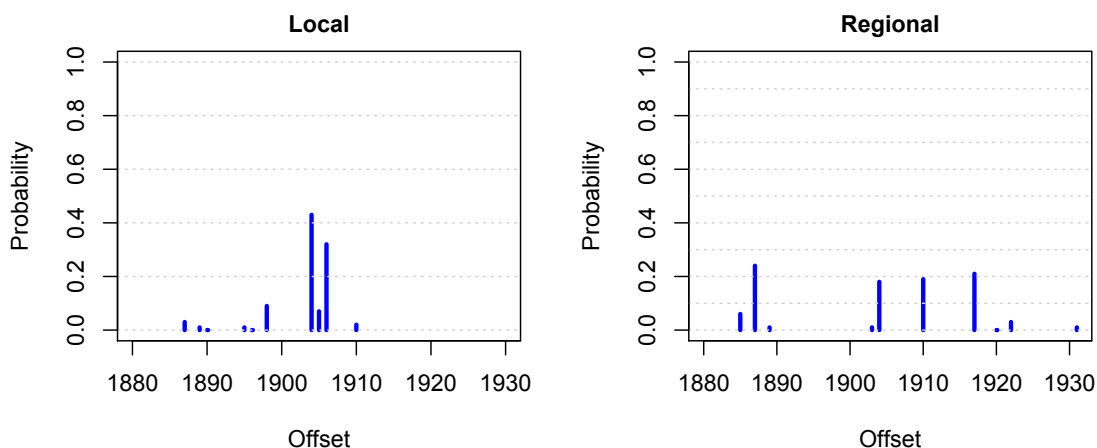
Figure 8.5: Histogram plot of the highest ten possible offsets for the experiment of matching undated site chronology of length 100 years from Sheffield to a pseudo local master chronology (*left*) and a pseudo regional master chronology (*right*), both generated from the VSLite model given local and regional climate data records respectively. x-axis represents possible offsets of the matches and y-axis represents posterior probability of the match. The true offset of the undated sequences is 1904.

Figure 8.5, left panel, shows that the possible offsets of the match are focused around the true offset with a short period, while the right panel shows that the possible offsets of the match are dispersed from the true offset with a long period. In other words, we are 92% sure that the start date of the undated sequence is one of the four calendar dates (1904, 1906, 1898, 1905) with only 1.25 years expected loss, when matching to the local chronology (left panel). However, we are 91% percent sure that the starting date for the undated sequences is one of the six calendar dates (1917, 1898, 1911, 1904, 1885, 1922) with a high expected loss of 7.39 years, when matching to the regional chronology.

In the situation where no dated master chronologies exist, matching to pseudo-master chronologies generated from the VSLite model has provided an alternative way for dating. This is clearly useful if there is no dated ring-width data available; since, instead of knowing nothing about the true date of the undated sequences at this location, we can date it, albeit with greater uncertainty.

187

Our VSLite-based approach has provided more reliable results when matching to the pseudo-local chronologies rather than the pseudo-regional ones. This is unsurprising since the VSLite model was originally developed for modelling local tree-ring sequences as the function of local climates (Tolwinski-Ward *et al.*, 2013). Hence, the model has the potential to capture the mechanism of tree-ring width formation in locally spatial scales, but it might not be able to capture additional regional mechanisms. To capture the extra smoothing induced by averaging climate regionally, would require amendment of the model, which is not explored here, but is discussed in the future work section of the next chapter.

8.7 Summary of Chapter

Many tree-ring sequences from historic timbers have remained undated due to the lack of master chronologies (Jones, 2013). In this chapter we consider the problem of matching undated sequences when the master chronologies are missing. A pseudo-master chronology is generated from a process-based model, and then used in the matching process. Such a cross-matching process in the Bayesian framework promises to provide an alternative and reliable way of matching undated timbers when real dated master chronologies are missing.

A hierarchical Bayes modelling approach for matching tree-ring width sequences is introduced and demonstrated in a relatively small but computationally challenging exercise. The Bayesian inference and matching process via MCMC includes evaluating the likelihood of the model parameters at every possible date offset which allows the posterior distribution of the unknown date for the undated sequences to be estimated. Implementation involves two main tasks: generating dated pseudo-chronologies from a mechanistic model given dated climatic variables, and matching undated sequences to the generated pseudo-chronologies thus providing a posterior estimate of the match. These tasks have been implemented via a two-stage Markov chain Monte Carlo method, which enabled us to speed up

our model implementation.

Experiments of applying the method at the UK chronologies, showed the efficiency of the suggested approach. Considering situations where no master chronologies exist, the approach has successfully matched the undated sequences to the pseudo-master chronology and hence provided useful information about the most likely offsets. Although this method is beneficial to the dendrochronology community, as it allows them to date undated timbers in terms of their climate variables where no master chronology is available, it is limited by the availability of historical temperature and precipitation records in a monthly time-step. Such climate data are, unfortunately, not available for all geographical locations around the world, hence our suggested method will be beneficial for limited regions such as the UK and USA where a relatively long historical climate records are available from nearby or have been constructed by previous researchers as part of the work to interpolate past global climates.

To conclude, based on our suggested method it is possible to date any undated tree-ring width sequences even if no dated master chronologies exist, providing that long historical temperature and precipitation are available. This is achieved by matching undated trees to a pseudo master chronology generated from the VS-Lite model given the climate data.

Chapter 9

Conclusions and Future Research

This final chapter presents a brief summary of the main conclusions from the thesis alongside some suggestions for further research work that are needed for current and future modelling of ring-width growth to enable a fully Bayesian framework for dendrochronology.

9.1 Conclusions

Two different type of models have been discussed in **Chapter 3** for simulating tree-ring width growth: a well-known descriptive statistical model by Litton and Zainodin (1991) and the mechanistic forward model by Tolwinski-Ward *et al.* (2013). As the main focus of this thesis was to investigate the potential of using the VSLite model for Bayesian dendrochronology, we first evaluated this model and explored its uncertainty in **Chapter 4**. The model has successfully been implemented to simulate tree-ring width sequences at different geographical locations around the world, and the model's efficiency has been checked. We conclude that the VSLite model does efficiently and reliably generate tree-ring width sequences at any location where local historical climate data exist. The Bayesian Sensitivity Analysis (which uses a Gaussian process to build an emulator for the model) has also been used systematically to investigate uncertainty in the VSLite model output by examining the influence of each uncertain parameter on the model output variability.

We concluded that just three of the 11 VSLite model parameters (T_1, T_2 and M_2) appeared to have the biggest contribution to the model output variation. The degree of impact among these three parameters varies from one site to another. The conclusion is that if the site under study is temperature-limited then T_1 and T_2 are the most influential parameters, and if it is soil moisture-limited then M_2 is the most influential parameter.

In **Chapter 5** we used a hierarchical Bayesian modelling approach to estimate the VSLite model growth threshold parameters at a range of geographical locations in the UK where both tree-ring chronologies (with Pinus and Quercus species) and historical climate data are available. We concluded that there is some evidence for species-dependent distributions for the UK tree-ring chronologies. For Pinus trees, our estimates of temperature threshold parameters, T_1 and T_2, were lower than for Quercus trees, while M_2 was higher for Pinus trees. These indicate that the Pinus trees are more sensitive to lower temperature and upper soil moisture growth threshold values. However, there is no such evidence for species-dependent values observed for parameter M_1 in the UK chronologies since the results showed that the VSLite does not model this parameter very well.

In **Chapter 6** the Bayesian implementation of the VSLite model has been extended to include a matching process to allow its use in tree-ring dating. Experiments showed that the VSLite model could successfully be used at the core of Bayesian tree-ring dating. We showed that there is a strong relationship between the signal-to-noise ratio and the posterior probability of a match at the true offset. As signal-to-noise ratio increases, the model noise variance decreases and the similarity among individual samples within the chronology increases; thus the posterior probability of a match at the true offset increases. Results also showed that as the number of samples in the undated site chronology increases, the posterior probability of a match at the true offset increases.

In order to investigate the behaviour of the Bayesian approach to dendrochronology using the two models (one process-based and the other purely statistical),

results from the two approaches were compared using several experiments of simulated data. The conclusion is that when considering high signal-to-noise ratio for data, the performance of both models was indistinguishable. However, when considering low signal-to-noise ratio for data, the VSLite-based approach outperforms Jones' approach by providing larger posterior probabilities of a match at the true offset.

In **Chapter 7** we investigated the potential for reducing the amount of preprocessing which currently used prior to tree-ring dating. We extended the Bayesian model to include a rescaling term to ensure that the dated and undated tree-ring sequences are on the same scale before cross-matching them. The new data-adaptive rescaling approach has been explored using a series of experiments of simulated and real data and results showed that the matching process with the rescaling effect performs better in dating tree-ring sequences. This increase in performance is to be expected since by reducing the preprocessing we retain more of the structure in the data. The proposed approach has also been used for matching individual trees with each other, which could be beneficial for building master chronologies. Instead of constructing such chronologies from auto-rescaled tree-ring sequences (using current methods which apply fully processed data), the new Bayesian approach can be used for this purpose.

In **Chapter 8** we tackled the problem of matching undated trees in the presence of missing master chronologies. Pseudo-master tree-ring chronologies were generated from historical climate data using VSLite model, and then used in the dendrochronological matching process. This approach has been successfully implemented by extending our Bayesian framework using a two-stage Markov chain Monte Carlo method. Experiments of applying the model at the UK chronologies, showed the efficiency of the suggested approach. In situations where no master chronologies exist, the approach can successfully be used to match undated sequences to the pseudo-master chronology generated from the VSLite model. This

approach could be beneficial to the dendrochronology community, allowing them to date undated timbers where no master chronology is available. However, it is limited by the availability of historical temperature and precipitation records which are not available for all geographical locations.

9.2 Future Research

Tree-ring analysis remains as one of the most accurate dating methods available for historians and archaeologists. Due to a continuously growing database of tree-ring chronologies alongside developing models for tree-ring-climate relationship, dendrochronology has the possibility to become even more successful. This thesis has concentrated on developing Bayesian methodologies for dendrochronology using both statistical and mechanistic models, but there is considerable scope for further research. This section highlights the main limitations of the methodologies suggested, and discusses further work, based on implementations within this thesis and some aspects of dendrochronology which might usefully be investigated further, in order to move further towards a fully probabilistic framework.

9.2.1 Developing Software for Practical Use

If the proposed approaches investigated in this thesis are successful, they could in future become routine practise in dendrochronology, thus providing probabilistic estimates of the date of undated timbers instead of using classical methods, such as t-values. However, before such approaches can be routinely applied, the following issues should be considered.

- The need to improve the speed and efficiency of the current code. Although we have provided code written in R (R Core Team, 2015) for implementing the approaches suggested within this thesis, the current code is not quick enough to be used for daily practice in dendrochronology labs. Therefore a more effi-

cient program, based on the current code, needs to be developed. This can be done, for example, by recoding some functions in a lower level programming language (such as C or C++) in order to speed up the program and make it of greater practical use. Fortunately, the R package "*Rcpp*" developed by Eddelbuettel and François (2011) can be used for this purpose which allows writing of R functions in the C++ programming language without the need to learn much about compiling issues.

- Develop a software package in the R statistical programming environment for Bayesian dendrochronology. A similar package to that introduced by Bunn (2008) for classical dendrochronology can be developed, using our current code written in R, to implement the Bayesian approaches suggested in this thesis. Developing such a software package might open new potentials for researchers (Bayesian statisticians and dendrochronologists) to investigate further the value and utility of a fully probabilistic framework for tree-ring dating.

9.2.2 Developing Methods for Building Chronologies

The Bayesian approaches proposed within this thesis assume that a group of trees, either dated or undated, exist in a particular geographical location which have already been crossmatched to each other with a view to constructing a master chronology. The classical methods for averaging individual tree-ring width sequences and building site master chronologies are detailed in Section 2.3, which pairwise crossmatch tree-ring sequences using statistical measures given in Section 2.2.2. Specifically, pairs of sequences are aligned at the 'best' match to produce a single average sequence and the process begins again matching one more sample at a time. In order for dendrochronology to be fully Bayesian, a probabilistic framework is required for building a master chronology from single samples. Our developed Bayesian approach for matching an undated sample to a dated sample is described in Chapter 7, which uses data-adaptive rescaling between the two samples. The work in Chapter 7 does not require the data to be fully processed

and may provide a useful starting point for the construction of an algorithm using Bayesian techniques for grouping samples. This would then allow the construction of robust site and regional master chronologies, which do not only rely on sequential pairwise matching but also allow constructing such chronologies from crossmatching a group of trees simultaneously.

9.2.3 Further Use of Forward models in Palaeoclimatology

More recently, dendroclimatologists have started using process-based forward models to investigate the relationship between climate proxy (tree-ring) observations and the climate. These forward models aim to capture the mechanisms of key features of the complex system which links climate to tree-ring growth. Such forward models, VS and VSLite, have been investigated by different dendroclimatologists including Anchukaitis *et al.* (2006); Evans *et al.* (2006); Shi *et al.* (2008); Tolwinski-Ward *et al.* (2011); Vaganov *et al.* (2006). They have found that the forward models produce simulations of tree-ring data which are significantly correlated with actual raw data (Tolwinski-Ward *et al.*, 2011, p.2426). Therefore, such forward models can be inverted with a view to reconstructing past climate.

Although it is not an area investigated in this thesis, there are many other types of climate proxy data, such as ice and sediment cores, used for paleoclimate reconstruction. However, the way in which past climates are reconstructed from these proxies is not always using mechanistic models. In this thesis we have explored the value of using mechanistic forward models for modelling ring-width growth and investigating the use of such models in a fully probabilistic framework for tree-ring dating. Therefore, more investigations of using forward models are needed in the future dendrochronology and palaeoclimatology studies. Using such forward models for paleoclimate reconstruction will be of great benefit to the dendrochronologists. The reconstructed climates, such as those reconstructed from pollen data by Haslett *et al.* (2006), would make useful inputs to VSLite if we have managed to account for the uncertainty in such reconstructed data in the model.

9.2.4 Further Simplification of VSLite Model

Besides efforts continuously to improve applied methodologies for practical den-
drochronology and dendroclimatology, advances in the development of mechanistic
forward models are essential. Such dynamical process-based models should be as
straightforward as possible, while still capturing all relevant features between cli-
mate and tree-ring growth to appropriately represent all related climatic processes.
One of the potential modifications to the current version of the VSLite model
would be by taking out the Leaky Bucket (a sub-model to calculate soil moisture
M content, described in Section 3.6) outside the VSLite model. This will further
simplify the model hence contribute to the speed of the model implementation, as
well as increasing the interpretation of the input-output relationship in which the
climate variables and tree ring-widths are linked in the model. Calculation of soil
moisture is totally independent of modelling tree-ring width formation, hence it
can be calculated separately by first running the Leaky Bucket model, saving the
obtained soil moisture estimates to a file, and then using them as inputs to the
model. In such a case, the new simplified VSLite model would become as shown
in Figure 9.1.
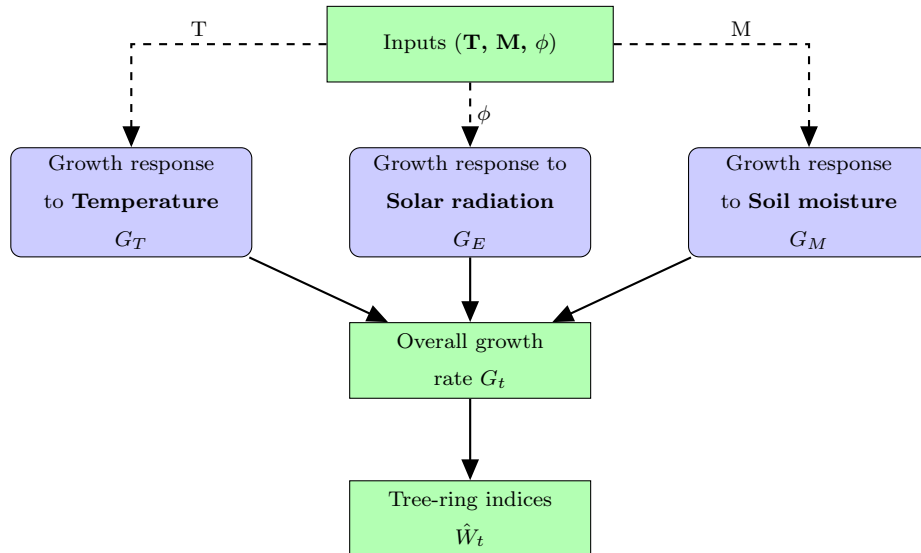
Figure 9.1: Schematic representation of a simplified VSLite model which shows the rela-
tionship between climate variables and simulated ring-width indices.

9.2.5 Adding Regional Hierarchy Layer to VSLite Model

The VSLite model describes the relationship between the ring-width index of a tree and the local climate in that year. The model has the potential to capture the mechanism of tree-ring width growth at a local (subregional) scale, which assumes that all the trees located within the subregion have experienced the same climatic conditions. When implementing the VSLite model for matching undated trees to the regional master chronologies, the model does not perform very well. This is because the current version of the model is developed for modelling local chronologies, and it does not contain a mechanism to generate the smoothness in regional master chronologies.

Given the hierarchical nature of the Bayesian modelling structure discussed in this thesis, however, the VSLite model could be extended to include an additional parameter which represents the local climate within the subregion in which the trees are located. The extended model exploits the hierarchical structure that is present in the data which has not been exploited in VSLite model (when implemented at a regional level). The first level of hierarchy would describe a group of tree-ring sequences from several trees grown in the same geographical locality, a subregion; while the second level of hierarchy would represents a region within which several subregions are grouped into a larger geographical area.

To allow for this extension, we assume γ_j to be the effect of subregion j, the tree-ring index in year t ($t = 1, 2, \ldots, n$) for sample i ($i = 1, 2, \ldots, I$) and subregion j ($j = 1, 2, \ldots, J$) is given by

$$y_{tij} = \beta + \hat{W}_t + \gamma_j + \epsilon_{tij},$$

where $\hat{W}_t$ is the climatic signal for the whole region, γ_j is the subregional signal, and ϵ_{tij} is the noise. For simplicity we could assume that the climatic signal $\hat{W}_t$, γ_j and ϵ_{tij} are independent which might not be appropriate and therefore would need exploring. It seems likely that implementation of the suggested extension would be more successful for matching trees to the regional chronologies than the implementation of the original version of the model for that purpose.

9.3 Priorities for Near Future

The future work listed above is all interrelated and there is not an obvious single way forward. However, our priority for the coming year would be to work on developing software to make the Bayesian approach proposed in this thesis accessible to dendrochronologists. Clearly, the ability to construct master chronologies will be a key part of such software and therefore further development of the ideas in Section 9.2.2 will be a priority.

Appendices

I Full Conditional Distributions for VSLite Parameters in Bayesian Matching Process

The VSLite-based model for Bayesian tree-ring dating, the likelihood of the dated and undated site chronologies, the priors of and the joint posterior distribution of the unknown model parameters are described in Section 6.2 in the main text. The full conditional distribution for each parameter can be obtained from the joint posterior distribution as follows.

i The Conditional Posterior Distribution of T_1

With the prior distribution of $T_1 \sim \Gamma(\alpha_{T_1}, \beta_{T_1})$, and the likelihood of data $\pi(\mathbf{y}|\mathbf{T}, \mathbf{P}, T_1, T_2, M_1, M_2, \sigma_\epsilon^2, \Delta^*) \sim N(\sqrt{1 - \sigma_\epsilon^2}\hat{W}_t, \sigma_\epsilon^2)$, the full conditional distribution of T_1 is:

$$
\begin{aligned}
\pi(T_1|\mathbf{y}, \mathbf{T}, \mathbf{P}, \boldsymbol{\theta}_{-T_1}, \sigma_\epsilon^2, \Delta^*) &\propto \pi(T_1) \times \pi(\mathbf{y}|\mathbf{T}, \mathbf{P}, T_1, T_2, M_1, M_2, \sigma_\epsilon^2, \Delta^*) \\
&\propto \pi(T_1) \times \pi(\mathbf{y^D}|\mathbf{T}, \mathbf{P}, T_1, T_2, M_1, M_2, \sigma_\epsilon^2) \times \\
&\quad \pi(\mathbf{y^{UD}}|\mathbf{T}, \mathbf{P}, T_1, T_2, M_1, M_2, \sigma_\epsilon^2, \Delta^*) \\
&\propto T_1^{(\alpha_{T_1}-1)}\ e^{-T_1/\beta_{T_1}} \times \\
&\quad \prod_{i=1}^{I}\left[\prod_{t=\delta_i}^{\delta_i+l_i-1}(\frac{1}{\sigma_\epsilon^2})^{\frac{1}{2}}\exp\Big(-\frac{1}{2\sigma_\epsilon^2}(y_{ti}-\sqrt{1-\sigma_\epsilon^2}\hat{W}_t)^2\Big)\right] \times \\
&\quad \prod_{i=1+I}^{I+I^*}\left[\prod_{t=\Delta^*+r_i}^{\Delta^*+r_i+l_i-1}(\frac{1}{\sigma_\epsilon^2})^{\frac{1}{2}}\exp\Big(-\frac{1}{2\sigma_\epsilon^2}(y_{ti}-\sqrt{1-\sigma_\epsilon^2}\hat{W}_t)^2\Big)\right].
\end{aligned}
$$

Where $\boldsymbol{\theta}_{-T_1}$ denotes the vector of the four growth threshold parameters except T_1. The full conditional distribution for the parameter T_1 is not a standard distribution, thus we used the Metropolis-Hastings update instead of a Gibbs update.

ii   The Conditional Posterior Distribution of T_2

With the prior distribution of $T_2 \sim \Gamma(\alpha_{T_2}, \beta_{T_2})$, and the likelihood of data $\pi(\mathbf{y}|\mathbf{T}, \mathbf{P}, T_1, T_2, M_1, M_2, \sigma_\epsilon^2, \Delta^*) \sim N(\sqrt{1-\sigma_\epsilon^2}\hat{W}_t, \sigma_\epsilon^2)$, the full conditional distribution of T_2 is:

$$\pi(T_2|\mathbf{y}, \mathbf{T}, \mathbf{P}, \boldsymbol{\theta}_{-T_2}, \sigma_\epsilon^2, \Delta^*) \propto \pi(T_2) \times \pi(\mathbf{y}|\mathbf{T}, \mathbf{P}, T_1, T_2, M_1, M_2, \sigma_\epsilon^2, \Delta^*)$$

$$\propto \pi(T_2) \times \pi(\mathbf{y^D}|\mathbf{T}, \mathbf{P}, T_1, T_2, M_1, M_2, \sigma_\epsilon^2) \times$$

$$\pi(\mathbf{y^{UD}}|\mathbf{T}, \mathbf{P}, T_1, T_2, M_1, M_2, \sigma_\epsilon^2, \Delta^*)$$

$$\propto T_2^{(\alpha_{T_2}-1)} \, e^{-T_2/\beta_{T_2}} \times$$

$$\prod_{i=1}^{I} \left[\prod_{t=\delta_i}^{\delta_i+l_i-1} (\frac{1}{\sigma_\epsilon^2})^{\frac{1}{2}} \exp\left(-\frac{1}{2\sigma_\epsilon^2}(y_{ti} - \sqrt{1-\sigma_\epsilon^2}\hat{W}_t)^2\right) \right] \times$$

$$\prod_{i=1+I}^{I+I^*} \left[\prod_{t=\Delta^*+r_i}^{\Delta^*+r_i+l_i-1} (\frac{1}{\sigma_\epsilon^2})^{\frac{1}{2}} \exp\left(-\frac{1}{2\sigma_\epsilon^2}(y_{ti} - \sqrt{1-\sigma_\epsilon^2}\hat{W}_t)^2\right) \right].$$

Where $\boldsymbol{\theta}_{-T_2}$ denotes the vector of the four growth threshold parameters except T_2. The full conditional distribution for the parameter T_2 is not a standard distribution, thus we used the Metropolis-Hastings update instead of a Gibbs update.

iii   The Conditional Posterior Distribution of M_1

With the prior distribution of $M_1 \sim \Gamma(\alpha_{M_1}, \beta_{M_1})$, and the likelihood of data $\pi(\mathbf{y}|\mathbf{T}, \mathbf{P}, T_1, T_2, M_1, M_2, \sigma_\epsilon^2, \Delta^*) \sim N(\sqrt{1-\sigma_\epsilon^2}\hat{W}_t, \sigma_\epsilon^2)$, the full conditional distribution of M_1 is:

$$\pi(M_1|\mathbf{y}, \mathbf{T}, \mathbf{P}, \boldsymbol{\theta}_{-M_1}, \sigma_\epsilon^2, \Delta^*) \propto \pi(M_1) \times \pi(\mathbf{y}|\mathbf{T}, \mathbf{P}, T_1, T_2, M_1, M_2, \sigma_\epsilon^2, \Delta^*)$$

$$\propto \pi(M_1) \times \pi(\mathbf{y^D}|\mathbf{T}, \mathbf{P}, T_1, T_2, M_1, M_2, \sigma_\epsilon^2) \times$$

$$\pi(\mathbf{y^{UD}}|\mathbf{T}, \mathbf{P}, T_1, T_2, M_1, M_2, \sigma_\epsilon^2, \Delta^*)$$

$$\propto M_1^{(\alpha_{M_1}-1)} \, e^{-M_1/\beta_{M_1}} \times$$

$$\prod_{i=1}^{I} \left[\prod_{t=\delta_i}^{\delta_i+l_i-1} (\frac{1}{\sigma_\epsilon^2})^{\frac{1}{2}} \exp\left(-\frac{1}{2\sigma_\epsilon^2}(y_{ti} - \sqrt{1-\sigma_\epsilon^2}\hat{W}_t)^2\right) \right] \times$$

$$\prod_{i=1+I}^{I+I^*} \left[\prod_{t=\Delta^*+r_i}^{\Delta^*+r_i+l_i-1} (\frac{1}{\sigma_\epsilon^2})^{\frac{1}{2}} \exp\left(-\frac{1}{2\sigma_\epsilon^2}(y_{ti} - \sqrt{1-\sigma_\epsilon^2}\hat{W}_t)^2\right) \right].$$

Where $\boldsymbol{\theta}_{-M_1}$ denotes the vector of the four growth threshold parameters except M_1. The full conditional distribution for the parameter M_1 is not a standard distribution, thus we used the Metropolis-Hastings update instead of a Gibbs update.

iv The Conditional Posterior Distribution of M_2

With the prior distribution of $M_2 \sim \Gamma(\alpha_{M_2}, \beta_{M_2})$, and the likelihood of data $\pi(\mathbf{y}|\mathbf{T}, \mathbf{P}, T_1, T_2, M_1, M_2, \sigma_\epsilon^2, \Delta^*) \sim N(\sqrt{1-\sigma_\epsilon^2}\hat{W}_t, \sigma_\epsilon^2)$, the full conditional distribution of M_2 is:

$$
\begin{aligned}
\pi(M_2|\mathbf{y}, \mathbf{T}, \mathbf{P}, \boldsymbol{\theta}_{-M_2}, \sigma_\epsilon^2, \Delta^*) &\propto \pi(M_2) \times \pi(\mathbf{y}|\mathbf{T}, \mathbf{P}, T_1, T_2, M_1, M_2, \sigma_\epsilon^2, \Delta^*) \\
&\propto \pi(M_2) \times \pi(\mathbf{y^D}|\mathbf{T}, \mathbf{P}, T_1, T_2, M_1, M_2, \sigma_\epsilon^2) \times \\
&\quad \pi(\mathbf{y^{UD}}|\mathbf{T}, \mathbf{P}, T_1, T_2, M_1, M_2, \sigma_\epsilon^2, \Delta^*) \\
&\propto M_2^{(\alpha_{M_2}-1)} e^{-M_2/\beta_{M_2}} \times \\
&\quad \prod_{i=1}^{I} \left[\prod_{t=\delta_i}^{\delta_i+l_i-1} (\frac{1}{\sigma_\epsilon^2})^{\frac{1}{2}} \exp\Big(-\frac{1}{2\sigma_\epsilon^2}(y_{ti} - \sqrt{1-\sigma_\epsilon^2}\hat{W}_t)^2\Big) \right] \times \\
&\quad \prod_{i=1+I}^{I+I^*} \left[\prod_{t=\Delta^*+r_i}^{\Delta^*+r_i+l_i-1} (\frac{1}{\sigma_\epsilon^2})^{\frac{1}{2}} \exp\Big(-\frac{1}{2\sigma_\epsilon^2}(y_{ti} - \sqrt{1-\sigma_\epsilon^2}\hat{W}_t)^2\Big) \right].
\end{aligned}
$$

Where $\boldsymbol{\theta}_{-M_2}$ denotes the vector of the four growth threshold parameters except M_2. The full conditional distribution for the parameter M_2 is not a standard distribution, thus we used the Metropolis-Hastings update instead of a Gibbs update.

v The Conditional Posterior Distribution of σ_ϵ^2

The inverse-gamma distribution is a conjugate prior for the variance parameter (σ_ϵ^2) since it results in a posterior distribution that is also inverse-gamma and thus it is simple to sample. With the prior distribution $\sigma_\epsilon^2 \sim \Gamma^{-1}(\alpha_\epsilon, \beta_\epsilon)$ and the likelihood of data $\pi(\mathbf{y}|\mathbf{T}, \mathbf{P}, T_1, T_2, M_1, M_2, \sigma_\epsilon^2, \Delta^*) \sim N(\sqrt{1-\sigma_\epsilon^2}\hat{W}_t, \sigma_\epsilon^2)$, and when the overall number of observations is equal to $(N + N^*)$, the full conditional distribution of σ_ϵ^2

is:

$$\pi(\sigma_\epsilon^2|\mathbf{y},\mathbf{T},\mathbf{P},\boldsymbol{\theta},\Delta^*) \propto \pi(\sigma_\epsilon^2) \times \pi(\mathbf{y}|\mathbf{T},\mathbf{P},T_1,T_2,M_1,M_2,\sigma_\epsilon^2,\Delta^*)$$

$$\propto \pi(\sigma_\epsilon^2) \times p(\mathbf{y^D}|\mathbf{T},\mathbf{P},T_1,T_2,M_1,M_2,\sigma_\epsilon^2) \times$$

$$\pi(\mathbf{y^{UD}}|\mathbf{T},\mathbf{P},T_1,T_2,M_1,M_2,\sigma_\epsilon^2,\Delta^*)$$

$$\propto \left(\sigma_\epsilon^2\right)^{-(\alpha_\epsilon+1)} \exp\left(\frac{\beta_\epsilon}{\sigma_\epsilon^2}\right) \times$$

$$\prod_{i=1}^{I}\left[\prod_{t=\delta_i}^{\delta_i+l_i-1}(\frac{1}{\sigma_\epsilon^2})^{\frac{1}{2}}\exp\left(-\frac{1}{2\sigma_\epsilon^2}(y_{ti}-\sqrt{1-\sigma_\epsilon^2}\hat{W}_t)^2\right)\right] \times$$

$$\prod_{i=1+I}^{I+I^*}\left[\prod_{t=\Delta^*+r_i}^{\Delta^*+r_i+l_i-1}(\frac{1}{\sigma_\epsilon^2})^{\frac{1}{2}}\exp\left(-\frac{1}{2\sigma_\epsilon^2}(y_{ti}-\sqrt{1-\sigma_\epsilon^2}\hat{W}_t)^2\right)\right]$$

$$\propto\left(\sigma_\epsilon^2\right)^{-(\frac{N+N^*}{2}+\alpha_e+1)}\exp\left(-\frac{1}{\sigma_\epsilon^2}\left\{\sum_{i=1}^{I}\left(\sum_{t=\delta_i}^{\delta_i+l_i-1}\frac{(y_{ti}-\sqrt{1-\sigma_\epsilon^2}\hat{W}_t)^2}{2}\right)+\right.\right.$$

$$\left.\left.\sum_{i=I+1}^{I+I^*}\left(\sum_{t=\Delta^*+r_i}^{\Delta^*+r_i+l_i-1}\frac{(y_{ti}-\sqrt{1-\sigma_\epsilon^2}\hat{W}_t)^2}{2}\right)+\beta_\epsilon\right\}\right).$$

The final expression is the kernel of a inverse-gamma distribution. Therefore, the distribution of the variance parameter is also inverse-gamma $\pi(\sigma_\epsilon^2) \sim \Gamma^{-1}(\acute{\alpha}_\epsilon, \acute{\beta}_\epsilon)$ with $\acute{\alpha}_\epsilon = \frac{N+N^*}{2} + \alpha_\epsilon$, and
$\acute{\beta}_\epsilon = \sum_{i=1}^{I}\left(\sum_{t=\delta_i}^{\delta_i+l_i-1}\frac{(y_{ti}-\sqrt{1-\sigma_\epsilon^2}W_t)^2}{2}\right) + \sum_{i=I+1}^{I+I^*}\left(\sum_{t=\Delta^*+r_i}^{\Delta^*+r_i+l_i-1}\frac{(y_{ti}-\sqrt{1-\sigma_\epsilon^2}\hat{W}_t)^2}{2}\right) + \beta_\epsilon.$

vi The Conditional Posterior Distribution of Δ^*

Having estimated all the model parameters, the conditional distribution of the match at the true offset can be obtained. With the discrete uniform prior distribution $\pi(\Delta^*) \sim U[\Delta_{min} = \Delta_s - l^* + q, \Delta_{max} = \Delta_e - q + 1]$ and the likelihood of dated and undated data $p(\mathbf{y}|\mathbf{T},\mathbf{P},T_1,T_2,M_1,M_2,\sigma_\epsilon^2,\Delta^*) \sim N(\sqrt{1-\sigma_\epsilon^2}\hat{W}_t, \sigma_\epsilon^2)$, and when the overall number of observations in the undated site master chronology is equal to (N^*), the full conditional distribution of Δ^* for $\Delta^* = \Delta_{min}, \ldots, \Delta_{max}$

is:

$$\pi(\Delta^*|\mathbf{y}, \mathbf{T}, \mathbf{P}, \boldsymbol{\theta}, \sigma_\epsilon^2) \propto \pi(\Delta^*) \times \pi(\mathbf{y}|\mathbf{T}, \mathbf{P}, T_1, T_2, M_1, M_2, \sigma_\epsilon^2, \Delta^*)$$

$$\propto \pi(\Delta^*) \times \pi(\mathbf{y^D}|\mathbf{T}, \mathbf{P}, T_1, T_2, M_1, M_2, \sigma_\epsilon^2) \times$$

$$\pi(\mathbf{y^{UD}}|\mathbf{T}, \mathbf{P}, T_1, T_2, M_1, M_2, \sigma_\epsilon^2, \Delta^*)$$

$$\propto \pi(\mathbf{y^{UD}}|\mathbf{T}, \mathbf{P}, T_1, T_2, M_1, M_2, \sigma_\epsilon^2, \Delta^*)$$

$$\propto \prod_{i=1+I}^{I+I^*} \left[\prod_{t=\Delta^*+r_i}^{\Delta^*+r_i+l_i-1} (\frac{1}{\sigma_\epsilon^2})^{\frac{1}{2}} \exp\left(-\frac{1}{2\sigma_\epsilon^2}(y_{ti} - \sqrt{1-\sigma_\epsilon^2}\hat{W}_t)^2\right) \right]$$

$$\propto \left(\frac{1}{\sigma_\epsilon^2}\right)^{\frac{N^*}{2}} \prod_{i=1+I}^{I+I^*} \left[\prod_{t=\Delta^*+r_i}^{\Delta^*+r_i+l_i-1} \exp\left(-\frac{1}{2\sigma_\epsilon^2}(y_{ti} - \sqrt{1-\sigma_\epsilon^2}\hat{W}_t)^2\right) \right]$$

Now, taking the logarithm of both sides,

$$\log\left[\pi(\Delta^*|\mathbf{y}, \mathbf{T}, \mathbf{P}, \boldsymbol{\theta}, \sigma_\epsilon^2) \right] = \frac{N^*}{2} \log(\frac{1}{2\sigma_\epsilon^2}) - \frac{1}{2\sigma_\epsilon^2} \sum_{i=I+1}^{I+I^*} \left[\sum_{t=\Delta^*+r_i}^{\Delta^*+r_i+l_i-1} \left(y_{ti} - \sqrt{1-\sigma_\epsilon^2}\hat{W}_t \right)^2 \right]$$

$$= -\frac{1}{2\sigma_\epsilon^2} \sum_{i=1+I}^{I+I^*} \left[\sum_{t=\Delta^*+r_i}^{\Delta^*+r_i+l_i-1} \left(y_{ti} - \sqrt{1-\sigma_\epsilon^2}\hat{W}_t \right)^2 \right] + constant$$

Hence calculate the posterior probability of the match at each possible date offset $p(\Delta^* = \Delta_s - l^* + q), \ldots, p(\Delta^* = \Delta_s), \ldots, p(\Delta^* = \Delta_e), \ldots, p(\Delta^* = \Delta_e - q + 1)$. We then followed (Jones, 2013, p.72) to normalise the posterior estimates, and sample $\Delta^{*(1)}$ by inverting the distribution function of Δ^*.

II VSLite Model and Matching Process Results

This Appendix comprises results of different experiments of matching undated sequences to a dated master chronology using our extension of the VSLite model and the matching process. The matching process using the VSLite model is detailed in Chapter 6.

Experiment (A)

Matching an undated site chronology with **2** samples covering **50** years, to a dated site master chronology with **10** samples covering **200** years. The MCMC were thinned every 10 iterations and results were reproducible after 100,000 iterations.

SNR	σ_ϵ^2	Posterior Probability		$\hat{\sigma}_\epsilon^2$	t-value
		Offset	Probability		
0.5	0.667	100	1.00	0.65	5.66
		22	0.00		2.72
0.4	0.714	100	0.98	0.696	3.97
		22	0.01		2.846
0.3	0.769	100	0.83	0.758	3.64
		22	0.13		2.89
		91	0.13		2.62
0.2	0.833	100	0.53	0.817	2.91
		91	0.21		2.38
		22	0.17		2.04
		103	0.05		1.81
0.1	0.899	22	0.36	0.876	2.36
		100	0.29		2.27
		91	0.20		2.11
		103	0.11		2.08

Table 1: Results of matching undated sequences of length 50 years created from 2 samples to a dated master chronology of length 200 years. The true offset of the undated site chronology is 100. The signal-to-noise ratio (SNR) varies from 0.5 to 0.1.

- While SNR is bigger than or equal to 0.5, the posterior probability of a match at the correct offset is 1. As signal-to-noise ratio decreases, the similarity between individual trees within the chronology decreases, and the posterior probability of a match at the correct offset decreases.

Experiment (B)

Matching an undated site chronology with **5** samples covering **50** years, to a dated master chronology with **10** samples covering **200** years. The MCMC were thinned every 10 iterations and results were reproducible after 50,000 iterations.

SNR	σ_ϵ^2	Posterior Probability		$\hat{\sigma}_\epsilon^2$	t-value
		Offset	Probability		
0.3	0.769	100	1.00	0.764	6.16
		48	0.00		3.39
0.2	0.833	100	0.98	0.829	4.91
		48	0.01		3.75
		95	0.00		2.77
0.1	0.899	100	0.54	0.902	3.82
		95	0.23		3.55
		40	0.12		2.83
		18	0.07		2.69

Table 2: Results of matching undated sequences of length 50 years created from 5 samples to a dated master chronology of length 200 years. The true offset of the undated site chronology is 100. The signal-to-noise ratio (SNR) varies from 0.3 to 0.1.

- When SNR is bigger than or equal to 0.3, the posterior probability of a match at the correct offset is 1. As signal-to-noise ratio decreases, the similarity between individual trees within the chronology decreases, and the posterior probability of a match at the correct offset decreases. For SNR equal to 0.1, posterior probability was relatively low (0.54).

206

Experiment (C)

Matching an undated site chronology with **2** samples covering **100** years, to a dated site master chronology with **10** samples covering **200** years. The MCMC were thinned every 10 iterations and results were reproducible after 90,000 iterations.

SNR	σ_ϵ^2	Posterior Probability		$\hat{\sigma}_\epsilon^2$	t-value
		Offset	Probability		
0.4	0.714	100	1.00	0.708	5.71
		82	0.00		3.42
0.3	0.769	100	0.99	0.781	5.04
		82	0.00		3.19
0.2	0.833	100	0.88	0.822	3.91
		82	0.09		2.85
		79	0.02		2.14
0.1	0.899	100	0.63	0.888	3.36
		82	0.24		2.13
		101	0.06		2.01
		79	0.03		1.78

Table 3: Results of matching undated sequences of length 100 years created from 2 samples to a dated master chronology of length 200 years. The true offset of the undated site chronology is 100. The signal-to-noise ratio (SNR) varies from 0.4 to 0.1.

- When SNR is bigger than or equal to 0.4, the posterior probability of a match at the correct offset is 1. As signal-to-noise ratio decreases, the similarity between individual trees within the chronology decreases, and the posterior probability of a match at the correct offset decreases.

Experiment (D)

Matching an undated site chronology with **5** samples covering **100** years, to a dated master chronology with **10** samples covering **200** years. The MCMC were thinned every 10 iterations and results were reproducible after 50,000 iterations.

SNR	σ_ϵ^2	Posterior Probability		$\hat{\sigma}_\epsilon^2$	t-value
		Offset	Probability		
0.3	0.769	100	1.00	0.748	6.73
		112	0.00		2.89
0.2	0.833	100	1.00	0.826	6.15
		112	0.01		2.61
0.1	0.899	100	0.96	0.886	4.39
		112	0.02		2.76
		33	0.01		2.03
		21	0.00		1.98

Table 4: Results of matching undated sequences of length 100 years created from 5 samples to a dated master chronology of length 200 years. The true offset of the undated site chronology is 100. The signal-to-noise ratio (SNR) varies from 0.3 to 0.1. When SNR is bigger than or equal to 0.2, the posterior probability of a match at the correct offset is 1.

III   Comparison between results from VSLite and Jones' models

This Appendix comprises different experiments of comparing the results obtained from using our extension to the VSLite model with those from Jones' model, and the traditional t-value based method when matching undated sequences to a dated master chronology. The matching process using the VSLite model is detailed in Chapter 6.

Experiment 1: Comparing the results of using VSLite-based model with those of using Jones' model, and the traditional t-value for the experiment of matching an undated site chronology with **5** samples covering **50** years, to a dated master chronology with **10** samples covering **200** years.

SNR	σ_ϵ^2	VSLite Model			Jones' Model			Trad. Results
		Offset	Prob.	$\hat{\sigma}_\epsilon^2$	Offset	Prob.	$\hat{\sigma}_\epsilon^2$	t-value
0.3	0.769	100	1.00	0.764	100	1.00	0.761	5.16
		48	0.00		141	0.00		3.39
		95	0.00		84	0.00		2.65
0.2	0.833	100	0.98	0.829	100	0.94	0.843	3.91
		48	0.01		141	0.06		3.75
		95	0.00		84	0.00		2.77
0.1	0.899	100	0.54	0.902	141	0.48	0.905	3.12
		95	0.23		100	0.25		3.55
		40	0.12		84	0.10		2.83
		18	0.07		45	0.05		2.69

Table 5: Results of matching 5 undated trees of length 50 years to a dated master chronology, with 10 samples, covering 200 years, when using our extension of the VSLite model, Jones' model, and the traditional method (t-value). The true offset of the undated site chronology is 100. The signal-to-noise ratio (SNR) varies from 0.3 to 0.1.

- The posterior estimate of the match at the true offset depends on the signal-to-noise ratio. As SNR decreases, the posterior probability of a match decreases.

- When signal-to-noise ratio is bigger than or equal to 0.3, the performance of both VSLite and Jones' models were indistinguishable and both provided the posterior probability of a match at the true offset equals to 1. However, for lower signal-to-noise ratio values (≤ 0.2), the VSLite model provided slightly higher posterior probabilities of a match at the correct offset.

- When SNR is 0.1, the VSLite model provided a posterior probability of a match at the true offset equal to 0.54; however, Jones' model led to the highest posterior probability of 0.48 being associated with an incorrect offset.

- The mean posterior estimate of the model noise parameter $\hat{\sigma}_e^2$ were almost similar from both models.

Experiment 2: Comparing the results of using VSLite-based model with those of using Jones' model, and the traditional t-value method for the experiment of matching an undated site chronology with **1** sample covering **100** years, to a dated master chronology with **10** samples covering **200** years.

SNR	σ_ϵ^2	VSLite Model			Jones' Model			Trad. Results
		Offset	Prob.	$\hat{\sigma}_\epsilon^2$	Offset	Prob.	$\hat{\sigma}_\epsilon^2$	t-value
0.4	0.714	100	1.00	0.702	100	1.00	0.644	5.10
		-31	0.00		40	0.00		3.89
0.3	0.769	100	0.98	0.748	100	0.98	0.692	4.19
		-31	0.00		40	0.01		3.68
		100	0.74		100	0.50		3.33
0.2	0.833	126	0.01	0.829	40	0.16	0.753	3.11
		-13	0.01		-17	0.13		2.82
		126	0.44		40	0.39		2.92
0.1	0.899	100	0.36	0.91	-17	0.27	0.931	2.81
		28	0.15		100	0.11		1.22

Table 6: Results of matching 1 undated tree of length 100 years to a dated master chronology, with 10 samples, covering 200 years, when using our extension of the VSLite model, Jones' model, and the traditional method (t-value). The true offset of the undated site chronology is 100. The signal-to-noise ratio (SNR) varies from 0.4 to 0.1.

- When signal-to-noise ratio is bigger than or equal to 0.4, the performance of both VSLite and Jones' models were indistinguishable and both provided the posterior probability of a match at the true offset equals to 1. However, for lower signal-to-noise ratio values (≤ 0.3), the VSLite model provided slightly higher posterior probabilities of a match at the correct offset.

- When signal-to-noise ratio is 0.1, both models provided the highest posterior probability associated with an incorrect offset.

- The mean posterior estimate of the model noise parameter $\hat{\sigma}_e^2$ were almost similar from both models.

Experiment 3: Comparing the results of our extension of the VSLite model with those from Jones' model, and the traditional t-value method for the experiment of matching **5** undated sample covering **100** years, to a dated site master chronology with **10** samples covering **200** years.

SNR	σ_ϵ^2	VSLite Model			Jones' Model			Trad. Results
		Offset	Prob.	$\hat{\sigma}_\epsilon^2$	Offset	Prob.	$\hat{\sigma}_\epsilon^2$	t-value
0.2	0.833	100	1.00	0.83	100	1.00	0.83	5.15
		112	0.00		80	0.00		2.61
0.1	0.899	100	0.99	0.886	100	0.96	0.89	3.89
		112	0.02		80	0.00		2.76
		33	0.01		80	0.00		2.03
		21	0.00		80	0.00		1.98

Table 7: Results of matching 5 undated tree of length 100 years to a dated master chronology, with 10 samples, covering 200 years, when using our extension of the VSLite model, Jones' model, and the traditional method (t-value). The true offset of the undated site chronology is 100.

- The performance of both VSLite and Jones' models were almost similar. However, when signal-to-noise ratio is 0.1, VSLite model provided a slightly higher posterior probability of a match at the true offset.

- The mean posterior estimate of $\hat{\sigma}_e^2$ were almost similar from both models.

IV Matching Trees to Pseudo Local Chronologies

i Matching individual trees from Oxford to the pseudo local site chronology generated from VSLite model

Undated Tree	Possible Offset	Posterior Probability	Cumulative Posterior Probability	Loss (L)	Expected Loss E(L)
	1879	0.77	0.77	0	0.00
	1899	0.06	0.83	20	1.20
Sample 1	1862	0.05	0.88	17	2.05
	1858	0.04	0.92	21	2.89
	1911	0.02	0.94	32	3.53
	1879	0.75	0.75	0	0.00
	1878	0.08	0.83	1	0.08
Sample 2	1893	0.03	0.86	14	0.50
	1898	0.02	0.88	19	0.68
	1883	0.01	0.89	4	0.72
	1879	0.76	0.76	0	0.00
	1892	0.13	0.89	13	1.69
Sample 3	1889	0.05	0.94	10	2.19
	1899	0.03	0.97	20	2.79
	1880	0.01	0.98	1	2.80
	1879	0.89	0.89	0	0.00
	1881	0.05	0.94	2	0.10
Sample 4	1892	0.04	0.98	13	0.62
	1891	0.01	0.99	12	0.74
	1893	0.00	0.99	14	0.74
	1879	0.39	0.39	0	0.00
	1892	0.23	0.62	13	2.99
Sample 5	1881	0.17	0.79	2	3.33
	1878	0.10	0.89	1	3.43
	1887	0.03	0.92	8	3.67
	1879	0.79	0.79	0	0.00
	1856	0.09	0.88	23	2.07
Sample 6	1894	0.04	0.92	15	2.67
	1892	0.01	0.93	13	2.80
	1857	0.01	0.94	22	3.02
	1879	0.96	0.96	0	0.00
	1878	0.01	0.97	1	0.01
Sample 7	1914	0.01	0.98	35	0.36
	1865	0.00	0.98	14	0.36
	1882	0.00	0.98	3	0.36
	1879	0.80	0.8	0	0.00
	1882	0.08	0.88	3	0.24
Sample 8	1856	0.04	0.92	23	1.16
	1892	0.01	0.93	13	1.29
	1883	0.01	0.94	4	1.33

Table 8: Results of matching 8 individual trees of length 100 years at "Oxford" site. Each tree is crossmatched to the pseudo site chronology of length 162 years, using our new Bayesian approach. The true offset is 1879, and only 5 possible offsets are reported.

ii Matching individual trees from Southampton to pseudo local site chronology generated from VSLite model

Undated Tree	Possible Offset	Posterior Probability	Cumulative Posterior Probability	Loss (L)	Expected Loss E(L)
Sample 1	1910	0.49	0.49	0	0.00
	1898	0.18	0.67	12	2.16
	1891	0.17	0.84	19	5.39
	1896	0.08	0.92	14	6.51
	1888	0.01	0.93	22	6.73
Sample 2	1910	0.75	0.75	0	0.00
	1889	0.21	0.96	21	4.41
	1911	0.01	0.97	1	4.42
	1913	0.00	0.97	3	4.42
	1870	0.00	0.97	40	4.42
Sample 3	1910	0.62	0.62	0	0.00
	1897	0.27	0.89	13	3.51
	1889	0.04	0.93	21	4.35
	1894	0.02	0.95	16	4.67
	1891	0.01	0.96	19	4.86
Sample 4	1897	0.36	0.36	13	4.68
	1910	0.28	0.64	0	4.68
	1911	0.19	0.83	1	4.87
	1882	0.07	0.90	28	6.83
	1896	0.05	0.95	14	7.53
Sample 5	1910	0.45	0.45	0	0.00
	1898	0.25	0.70	12	3.00
	1906	0.14	0.84	4	3.56
	1882	0.12	0.96	28	6.92
	1896	0.03	0.99	14	7.34
Sample 6	1910	0.56	0.56	0	0.00
	1883	0.25	0.81	27	6.75
	1886	0.10	0.91	24	9.15
	1901	0.03	0.94	9	9.42
	1909	0.01	0.95	1	9.43
Sample 7	1910	0.59	0.59	0	0.00
	1883	0.18	0.77	27	4.86
	1898	0.06	0.83	12	5.58
	1862	0.03	0.86	48	7.02
	1884	0.02	0.88	26	7.54
Sample 8	1910	0.74	0.74	0	0.00
	1887	0.12	0.86	23	2.76
	1893	0.05	0.91	17	3.61
	1877	0.01	0.92	33	3.94
	1911	0.01	0.93	1	3.95

Table 9: Results of matching 8 individual trees of length 100 years at "Southampton" site. Each tree is crossmatched to the pseudo site chronology of length 160 years, using our new Bayesian approach. The true offset is 1910, and only 5 possible offsets with the highest posterior probabilities are reported.

Bibliography

Akaike, H. (1973). "Information Theory and an Extension of the Maximum Likelihood Principle." In Petrov, B. N. and Gsaki, F. (eds.), *2nd International Symposium on Information Theory*, 267–281. Akadeimia Kiado, Budapest.

Anchukaitis, K., Evans, M., Kaplan, A., Vaganov, E. A., Hughes, M. K., Grissino-Mayer, H. D., and Cane, M. A. (2006). "Forward modeling of regional scale tree-ring patterns in the southeastern United States and the recent influence of summer drought." *Geophysical Research Letter*, 33: L04705.

Baillie, M. G. L. (1977). "An Oak Chronology for South Central Scotland." *Tree-ring Bulletin*, 37: 33–44.

— (1982). *Tree-Ring Dating and Archaeology*. Croom Helm. London.

— (1995). *A Slice Through Time*. BT. Batsford Ltd, London.

Baillie, M. G. L. and Pilcher, J. R. (1973). "A Simple Crossdating Program for Tree-ring Research." *Tree-ring Bulletin*, 33: 7–14.

Bayarri, M. J., Berger, J. O., Paulo, R., Sacks, J., Cafeo, J. A., Cavandish, J., Lin, C. H., and Tu, J. (2007). "A framework for Validation of computer models"." *Technometrics*, 49: 138–154.

Bhattacharya, S. and Haslett, J. (2007). "Importance re-sampling MCMC for cross-validation in inverse problems." *Bayesian Anal.*, 2(2): 385–407.

Bowman, S. (1990). *Interpreting the past: Radiocarbon Dating*. London: British Museum Publication.

Box, G. E. P., Jenkins, G. M., and Reinsel, G. C. (1994). *Time Series Analysis: Forecasting and Control*. Prentice-Hall International (UK) Ltd, London, third edition.

Breitenmoser, P., Brönnimann, S., and Frank, D. (2014). "Forward modelling of tree-ring width and comparison with a global network of tree-ring chronologies." *Climate of the Past*, 10(2): 437–449.

Bridge, M. C. (1988). "The Dendrochronological Dating of Buildings in Southern England." *Medieval Archaeology*, 32: 166–174.

Bronk Ramsey, C. (1995). "Radiocarbon calibration and analysis of stratigraphy: The OxCal program." *Radiocarbon*, 37: 425–430.

Brown, D. M., Munro, M. A. R., Baillie, M. G. L., and Pilcher, J. R. (1986). "Dendrochronology- the Absolute Irish Standard." *Radiocarbon*, 28: 279–283.

Buck, C. E., Cavanagh, W. G., and Litton, C. D. (1996). *The Bayesian Approach to Interpreting Archaeological Data*. Wiley, Chichester.

Buck, C. E., Christen, J. A., and James, G. N. (1999). "BCal: an On-line Bayesian Radiocarbon Calibration Tool." *Internet Archaeology*, 7.

Buck, C. E. and Millard, A. R. (eds.) (2004). *Tools for Constructing Chronologies: Crossing Disciplinary Boundaries*. Springer, London.

Bunn, A. G. (2008). "A dendrochronology program library in R (dplR)." *Dendrochronologia*, 26(2): 115 – 124.

Cairns, D. A. (2005). "Detecting Ring Anomalies in Dendrochronology." Ph.D. thesis, University of Sheffield.

Christen, J. A. and Fox, C. (2005). "Markov Chain Monte Carlo Using an Approximation." *Journal of Computational and Graphical Statistics*, 14(4): 795–810.

Cook, E., Briffa, K., Shiyatov, S., and Mazepa, V. (1990). "Tree-Ring Standardization and Growth-Trend Estimation." In Cook, E. R. and Kairiukstis, L. A.

(eds.), *Methods of Dendrochronology: Applications in the Environmental Sciences*, 104–123. Kluwer Academic Publishers, The Netherlands.

Cook, E. R. (1981). "The Smoothing Spline: A New Approach to Standardizing Forest Interior Tree-Ring Width Series for Dendroclimatic Studies." *Tree-Ring Bulletin*, 41: 45–53.

Eddelbuettel, D. and François, R. (2011). "Rcpp: Seamless R and C++ Integration." *Journal of Statistical Software*, 40(8): 1–18.

Evans, M., Reichert, B. K., Kaplan, A., Anchukaitis, K., Vaganov, E. A., Hughes, M. K., and Cane, M. A. (2006). "A forward modeling approach to paleoclimatic interpretation of tree-ring data." *Geophysical Research*, 111: G03008.

Evans, M. N., Smerdon, J. E., Kaplan, A., Tolwinski-Ward, S. E., and Gonzlez-Rouco, J. F. (2014). "Climate field reconstruction uncertainty arising from multivariate and nonlinear properties of predictors." *Geophysical Research Letters*, 41(24): 9127–9134. 2014GL062063.

Fritts, H. C. (1963). "Computer Programs for Tree-Ring Research." *Tree-ring Bulletin*, 25: 2–7.

— (1976). *Tree Rings and Climate*. Academic Press Inc. London Ltd.

Fritts, H. C., Mosimann, J. E., and Bottorff, C. P. (1969). "A Revised Computer Program for Standardizing Tree-Ring Series." *Tree-ring Bulletin*, 29: 15–20.

Gelman, A. (2006). "Prior Distributions for Variance Parameters in Hierarchical Models." *Bayesian Analysis*, 1: 515–533.

Gelman, A. and Rubin, D. (1992). "Inference from iterative simulation using multiple sequences." *Stat. Sci.*, 7: 457–472.

Geman, S. and Geman, D. (1984). "Stochastic Relaxation, Gibbs Distributions, and the Bayesian Restoration of Images." *IEEE Transactions on Pattern Analysis and Machine Intelligence*, PAMI-6(6): 721–741.

Gilks, W. R., Richardson, S., and Spiegelhalter, D. J. (1996). *Markov Chain Monte Carlo in Practice*. Chapman & Hall, London.

Ginting, V., Pereira, F., Presho, M., and Wo, S. (2011). "Application of the two-stage Markov chain Monte Carlo method for characterization of fractured reservoirs using a surrogate flow model." *Computational Geosciences*, 15(4): 691–707.

Guiot, J., Boucher, E., and Gea Izquierdo, G. (2014). "Process models and model-data fusion in dendroecology." *Frontiers in Ecology and Evolution*, 2(52).

Harris, I., Jones, P., Osborn, T., and Lister, D. H. (2014). "Updated high-resolution grids of monthly climatic observations- the CRU TS3.10 Dataset." *Int J Climatol*, 34.

Haslett, J., Whiley, M., Bhattacharya, S., Salter-Townshend, M., Wilson, S. P., Allen, J. R. M., Huntley, B., and Mitchell, F. J. G. (2006). "Bayesian palaeoclimate reconstruction." *Journal of the Royal Statistical Society: Series A (Statistics in Society)*, 169(3): 395–438.

Hastings, W. K. (1970). "Monte Carlo sampling methods using Markov chains and their applications." *Biometrika*, 57(1): 97–109.

Haung, J., van den Dool, H. M., and Georgankakos, K. P. (1996). "Analysis of model-calculated soil moisture over the United States (1931–1993) and applications to long-range temperature forecasts." *J Clim*, 9: 1350–1362.

Haylock, R. G. and OHagan, A. (1996). "On inference for outputs of computationally expensive algorithms with uncertainty on the inputs." *SIAM*, 2: 106–125.

Hillam, J. (1998). "Dendrochronology: Guidelines on Producing and Interpreting Dendrochronological Dates." English Heritage, London.

Jones, E. M. (2013). "Practical Bayesian dendrochronology." Ph.D. thesis, University of Sheffield, UK.

217

Kennedy, M. C. and O'Hagan, A. (2001). "Bayesian Calibration of Computer Models" (with discussion)." *Journal of the Royal Statistical Society*, 63: 25–464.

Korner, C. (2012). *Alpine tree-lines: functional ecology of the global high elevation tree limits*. Switzerland: Springer Basel.

Laxton, R. R. and Litton, C. D. (1983). "Information theory and dendrochronology; The Effect of Prewhitening." *Computer Applications and Archaeology*, 11: 137–149.

— (1988). *An East Midlands master tree-ring chronology and its use for dating vernacular buildings*. University of Nottingham.

Litton, C. D. and Zainodin, H. J. (1987). "Grouping Methods for Dendrochronology." *Science and Archaeology*, 29: 14–24.

— (1991). "Statistical models of dendrochronology." *Journal of Archaeological Science*, 18: 429–440.

Manley, G. (1974). "Central England Temperatures: monthly means 1659 to 1973." *Q.J.R. Meteorol. Soc.*, 100: 389–405.

Matalas, N. C. (1962). "Statistical Properties of Tree-Ring Data." *Publications of the International Association of Scientific Hydrology*, 7: 39–47.

Maxwell, R. S., Wixom, J. A., and Hess, A. E. (2011). "A comparison of two techniques for measuring and crossdating tree rings." *Dendrochronologia*, 29: 237–243.

McKay, M., Beckman, R., and Conover, W. (1979). "A comparison of three methods for selecting values of input variables in the analysis of output from a computer code." *Technometrics*, 21: 239–245.

Mills, C. (1988). "Dendrochronology: the Long and the Short of it." In Slater, E. A. and Tate, J. (eds.), *Science and Archaeology*, 549–565. BAR Brit. Ser. 196, Oxford.

Monserud, R. A. (1986). "Time-series Analyses of Tree-ring Chronologies." *Forest Science*, 32: 349–372.

Munro, M. A. R. (1984). "An Improved Algorithm for Crossdating Tree-Ring Series." *Tree-ring Bulletin*, 44: 17–27.

Oakley, J. E. and O'Hagan, A. (2002). "Bayesian inference for the uncertainty distribution of computer model outputs"." *Biometrika*, 89: 769–784.

— (2004). "Probabilistic sensitivity analysis of complex models: a Bayesian approach."." *Journal of the Royal Statistical Society*, 66: 751–769.

Okasha, M. K. M. (1987). "Statistical Methods in Dendrochronology." Ph.D. thesis, University of Sheffield.

Orton, C. R. (1983). "The use of Student's t test for matching treering patterns." *Bulletin University London Institute of Archaeology*, 20: 101–105.

OHagan, A. (2004). "Bayesian analysis of computer code outputs: a tutorial." *Reliability Engineering and System Safety*.

Parker, D. E. and Horton, E. (2005). "Uncertainties in the Central England Temperature series since 1878 and some changes to the maximum and minimum series." *International J.Climatology*, 25: 1173–1188.

Parker, D. E., Legg, T., and Folland, C. (1992). "A new daily Central England Temperature Series, 1772-1991." *International J.Climatology*, 12: 317–342.

Pilcher, J. R. (1990). "Sample Preparation, Cross-dating, and Measurement." In Cook, E. R. and Kairiukstis, L. A. (eds.), *Methods of Dendrochronology: Applications in the Environmental Sciences*, 40–50. Kluwer Academic Publishers, The Netherlands.

Pilcher, J. R., Baillie, M. G. L., Brown, D. M., McCormac, F. G., MacSweeney, P. B., and McLawrence, A. S. (1995). "Dendrochronology of Subfossil Pine in the North of Ireland." *Journal of Ecology*, 83: 665–671.

Plummer, M., Best, N., Cowles, K., and Vines, K. (2006). "CODA: Convergence Diagnosis and Output Analysis for MCMC." *R News*, 6(1): 7–11.

R Core Team (2015). *R: A Language and Environment for Statistical Computing*. R Foundation for Statistical Computing, Vienna, Austria.
URL `https://www.R-project.org/`

Raftery, A. E. and Lewis, S. L. (1992). "How Many Iterations in the Gibbs Sampler?" In Berger, J. O., Bernado, J. M., Dawid, A. P., and Smith, A. F. M. (eds.), *Bayesian Statistics*, 763–773. Oxford University Press, New York.

Reinsch, C. H. (1967). "Smoothing by Spline Functions." *Numerische Mathematik*, 10: 177–183.

Sacks, J., Welch, W. J., Mitchell, T. J., and Wynn, H. P. (1989). "Design and Analysis of Computer Experiments." *Statist. Sci.*, 4(4): 409–423.

Saltelli, A., Chan, K., and Scott, E. (2000). *Sensitivity Analysis*. Wiley. Wiley Series in Probability and Statistics.

Saltelli, A., Ratto, T., M.and Andres, Campolongo, F., Cariboni, J., Gatelli, D., Saisana, M., and Tarantola, S. (2008). *Global sensitivity analysis: the primer*. Wiley. Chichester.

Saltelli, A., Tarantola, S., Campolongo, F., and Ratto, M. (2004). *Sensitivity analysis in practice: A guide to assessing scientific models*. Wiley.

Sander, C. and Levanic, T. (1996). "Comparison of t-values Calculated in Different Dendrochronological Programmes." *Dendrochronologia*, 14: 269–272.

Schweingruber, F. (1988). *Tree Rings: Basics and Applications of Dendrochronology*. Kluwer Academic Publishers, Dordrecht, Holland.

Shi, J., Liu, Y., Vaganov, E. A., Li, J., and Cai, Q. (2008). "Statistical and process-based modeling analyses of tree growth response to climate in semi-arid

area of north central China: A case study of Pinus tabulaeformis." *Geophysical Research*, 113: G01026.

Smith, B. J. (2007). "boa: An R Package for MCMC Output Convergence Assessment and Posterior Inference." *Journal of Statistical Software*, 21(11): 1–37.

Steward, S. (1983). "Statistical Dendrochronology." Master's thesis, University of Sheffield.

Stokes, M. A. and Smiley, T. L. (1968). *An Introduction to Tree-ring Dating*. University of Arizona Press, Tucson, AZ.

Strong, M. and Oakley, J. (2014). "When is a model good enough? Deriving the expected value of model improvement via specifying internal model discrepancies'." *SIAM*, 2: 106–125.

Tolwinski-Ward, S. E. (2015). "Uncertainty quantification for a climatology of the frequency and spatial distribution of North Atlantic tropical cyclone landfalls." *Journal of Advances in Modeling Earth Systems*, 7(1): 305–319.

Tolwinski-Ward, S. E., Anchukaitis, K., and Evans, M. (2013). "Bayesian parameter estimation and interpretation for an intermediate model of tree-ring width." *Climate of the Past Discussions*, 9: 615–645.

Tolwinski-Ward, S. E., Evans, M. N., Hughes, M. K., and Anchukaitis, K. J. (2011). "An efficient forward model of the climate controls on interannual variation in tree-ring width." *Climate Dynamics*, 36: 2419–2439.

Tolwinski-Ward, S. E., Tingley, M. P., Evans, M. N., Hughes, M. K., and Nychka, D. W. (2015). "Probabilistic reconstructions of local temperature and soil moisture from tree-ring data with potentially time-varying climatic response." *Climate Dynamics*, 44(3): 791–806.

Touchan, R., Shishov, V. V., Meko, D. M., and Grachev, A. (2012). "Process based model sheds light on climate sensitivity of Mediterranean tree-ring width." *Biogeosciences*, 9: 965–972.

Vaganov, E. A., Hughes, M. K., Shashkin, A. V., and Grachev, A. (2006). *Growth Dynamics of Conifer Tree Rings, Image of Past and Future Environments*. Springer-Verlag Berlin Heidelberg.

Walker, M. (2005). *Quaternary Dating Methods*. John Wiley and Sons.

Warren, W. G. (1980). "On Removing the Growth Trend from Dendrochronological Data." *Tree-Ring Bulletin*, 40: 35–44.

Warren, W. G. and MacWilliam, S. L. (1981). "Test of a New Method for Removing the Growth Trend from Dendrochronological Data." *Tree-Ring Bulletin*, 41: 55–66.

Wigley, T. M. L., Jones, P. D., and Briffa, K. R. (1987). "Cross-dating Methods in Dendrochronology." *Journal of Archaeological Science*, 14: 51–64.

Yamaguchi, D. K. (1986). "Interpretation of Cross Correlation Between Tree-Ring Series." *Tree-Ring Bulletin*, 46: 47–54.

Zainodin, H. J. (1988). "Statistical models and techniques for dendrochronology." Ph.D. thesis, University of Nottingham, UK.

Zhang, Y. X., Shao, X. M., Xu, Y., and Martin, W. (2011). "Process-based modeling analyses of Sabina przewalskii growth response to climate factors around the northeastern Qaidam Basin." *Chinese Sci Bull*, 56: 1518–1525.